Late Quaternary ecosystem and climate interactions in SW Balkans inferred from Lake Prespa sediments

Inaugural-Dissertation

zur

Erlangung des Doktorgrades

der Mathematisch-Naturwissenschaftlichen Fakultät

der Universität zu Köln

vorgelegt von

Konstantinos Panagiotopoulos

aus Athen

Köln, 2013

Berichterstatter:	Prof. Dr. Frank Schäbitz
	Prof. Dr. Helmut Brückner
Vorsitzender der Prüfungskommission:	Prof. Dr. Martin Melles
Tag der mündlichen Prüfung:	3. Juli 2013

Kumulative Dissertation – Vorlage und Gliederung gemäß Anhang 4 der Promotionsordnung der Mathematisch-Naturwissenschaflichen Fakultät der Universität zu Köln vom 2. Februar 2006 (geändert durch Artikel I Absatz 10 der Ordnung zur Änderung der Promotionsordnung von 10. Mai 2012).

στους γονείς μου

Acknowledgements

For the successful completion of this PhD project I owe my appreciation to my supervisor Frank Schäbitz and my advisor Bernd Wagner. Helmut Brückner is also gratefully acknowledged for reviewing this dissertation, which was generously funded by the German Science Foundation (DFG) within the framework of the CRC 806 "Our Way to Europe".

It was in 2006, while studying in Cologne, when I got a brief introduction to the world of paleoclimate and pollen analysis by Frank. I was instantly intrigued with the idea that these magnificent microfossils had a story to tell to those willing to dig beyond the surface. A couple of years later, Frank offered me the unique opportunity to immerse myself in this minuscule world on a project located in the Balkans and in specific at Lake Prespa. Frank, I am thankful for your trust and support during all these years. Bernd was instrumental in conceiving and planning this project as he has been active in the region over several years. Thanks for the insightful comments, advice and witty conversations. My introduction and training in pollen identification was made possible through the unconditional support of Jutta Meurers-Balke, head of the Laboratory of Archaeobotany, and her working group at the Institute of Prehistoric Archaeology. My special thanks are due to Ingrid Kloß who generously shared with me her counting routine, enthusiasm and knowledge of European pollen grains and spores. Martin Melles is acknowledged for providing drilling equipment and laboratory facilities at the Institute of Geology and Mineralogy, Hendrik Vogel for leading the successful field campaign at Lake Prespa in October/ November 2009 and Hanna Cieszynski for help with SEM photography. Special credits go to Anne Böhm (Aufgebauer) my PhD partner in Geology with whom we shared countless hours at the lab, the office and the field. This thesis benefited greatly from our close collaboration. We are both obliged to a number of people at the Institute of Geology and Mineralogy that provided help in the lab and in the field.

In addition, I would like to thank all colleagues (and friends) from the Laboratory of Palynology (Geography), especially Jean-Pierre Francois (mi compañero de la oficina), Karsten Schittek (for the German translation of the summary), Jonathan Hense, Verena Foerster, Tsige Gebru-Kassa, Flavia Quintana, Wilfried Schulz, Michael Wille for stimulating conversations, bright ideas, and numerous extra curriculum activities. Steffi Reusch, René Kabacinski, Carina Casimir, Markus Dzakovic, Dominik Berg, Jonas Urban and Jan Wowrek, offered invaluable help in the lab. Tips on cartography and graphical design issues from Frederik von Reumont and Lutz Hermsdorf-Knauth are really appreciated. I am indebted to Iris Breuer and Werner Schuck for help with administrative and financial matters. This project profited significantly from cooperation with several researchers within and outside the CRC 806. I am particularly grateful to Melanie Leng, Thomas Litt, Andreas Hense, Norbert Kühl, Zlatko Levkov, Finn Viehberg, Andreas Andrinopoulos, Marianthi Stefouli, Elena Marinova, Thomas Giesecke, Bernhard Weninger, Valery Sitlivy, Giovanni Zanchetta, Roberto Sulpizio, Lyudmila Shumilovskikh, Benno Thoma, and to several IRTG members. The administrations of the Galičica and Pelister National Parks, the Hydrobiological Institute at Ohrid, the Greek Biotope/Wetland Center (EKBY) at Thessaloniki, and the Society for the Protection of Prespa (SPP) at Prespa are gratefully acknowledged.

I remain of course responsible for any errors.

Last but not least I would like to express my sincerest gratitude to my friends, the Müller family and my family for their unreserved support.

Abbreviations

a.s.l.	above sea level
AMS	accelerator mass spectrometry
AP	arboreal pollen
CRC	collaborative research center
D-O	Dansgaard-Oeschger
ESR	electron spin resonance
GI	Greenland interstadials
GMWL	global meteoric water line
GS	Greenland stadial
H1	Heinrich event 1
HI	hydrogen index
IRD	ice rafted debris
ka cal BP	thousand years calibrated before present
LEL	local evaporation line
LGM	last glacial maximum
LZ (or L)	lithozone
MIS	marine isotope stage
MMWL	Mediterranean meteoric water line
NAP	non arboreal pollen
NGRIP	north Greenland ice core project
OI	oxygen index
OM	organic matter
P-1(a)	Prespa pollen assemblage (sub)zone 1(a)
PAZ(s)	pollen assemblage zone(s)
PBO	Preboreal oscillation
PCA	principal component analysis
S1	Sapropel 1
SEM	scanning electron microscope
SST(s)	sea surface temperature(s)
TC	total carbon
TIC	total inorganic carbon
TIDC	total dissolved inorganic carbonate
TN	total nitrogen
TOC	total organic carbon
TS	total sulfur
XRD	x-ray diffraction
XRF	x-ray fluorescence
YD	Younger Dryas

Contents

Figures

Tables

I Introduction

1.1 Preface

How can fossil pollen grains originating from a remote area of the Balkan Peninsula be relevant to pressing policy issues dealing with the biodiversity and climate change agenda? In what way does the paleoecological archive of Lake Prespa contribute to our knowledge of spatial and temporal vegetational patterns in southeastern Europe? Did the study area serve as a refugium of plant species during the Last Glacial? Which ecological and/or environmental factors controlling changes in terrestrial and aquatic ecosystems within the watershed are identified besides climate variability? Is it possible to infer the duration, nature and extent of climate oscillations from the paleovegetation record? Did regional environmental and climatic conditions facilitate or hinder the establishment of hominid populations at Prespa and its vicinity? Is it possible to trace the imprint of anthropogenic activity on the landscape and discern it from natural processes?

In order to address the issues raised above, there is a need to put the research undertaken within this dissertation into a broader perspective. To begin with, in 1988 the United Nations Environmental Program (UNEP) and the World Meteorological Organization (WMO) established the Intergovernmental Panel on Climate Change (IPCC), a scientific body assigned to investigate the potential environmental and socio-economic impacts of climate change and assess options for mitigation and adaptation. Hitherto, the IPCC has produced four comprehensive assessment reports and played an instrumental role in the creation of the UN Framework Convention of Climate Change (UNFCCC), which was opened for signature in June 1992 at the UN Conference on Environment and Development at Rio de Janeiro. The Convention on Biological Diversity (CBD) was also ready for signature during the "Rio Earth Summit" and entered into force in 1993 while the UNFCC in 1994. The ensuing Protocols (e.g. Kyoto and Nagoya) were conceived as the legal instruments for implementing the objectives laid down by the respective conventions. The overarching goal of the two conventions are to prevent human interference with the climate system (UNFCCC, 1992) and to conserve genetic, species and ecosystem diversity (CBD, 1992).

In the latest IPCC Assessment Report (AR4) released in 2007, it is described that atmospheric concentration of greenhouse gases has grown significantly since pre-industrial times. For instance, carbon dioxide global atmospheric concentration has increased from about 280 ppm in 1850 to 379 ppm in 2005 exceeding by far the natural range over the last 650,000 years (i.e. 180 to 300 ppm) as determined from ice cores. In addition, the average global surface temperature has risen by 0.74 °C since 1899 as a result of anthropogenic activities (IPCC, 2007). A warming of about 0.2 °C per decade is projected for a range of emission scenarios, summing up to 1.8-4 °C by the year 2100 if no action is taken. Even if greenhouse gas concentrations were to be stabilized, anthropogenic warming and sea level rise would continue for centuries (IPCC, 2007).

The Millennium Ecosystem Assessment (MEA, 2005) concluded that human-induced changes in ecosystems have accelerated and intensified over the last 50 years leading to unprecedented losses in global biodiversity. Changes in land use, climate, atmospheric CO_2 concentrations and

eutrophication have been identified as major drivers of global biodiversity change (e.g. Sala et al., 2000; Pereira et al., 2010). At a global scale, Mediterranean and alpine ecosystems are projected to experience large biodiversity losses due to land-use and climate change respectively (Sala et al., 2000), while freshwater ecosystems are expected to experience increasing pressure due to climate change and eutrophication (Leadley et al., 2010). In Europe, abandonment of agricultural land and subsequent expansion of forests is modeled to lead to a net carbon uptake in terrestrial ecosystems between 1990 and 2100, but most likely it will be offset by increasing CO_2 emissions and human-induced climate change (e.g. Zaehle et al., 2007).

The Mediterranean basin is one of the world's biodiversity hotspots featuring high species richness and an exceptional concentration of endemic species (4.3% or 13,000 of the world's 300,000 plant species as endemics), but only an estimated 4.7% of the original extent of primary vegetation remains undisturbed (Myers et al., 2000). Factors limiting the geographical range (habitat distribution) of species pose a serious threat to local populations and increase their extinction risk (e.g. Thomas et al., 2004). In the light of projected climate warming for the Mediterranean (IPCC, 2007), the occurrence of frequent droughts and changes in fire regime are estimated to affect plant species distribution in this region significantly. Niche-based models predict an excess of species loss for Mediterranean mountain regions, such as in the Balkans and the Carpathians, considering the marginal character of these habitats for many species (Thuiller et al., 2005). Given the higher disturbance frequency (e.g. wildfires) and human-induced habitat fragmentation associated with changes in land use, Mediterranean mountain plant species become more vulnerable and are expected to face increasing extinction risk (endemics in particular) due to their limited migration potential. However, the survival of species in favorable locations (i.e. refugia) in mountain regions can not be accurately estimated considering the grid scale applied in most studies (e.g. 50 x 50 km in Thuiller et al., 2005).

Paleoecological data underscore the potential of Mediterranean mountain regions to serve as refugia for flora and fauna during preceding climate oscillations (e.g. Griffiths et al., 2004; Médail and Diadema, 2009). Quaternary refugia preserved plant diversity over multiple glacial cycles and frequently coincide with regional biodiversity hotspots (Médail and Diadema, 2009). Archives of past biodiversity changes have the potential to extent existing ecological datasets over millennial time scales allowing to test models and hypotheses, and to improve our understanding over ecological and evolutionary processes. In this regard, paleoecological input is critical in comprehending the rate and nature of biotic response to climate change. Paleoarchives record the complex interplay between abiotic and biotic factors and processes -such as species migration and extinction as well as rapid compositional turnover and resilience of ecosystems- and provide an important resource for conservation planning (e.g. Taberlet and Cheddadi, 2002; Willis et al., 2010).

1.2 Research objectives, methodology and thesis structure

This study investigates sediments retrieved from Lake Prespa by means of palynological analyses and forms an integral part of Project B2 within the Collaborative Research Center (CRC) 806 'Our Way to Europe: Culture-Environment Interaction and Human Mobility in the Late Quaternary'. The CRC 806 takes on the dispersal of modern humans from Africa into Europe applying a wide range of archaeological, ethnological and geoscientific methods (Richter et al., 2012a). In this framework, Project B2 aims at providing paleoenvironmental data in order to infer climate oscillations over the Last Glacial and the Holocene at a local and regional scale. Considering the location of the study area on the Balkan Peninsula, the principal corridor of human migration into Europe, the Lake Prespa paleoarchive offers new insights into past climate change and its potential impacts on hominid populations in the region.

The recent development of core scanning and multi-sensor logging instruments took the paleoresearch community by storm overshadowing more laborious techniques, such as palynology. Despite its undisputable time-efficiency and high-resolution output, it can prove challenging for researches to reconstruct past environmental changes without employing other methods (e.g. Section **3.1** in Chapter **III**). Biological proxies offer direct insights into the biotic component and mechanisms governing the rate and nature of ecosystem change through time and space. Understanding the complexity of biotic processes (e.g. immigration, competition and succession) and the interaction between abiotic and biotic factors (e.g. nutrient cycles) is a prerequisite for reconstructing paleoenvironments and deducing paleoclimate. This thesis profited greatly from the application of a multi-proxy approach and in particular from the close cooperation with my colleagues at the Institute of Geology and in particular with my B2 Project partner, Anne Böhm (Aufgebauer). In addition to palynological analyses (performed at the Institute of Geography by the author), multiple other proxies were investigated in collaboration with other researchers and institutes (**Figure 1.1)**, which are explicitly listed in each chapter.

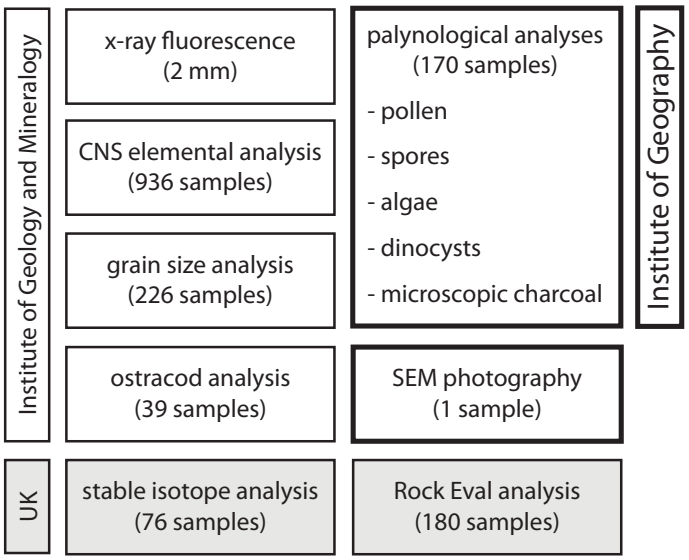

Figure 1.1: Synopsis of analyses already performed on material from Lake Prespa and included in this thesis. Note that for non-destructive methods sampling intervals are given in mm.

Three hypotheses are tested in the ensuing chapters (Chapter II-VII):

- the potential of the study area to record past changes in abiotic and biotic components of local ecosystems without significant time lags in comparison to other paleoarchives,
- the sensitivity to orbital- and suborbital-scale climate variability,
- and the refugial character of the watershed in terms of fostering mesophilous trees during the Last Glacial.

In addition, this thesis focuses on the following key themes:

- Floristic composition and representation in pollen spectra.
- Spatial vegetation patterns in the landscape through time (e.g. treeline shifts, vegetation belts, landscape openness).
- Species immigration, competition, displacement and succession.
- Occurrence of natural or anthropogenic disturbance (e.g. fire) and resilience of ecosystems.
- Parameters and mechanisms controlling aquatic, littoral and terrestrial ecosystem dynamics in response to climate oscillations (e.g. water pH, mixing regime, lake-level change, soil development).
- Human-environment interaction through time (e.g. agriculture, pastoralism, forest clearance, potential migration barriers)

Chapter **II** and **III** deal with environmental and climatic changes over the last 17,000 years (320 cm) spanning the Last Glacial termination, the Lateglacial transition and the Holocene intervals. In specific, Chapter **II** introduces the chronology, lithology, sedimentology, geochemistry, as well as summary pollen and ostracod data from a new sediment core (Co1215) recovered from Lake Prespa during the 2009 field campaign. Chapter **III**, presents pollen, phytoplankton, and microscopic charcoal data and discusses vegetation dynamics, fire history and human impact on the landscape. Chapter **IV**, presents sedimentological, geochemical, isotope, and summary palynological data and examines the limnological and environmental response over the last 80,000 years (1575 cm). In Chapter **V**, after the addition of 2 m obtained during the 2011 field campaign, are presented sedimentological, geochemical and palynological data from the longest sequence to date (1776 cm) spanning the last 92,000 years. Chapter **VI**, showcases several case studies originating from CRC 806 projects in an effort to bring together the principles of geoscientific, archaeological and socio-cultural anthropological research under the scope of an adaptive cycle model. Chapter **VII** takes on numerical analyses of the data and shows results that have not been published yet. At last, Chapter **VIII** synthesizes data presented in previous chapters, evaluates the findings with qualitative and quantitative means, and reconstructs environmental responses (vegetational and limnological) to past climate variability.

1.3 General setting

1.3.1 Study area

The Prespa watershed is shared between Albania, the Former Yugoslav Republic of Macedonia (FYROM) and Greece (**Figure 1.2**). It comprises two transboundary lakes (Megali and Mikri Prespa), separated by an alluvial isthmus, and is surrounded by mountains rising over 2,000 m. Together with Lake Ohrid (Albania, FYROM) and the former Lake Maliq (Albania), which was drained after World War II, comprised the Dessarete Lake group (Stanković, 1960). Lake Prespa (Megali Prespa), situated at 849 m a.s.l. has no surface outflow, but is hydrologically connected with underground karst channels (Matzinger et al., 2006; Amataj et al., 2007; **Figure 1.5**) to Lake Ohrid located at 693 m a.s.l., which eventually drains into the Adriatic sea.

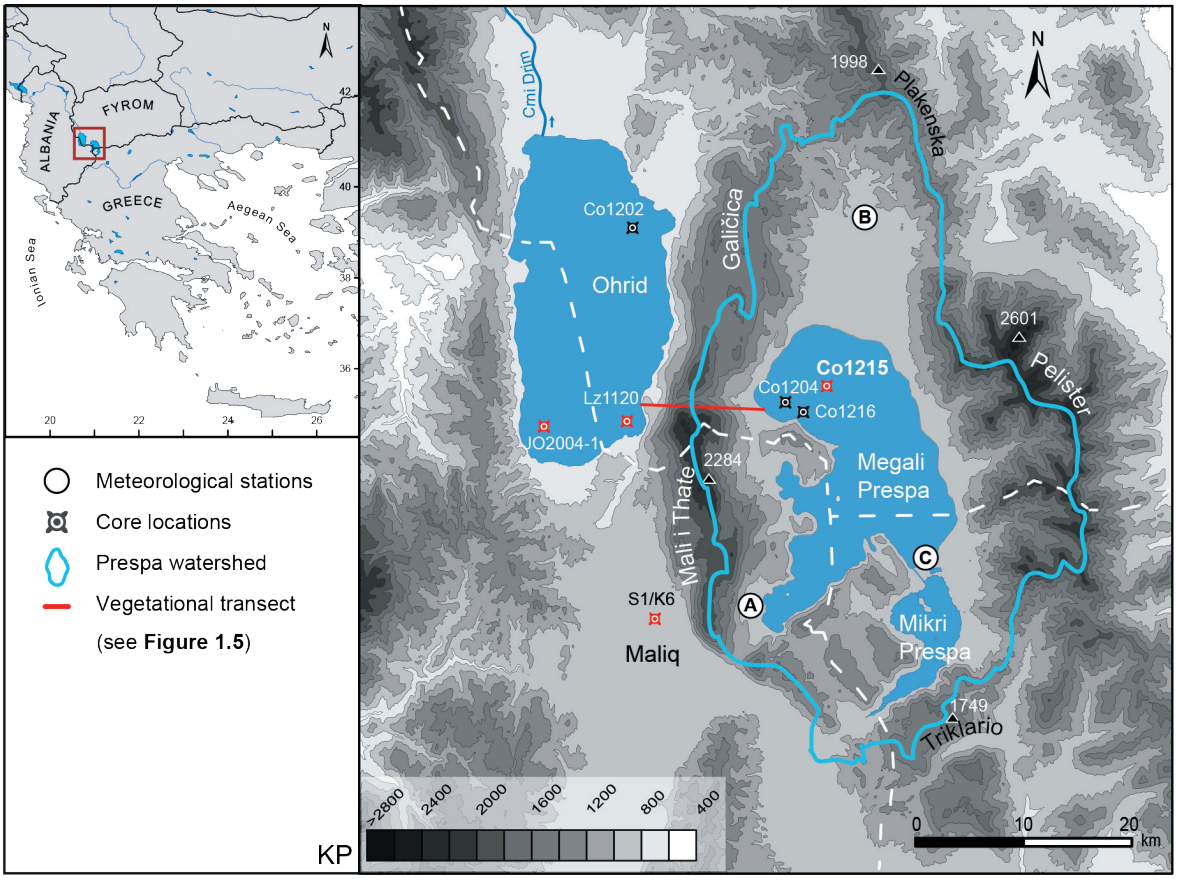

Figure 1.2: Location of study area in southwestern Balkans and topography. Locations and codes of palaeorecords mentioned in the text: Co1215 (this study), Co1216 (Wagner et al., 2012), Co1204 (Leng et al., 2010; Wagner et al., 2010), Co1202 (Vogel et al., 2010a, b; Wagner et al., 2010), JO2004-1 (Belmecheri et al., 2009; Lézine et al., 2010), Lz1120 (Wagner et al., 2009, 2010), and S1/K6 (Denèfle et al., 2000; Bordon et al., 2009). Pollen archives are indicated in red (SRTM Data: Jarvis et al., 2008).

1.3.2 Geology

The Lake Prespa region was uplifted during the Alpine orogeny, while Lake Prespa is a result of subsequent subsidence (Aliaj et al., 2001; Dumurzanov et al., 2005). Consequently, Lake Prespa is deduced to be of Pliocene origin, c. 3.5 million years (Stanković, 1960; Popovska and Bonacci, 2007). The Prespa graben is characterized by active faults running parallel to the N–S direction of the basin (Dumurzanov et al., 2005; Wagner et al., 2012). On the west and south, the Galičica and Mali i Thate mountains comprise intensively karstified triassic limestone, while carbonate rocks (limestone and dolomite) dominate the southern part of the basin as well. Paleozoic metamorphic and intrusive rocks (schists, gneisses, granites) outcrop in the northern and eastern part of the basin (Geological Maps of Yugoslavia, 1977; Geological Maps of Albania, 1983; Hydrogeological map of western Macedonia water district (09), 2010). The lowlands of the basin are filled by c. 50–60 m of alluvial Quaternary sediments (Dumurzanov et al., 2005).

1.3.3 Climate

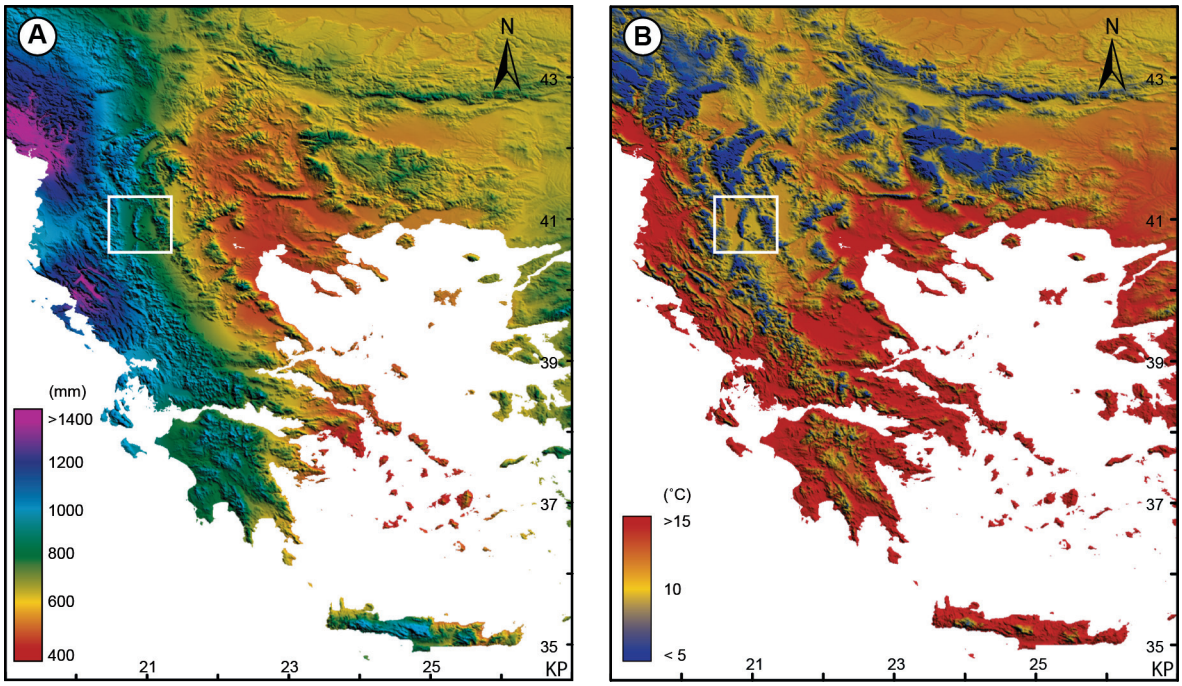

Figure 1.3: Mean annual precipitation and temperature (data from WorldClim; Hijmans et al., 2005).

The Prespa catchment lies in a transitional climatic zone where the warm and humid air from the west and south meet the cold and dry air masses from the north. Despite the close proximity to the Adriatic sea, the study area does not feature a typical Mediterranean climate. The Prespa region is situated northeast of the Pindos mountain range, which is responsible along with the prevailing westerlies for the precipitation gradient occurring across the southern tip of the Balkan Peninsula (**Figure 1.3** a). The present-day mean annual temperatures for mountain-

ous areas in this region are below the 10 °C (**Figure 1.3** b). There are several meteorological stations within the catchment operating since the 1950s (Strubenhoff and Hoyos, 2005) and the ones with the longest record from each country are presented (locations are shown in **Figure 1.2**; **Figure 1.4**).

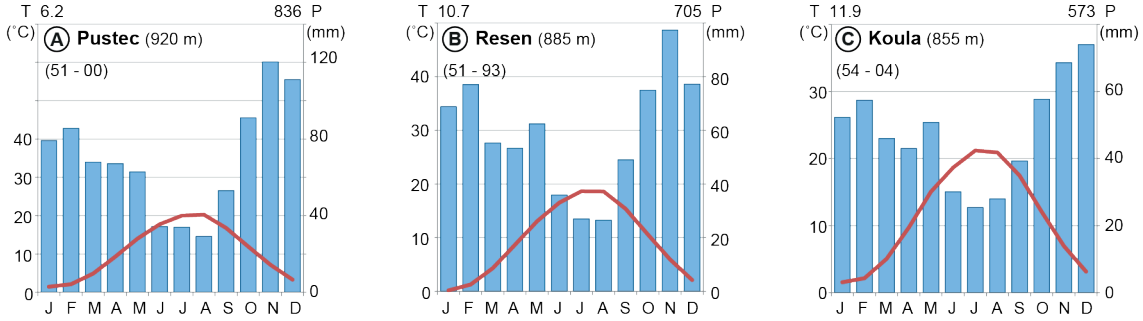

Figure 1.4: Ombrothermic diagrams of selected meteorological stations within the Prespa catchment (data compiled from Strubenhoff and Hoyos, 2005).

The climate of the area is transitional and can be classified as sub-Mediterranean with continental influences. Mean July and January temperatures in the lowlands are 21°C and 1°C respectively, with a mean annual temperature of 11°C. Precipitation peaks in winter (when snowfalls are frequent) and drops in summer. It varies from 750 mm in the lowlands to over 1,200 mm in the mountains. Owing to the diverse topography, exposure of slopes and valleys, as well as the presence of a large water body a complex patchwork of microclimates occurs in the catchment that is also reflected in the vegetation.

1.3.4 Vegetation

The landscape heterogeneity of the Prespa watershed and its location at a transitional climate zone gave rise to an assemblage of central European, Mediterranean and Balkan endemic plants (Polunin, 1980). With an estimated total of 1,500 plant species (cf. Society for the Protection of Prespa, 2011), the study area contains approximately 6% of the 25,000 plant species encountered in the entire Mediterranean Basin (cf. Myers et al., 2000).

A considerable area of Prespa's wetlands and adjacent mountain biotopes are protected under international treaties (Ramsar, Natura 2000) as well as national legislation (**Table 1.1**). In 2000, the prime ministers of the three countries established the transboundary Prespa Park and in 2010 signed an agreement committing to the conservation and sustainable development of the area.

Despite the remote character of the area and early conservation efforts, human impact on Prespa landscapes under protection is still visible today (e.g. treeline depression due to logging or grazing). Nevertheless, the diversity of communities and species encompassed in the aquatic, littoral and terrestrial habitats are remarkable with regard to the size of the catchment.

Table 1.1: Designated protected areas within the Prespa catchment (data from Society for the Protection of Prespa).

Country	Name	Protected Area (km²)	Year
Albania	Prespa National Park	277	1999
F.Y.R. of Macedonia	Galičica National Park	250	1958
F.Y.R. of Macedonia	Pelister National Park	125	1948
F.Y.R. of Macedonia	Ezerani Reserve	21	1996
Greece	Prespa National Park	257(327)	1974(2009)

In the lowlands, extensive reed beds, sedge- and grasslands comprising Poaceae (e.g. *Phragmites australis*), Typhaceae, Cyperaceae, and Juncaceae dominate the littoral zone. Outside of protected areas, the plains are covered with apple tree orchards in the north and bean plantations in the south. Thermophilous species such as *Phillyrea latifolia*, *Fraxinus ornus*, *Pistacia terebinthus*, *Juniperus excelsa*, *J. foetidissima*, *Buxus sempervirens*, *Quercus trojana*, *Carpinus orientalis*, *Ostrya carpinifolia* are encountered at lower elevations mostly on limestone hills in the east and south. They form transitional communities (pseudomaquis) comprising evergreen and deciduous species and their distribution depends on factors such as slope exposure and soil moisture content. Mixed deciduous oak forests (dominated by *Q. cerris*, *Q. frainetto*, *Q. pubesens*, *Q. petraea*) grow below 1,600 m a.s.l., while montane mesophilous forests (dominated by *Fagus sylvatica* in association with *Carpinus betulus*, *Corylus colurna* and *Acer obtusatum*) below 1,800 m. Beech forests codominated by *Abies borisii-regis* are encountered below 1,900 m. A characteristic transitional

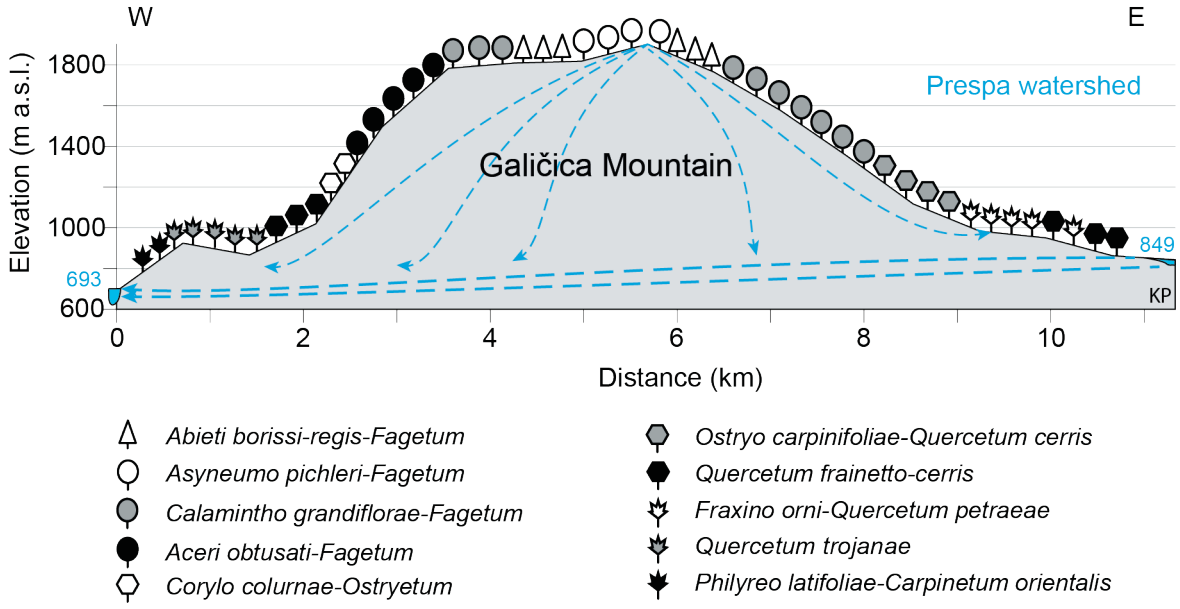

Figure 1.5: Vegetational transect across the Galičica Mountain and schematic underground connection between Lake Prespa and Lake Ohrid (SRTM Data: Jarvis et al., 2008; adapted after Matevski et al., 2011; Popovoska and Benacci, 2007).

plant community dominating the mountainous landscape in the eastern part is the distinctive climax communities of *Pinus peuce,* growing up to an altitude of 2,200 m a.s.l., associated with *Pteridium aquilinum* or *Vaccinium myrtillus* (at higher elevations). Extensive subalpine and alpine meadows occur above the tree-line (Polunin, 1980; Pavlides 1997; Matevski et al., 2011). A characteristic vegetational profile from the western part of the catchment as well as typical forest ecosystems are shown in **Figure 1.5** and **Figure 1.6** respectively.

Figure 1.6: Typical forest ecosystems: *Pinus peuce* forming the treeline with *Vaccinium myrtillus* as dominant understory species on Pelister (a, b), *Fagus sylvatica* with *Abies borisii-regis* forming the treeline on Galičica (c), pure *Fagus sylvatica* stand (d), mixed thermophilous oak-dominated forests on the eastern flank of Galičica Mountain near the village of Stenje (e), *Quercus* cerris stand on Galičica (f). Note the rich herbaceous layer of the oak stand (f) in contrast to the beech one (d). Photos taken during the June 2011 field campaign by the author.

1.3.5 Lake Prespa morphology and hydrology

Lake Prespa is a rather shallow lake (mean depth 14 m) in comparison with Lake Ohrid (mean depth 155 m) despite their similar size (254 km^2 and 358 km^2 respectively). Lake Mikri Prespa has a lake surface of only 53 km^2 and a mean water depth of 4 m (**Table 1.2**). On the Greek side, the Prespa Lakes are connected by a canal ending at a four-sluice gate system with a total extend of 9 m, which lets excess water to overflow from Lake Mikri Prespa into Lake Prespa (Malakou, 2007; Parisopoulos et al., 2009). In addition, Lake Prespa has an underground connection with Lake Ohrid via karst channels (Matzinger et al., 2006; Amataj et al., 2007; **Figure 1.5**).

Table 1.2: Characteristics of the Prespa Lakes (compiled from Zacharias et al., 2002 and Matzinger et al., 2006).

	Lake (Megali) Prespa	Lake Mikri Prespa
Watershed (km^2)	1,000	260
Lake surface (km^2)	254	53
Volume (km^3)	3.6	0.22
Altitude (m a.s.l.)	849	853
Depth max. (m)	55	8.4
Depth mean (m)	14	4.1
Residence time (yrs)	11	3.4
Surface temperature max. (°C)	25	28
pH mean	8.3	8.3
Mixing mechanism	monomictic	dimictic

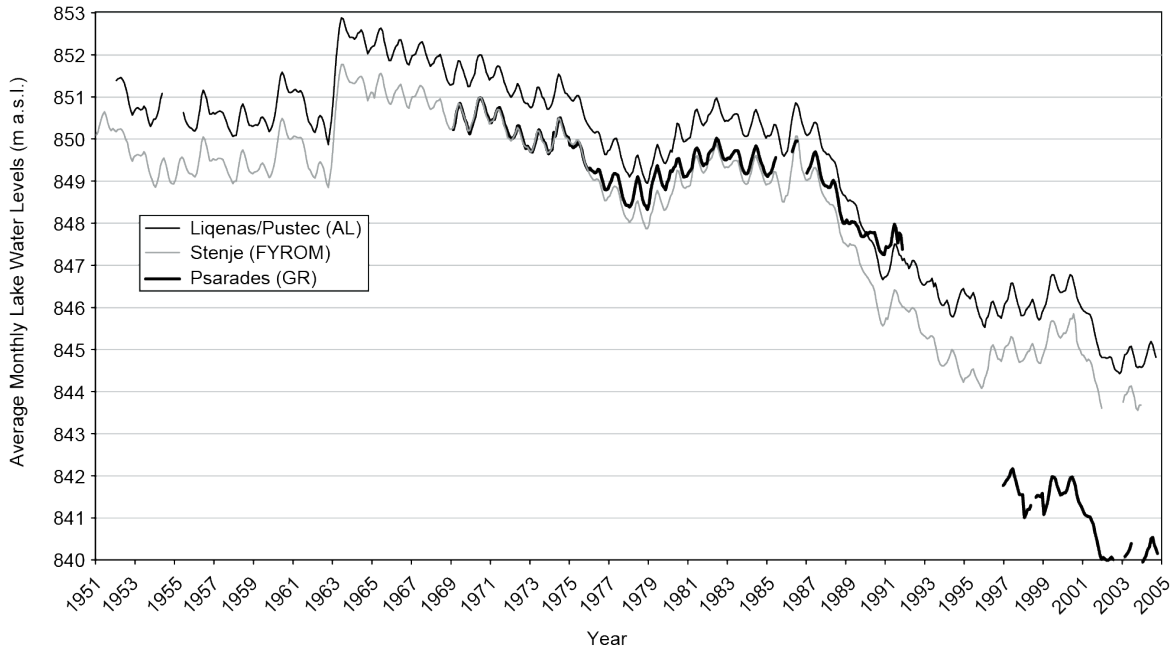

Figure 1.7: Lake-level fluctuations of Lake Prespa (from Strubenhoff and Hoyos, 2005).

In the absence of natural surface outlet, water from Lake Prespa is mostly evaporated (52%), fed through the karst aquifer (46%) to Ohrid springs, and 2% is used for irrigation (Matzinger et al., 2006). Increasing anthropogenic pressure combined with precipitation patterns and the closed nature of the watershed account for the annual lake level change and an estimated residence time of 11 years. The annual high stand occurs in late spring partly due to snowmelt and low stand in autumn and early winter months (Hollis and Stevenson, 1997).

Apart from seasonal fluctuations, lake levels have oscillated historically up to several meters (**Figure 1.7**). Between 1951 and 1963 the water level of Lake Prespa oscillated around a relatively high level of c. 851 m a.s.l (according to the Albanian record). In 1963 the water level reached its maximum stand of c. 853 m a.s.l. and declined till 1979 when it fell below 849 m a.s.l. Between 1979 and 1987 water levels remained above 849 m a.s.l., and between 1987 and 1994 declined steadily reaching a low of c. 846 m a.s.l. After 2000 lake levels dropped further to reach 844.5 m a.s.l. the lowest stand recorded within the period examined. An average water level drop of approximately 6 m is recorded between 1951 and 2005 (**Figure 1.7**).

Stefouli et al. (2011) detected in Landsat images for the period 1988–2010 recurring surface circulation patterns in the form of gyre systems (**Figure 1.8**). Prevailing northern winds during summer months produce counter- and clockwise gyres. Wagner et al. (2012) suggested that surface currents propagating in the water column in concert with geostrophic effects led to the formation of a contourite drift (**Figure 1.8**).

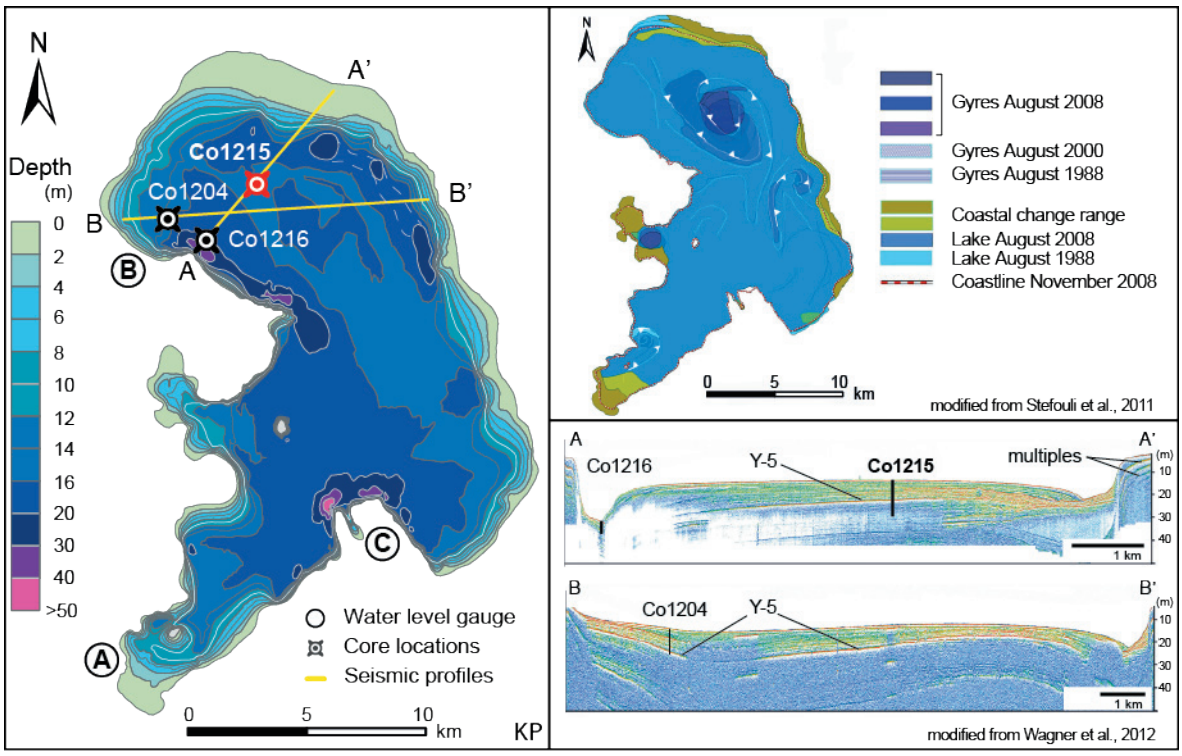

Figure 1.8: Simplified bathymetry of Lake Prespa (based on unpublished data from Andrinopoulos A. for IAEA Project RER/8/008; Stefouli M., personal communication). Locations of water-level gauges: (a) Liqenas/Pustec, (b) Stenje, (c) Psarades. Surface currents and hydroacoustic profiles are also shown.

1.4 State of research

1.4.1 Core lithology and correlation

Core Co1215 with a composite length of 1776 cm is the longest core from Lake Prespa to date and was retrieved from the northern part of the lake in October/November 2009 and June 2011. The coring location displays relatively undisturbed sedimentation, revealed after a shallow hydroacoustic survey (Wagner et al., 2012; **Figure 1.8**). In addition to Co1215 (focus of this study), two shorter sediment cores have already been analyzed with means of sedimentology and geochemistry (**Table 1.3**).

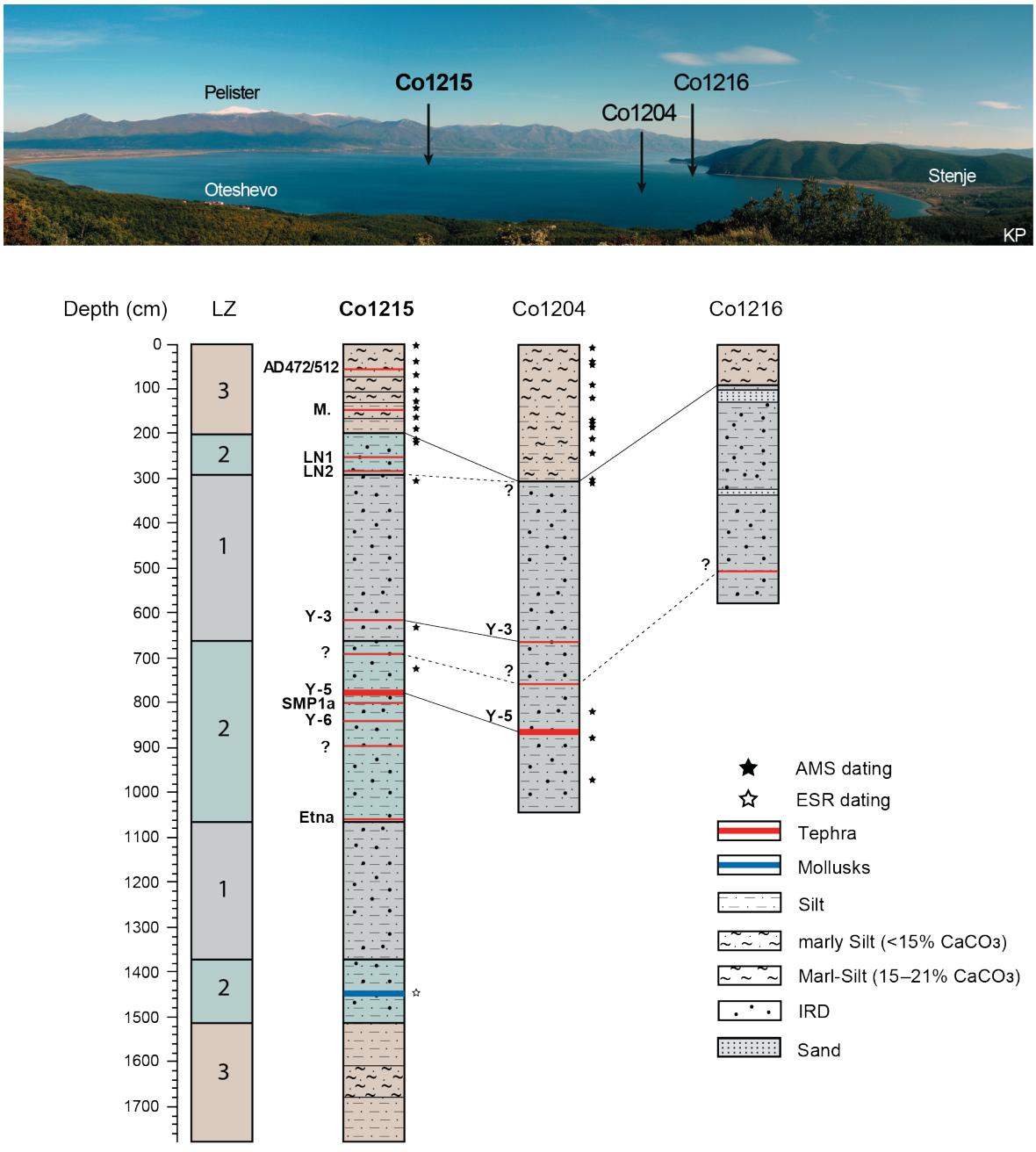

Figure 1.9: Panoramic view of Lake Prespa from the Galičica Mountain. Core locations and landmarks are indicated. Core lithology and correlations (adapted after Böhm, 2012; Wagner et al., 2012).

Table 1.3: Cores retrieved from Lake Prespa.

Core	Coordinates	Composite Length (cm)	Water Depth (m)	Recovery Date
Co1204	40°57'02'' N, 20°55'54'' E	1050	14	October 2007
Co1215	40°57'50'' N, 20°58'41'' E	1575 (1776)	14.5	October/November 2009 (June 2011)
Co1216	40°56'22'' N, 20°56'57'' E	577	32.3	October 2009

Three lithofacies (L3, L2, L1) occur in Co1215 (described in Böhm, 2012; Damaschke et al., 2013), and have been distinguished based on color, grain-size composition and chemistry (**Figure 1.9**). Lithofacies 3 (1776–1516 and 204–0 cm) sediments are characterized by olive-brown colored bioturbated silt, relatively high organic matter and calcium carbonate (calcite) and low to intermediate clastic content. Lithofacies 2 (1516–1380, 1066–662, and 292–204 cm) has gray-olive, non-laminated silts with intermediate organic content, and generally low carbonate content but with distinct TIC (calcite and siderite) and Fe spikes. Sporadic occurrence of sand and gravel was recorded in L2. Lithofacies 1 (1380–1066 and 662–292 cm) sediments are gray, bioturbated, dominated by silt and with very low organic content. Conspicuous TIC (siderite) and (Fe) spikes are present between 1380 and 1066 cm, and an irregular black-greenish lamination associated with black spots and high Fe and Mn (between 662 and 292 cm). Coarse sand and gravel were present intermittently throughout L1.

In Co1204 (described in Leng et al., 2010; Wagner et al., 2010, 2012) sediments between 1050–314 cm are gray, have a low TOC and high K content, and were deposited during the Last Glacial. Distinct Mn and Fe peaks are recorded during this interval which indicate shifts in the redox conditions and were correlated with Heinrich events (Wagner et al., 2010). Sediments between 314–0 cm are characterized by a brownish color, higher organic content and were deposited during the Holocene (for radiocarbon ages from Co1204 see Wagner et al., 2012)

In Co1216 (described in Wagner et al., 2012) sediments between 577–86 cm have a gray color, low TOC and TIC, high K and several Mn and Fe peaks, while between 86–0 cm are brown, have high organic content and low K. Although no reliable age control points exist for this core, Wagner et al. (2012) proposed the correlation of the uppermost 86 cm to the Holocene and between 577–86 to the Last Glacial. The authors interpreted discontinuities in the sedimentation as the result of erosion and redeposition caused by wave action and fluctuating lake levels.

1.5 Chronology of core Co1215

The age model of core Co1215 (1776 cm) is based on accelerator mass spectrometry (AMS) ^{14}C ages (**Table 1.4**), electron spin resonance (ESR) dating (**Table 1.5**), tephrochronology (**Table 1.6**) and cross correlation with the NGRIP ice core record. Aufgebauer et al. (2012), Wagner et al. (2012), Böhm (2012), and Damaschke et al. (2013) discuss the AMS dates obtained and used in the age model, elaborate on the composition and correlation of the identified tephra layers, as well as on the ESR dating of a shell horizon between 1458 and 1463 cm. According to the proposed age model, the base of the sediment sequence can be extrapolated to c. 92 ka cal BP (Damaschke et al., 2013).

Table 1.4: Radiocarbon dating carried out at the AMS facilities of the Federal Institute of Technology (ETH) Zurich (Switzerland). The radiocarbon ages were converted into calendar years (a cal BP) using CALIB 6.1.0 (Stuiver et al., 2012), based on the INTCAL09 calibration curve (Reimer et al., 2009). Sample ETH–40050 was calibrated using the Levin.14c dataset (Levin and Kromer, 2004).

Sample	Depth (cm)	Material	^{13}C (‰)	^{14}C Age (a BP)	Calendar Age (a cal BP [2σ]
ETH–40050	4 – 6	shell (*Dreissena presbensis*)	-0.8	-1190 ± 30	(-15) ± 1
Col1030	42 – 44	plant (*Carex* sp.)	-16.5	715 ± 28	630 ± 64
ETH–40051	74 – 76	plant (*Phragmites australis*)	-27.9	2080 ± 35	2066 ± 80
ETH–40052	74 – 76	bulk organic matter	-26.9	3095 ± 35	3312 ± 73
Col1031	104 – 108	bulk organic matter	-30.2	6003 ± 28	6842 ± 90
ETH–40054	128 – 130	bulk organic matter	-28.3	7055 ± 40	7892 ± 70
ETH–40055	146 – 147	bulk organic matter	-26.8	8205 ± 40	9157 ± 127
ETH–40056	166 – 168	plant (*Phragmites australis*)	-26.2	8755 ± 35	9752 ± 152
ETH–40057	166 – 168	bulk organic matter	-27.8	9090 ± 35	10244 ± 50
ETH–40059	184 – 186	bulk organic matter	-26.5	9840 ± 35	11241 ± 40
ETH–40060	212 – 214	fish remain	-12.5	10837 ± 132	12815 ± 261
ETH–40062	214 – 216	fish remain	-17.1	11466 ± 121	13358 ± 250
ETH–40063	214 – 216	bulk organic matter	-24.3	11005 ± 40	12889 ± 187
Col1032	301 – 303	plant (aquatic)	-5.4	14056 ± 71	17159 ± 301
ETH–40064	633 – 635	plant remains	-28.2	26345 ± 105	31011 ± 202
ETH–40065	728 – 729	plant remains	-28.2	33075 ± 210	37762 ± 808

Table 1.5: ESR dating performed at the Geochronological Laboratory of the Institute of Geography (University of Cologne) and dose rate calculation of internal (shells) and external (bulk) radionuclide content were determined at the by ICP-MS analysis at the Institute of Geology and Mineralogy (University of Cologne), the VKTA Laboratory (Dresden) and the Geochronological Laboratory (University of Cologne).

Sample	Depth (cm)	U (‰) [shells, ICP-MS]	Dose Rate (Gy a^{-1})	Equivalent Dose (Gy)	ESR Age (a cal BP [1σ])
K-5800	1458 – 1463	0.08 ± 0.01	1360 ± 100	100.2 ± 11.2	73900 ± 9900
K-5835a	1470 – 1488	0.06 ± 0.01	1360 ± 100	93.71 ± 2.03	68900 ± 5100
K-5836a	1458 – 1470	0.06 ± 0.01	1360 ± 100	114.41 ± 6.73	84100 ± 7800

Table 1.6: Tephra layers identified in Co1215. Tephra identification and correlation were performed at the Institute of Geology and Mineralogy (University of Cologne) and the Earth Sciences Department of the University of Pisa (Italy).

Sample	Depth (cm)	Correlated to	Calendar Age (a cal BP)	Age Reference
PT0915–1	55.4 – 55.6	AD 472/512	1478/1438	Santacroce et al., 2008
PT0915–2	155.6 – 156.2	Mercato	8540 ± 50	Zanchetta et al., 2011
PT0915–3	265 – 267	LN1	14697 ± 519	Siani et al., 2004
PT0915–4	287 – 289	LN2	15551 ± 621	Siani et al., 2004
PT0915–5	616.8 – 617.8	Y–3	30500 ± 500	Zanchetta et al., 2008
PT0915–6	690 – 693.2	—	—	—
PT0915–7	764.5 – 783.8	Y–5	39280 ± 110	De Vivo et al., 2001
PT0915–8	842 – 844	SMP1-a	45000 ± 6000	Di Vito et al., 2008
PT0915–9	854 – 856	Y–6	~45000	Keller et al., 1978
PT0915–10	900.8 – 901	—	—	—
PT0915–11	1078.6 – 1079.6	Etna	—	—

II Climate and environmental change in the Balkans over the last 17 ka recorded in sediments from Lake Prespa (Albania/F.Y.R. of Macedonia/Greece)*

Abstract

This paper presents sedimentological, geochemical, and biological data from Lake Prespa (Albania/ Former Yugoslav Republic of Macedonia/Greece). The 320 cm core sequence (Co1215) covers the last 17 ka cal BP and reveals significant change in climate and environmental conditions on a local and regional scale. The sediment record suggests typical stadial conditions from 17.1 to 15.7 ka cal BP, documented through low lake productivity, well-mixed conditions, and cold-resistant steppe catchment vegetation. Warming is indicated from 15.7 ka cal BP with slightly increased in-lake productivity, gradual expansion of trees, and decreasing erosion through disappearance of local ice caps. Between 14.5 and 11.5 ka cal BP relatively stable hydrological conditions are documented. The maximum in tree taxa percentages during the Bølling/Allerød interstadial (14.5-13.2 ka cal BP) indicates increased temperatures and moisture availability, whereas the increase of cold-resistant open steppe vegetation taxa percentages during the Younger Dryas (13.2-11.5 ka cal BP) is coupled with distinct colder and drier conditions. The Holocene sequence from 11.5 ka cal BP indicates ice-free winters, stratification of the water column, a relatively high lake trophic level and dense vegetation cover over the catchment. A strong climate related impact on the limnology and physical parameters in Lake Prespa is documented around 8.2 ka through a significant decrease in productivity, enhanced mixing, strong decomposition and soil erosion, and a coeval expansion of herbs implying cool and dry climate conditions. Intensive human activity in the catchment is indicated from around 1.9 ka cal BP. This multiproxy approach improves our understanding of short- and long-term climate fluctuations in this area and their impact on catchment dynamics, limnology, hydrology, and vegetation.

Keywords: Lake Prespa, Mediterranean, paleolimnology, Late Glacial, Holocene, climate change

* This chapter is based on Aufgebauer A., Panagiotopoulos K., Wagner B., Schäbitz F., Viehberg F. A., Vogel H., Zanchetta G., Sulpizio R., Leng M. J., Damaschke M., 2012, Climate and environmental change in the Balkans over the last 17 ka recorded in sediments from Lake Prespa (Albania/F.Y.R. of Macedonia/Greece), Quaternary International 274, 122-135, dx.doi.org/10.1016/j.quaint.2012.02.015.

2.1 Introduction

Lake Prespa is one of the three largest lakes on the Balkan Peninsula (**Figure 2.1** a) and is, with a supposed age of more than three million years (Stankovic, 1960; Levkov et al., 2007), one of the oldest lakes in Europe. As Lake Prespa has a relatively small volume for its large surface area, it supposedly reacts sensitively to climatic and environmental change. The lake drains into Lake Ohrid via karst aquifers (Popovska and Bonacci, 2007). Both lakes Prespa and Ohrid are known for high degrees of endemism and form unique ecosystems within the Balkan region (Stankovic, 1960; Levkov et al., 2007; Albrecht and Wilke, 2008). Several paleolimnological studies exist from Lake Ohrid (e.g. Belmecheri et al., 2009; Wagner et al., 2009, 2010; Lézine et al., 2010; Vogel et al., 2010a) and also from Lake Maliq (Denèfle et al., 2000; Bordon et al., 2009; Fouache et al., 2010), which is drained today and located only a few kilometers to the south of lakes Ohrid and Prespa. The records from Lake Ohrid span up to 140 ka, and those from Lake Maliq span the last 16 ka cal BP. Only one longer sediment record has been described from Lake Prespa. This record originates from the northwestern lateral part of the lake and covers the last c. 50 ka (Leng et al., 2010; Wagner et al., 2010).

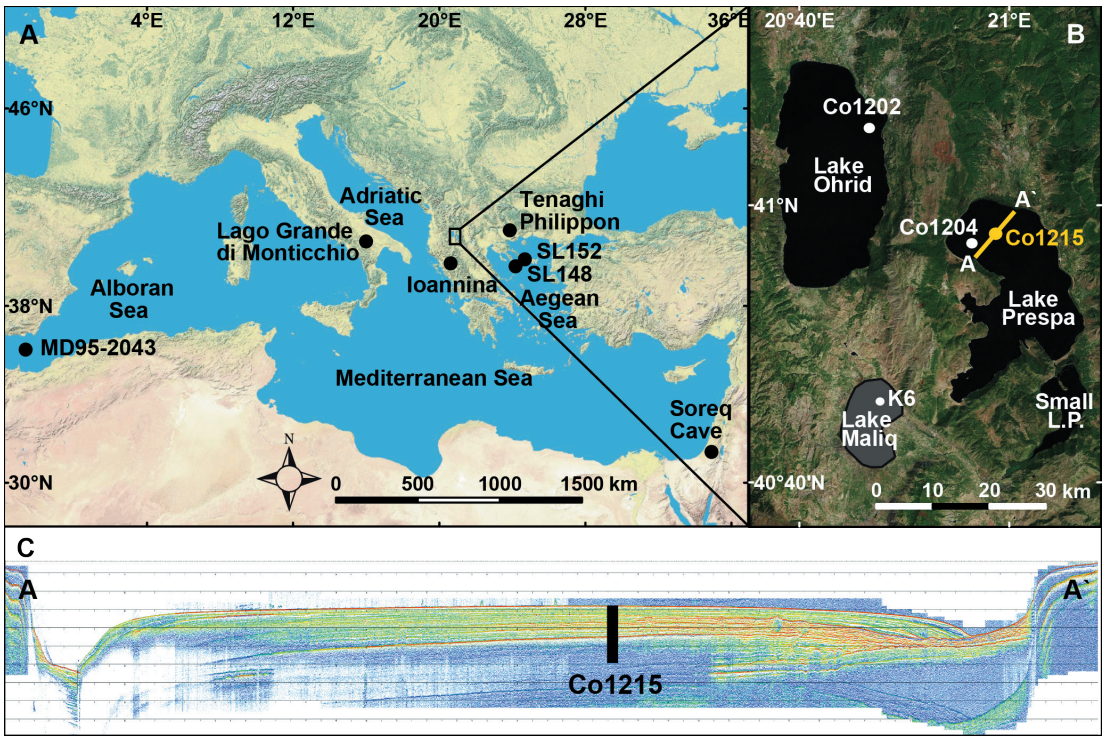

Figure 2.1: Map of the Mediterranean region (a) showing the location of lakes Prespa, Ohrid and Maliq (gray rectangle) on the Balkan Peninsula and palaeoenvironmental reconstruction key sites referred to in the text (black dots): MD95-2043 (Cacho et al., 1999), Lago Grande di Monticchio (Allen et al., 1999, 2002), Ioannina (Tzedakis et al., 2002; Lawson et al., 2004), Tenaghi Philippon (Kotthoff et al., 2008; Müller et al., 2011), SL148 and SL152 (Kotthoff et al., 2008, 2011), Soreq Cave (Bar-Matthews et al., 1999, 2003). (b) Detailed map of lakes Prespa, Ohrid and Maliq showing coring location Co1215 (yellow dot) at Lake Prespa with seismic profile (A-A') across the coring location. (c) and other sites nearby (white dots) referred to in the text: Lake Prespa Co1204 (Leng et al., 2010; Wagner et al., 2010), Lake Ohrid Co1202 (Vogel et al., 2010a, 2010b; Wagner et al., 2010) and Lake Maliq (today dried up) K6 (Bordon et al., 2009).

The Pleistocene to Holocene transition in lakes Ohrid, Maliq and Prespa can hardly be compared. This is partly because some of the cores (Co1204/Lake Prespa, Wagner et al., 2010; Lz1120/Lake Ohrid, Wagner et al., 2009) show at least some indication for a hiatus at the transition and/or because the start of full interglacial conditions seems to be delayed (Co1202/Lake Ohrid, Vogel et al., 2010a) compared to ice core records from Greenland (e.g. Grootes et al., 1993; Alley, 2000), marine records (Cacho et al., 1999, 2001; Ehrmann et al., 2007; Kotthoff et al., 2011), or other terrestrial records around the Mediterranean (Allen et al., 1999, 2002; Bar-Matthews et al., 1999, 2003; Tzedakis et al., 2002; Lawson et al., 2004, 2005; Brauer et al., 2007; Müller et al., 2011).

The focus of this study is to reconstruct the climatic and environmental history of the Balkan region during the Late Glacial and Holocene on a sub-millennial scale. For this purpose, the Co1215 sediment record from the northern part of Lake Prespa was investigated using sedimentological, geochemical and biological methods. The results of this study enhance understanding of changes in lake productivity, ecology, hydrology, and catchment dynamics and thus improve the knowledge of regional climatic, environmental, and anthropogenic change.

2.2 Regional setting

Lake Prespa (40°46'-41°00' N, 20°54'-21°07' E) is located at an altitude of 849 m above sea level (a.s.l.), and is shared by the Republics of Albania, F.Y.R. of Macedonia and Greece (**Figure 2.1**). The catchment (c. 1300 km^2, Matzinger et al., 2006) of Lake Prespa is characterized by karstified Triassic limestones in the west and southwest and by Paleozoic and Mesozoic metasediments and magmatites in the north, east, and southeast (Geological Maps of Yugoslavia, 1977).

Lake Prespa has a surface area of 254 km^2, a maximum water depth of 48 m, a mean water depth of 14 m, and a volume of 3.6 km^3 (Matzinger et al., 2006). The lake is fed by river runoff from several small streams (56%), direct precipitation on its surface (35%), and by inflow from Small Lake Prespa (9%), which is located 1 km to the south and connected to Lake Prespa by a man-made channel. Lake Prespa has no surface outflow. Water loss derives through evaporation (52%), irrigation (2%), and underground outflow (46%). A large quantity of water is discharged through karst channels into Lake Ohrid, which is located at 693 m a.s.l. (Matzinger et al., 2006; Popovska and Bonacci, 2007). A lake level decrease of nearly 8 m was documented for Lake Prespa for the period between 1963 and 1995 and might have resulted from reduced precipitation and intensified water irrigation for agriculture (Popovska and Bonacci, 2007). An additional lowering of at least 1 m between 1995 and 2009 (Wagner et al., 2010) has been compensated by a subsequent lake level increase of c. 2 m (data from a field campaign in 2011). The isotope composition of modern water from Lake Prespa shows that the lake is highly susceptible to moisture balance and seasonality (Leng et al., 2010).

The climate at Lake Prespa is today influenced by Mediterranean climate to the south and continental climate to the north. Average temperatures range from + 1 °C in January to + 22°C in July. The precipitation is highest in winter and strongly controlled by the local morphology. Annual precipitation ranges from 750 mm in the lowlands of Prespa valley to over 1200 mm on

the mountains with maximum altitudes of 2420 m a.s.l. The highest water levels in Lake Prespa are recorded during May and June due to snowmelt (Hollis and Stevenson, 1997).

The location of Lake Prespa at a transitional climatic zone leads to a vegetation, which is composed by a mixture of Balkan endemic, central European, and Mediterranean species (Polunin, 1980). The relatively large size and diversity of the catchment area, which includes several national parks, does not allow classification in a single zonation scheme for the entire area. The major altitudinal formations present in the greater area are the mixed deciduous oak forests (with *Quercus trojana*) up to 1200 m a.s.l., the montane deciduous forests (mainly beech forests) up to 1800 m a.s.l., the montane conifer forests (including the Balkan endemic *Pinus peuce*) up to 2000 m a.s.l., and the subalpine and alpine meadows above the treeline.

2.3 Material and methods

2.3.1 Core recovery

Core Co1215 (40˚57'50" N, 20˚58'41" E) was recovered in autumn 2009 from the central northern part of Lake Prespa. The coring site was selected on the basis of a 3.5 kHz hydroacoustic survey, which indicated a water depth of 14.5 m and an acoustically well stratified sediment succession in the close surrounding (**Figure 2.1** b, c; Wagner et al., 2012). Coring was conducted from a floating platform using a gravity corer for undisturbed surface sediments and a 3-m-long percussion piston corer (UWITEC Co. Austria) for deeper sediments. After recovery, the overlapping 3-m-long sediment cores were cut into segments of up to 1 m length and stored in the dark at 4 ˚C until further processing.

2.3.2 Analytical work

The analytical work presented here focuses on the uppermost 320 cm of core Co1215, which comprise the Late Pleistocene and Holocene sediment succession. Individual core segments were split into two halves in the laboratory. Subsequently, one core half was photographed, described, and used for high-resolution X-ray fluorescence (XRF) scanning. The XRF scanner (ITRAX core scanner; COX Ltd., Sweden) was equipped with a Mo-tube set to 30 kV and 30 mA, and a Si-drift chamber detector. XRF scanning was per- formed at a resolution of 2 mm and an analysis time of 10 s per measurement. The obtained count rates for individual elements can be used as semi-quantitative estimates of their relative concentrations. Only a selection of elemental data from the XRF scanning is presented here.

The other core half was continuously sampled at 2 cm intervals. Prior to biogeochemical analyses, aliquots of the freeze-dried and homogenized subsamples were ground to a particle size <63 mm using an agate ball mill. Total carbon (TC) and total inorganic carbon (TIC) concentrations were determined with a DIMATOC 200 (DIMATEC Co.). Total organic carbon (TOC) was calculated from the difference between TC and TIC. The identification of carbonate species was done using X-Ray Diffraction (XRD) analysis, on a Bruker D8 Advance powder diffractometer with Da Vinci, over the scan range 4-90˚ 2-theta. The carbonate match (calcite and substituted

siderite) was performed using Bruker Diffrac Plus EVA software interfaced with the ICDD PDF-4+ Scholar database. The substituted siderite structure [$(Fe,Mg,Ca)CO_3$] was published by Heiss (1988). Total nitrogen (TN) and total sulfur (TS) were measured with a Vario Micro Cube combustion CNS elemental analyzer (VARIO Co.).

For grain-size analysis, 39 raw sediment samples with a dry weight of 1 g each were selected at 6-10 cm intervals. Carbonate and iron sulfides, organic matter, and biogenic silica were removed from the subsamples using 10% HCl, 30% H_2O_2 and NaOH, respectively. Grain-size analysis on the remaining, presumably allochthonous clastic fraction was carried out after removing the >630 mm fraction by sieving and using a Micromeritics Saturn DigiSizer 5200 laser particle analyzer. The volume percentages (vol %) of the individual grain-size fractions were calculated from the average values of 3 runs.

Pollen analysis was carried out on 51 samples taken at 2-8 cm intervals. Approximately 1 g of dried raw sediment was treated with HF and acetolysis (Fægri et al., 2000). Identification of pollen and other palynomorphs was performed with relevant keys and atlases (Punt and Clarke, 1980; Moore et al., 1991; Punt and Blackmore, 1991; Reille, 1998, 1999; Beug, 2004), as well as the reference collection of the Laboratory of Palynology at the Seminar of Geography and Education, University of Cologne. The relative percentages of the presented taxa and groups are based upon the sum of terrestrial pollen (excluding aquatics, spores and algae). A minimum of 500 pollen grains was counted per sample.

Ostracod analyses are based on 38 subsamples, which were taken at 4-10 cm intervals and had a dry weight of 2-6 g each. The material was wet-sieved and the >125 mm fraction subsequently freeze-dried. All ostracod valves were picked, enumerated, and identified under a dissecting microscope. The results were standardized to 5 g dry weights in the diagram. Identification and taxonomy follow Klie (1939a, 1939b, 1942), Petkovski (1960), Meisch (2000), and Petkovski et al. (2002).

Radiocarbon dating and tephrostratigraphy were used to establish an age-depth model for the sediment sequence Co1215. Material for radiocarbon dating was selected from eleven horizons and comprises plant macrofossils, fish bones, shell remains, and bulk sediment, if no macrofossils were available. All samples were measured by accelerator mass spectrometry (AMS) at the ETH Laboratory of Ion Beam Physics in Zurich, Switzerland (Table 1). The radiocarbon ages of all samples were calibrated into calendar years before present (a cal BP) using the INTCAL09 calibration curve (Reimer et al., 2009), except for sample ETH-40050 which used the Levin ^{14}C dataset (Levin and Kromer, 2004).

Tephrostratigraphic work was mainly carried out at the Dipartimento di Scienze della Terra, University of Pisa, Italy. Potential horizons containing tephra were identified from macroscopic inspection of the sediment successions and/or from significant Sr, K, and Rb abundances from XRF scanning. All samples were analyzed following methods described elsewhere (cf. Sulpizio et al., 2010; Vogel et al., 2010b). After correlation of the tephra from core Co1215 with known tephra, an age-depth model was established based on linear interpolation between the chronological tie points and using calendar ages (**Figure 2.2**).

2.4 Results

2.4.1 Lithology and biogeochemistry

The 320-cm-long sediment sequence is subdivided in three lithozones (LZ-1 to LZ-3; **Figure 2.3**). LZ-1 (320-292 cm; **Figure 2.3**) is light to medium gray. The grain-size composition is dominated by silt and clay, but coarse sand and gravel grains occur sporadically. In general, the sediment in LZ-1 appears homogeneous, lacking sedimentary structures, except for an irregular lamination consisting of dark grayish to black spots with peaks in Fe and Mn between 320 and 317 cm depth. Furthermore, a distinct Fe/Ti peak and a vivianite concretion (6 mm in diameter) occur at 319 cm depth (**Figure 2.3**). K is relatively high throughout LZ-1. Carbonate is mostly negligible, and low TOC and TS suggest minimal organic matter.

LZ-2 (292-204 cm; **Figure 2.3**) is medium gray to light brown. The grain-size composition is dominated by silt and fine sand, but coarse sand and gravel occur sporadically. In general, the sediment in LZ-2 appear homogeneous, however, a subtle change in clastic and organic matter composition allows a sub-division of this lithozone: LZ-2a (292-265 cm) is characterized by a slight increase in TOC and C/N, the absence of TIC, a distinct decrease in K, and a slight increase of Fe/Ti. LZ-2b (265-204 cm) is characterized by a TOC content of c. 2%, C/N of about 6-7, a slight peak in TIC, stable K, and slightly higher Fe/Ti. A vivianite concretion (2 cm in diameter) was found between 254 and 256 cm. TS shows a distinct increase, but overall remains <0.3%. The increase of TS is likely caused by finely dispersed iron sulfides, which appear as dark grayish to black spots and irregular lamination between 232 and 218 cm depth and as fine layer (1 mm) at 236 cm.

LZ-3 (204-0 cm; **Figure 2.3**) sediments are brown to gray. The grain-size composition is dominated by silt, the amount of sand decreases toward the top of the core. Coarse sand and gravel grains are absent. Although the sediment appears homogeneous, distinct changes in the sediment composition imply a sub-division into five sub-lithozones (LZ-3a-e; **Figure 2.3**). LZ-3a (204-164 cm) is characterized by relatively high fine sand content, a distinct increase in TOC, TS, and Fe/Ti, and a distinct decrease in K. The TIC content is low. LZ-3b (164-148 cm) has a similar grain-size composition, but high TOC, TS, and TIC content, and Fe/Ti maxima. K shows a distinct minimum, except of a peak at 156 cm. LZ-3c (148-130 cm) has minima in sand content, TOC, TS, TIC, and Fe/Ti and a maximum in K. LZ-3d (130-70 cm) has a similar grain-size composition as LZ-3a, but high and fluctuating TOC, TS, C/N, and TIC, a broad and fluctuating maximum in Fe/Ti, and lowest values in K. LZ-3e (70-0 cm) is characterized by high silt and clay and low sand content. TOC, TS, and Fe/Ti, show fluctuations with a maximum between 48 and 35 cm and relatively low values below and above. TIC and K also show fluctuations with distinct minima occurring between 48 and 35 cm, and also close to the sediment surface. A distinct peak in K is centered at 56 cm.

2.4.2 Pollen record

The major pollen zones (PZ-I-III; **Figure 2.4**) in the Co1215 sediment sequence reflect the main phases of vegetation development. The groups included here (**Figure 2.4**) contain the following

taxa: the genus *Quercus* comprises deciduous and evergreen species; the group of mixed deciduous (temperate) trees includes *Carpinus*, *Ostrya*, *Corylus*, *Fraxinus*, *Tilia*, *Alnus*, *Ulmus*, *Fagus*, and *Acer*. The Mediterranean group consists of *Phillyrea*, *Olea*, and *Pistacia*, and the anthropogenic group of Cerealia, *Juglans*, *Vitis vinifera*, and *Plantago lanceolata*. Given the size of the catchment and its surface area, the source area of the pollen of Lake Prespa can be assumed to be mainly of regional origin (cf. Jacobson and Bradshaw, 1981; Davis, 2000).

PZ-I (320-204 cm; **Figure 2.4**) is characterized by distinct changes between *Pinus* and herbs (mainly *Artemisia* and Chenopodiaceae), which dominate the pollen assemblage with up to 56% and up to 60%, respectively. For instance, a decrease of herbs at 295 cm correlates with an increase of *Pinus*, and an increase of herbs around 240 cm corresponds with a decrease of *Pinus*. *Abies* shows slightly increased values between 271 and 242 cm and from 213 cm toward the top of PZ-I. Throughout this zone, *Quercus* and other deciduous trees increase to values of 30% and 5%, respectively. Mediterranean and anthropogenic taxa occur sporadically with very low percentages.

PZ-II (204-70 cm; **Figure 2.4**) is characterized by the highest percentages of trees. The tree assemblage shows, however, variations with overall increasing *Pinus* and temperate trees and with broad maxima of *Quercus* between 204 and 148 cm depth and *Abies* between 172 and 112 cm depth. Herbs decrease from 33% at the bottom of this zone to 10% at the top. A peak of *Artemisia* around 138 cm is correlated with a minimum in arboreal taxa. Mediterranean taxa can be observed at low percentages from 180 cm toward the top. Anthropogenic taxa are negligible throughout this zone.

PZ-III (70-0 cm; **Figure 2.4**) is characterized by an overall decrease of tree and an increase in herb taxa percentages. The arboreal component consists mainly of *Quercus* and other temperate tree taxa with a distinct peak at 50 cm (41% and 32%, respectively). Mediterranean and anthropogenic taxa have values of up to 6% and 10%.

2.4.3 Ostracod record

The ostracod record in Co1215 (**Figure 2.4**) is based on the number of valves in the studied sediment samples. Only 13 samples yielded ostracod valves. The identified ostracod species belong to six benthic species: *Amnicythere* (*Leptocythere*) *karamani*, *A*. (*L*.) *prespensis*, *Candona hartmanni*, *C*. cf. *vidua*, *Paralimnocythere alata*, and *Paralimnocythere karamani*. In LZ-1 and 3a, there are no or only a few ostracod valves preserved, such as the single occurrence of valves of *Amnicythere karamani* and *Candona hartmanni* specimens at 224 cm and from 194 to 180 cm. LZ-3b and LZ-3c are dominated by *P. karamani* and accompanied by *A. karamani*. One valve of *Candona* cf. *vidua* is recorded at 144 cm depth. LZ-3d contains no ostracods. LZ-3e is characterized by the sporadic presence of a few ostracods of *P. karamani* and *Candona* cf. *vidua* from 70 to 40 cm, and the presence of *A. karamani*, *Amnicythere prespensis*, and *Candona* cf. *vidua*, complemented by few valves of *P. alata* and *C. hartmanni* from 40 to 0 cm.

The ostracods from Lake Prespa represent almost exclusively endemic species, which differ from those found in Lake Ohrid (cf. Belmecheri et al., 2010) and are poorly known with respect to

their specific ecological requirements. Therefore, an ecological interpretation of the Lake Prespa ostracod record is mostly restricted to changes in diversity and abundance. The adult ostracod valves were grouped in orders of *Cypridoidea* (*C. hartmanni*, *C.* cf. *vidua* and *Cypria lacustris*) and *Cytheroidea* (*P. karamani*, *P. alata* and *A. karamani*).

2.4.4 Chronology

The chronology of the uppermost 320 cm of core Co1215 is based on radiocarbon dating (**Table 2.1**) and tephrostratigraphy (**Table 2.2** and **Table 2.3**). The radiocarbon ages should be treated with caution, since reservoir and/or hard-water effects can bias the real ages. Bulk organic carbon from Lake Ohrid is known to indicate ages, which are up to c. 1500 years too old (Wagner et al., 2008; Vogel et al., 2010b). A potential source of old carbon could be dissolved bicarbonate from Triassic limestone in the catchment. Today, a relatively short residence time of eleven years and the warm monomictic character of Lake Prespa (Matzinger et al., 2006) should result in good exchange of carbon with the atmosphere and a low reservoir effect (cf. Cohen, 2003).

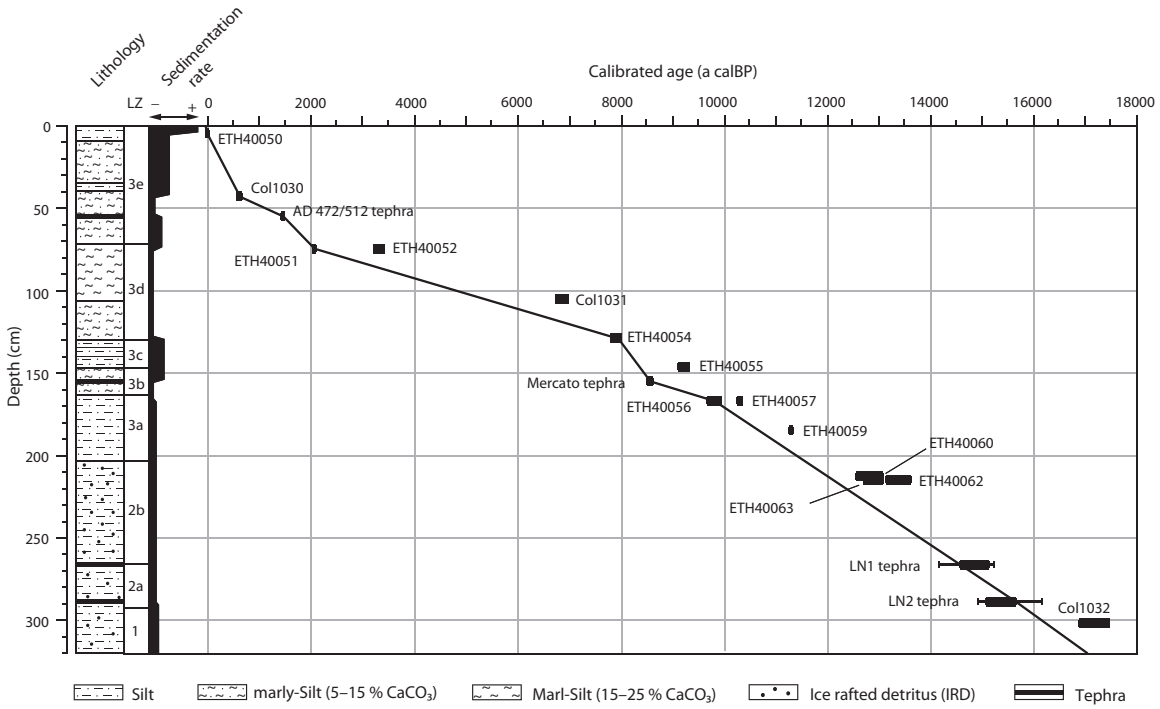

Figure 2.2: Age-depth model for core Co1215 (320-0 cm depth) based on radiocarbon dating and tephrostratigraphy. The calibrated ages of tephras LN1 and LN2 are given in 1σ (thick line) and 2σ (thin line) ranges. Reliable chronological tie points were interpolated on a linear basis. The lithology, lithozones (LZ) and the sedimentation rate are also indicated.

An estimate of how much the radiocarbon ages are biased in the past is given by parallel dating of bulk sediment and macrofossils in two horizons. The plant macrofossil sample (ETH-40051) and the bulk organic carbon sample (ETH-40052) at 74-76 cm depth yield a difference of 1015 years. The difference of the plant macrofossil sample (ETH-40056) and the bulk organic carbon

sample (ETH40057) from 166 to 168 cm depth is only 235 years. The large discrepancy between these offsets indicates that the environmental conditions and hard-water and/or reservoir effects have not been constant over time. Therefore, the bulk organic carbon samples are regarded as providing only maximum ages. The shell fragment of *Dreissena presbensis* (sample ETH-40050) from 4 to 6 cm depth is calibrated to -15 ± 1 ca BP and is presumed to provide a reliable age. Furthermore, the ages of the macrofossil remains of *Carex* sp. from 42 to 44 cm depth (sample Col1030) and *Phragmites australis* from 74 to 76 cm depth (sample ETH-40051) are presumed to be reliable, because these plants are semi-aquatic macrophytes, which assimilate mainly atmospheric CO_2 through photosynthesis. The lowermost sample used for radiocarbon dating is from 301 to 303 cm depth and derives from an aquatic plant. This sample (Col1032) indicates probably an over-estimated age, as aquatic plants assimilate HCO_3^- from the water column and thus potentially suggests a significant hard-water and/or reservoir effect. The fish remains (ETH-40060 and ETH-40062) from 212 to 216 cm depth probably provide also an over-estimated age due to hard-water and/or reservoir effect, as ETH-40062 with an age of 13,358 ± 250 cal BP is distinctly older than the bulk organic carbon sample ETH-40063 (12,889 ± 187 cal BP) from the same horizon. The only bulk organic carbon sample (ETH-40054), which probably provides a reliable age is from 128 to 130 cm depth and has an age of 7892 ± 70 cal BP. This depth in core Co1215 is characterized by a significant increase of TIC (**Figure 2.3**), which can be correlated with a similar increase in another core (Co1204, Wagner et al., 2010) from Lake Prespa. A terrestrial macrofossil from this horizon in core Co1204 provided an age of 7800 ± 50 cal BP.

Table 2.1: AMS dates and $\delta^{13}C$ from Lake Prespa core Co1215, which were measured at the ETH Laboratory of Ion Beam Physics in Zurich, Switzerland. Depths, materials chosen as well as radiocarbon ages and calendar ages are given. The radiocarbon ages of all samples were calibrated into calendar years before present (a cal BP) using the INTCAL09 calibration curve (Reimer et al., 2009), except of sample ETH-40050, which was calibrated with the Levin.14c dataset (Levin and Kromer, 2004).

Sample	Corr. Depth (cm)	Material	$\delta^{13}C$ (‰)	^{14}C Age (a BP)	Calendar age (a calBP [2σ])
ETH-40050	0 - 6	shell (*Dreissena presbensis*)	-0.8 ± 1.1	–1190 ± 30	(–15) ± 1
Col1030	42 - 44	plant (*Carex* sp.)	-16.5 ± 0.1	715 ± 28	630 ± 64
ETH-40051	74 - 76	plant (*Phragmites australis*)	-27.9 ± 1.1	2080 ± 35	2066 ± 80
ETH-40052	74 - 76	bulk organic matter	-26.9 ± 1.1	3095 ± 35	3312 ± 73
Col1031	104 - 108	bulk organic matter	-30.2 ± 0.1	6003 ± 28	6842 ± 90
ETH-40054	128 - 130	bulk organic matter	-28.3 ± 1.1	7055 ± 40	7892 ± 70
ETH-40055	146 - 147	bulk organic matter	-26.8 ± 1.1	8205 ± 40	9157 ± 127
ETH-40056	166 - 168	plant (*Phragmites australis*)	-26.2 ± 1.1	8755 ± 35	9752 ± 152
ETH-40057	166 - 168	bulk organic matter	-27.8 ± 1.1	9090 ± 35	10244 ± 50
ETH-40059	184 - 186	bulk organic matter	-26.5 ± 1.1	9840 ± 35	11241 ± 40
ETH-40060	212 - 214	fish remain	-12.5 ± 0.0	10837 ± 132	12815 ± 261
ETH-40062	214 - 216	fish remain	-17.1 ± 0.0	11466 ± 121	13358 ± 250
ETH-40063	214 - 216	bulk organic matter	-24.3 ± 1.1	11005 ± 40	12889 ± 187
Col1032	301 - 303	plant (aquatic)	-5.4 ± 0.1	14056 ± 71	17159 ± 301

In addition to the radiocarbon ages, four tephra were identified and used for the establishment of the age-depth model. The tephra have been labeled according to their origin (PT for Prespa Tephra), recovery year (09 for 2009) and last two identification numbers of the core Co1215. Tephra PT0915-1 (55.4-55.6 cm) and PT0915-2 (155.6-156.2 cm) were fairly easy to correlate to distinctive eruptions due to characteristic geochemical compositions (**Table 2.2**) and their stratigraphic position. PT0915-1 shows mainly foiditic to tephriphonolitic composition and corresponds with the AD 472 (1478 cal BP) and/or AD 512 (1438 cal BP) eruptions of Somma-Vesuvius (**Table 2.3**; Rosi and Santacroce, 1983; Sulpizio et al., 2005; Santacroce et al., 2008). The composition of these two eruptions is relatively similar, probably because they evolved from the same magma chamber over a short time interval (Santacroce et al., 2008; Vogel et al., 2010b). PT0915-2 shows homogeneous phonolitic composition and correlates with the Mercato eruption of Somma-Vesuvius (**Table 2.3**; Santacroce, 1987; Santacroce et al., 2008) dated to 8540 ± 50 cal BP (Zanchetta et al., 2011). Both tephras have also been found in other Balkan lakes (Sulpizio et al., 2009, 2010; Vogel et al., 2010b).

Table 2.2: Major element compositions of tephras identified in core Co1215.

Sample	depth (cm)	Shard	SiO_2	TiO_2	Al_2O_3	FeO_{tot}	MnO	MgO	CaO	Na_2O	K_2O	P_2O_5	ClO	Total alk.	Alk. ratio
PT0915-1	55.4-55.6	Mean	48.61	0.95	20.69	6.85	0.19	2.00	8.43	4.72	6.33	0.20	1.04	11.05	1.38
		SD	1.5	0.18	1.04	0.82	0.09	0.42	1.41	0.53	1.48	0.12	0.11	1.23	0.49
PT0915-2	155.6-156.2	Mean	58.34	0.18	21.59	1.92	0.15	0.24	1.97	7.93	6.85	0.09	0.73	14.79	0.86
		SD	0.31	0.05	0.40	0.12	0.07	0.10	0.44	0.26	0.19	0.19	0.06	0.34	0.03
PT0915-3	265-267	Mean	61.33	0.43	18.98	2.86	0.14	0.55	2.17	4.36	8.62	0.00	0.55	12.98	1.99
		SD	0.31	0.11	0.13	0.15	0.08	0.07	0.14	0.31	0.54	0.00	0.03	0.45	0.22
PT0915-4	287-289	Mean	61.07	0.45	19.08	2.83	0.17	0.54	2.19	4.22	8.87	0.00	0.56	13.09	2.11
		SD	0.61	0.10	0.69	0.15	0.09	0.08	0.1	0.23	0.25	0.00	0.05	0.36	0.12

Table 2.3: Geochemical data of correlated tephra layers.

Tephra	Shard	SiO_2	TiO_2	Al_2O_3	FeO_{tot}	MnO	MgO	CaO	Na_2O	K_2O	P_2O_5	ClO	Total alk.	Alk. ratio
AD 472*	Mean	49.79	0.50	22.23	4.95	0.15	1.01	5.63	9.2	5.41	0.00	1.12	14.62	0.73
	SD	1.65	0.16	0.92	1.38	0.07	0.47	1.51	2.35	2.29	0.00	0.53	1.87	0.82
AD 512*	Mean	47.81	1.05	19.40	7.97	0.20	2.97	9.11	4.6	5.85	0.31	0.75	10.45	1.28
	SD	0.98	0.17	0.61	0.53	0.13	0.80	1.05	0.53	0.58	0.15	0.14	0.85	0.18
OT0702-1**	Mean	48.82	0.88	20.58	7.08	0.27	1.39	8.04	6.19	5.61	0.06	1.08	11.80	0.92
	SD	1.12	0.14	0.84	0.58	0.10	0.34	1.51	0.58	0.72	0.04	0.10	0.55	0.18
Mercato*	Mean	58.51	0.13	21.70	1.76	0.14	0.09	1.66	8.56	6.93	0.00	0.52	15.49	0.82
	SD	0.72	0.08	0.41	0.19	0.10	0.08	0.26	0.62	0.38	0.00	0.09	0.49	0.11
OT0702-3**	Mean	59.1	0.17	21.58	1.95	0.17	0.16	1.76	7.56	7.02	0.00	0.52	14.58	0.93
	SD	0.55	0.09	0.13	0.11	0.07	0.09	0.13	0.56	0.27	0.00	0.03	0.70	0.07
LN1***	Mean	61.66	0.45	18.12	2.72	0.24	0.27	2.06	5.35	8.7	0.06	0.30	14.05	1.63
	SD	0.35	0.12	0.31	0.26	0.14	0.10	0.15	0.30	0.22	0.08	0.39	0.33	0.12
LN2***	Mean	62.14	0.43	18.09	2.62	0.18	0.25	1.88	5.34	8.51	0.07	0.41	13.85	1.61
	SD	0.63	0.12	0.32	0.31	0.11	0.17	0.34	0.49	0.49	0.09	0.04	0.33	0.22

*Proximal deposit (Santacroce et al., 2008), **(Vogel et al., 2010b), ***(Siani et al., 2004). Bold signature indicates tephra deposits correlated to Lake Prespa tephras.

Cryptotephra PT0915-3 (in the sample from 265 to 267 cm depth) and PT0915-4 (in the sample from 287 to 289 cm depth) have relatively similar geochemical compositions (**Table 2.2**) described as homogeneous trachytic according to Le Bas et al. (1986). The composition and the existence of two separated tephra layers make it unlikely that these cryptotephra correlate with the widespread 'Neapolitan Yellow Tuff' tephra (NYT, 12,300 ± 300 BP; Rosi and Sbrana, 1987; Orsi et al., 1992), particularly because NYT is bimodal in composition. More likely, PT0915-3 and PT0915-4 correspond to pre-NYT erupted tephra layers. Pre-NYT deposits form highly evolved trachyte assemblages and originate from the same parent magma as NYT (Pabst et al., 2008). However, there is little geochemical data from pre-NYT available, which makes a correlation difficult. Three main distal deposits of pre-NYT eruptions are known from marine and lacustrine sediment cores. Siani et al. (2004) found a cluster of tephra layers preceding the NYT, which they related to the Phlegraean Fields GM1 eruption (recovered on the northwestern flanks of Somma-Vesuvius; Andronico et al., 1996; Zanchetta et al., 2000) and the Lagno Amendolare eruption (LAM, 13,070 ± 90 BP; Andronico, 1997). Another pre-NYT tephra layer, named 'Tufi Biancastri', was recovered from Lago Grande di Monticchio and dates at 14.6 ka BP (Pappalardo et al., 1999; Wulf et al., 2004). PT0915-3 and PT0915-4 are, however, different in geochemical compositions and in glass appearance to LAM (e.g. black pumice of LAM) and Tufi Biancastri. According to the geochemical and stratigraphic characteristics, PT0915-3 and PT0915-4 can be better correlated with the marine tephra layers LN1 and LN2, which were found in the South Adriatic Sea (Siani et al., 2004) and show a similar trachytic composition (**Table 2.3**). LN1 and LN2 have been dated to 12,660 ± 110 BP and 12,870 ± 100 BP, which can be calibrated to 14,697 ± 519 cal BP and 15,551 ± 621 cal BP, respectively. According to the age-depth model, which is based on reliable radiocarbon ages and the tephra ages, the base of the studied Co1215 sequence can be extrapolated to 17.1 ka cal BP.

2.5 Discussion and interpretation

2.5.1 Late Glacial (17.1 - 15.7 ka cal BP)

Based on the age-depth model, the sediments of LZ-1 were deposited during the Late Glacial between 17.1 and 15.7 ka cal BP (**Figure 2.5**). The sporadic occurrence of coarse sand and gravel within these glacial sediments can best be explained by ice floe transport and is thus interpreted as ice rafted debris (IRD). IRD and the fine grain-size composition in LZ-1 imply significantly more ice cover than today when the lake remains mostly ice free during winters (Wagner et al., 2010) and sedimentation under relatively calm conditions. Calm conditions are likely a result of the location of site Co1215 in the central northern basin, where no significant riverine inflow affects the sedimentation. The lack of lamination during the Late Glacial implies bioturbation. Lower temperatures likely in the Late Glacial imply that the lake was probably dimictic, with at least partial ice cover in winter constraining mixing and complete turnover of the water column during spring and autumn. Today, Lake Prespa water is mixed from September to April/May with complete mixing of the water column and stratified with anoxic conditions below 15 m water depth during the summers (Matzinger et al., 2006). Also low TOC and TS during the

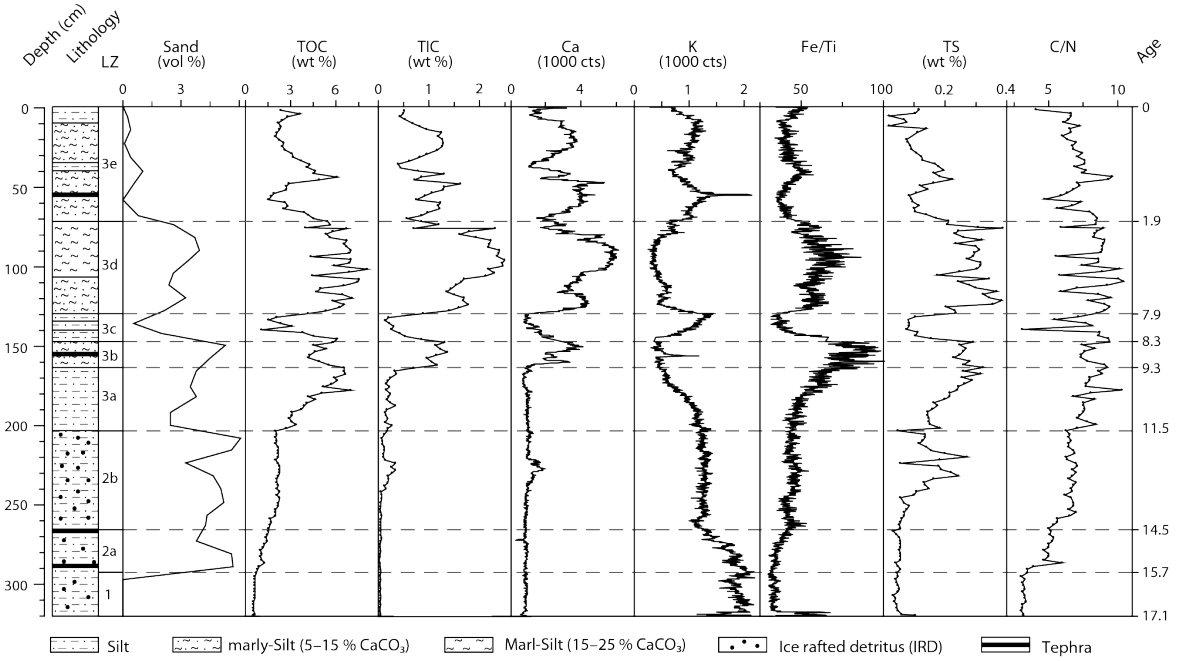

Figure 2.3: Lithology, lithozones (LZ), sand content (vol %), total organic carbon (TOC) and total inorganic carbon (TIC) content (wt %), calcium (Ca) and potassium (K) intensities (10^3 counts), iron/titanium (Fe/Ti) ratio, total sulfur (TS) content (wt %), carbon/nitrogen (C/N) ratio and age (ka cal BP) of LZ of core Co1215 from Lake Prespa (320-0 cm depth). Dashed lines in the figure mark transitions of lithozones.

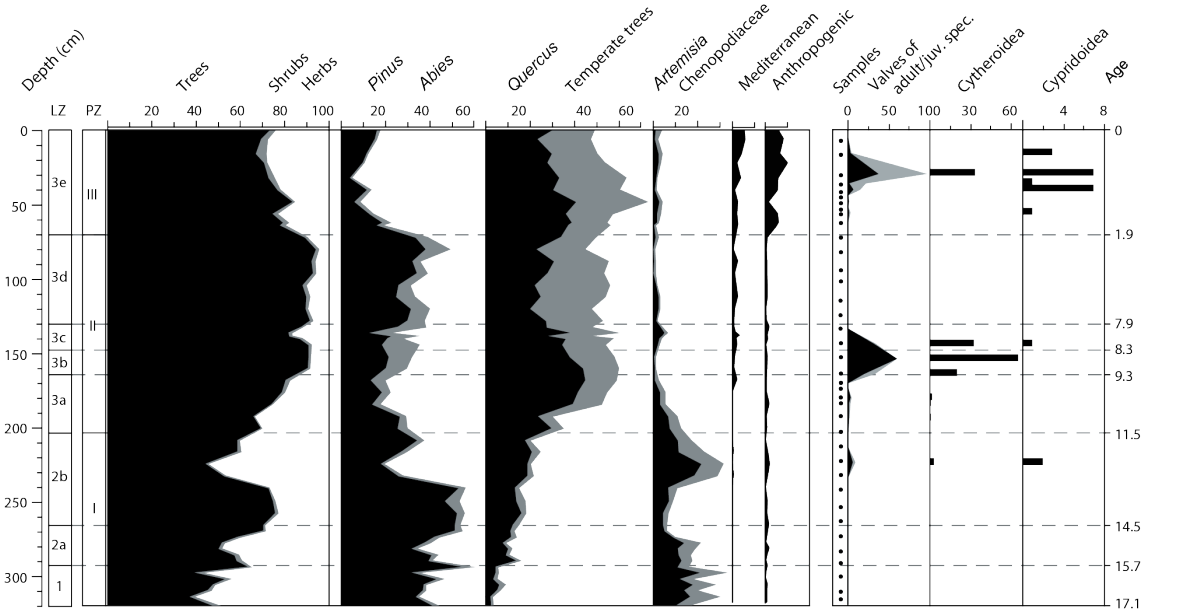

Figure 2.4: Pollen zones (PZ), pollen percentages of trees, shrubs, herbs, *Pinus*, *Abies*, *Quercus*, mixed deciduous (temperate) trees, *Artemisia*, Chenopodiaceae, Mediterranean and anthropogenic taxa, as well as sample depths treated for ostracod analysis, total number of adult and juvenile ostracods (valves per 5 g), adult species of members of Cytheroidea, and members of Cypridoidea, and age (ka cal BP) of LZ of core Co1215 from Lake Prespa (320-0 cm depth). Dashed lines in the figure mark transitions of lithozones.

Late Glacial indicate a well-oxygenated low productivity environment fostering decomposition of organic matter, supported by very low C/N and Fe/Ti ratios. C/N is generally used to ascribe an organic matter source, but the very low values 6 are supposed to be due to decomposition (cf. Meyers and Ishiwatari, 1995). The Fe/Ti ratio likely reflects past redox conditions. Ti is a relatively immobile element and a tracer for detrital clastic material, while Fe forms relatively stable FeS mineral phases under reducing conditions, if sufficient S is available. As S is present in varying amounts and correlates relatively well to the Fe/Ti ratio in Lake Prespa, a high Fe/Ti ratio indicates more reducing conditions and a low Fe/Ti ratio more oxidizing conditions.

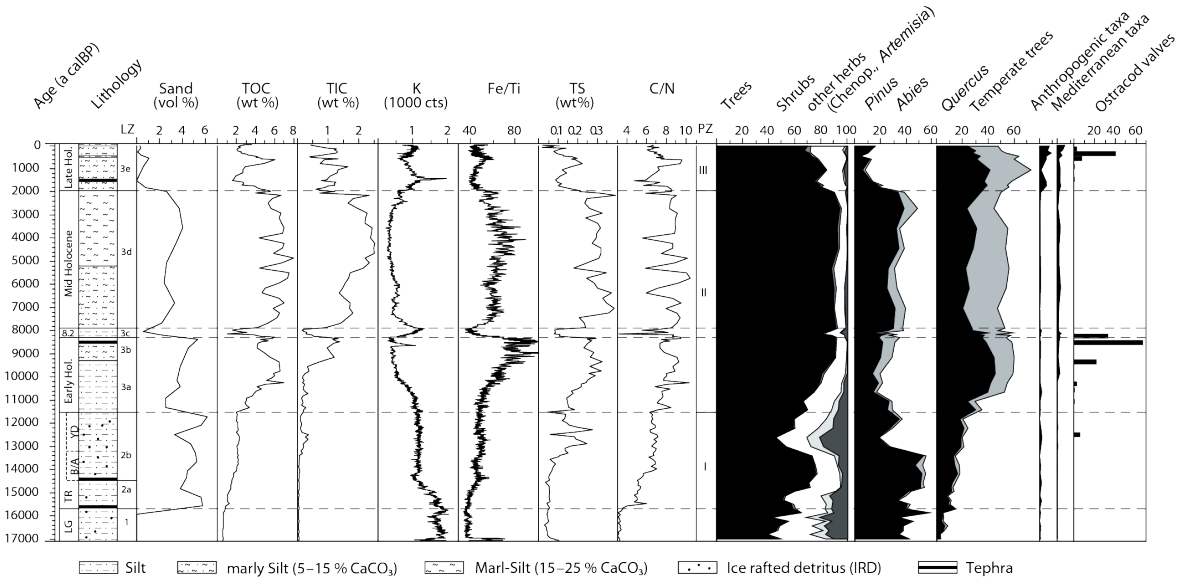

Figure 2.5: Lithology, lithozones (LZ), sand content (vol %), total organic carbon (TOC) and total inorganic carbon (TIC) content (wt %), potassium (K) intensities (103 counts), iron/ titanium (Fe/Ti) ratio, total sulfur (TS) content (wt %) and carbon/nitrogen (C/N) ratio, as well as pollen zones, pollen percentages of trees, shrubs, other herbs, Chenopodiaceae, Artemisia, Pinus, Abies, Quercus, mixed deciduous (temperate) trees, anthropogenic taxa, Mediterranean taxa and total number of adult ostracod (valves per 5 g) of core Co1215 from Lake Prespa (17,100-0 a calBP). Dashed lines in the figure mark transitions of time intervals discussed in Section 2.5. Explanation of abbreviations: LG = Late Glacial, TR = Late Glacial to Holocene Transition, B/A = Bølling/Allerød, YD = Younger Dryas, Hol. = Holocene.

The Fe and Mn concretionary horizon at onset of LZ-1 is interpreted as a paleo-redox front, which also occurs in other cores from lakes Prespa and Ohrid (cf. Wagner et al., 2010; Vogel et al., 2010a). The absence of TIC ($CaCO_3$) between 17.1 and 15.7 ka cal BP is assumed to be a result of low productivity, dissolution due to aerobic decomposition of organic matter (cf. Cohen, 2003), and/or inhibited supply of Ca_2^+ and HCO_3^- ions from the catchment (cf. Wagner et al., 2009; Vogel et al., 2010a). These conditions probably also explain the absence of ostracod valves. Restricted supply of Ca_2^+ and HCO_3^- ions to the lake was probably due to open steppe vegetation in the catchment, which likely promoted surface runoff and restricted soil formation and chemical weathering. Furthermore, the formation of local ice caps (Hughes et al., 2006; Belmecheri et al., 2009) likely reduced runoff during winter months, but led to pulsed spring- sum-

mer melt water discharges with a high erosional force as documented by high contents of detrital clastic matter (high K counts) in Prespa sediments during this period (**Figure 2.5**). Cold-tolerant herbs, such as *Artemisia* and Chenopodiaceae, and *Pinus* indicating typical stadial conditions dominate the vegetation. *Pinus* populations and isolated patches of *Abies* and *Quercus* at favorable locations in the surrounding valleys probably characterized the landscape. The presence of *Abies* and *Quercus* along with some other deciduous trees (*Carpinus*, *Ulmus*, *Alnus*, *Fraxinus*, and *Betula*) suggests their potential survival in sheltered habitats (refugia) with sufficient moisture and favorable temperature for growth (cf. Bennett et al., 1991; Tzedakis et al., 2002; Birks and Willis, 2008).

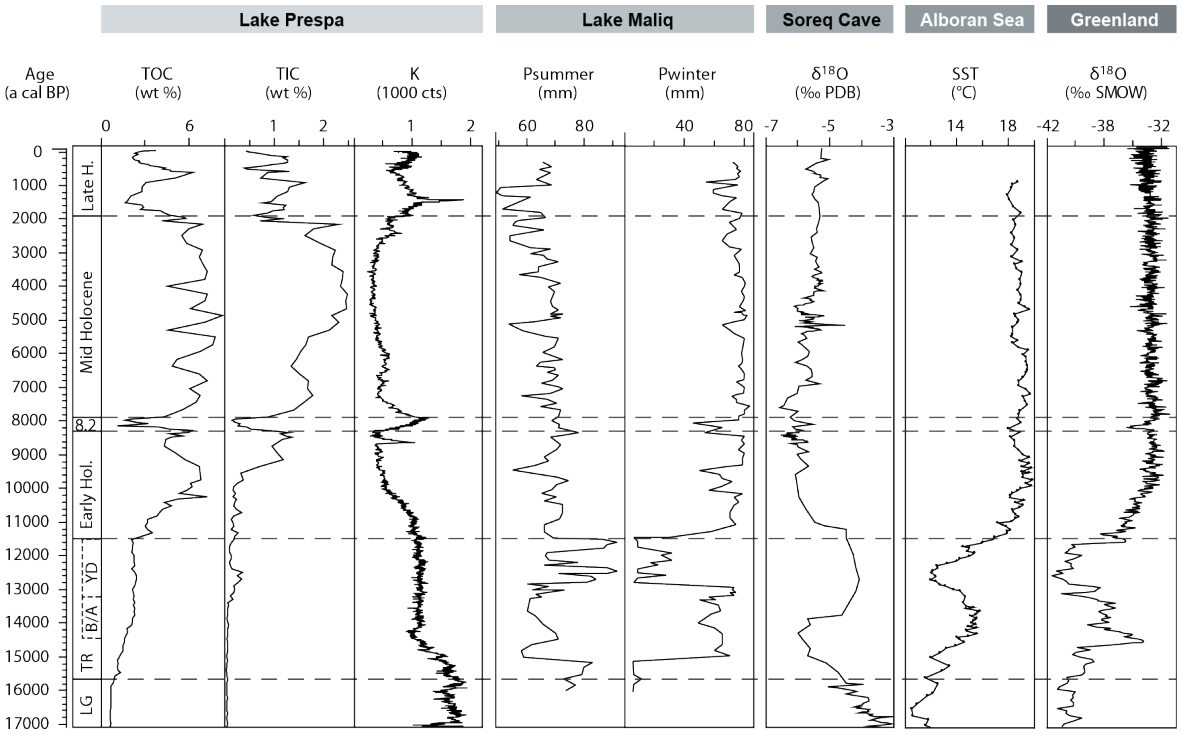

Figure 2.6: Total organic carbon (TOC) content (wt %), total inorganic carbon (TIC) content (wt %), and potassium (K) intensities (10^3 counts) of core Co1215 from Lake Prespa (17,100-0 a cal BP) in comparison with summer precipitation (Psummer) and winter precipitation (Pwinter) (mm) of pollen-based quantitative reconstructions from Lake Maliq (Bordon et al., 2009), $\delta^{18}O$ values (per mill PDB) from Soreq Cave speleothems (Bar-Matthews et al., 2003), Sea surface temperatures (SST) (°C) reconstructed from core MD95-2043 of the Alboran Sea (Cacho et al., 1999) and d18O values (per mill SMOW) of the GISP2 Greenland ice core (Grootes et al., 1993). Dashed lines in the figure mark transitions of time intervals discussed in chapter 2.5. Explanation of abbreviations: LG = Late Glacial, TR = Late Glacial to Holocene Transition, B/A = Bølling/Allerød, YD = Younger Dryas, Hol., H. = Holocene.

The general picture of relatively cold and dry climate conditions during the Late Glacial at Lake Prespa with enhanced mixing of the water column corresponds well with existing records from lakes Prespa and Ohrid (Wagner et al., 2009, 2010; Vogel et al., 2010a) and other records from the region (**Figure 2.6**). Marine records from the Alboran Sea indicate sea surface temperatures (SST) 5-6 °C lower during the Late Glacial than during the Holocene (Cacho et al., 2001;

Figure 2.6) and would lead to summer temperatures of around + 16 °C and winter temperatures as low as - 5 °C at Lake Prespa (cf. Hollis and Stevenson, 1997). This corresponds relatively well with pollen-based terrestrial temperature reconstructions for the Last Glacial Maximum (~20 ka cal BP), which indicate 8 °C lower temperatures than today in northern Greece and 7-10 °C lower temperatures in Italy (Peyron et al., 1998). Pollen records from Italy and Greece (Allen et al., 1999, 2002; Lawson et al., 2004; Müller et al., 2011) also indicate relatively dry conditions and predominance of open steppe vegetation, which correlates well to low precipitation inferred from speleothem records in the Eastern Mediterranean (Bar-Matthews et al., 1999, 2003; **Figure 2.6**).

2.5.2 Late Glacial to Holocene transition (15.7 - 11.5 ka cal BP)

The Late Glacial to Holocene transition from 15.7 to 11.5 ka cal BP is represented by LZ-2 (**Figure 2.5**). The occurrence of IRD implies that the lake was ice-covered during winter. Increased wave action and/or higher current activity perhaps explain the relatively high percentages of sand. Increased wave action could be due to a lake level lowering, which probably also occurred at Lake Ohrid and led to mass movements and potential hiati in the sediment records (Wagner et al., 2009; Vogel et al., 2010a). However, as changing abundances of *Artemisia* and Chenopodiaceae (indicative of a dry climate) do not correlate with changes of the grain-size distribution throughout this period (**Figure 2.5**), the high sand content in core Co1215 is likely a function of high aeolian activity (Vogel et al., 2010a) and is probably related to the formation of a contourite drift and channel-like structures in the lateral parts of the seismic profile across the coring location (**Figure 2.1** c; Wagner et al., 2012).

The increase of TOC between 15.7 and 14.5 ka cal BP suggests either increased productivity and/or, along with the increase in C/N, less decomposition. The increase of organic matter accumulation and higher abundance of *Pinus* indicate an increase in temperatures and the expansion of *Pinus* at higher elevations (ascendance of the tree-line) and/or a denser forest cover. The increasing abundance of trees likely led to less erosion and lower clastic input into the lake as suggested by decreasing K. Further reduction of clastic input is probably related to decreasing glacial melt water supply, as other terrestrial (Bar-Matthews et al., 1999) and marine records (Cacho et al., 2001, **Figure 2.6**; Ehrmann et al., 2007) indicated ongoing deglaciation around this time. More reducing bottom water conditions and less decomposition of organic matter due to warmer conditions between 15.7 and 14.5 ka cal BP is confirmed by a slight increase in the Fe/Ti ratio. The absence of TIC suggests little allochthonous carbonate input and restricted carbonate precipitation or post depositional carbonate dissolution.

Between 14.5 and 13.2 ka cal BP, which corresponds to the Bølling/ Allerød interstadial, relatively stable hydrological conditions are documented at Lake Prespa. Low and stable K suggests that the local ice caps disappeared from the catchment. Relatively constant TOC, C/N and Fe/Ti imply that organic matter accumulation and the mixing conditions did not change significantly. The broad maximum in tree taxa percentages (above 70%) during the Bølling/Allerød at Lake Prespa is mainly made by *Pinus* (around 50%) and the gradual expansion of *Quercus* and implies warmer temperature and/or more humid conditions. The diversity of trees also increases,

as deciduous trees expanded from their local refugia and occupied stretches at lower altitudes and other sheltered locations. Increased moisture, at least during several periods is indicated in slightly increased values of *Abies* (cf. Ellenberg, 2009). Quantitative temperature reconstructions from Lake Maliq and the Aegean Sea indicate that the mean annual temperatures increased by c. 10 °C at the onset of the Bølling and remained relatively stable subsequently (Bordon et al., 2009; Kotthoff et al., 2011). Interestingly, this temperature shift had little effect on the productivity and the mixing conditions in Lake Prespa. The maximum in tree pollen percentages and the relatively low values of *Artemisia* and Chenopodiaceae during this period are predominantly related to higher winter temperatures and more humid conditions in the region. More humid conditions during the Bølling/Allerød correspond with a relatively high amount of reconstructed annual rainfall at Lake Maliq (Bordon et al., 2009), in the Eastern Mediterranean (Bar-Matthews et al., 1999, 2003, **Figure 2.6**) and at Lago Grande di Monticchio in Italy (Allen et al., 1999, 2002). The cold setback of the Older Dryas, as documented in marine records from the Aegean Sea around 13.8 ka cal BP (Kotthoff et al., 2011) or from the GISP2 record from Greenland (Grootes et al., 1993; **Figure 2.6**), cannot be clearly identified in the Lake Prespa record.

The significant change in the vegetation pattern at around 13.2 ka cal BP can be correlated to the onset of the Younger Dryas chronozone (cf. Kotthoff et al., 2008). The distinct decrease of trees (mainly *Pinus*) and the coeval increase of *Artemisia* and Chenopodiaceae culminate at 12.6 ka cal BP and imply a significant decrease in temperature and/or more arid conditions in the catchment. The re-advancement of trees and decrease of mountain steppe herbs suggests the reversion to warmer and more humid climate conditions after 12.6 ka cal BP. Deciduous trees, including *Quercus*, appear to expand gradually between 13.2 and 11.5 ka cal BP, which suggests that moisture availability and temperature were not limiting factors for their growth. On the contrary, available conifer habitats were limited by the descending tree-line as well as the competition from deciduous trees in lower elevations. In contrast to the significant shifts in vegetation, stable values in K, TOC, C/N, and Fe/Ti imply relatively constant detrital input, productivity, decomposition and mixing conditions in the lake during this period. However, the higher TIC (siderite) between 13.2 and 12.3 ka cal BP and the distinct peak in TS during this time and between 12.3 and 11.5 ka cal BP implies diagenesis under reducing conditions (cf. Cohen, 2003) in the surface sediments and/or bottom waters. The high TS is probably due to the occurrence of iron sulfide in the sediment, which is likely formed through dissolution of allochthonous pyrite to sulfate and reprecipitation as a secondary sulfide (pyrite or greigite) in the sediments under strong reducing conditions. The strong reducing conditions in the lake during the Younger Dryas are probably a result of enhanced ice cover during winter. As this is the only horizon throughout the Late Glacial to Holocene transition, where ostracods are well preserved, somewhat higher reducing conditions restricted $CaCO_3$ dissolution.

The cold and dry conditions during the Younger Dryas at Lake Prespa correspond to those reported from other records in the Mediterranean region (e.g. Bar-Matthews et al., 1999, 2003; Allen et al., 2002; Lawson et al., 2005; Kotthoff et al., 2008; Bordon et al., 2009; Müller et al., 2011). The records from Lake Maliq (Bordon et al., 2009), Lago Grande di Monticchio (Allen et al., 2002), or the Aegean Sea (Kotthoff et al., 2011) suggest that this period was characterized

by c. 10 °C lower temperatures in the terrestrial environment, and c. 3-4 °C cooler temperatures in the Alboran Sea (Cacho et al., 2001; **Figure 2.6**). The distinct change in temperatures and precipitation during the Younger Dryas are explained by a stable high-pressure cell over the re-expanded North European ice sheet leading to S-flow of cold and dry northern air masses into the Mediterranean area (Bordon et al., 2009) and colder conditions in the Aegean Sea (Kotthoff et al., 2011). It is surprising that the extreme changes in temperatures and precipitation are not indicated in the hydrology of Lake Prespa, except of iron sulfide precipitation. The shifts in vegetation patterns at Lake Prespa during the Younger Dryas are probably related to predominantly lower winter temperatures and limited moisture availability, with overall limited effect on lake processes.

2.5.3 Early Holocene (11.5 - 8.3 ka cal BP)

The early Holocene is recorded by sediments of LZ-3a and -3b (**Figure 2.5**). The distinct decrease in sand content at the onset of the Holocene could be due to less current activity or wave action. Both could have been triggered by lower aeolian activity, which is, however, not indicated in other cores from the vicinity and in the seismic profiles (cf. Vogel et al., 2010a; Wagner et al., 2010, 2012). Reduced wave action could also be due to lake level increase. However, stable isotope data from Lake Prespa indicate only tentatively a lake level change (Leng et al., 2010) and precipitation changes during the early Holocene can hardly be inferred from the Co1215 record. Increased precipitation from c. 11.5 ka cal BP is reported from the North Aegean Sea (Kotthoff et al., 2011) and Lago Grande di Monticchio (Allen et al., 1999, 2002), and from around 11.3 ka cal BP from Lake Maliq (Bordon et al., 2009; **Figure 2.6**). The only indication for changes in precipitation at Lake Prespa comes from the pollen record, which shows a decrease in steppe vegetation taxa and an increase in *Abies* percentages during the early Holocene. However, these are more gradual changes and do not correlate with the more stepwise increase of precipitation reported from Lake Maliq (Bordon et al., 2009) and the Aegean Sea (Kotthoff et al., 2011).

A significant warming after 11.5 ka cal BP at Lake Prespa is indicated by the gradual expansion of trees and the coeval decrease in *Artemisia* and Chenopodiaceae percentages (**Figure 2.5**). Furthermore, the absence of IRD indicates increased winter temperatures, while increased TOC and the relatively constant C/N ratio of around 7 implies higher productivity and/or better preservation of the predominantly aquatic organic matter due to higher summer temperatures. However, the low TIC ($CaCO_3$) content during the Early Holocene implies that the increase in productivity was not correlated with $CaCO_3$ precipitation and/or preservation, probably because dissolution of $CaCO_3$ was fostered by primarily aerobic decomposition of organic matter when seasonal mixing occurred. During summer, the relatively high temperatures likely led to stratification of the water column, which is supported by increasing Fe/Ti and TS. Fe and S form early diagenetic FeS precipitates under reducing conditions in the surface sediments. The temperature increase at the onset of the Holocene correlates well with that reported from nearby Lake Maliq (Bordon et al., 2009), the Alboran Sea (Cacho et al., 2001; **Figure 2.6**) and the North Aegean Sea (Kotthoff et al., 2011). However, the proxies representing the hydrological conditions in Lake Prespa suggest a more gradual warming and do not support a rapid increase of c. 10 °C,

such as reported from the North Aegean Sea (Kotthoff et al., 2011), or from Lake Maliq (Bordon et al., 2009). The delayed response or more gradual pattern observed at Lake Prespa could be the result of a lagged catchment adaptation to rapid climate change. This might include lags in expansion of woodlands as seen in the pollen record (**Figure 2.5**) and associated lags in soil formation, overall hampering the export of nutrients and ions to the lake and thus productivity and $CaCO_3$ precipitation/preservation. In core Co1204, from a more lateral part of Lake Prespa, a rapid increase in TOC and TIC and a coeval decrease in K counts, together with a significant coarsening and change in the lithology were attributed to the Pleistocene/Holocene transition and dated to 10.5 ka cal BP (Wagner et al., 2010). As described above, potentially higher current activity in the lake at this time could have led to a hiatus in core Co1204 and would explain the discrepancies between the cores Co1204 and Co1215 during this period.

The decrease in K between 10.9 and 10.0 ka cal BP suggests higher accumulation of organic matter (increase of 3%) or less input of clastic material into the lake due to denser vegetation cover in the catchment. Increasing percentages of trees imply a denser forest cover in the catchment and/or the ascendance of the tree-line. Higher temperatures particularly during winter are documented in the first occurrence of Mediterranean taxa around 10 ka cal BP (**Figure 2.5**), which indicates immigration and/or expansion of relevant species.

Warmest temperatures during the early Holocene are indicated between 9.3 and 8.3 ka cal BP. The distinct increase in TIC ($CaCO_3$) from about 9.3 ka cal BP could be the result of increased lake productivity, as $CaCO_3$ in Lake Prespa is believed to derive mainly from photosynthesis-induced precipitation, higher ion concentrations in the lake, and/or improved preservation (cf. Wagner et al., 2010). Improved preservation of $CaCO_3$ is supported by the occurrence of ostracod valves in the sediment (**Figure 2.5**). The dominance of ostracod species of Cytheroidea throughout LZ-3b indicates well-oxygenized and pristine water conditions (Petkovski and Keyser, 1992; Meisch, 2000). Higher Ca_2^+ and HCO_3^- ion concentrations in the lake could be related to a complex interplay of factors including enhanced evaporation and increased ion supply from the catchment. Warm temperatures, increased precipitation, a dense vegetation cover and soil formation could have promoted the dissolution of $CaCO_3$ in the Lake Prespa catchment (cf. Vogel et al., 2010a) and may have restricted the erosion, such as indicated by low K counts (**Figure 2.5**) and a minimum in sedimentation rate (**Figure 2.2**). The decrease in TOC during this period is perhaps explained by the increase in $CaCO_3$ accumulation, which likely diluted the organic matter accumulation. Warmer temperatures and high productivity promoted decomposition and reducing conditions in the surface sediments, which are documented by the broad maxima in the Fe/ Ti ratio and TS. However, the bottom waters were apparently partly oxygenated, as ostracods are present. Members of Cytheroidea, which indicate oligo- to mesotrophic conditions, dominated the ostracod assemblage, but also Cypridoidea, which indicates rather eutrophic conditions, occur. The coeval occurrence of both genera indicates distinct shifts in the bottom water conditions and a better preservation of $CaCO_3$. These conditions are possible, if the water column is stratified during summer and completely mixed during winter.

2.5.4 The "8.2 ka event" (8.3 - 7.9 ka cal BP)

The period between 8.3 and 7.9 ka cal BP is characterized by sediments of LZ-3c (**Figure 2.5**). The distinct minimum in sand content at 8.3 ka cal BP is likely due to a significant decrease in current activity. Less wave action due to a lake level increase is unlikely, as winter precipitation around this time is low at Lake Maliq (Bordon et al., 2009; **Figure 2.6**). Restricted snowmelt will have led to a lower level of Prespa. A low lake level due to relatively dry climate conditions is supported by the distinct peak of *Artemisia* (**Figure 2.5**). The increase in steppic taxa percentages and also a distinct minimum in organic matter accumulation (less productivity and/or increased decomposition), and the low Fe/Ti and TS indicate well-oxygenated bottom water conditions and lower temperatures. These conditions could have fostered the dissolution of $CaCO_3$ and thus could have led to a decreasing number in the Cytheroidea-dominated ostracod assemblage. The opening of the forest and/or the lowering of the treeline at Lake Prespa likely promoted soil erosion, which is reflected in a high sedimentation rate (**Figure 2.2**). The low sand content and a maximum in K imply that mainly fine clastic matter caused the increase in sedimentation rate. The maximum in fine clastic supply at the very end of the period between 8.3 and 7.9 ka calBP implies a short delay between climate change, vegetation response and erosion.

The distinct shift in climate between 8.3 and 7.9 ka cal BP is likely related to the 8.2 ka cooling event, which lasted between 200 and 600 years and is reported to have occurred anywhere between 8.6 and 7.8 ka cal BP in the Northern Hemisphere (e.g. Magny et al., 2003; Rohling and Pälike, 2005), and between 8.4 and 8.0 ka cal BP in the North Atlantic and central Greenland (Alley et al., 1997; Barber et al., 1999). Pollen-inferred temperature reconstructions from Lake Maliq and from Tenaghi Philippon reveal up to 3 °C cooler winter temperatures during the 8.2 ka event, but relatively stable summer temperatures, and a decrease in annual precipitation of around 200 mm (Bordon et al., 2009; Pross et al., 2009).

2.5.5 Mid Holocene (7.9 - 1.9 ka cal BP)

The mid Holocene is recorded in the sediments of LZ-3d (**Figure 2.5**). The pollen record infers that the vegetation apparently had recovered relatively fast after the 8.2 ka event. Relatively high occurrence of *Pinus*, temperate trees, and *Quercus*, the latter though being less abundant compared to the early Holocene, imply a dense forest cover in the catchment of Lake Prespa. The pollen record in combination with absence of IRD, high organic matter accumulation (increased productivity and/or low degradation), high preservation of $CaCO_3$ and a C/N around 9 (aquatic productivity) indicate a rapid warming with relatively mild winter temperatures, ice-free conditions throughout the year, and more reducing conditions at 7.9 ka cal BP. However, the relatively slow return of K and Fe/Ti to values similar to those before the 8.2 ka event implies that sedimentation in Lake Prespa was still affected by high aeolian activity, as recorded at Lake Ohrid between 7.5 and 7.0 ka cal BP (Vogel et al., 2010a). The other explanation for the relatively slow reaction of K and Fe/Ti is an increase in annual precipitation and lake level as observed in Lake Maliq nearby (Bordon et al., 2009; Fouache et al., 2010; **Figure 2.6**).

Relatively low and stable K after 7.2 ka cal BP suggests low input of detrital clastic material by low erosion in the catchment. The relatively high organic matter and $CaCO_3$ content in Lake Prespa

between 7 and 5.1 ka cal BP imply higher lake productivity and/or that decomposition and dissolution was significantly restricted due to relatively mild winter temperatures and inhibited mixing. The high trophic level during this period likely led to oxygen depleted bottom water, which is also indicated in the broad and fluctuating maxima in Fe/Ti and TS and the complete absence of ostracod valves. The TIC ($CaCO_3$) maximum during the Mid Holocene suggests that the low abundance of ostracods is not caused by $CaCO_3$ dissolution. More likely, the low abundance of ostracods is related to redistribution and/or unfavorable living conditions in the bottom waters. Potential explanations for such conditions in Lake Prespa would be relatively warm temperatures, low precipitation, and/or a low lake level and increased ion concentration in the water column. However, the isotope record from Lake Prespa indicates wetter conditions especially during summers until c. 6.4 ka cal BP and a subsequent aridification (Leng et al., 2010). In lateral parts of lakes Ohrid and Prespa, $CaCO_3$ concentrations are increasing or high during the first period of the mid Holocene, and reach their highest and more stable values around 6 ka calBP (Wagner et al., 2009, 2010; Vogel et al., 2010a). The difference between these records and core Co1215 from the central part of Lake Prespa can be explained by a higher influence of inflow from a karst environment, ion and nutrient supply and probably also temperature.

The most prominent shift during the mid Holocene in core Co1215 occurs around 5.4 ka cal BP, when TIC ($CaCO_3$) increases to a broad peak. Until 2.8 ka cal BP the lowest values in K and a minimum in herbs suggest restricted erosion and relatively dense vegetation in the catchment. Slightly lower TS, a broad and fluctuating maximum in Fe/Ti, and the high and fluctuating TOC and C/ N could be related to further lake level lowering, with increased ion concentration in the water column, only sporadic mixing of the water column and low decomposition. The lake level lowering could have been initiated by a short period of reduced precipitation around 5.2 ka cal BP, such as described from Lake Maliq (Bordon et al., 2009; **Figure 2.6**), and is likely supported by progressive aridification, as indicated in other records from the region (e.g. Magny et al., 2007; Roberts et al., 2008; Wagner et al., 2009; Leng et al., 2010; Peyron et al., 2011). Alternatively, higher ion concentration in the lake could be a result of enhanced soil formation and chemical weathering. A short-term period of cooler and/or drier conditions around 4.2 ka cal BP, such as reported from other records in the region (e.g. Magny et al., 2009; Wagner et al., 2009, 2010; Vogel et al., 2010a), is not evident in core Co1215.

The decrease in TIC ($CaCO_3$), TOC, TS, Fe/Ti and C/N, and the increase in K around 2.7 ka cal BP correspond with the slight decrease in tree percentages (**Figure 2.5**) and probably results from enhanced human impact. The cultural development in the Eastern Mediterranean started to rise after the fall of the late Bronze Age and at the onset of the Iron Age (Roberts et al., 2011). Forest clearance, increased agriculture activity and enhanced erosion are also seen c. 200-300 years later in existing records from lakes Ohrid and Prespa (Wagner et al., 2009, 2010; Vogel et al., 2010a) and are probably related to settlements along the shores, such as found by archaeological explorations at Lake Ohrid (Kuzman, 2010a, 2010b). A correlation between the change in anthropogenic influence and a simultaneous climatic change around this time is likely, but difficult to unravel (Peyron et al., 2011; Roberts et al., 2011). Precipitation and lake level curves from Lake Maliq are controversial (cf. Bordon et al., 2009; Fouache et al., 2010)

for the period 2.7-1.9 ka cal BP, and the records from Lago Grande di Monticchio (Allen et al., 2002), the Eastern Mediterranean (Bar- Matthews et al., 1999) and the Aegean region (Kotthoff et al., 2008) do not indicate a significant climate change around this time.

2.5.6 Late Holocene (1.9 ka cal BP - present)

The late Holocene from 1.9 ka cal BP is characterized by sediments of LZ-3e (**Figure 2.5**). The decrease in TOC and C/N between 1.9 and 1.5 ka cal BP and low TIC ($CaCO_3$), together with the minima in Fe/Ti and TS, suggest enhanced decomposition and dissolution during more oxygenated bottom water conditions. The mixing of the water column in Lake Prespa could have been promoted by higher wind intensity or by a cooling. Neither is indicated at Lake Ohrid (Vogel et al., 2010a) or at Lake Maliq (Bordon et al., 2009). The record from Lake Maliq, however, shows decreasing summer precipitation and a lower lake level for this period (Bordon et al., 2009, **Figure 2.6**; Fouache et al., 2010). Drier conditions at Lake Prespa around this time are inferred by the decline of *Pinus* and *Abies* in the catchment. However, the increase of herbs, together with the significant occurrence of anthropogenic taxa in the catchment, indicates intensive human activity in the region. Forest clearance, increased agriculture activity and enhanced soil erosion have probably resulted in higher amounts of fine clastic material into the lake. This is indicated by the increase in K, the dominance of silt and clay (**Figure 2.5**), the increased sedimentation rate (**Figure 2.2**), and also by the decrease in organic matter and $CaCO_3$ (due to dilution by clastic material). Most likely, the anthropogenic activity in the region has overprinted the signature of natural climate variability at this time (cf. Wagner et al., 2009, 2010; Vogel et al., 2010a).

The increase in TOC, Fe/Ti, TS and C/N between 1.5 and 0.6 ka cal BP suggest the return to a higher trophic level, reduced mixing of the water column and reduced decomposition. This could be a result of slightly increased summer temperatures as indicated from Lake Maliq (Bordon et al., 2009). However, there is a sporadic occurrence of ostracod valves, which suggests that the living conditions at the bottom of Lake Prespa were favorable. Historical settlements from 0.85 to 0.75 ka cal BP imply that the lake level of Lake Prespa was relatively low at this time (Matzinger et al., 2006), and also the record from Lake Ohrid indicates a low lake level during this period (Wagner et al., 2009). The decrease in K and the low sedimentation rate between 1.5 and 0.6 ka cal BP are correlated with relatively high tree percentages and a low abundance of anthropogenic taxa, which suggests dense vegetation, relatively low human activity and restricted erosion in the catchment. This decrease in fine clastic material is also documented at Lake Ohrid (Vogel et al., 2010a).

Decreasing TOC, TS, C/N and Fe/Ti after 0.6 ka cal BP imply higher decomposition and improved mixing conditions with oxygenated bottom waters. However, the ostracod assemblage, which is dominated by members of Cypridoidea (**Figure 2.4**), indicates that the trophic level became mesotrophic to eutrophic (cf. Petkovski and Keyser; 1992; Meisch, 2000). Increasing K, together with a significant increase in the sedimentation rate, the decrease in tree taxa percentages, and the increase of anthropogenic taxa suggest increasing human impact throughout this period. The distinct increases in the sedimentation rate, TOC and Fe/Ti in the uppermost part

of the core can probably be correlated with intensive agricultural activity in the region and ongoing eutrophication in the past few decades (Matzinger et al., 2006).

2.6 Conclusions

This multiproxy study of core Co1215 from the northern central part of Lake Prespa in combination with results from former studies in the region add important information on climate-driven environmental change in the Balkan region during the Late Glacial and the Holocene and their imprint on limnology, hydrology, catchment dynamics and vegetation.

The Co1215 sediment record suggests typical stadial conditions from 17.1 to 15.7 cal BP, with low lake productivity, well mixing, and cold-resistant steppic vegetation. Warming is indicated from 15.7 ka cal BP with slightly increased organic matter accumulation, gradual expansion of trees, and decreasing erosion through disappearance of local ice caps. Between 14.5 and 11.5 ka cal BP, relatively stable hydrological conditions are documented in core Co1215. The significant shifts in vegetation development, with a maximum of *Pinus* during the Bølling/Allerød interstadial (14.5-13.2 ka cal BP), and an increase of cold-resistant open steppe vegetation during the Younger Dryas (13.2-11.5 ka cal BP), are therefore assumed to be related to predominantly changes in winter temperatures and moisture availability.

The early and mid Holocene sedimentation is characterized by significantly warmer climate conditions, with ice-free winters, stratification of the water column during summers, increased productivity, and maximum values in trees. A climate fluctuation around 8.2 ka is documented through a significant decrease in productivity, enhanced mixing, strong decomposition and soil erosion, and a coeval expansion of herbs implying cool and dry climate conditions. Vegetation surrounding Lake Prespa and lake-related processes recovered fairly quickly after the 8.2 ka event, whereas the relatively slow return of K and Fe/Ti implies that the region was still affected by high aeolian activity and/or higher precipitation and surface runoff. The highest trophic level of Lake Prespa is recorded during the mid Holocene between 5.2 and 2.8 ka cal BP and could be related to lake level lowering, only sporadic mixing of the entire water column, and increased ion concentration resulting in high carbonate precipitation. The significant change in the hydrological and environmental conditions at around 1.9 ka cal BP probably is a result of intensified human activity in the catchment.

2.7 Acknowledgments

The study was funded by the German Research Foundation (DFG) and forms part of project B2 of the CRC 806 “Our Way to Europe: Culture-Environment Interaction and Human Mobility in the Late Quaternary”. We would like to thank our colleagues at the Hydrobiological Institute in Ohrid for logistic support during the field campaigns in 2007, 2009 and 2011. Thank you to Robert from the police department in Stenje. Thank you to Ilaria Baneschi from the Instituto di Geoscienze e Georisorse in Pisa for previous comments to the results. We want to especially thank our colleagues from the Quaternary Geology group at the Institute of Geology and Mineralogy at Cologne University for their support.

2.8 References

Albrecht, C., Wilke, T., 2008. Ancient Lake Ohrid: biodiversity and evolution. Hydrobiologia 615, 103-140.

Allen, J.R.M., Brandt, U., Brauer, A., Hubberten, H.-W., Huntley, B., Keller, J., Kraml, M., Mackensen, A., Mingram, J., Negendank, J.F.W., Nowaczyk, N.R., Oberhänsli, H., Watts, W.A., Wulf, S., Zolitschka, B., 1999. Rapid environmental changes in southern Europe during the last glacial period. Nature 400, 740-743.

Allen, J.R.M., Watts, W.A., McGee, E., Huntley, B., 2002. Holocene environmental variability e the record from Lago Grande di Monticchio, Italy. Quaternary International 88, 69-80.

Alley, R.B., 2000. The Younger Dryas cold interval as viewed from central Greenland. Quaternary Science Reviews 19, 213-226.

Alley, R.B., Mayewski, P.A., Sowers, T., Stuiver, M., Taylor, K.C., Clark, P.U., 1997. Holocene climatic instability: a prominent, widespread event 8200 yr ago. Geology 6, 483-486.

Andronico, D., 1997. La stratigrafia dei prodotti dell'eruzione di Lagno Amendolare, Campi Flegrei, Napoli. In: Atti della Societa toscana di scienze naturali residente in Pisa, Memorie. Serie A 104, pp. 165-178.

Andronico, D., Calderoni, G., Cioni, R., Donahue, D.J., Marianelli, P., Santacroce, R., Sbrana, A., Sulpizio, R., November 7 1996. An Updated Chronostratigraphic Scheme of the Last 19,000 Years of Vesuvius Magmatic and Eruptive History. EOS, Electronic Supplement to the Member Newspaper of the American Geophysical Union (AGU), 671-672.

Bar-Matthews, M., Ayalon, A., Kaufman, A., Wasserburg, G.J., 1999. The Eastern Mediterranean paleoclimate as a reflection of regional events: Soreq Cave, Israel. Earth and Planetary Science Letters 166, 85-95.

Bar-Matthews, M., Ayalon, A., Gilmour, M., Matthews, A., Hawkesworth, C.J., 2003. Sea-land oxygen isotopic relationships from planktonic foraminifera and speleothems in the Eastern Mediterranean region and their implication for paleorainfall during interglacial intervals. Geochimica et Cosmochimica Acta 67, 3181-3199.

Barber, D.C., Dyke, A., Hillaire-Marcel, C., Jennings, A.E., Andrews, J.T., Kerwin, M.W., Bilodeau, G., McNeely, R., Southon, J., Morehead, M.D., Gagnonk, J.-M., 1999. Forcing of the cold event of 8,200 years ago by catastrophic drainage of Laurentide lakes. Nature 400, 344-348.

Belmecheri, S., Namiotko, T., Robert, C., von Grafenstein, U., Danielopol, D.L., 2009. Climate controlled ostracod preservation in Lake Ohrid (Albania, Macedonia). Palaeogeography, Palaeoclimatology, Palaeoecology 277, 236-245.

Belmecheri, S., von Grafenstein, U., Andersen, N., Eymard-Bordon, A., Régnier, D., Grenier, C., Lézine, A.-M., 2010. Ostracod-based isotope record from Lake Ohrid (Balkan Peninsula) over the last 140 ka. Quaternary Science Reviews 29, 3894-3904.

Bennett, K.D., Tzedakis, P.C., Willis, K.J., 1991. Quaternary refugia of north European trees. Journal of Biogeography 18, 103-115.

Beug, H.-J., 2004. Leitfaden der Pollenbestimmung für Mitteleuropa und angrenzende Gebiete. Pfeil, München.

Birks, H.J.B., Willis, K.J., 2008. Alpines, trees, and refugia in Europe. Plant Ecology and Diversity 1, 147-160.

Bordon, A., Peyron, O., Lézine, A.-M., Brewer, S., Fouache, E., 2009. Pollen-inferred Late-Glacial and Holocene climate in southern Balkans (Lake Maliq). Quaternary International 200, 19-30.

Brauer, A., Allen, J.R.M., Mingram, J., Dulski, P., Wulf, S., Huntley, B., 2007. Evidence for last interglacial chronology and environmental change from Southern Europe. PNAS 9, 450-455.

Cacho, I., Grimalt, J.O., Pelejero, C., Canals, M., Sierro, F.J., Flores, J.A., Shackleton, N.J., 1999. Dansgaard-Oeschger and Heinrich event imprints in the Alboran Sea paleotemperatures. Paleoceanography 14, 698-705.

Cacho, I., Grimalt, J.O., Canals, M., Sbaffi, L., Shackleton, N.J., Schönfeld, J., Zahn, R., 2001. Variability of the western Mediterranean Sea surface temperature during the last 25,000 years and its connection with the Northern Hemisphere climatic changes. Paleoceanography 16, 40-52.

Cohen, A.S., 2003. Paleolimnology. The History and Evolution of Lake Systems. Oxford University Press, Oxford.

Davis, M.B., 2000. Palynology after Y2K e understanding the source area of pollen in sediments. Annual Review of Earth and Planetary Sciences 28, 1-18.

Denèfle, M., Lézine, A.-M., Fouache, E., Dufaure, J.-J., 2000. A 12,000-year pollen record from Lake Maliq, Albania. Quaternary Research 54, 423-432.

Ehrmann, W., Schmiedl, G., Hamann, Y., Kuhnt, T., Hemleben, C., Siebel, W., 2007. Clay minerals in Late Glacial and Holocene sediments of the northern and southern Aegean Sea. Palaeogeography, Palaeoclimatology, Palaeoecology 249, 36-57.

Ellenberg, H., 2009. Vegetation Ecology of Central Europe, fourth ed. Cambridge University Press, Cambridge.

Fægri, K., Iversen, J., Kaland, P.E., Krzywinski, K., 2000. Textbook of Pollen Analysis, fourth ed. Blackburn Press, Caldwell.

Fouache, E., Desrulles, S., Magny, M., Bordon, A., Oberweiler, C., Coussot, C., Touchais, G., Lera, P., Lézine, A.-M., Fadin, L., Roger, R., 2010. Palaeogeographical reconstructions of Lake Maliq (Korça Basin, Albania) between 14,000 BP and 2000 BP. Journal of Archaeological Science 37, 525-535.

Geological Maps of Yugoslavia (ed. Geological Institute Belgrade), 1977. Maps 1:100 000; sheets K34-114 Podgradec, K34-102 Ohrid, K34-103 Bitola, K34-115 Lerin.

Grootes, P.M., Stuiver, M., White, J.W.C., Johnsen, S., Jouzel, J., 1993. Comparison of oxygen isotope records from the GISP2 and GRIP Greenland ice cores. Nature 366, 552-554.

Heiss, G., 1988. Crystal structure refinement of a synthetic Fe-Mg-Ca-carbonate phase. Zeitschrift für Kristallographie 185, 604. Hollis, G.E., Stevenson, A.C., 1997. The physical basis of the Lake Mikri Prespa systems: geology, climate, hydrology and water quality. Hydrobiologia 351, 1-19.

Hughes, P.D., Woodward, J.C., Gibbard, P.L., 2006. Quaternary glacial history of the Mediterranean mountains. Progress in Physical Geography 30, 334-364.

Jacobson, G.L., Bradshaw, R.H., 1981. The selection of sites for paleovegetational studies. Quaternary Research 16, 80-96.

Klie, W., 1939a. Studien über Ostracoden aus dem Ohridsee; I: Candocyprinae. Archiv für Hydrobiologie 35, 28-45.

Klie, W., 1939b. Studien über Ostracoden aus dem Ohridsee; II: Limnocythereinae und Cytherinae. Archiv für Hydrobiologie 35, 631-646.

Klie, W., 1942. Studien über Ostracoden aus dem Ohridsee; III: Erster Nachtrag. Archiv für Hydrobiologie 38, 254-259.

Kotthoff, U., Müller, U.C., Pross, J., Schmiedl, G., Lawson, I.T., van de Schootbrugge, B., Schulz, H., 2008. Late Glacial and Holocene vegetation dynamics in the Aegean region: an integrated view based on pollen data from marine and terrestrial archives. The Holocene 18, 1019-1032.

Kotthoff, U., Koutsodendris, A., Pross, J., Schmiedl, G., Bornemann, A., Kaul, C., Marino, G., Peyron, O., Schiebel, R., 2011. Impact of Lateglacial cold events on the northern Aegean region reconstructed from marine and terrestrial proxy data. Journal of Quaternary Science 26, 86-96.

Kuzman, P., 2010a. Important Archaeological Explorations, retrieved 08.03.11, from http://www.ohrid.com.mk/archaeology/archaeology.asp?ID1⁄4381.

Kuzman, P., May/June 2010b. Plaoshnik e Ohrid. Macedonian Archaeological News Number 7, II, 2010. Electronic newsletter, joint project of the Cultural Heritage Protection Office of the Republic of Macedonia and the Institute for Social Sciences and Humanities Euro-Balkan, retrieved 12.07.11, from www.mav.mk/article.php?lang1⁄4en&; article1⁄442.

Lawson, I.T., Frogley, M., Bryant, C., Preece, R., Tzedakis, P., 2004. The Lateglacial and Holocene environmental history of the Ioannina basin, north-west Greece. Quaternary Science Reviews 23, 1599-1625.

Lawson, I.T., Al-Omari, S., Tzedakis, P.C., Bryant, C.L., Christanis, K., 2005. Lateglacial and Holocene vegetation history at Nisi Fen and the Boras mountains, northern Greece. The Holocene 15, 873-887.

Le Bas, M.J., Le Maitre, R.W., Streckeisen, A., Zanettin, B., 1986. A chemical classification of volcanic rocks based on the total alkali-silica diagram. Journal of Petrology 27, 745-750.

Leng, M.J., Baneschi, I., Zanchetta, G., Jex, C.N., Wagner, B., Vogel, H., 2010. Late Quaternary palaeoenvironmental reconstruction from Lakes Ohrid and Prespa (Macedonia/Albania border) using stable isotopes. Biogeosciences 7, 3109-3122.

Levin, I., Kromer, B., 2004. The tropospheric $^{14}CO_2$ level in mid-latitudes of the Northern Hemisphere (1959-2003). Radiocarbon 46, 1261-1272.

Levkov, Z., Krstic, S., Metzeltin, D., Nakov, T., 2007. Diatoms of Lakes Prespa and Ohrid. About 500 Taxa from Ancient Lake System. Ganter, Ruggell.

Lézine, A.-M., von Grafenstein, U., Andersen, N., Belmecheri, S., Bordon, A., Caron, B., Cazet, J.P., Erlenkeuser, H., Fouache, E., Grenier, C., Huntsman-Mapila, P., Hur- eau-Mazaudier, D., Manelli, D., Mazaud, A., Robert, C., Sulpizio, R., Tiercelin, J.J., Zanchetta, G., Zeqollari, Z., 2010. Lake Ohrid, Albania, provides an exceptional multi-proxy record of environmental changes during the last glacial-interglacial cycle. Palaeogeography, Palaeoclimatology, Palaeoecology 287, 116-127.

Magny, M., Bégeot, C., Guiot, J., Peyron, O., 2003. Contrasting patterns of hydro- logical changes in Europe in response to Holocene climate cooling phases. Quaternary Science Reviews 22, 1589-1596.

Magny, M., de Beaulieu, J.-L., Drescher-Schneider, R., Vannière, B., Walter- Simonnet, A.-V., Miras, Y., Millet, L., Bossuet, G., Peyron, O., Brugiapaglia, E., Leroux, A., 2007. Holocene climate changes in the central Mediterranean as recorded by lake-level fluctuations at Lake Accesa (Tuscany, Italy). Quaternary Science Reviews 26, 1736-1758.

Magny, M., Vannière, B., Zanchetta, G., Fouache, E., Touchais, G., Petrika, L., Coussot, C., Walter-Simonnet, A.-V., Arnaud, F., 2009. Possible complexity of the climatic event around 4300-3800 cal. BP in the central and western Mediter- ranean. The Holocene 19, 1-11.

Matzinger, A., Jordanoski, M., Veljanoska-Sarafiloska, E., Sturm, M., Müller, B., Wüest, A., 2006. Is Lake Prespa jeopardizing the ecosystem of ancient Lake Ohrid? Hydrobiologica 553, 89-109.

Meisch, C., 2000. Freshwater ostracoda of Western and Central Europe. In: Schwoerbel, J., Zwick, P. (Eds.), 2000. Süßwasserfauna von Mitteleuropa, 8/3. Spektrum Akademischer Verlag, Heidelberg/Berlin.

Meyers, P.A., Ishiwatari, R., 1995. Organic matter accumulation records in lake sediments. In: Lerman, A., Imboden, D.M., Gat, J.R. (Eds.), Physics and Chemistry of Lakes. Springer, Berlin, 279-328.

Moore, P.D., Webb, J.A., Collinson, M.E., 1991. Pollen Analysis. Blackwell Scientific Publications, Oxford.

Müller, U.C., Pross, J., Tzedakis, P.C., Gamble, C., Kotthoff, U., Schmiedl, G., Wulf, S., Christanis, K., 2011. The role of climate in the spread of modern humans into Europe. Quaternary Science Reviews 30, 273-279.

Orsi, G., D'Antonio, M., de Vita, S., Gallo, G., 1992. The Neapolitan Yellow Tuff, a large magnitude trachytic phreatoplinian eruption: eruptive dynamics, magma withdrawal and caldera collapse. Journal of Volcanology and Geothermal Research 53, 275-287.

Pabst, S., Worner, G., Civetta, L., Tesoro, R., 2008. Magma chamber evolution prior to the Campanian Ignimbrite and Neapolitan Yellow Tuff eruptions (Campi Flegrei, Italy). Bulletin of Volcanology 70, 961-976.

Pappalardo, L., Civetta, L., D'Antonio, M., Deino, A., Di Vito, M., Orsi, G., Carandente, A., de Vita, S., Isaia, R., Piochi, M., 1999. Chemical and Sr-isotopical evolution of the Phlegrean magmatic system before the Campanian Ignimbrite and the Neapolitan Yellow Tuff eruptions. Journal of Volcanology and Geothermal Research 91, 141-166.

Petkovski, T.K., 1960. Zur Kenntnis der Crustaceen des Prespasees. Fragmenta Balcanica 3 (15), 117-131.

Petkovski, T.K., Keyser, D., 1992. Leptocythere ostrovskensis sp. n. (Crustacea, Ostracoda, Cytheridae) aus dem See Vegoritis (Ostrovsko Ezero) in NW Griechenland. In: Mitteilungen aus dem Hamburgischen Zoologischen Museum und Institut, vol. 89, pp. 227-237.

Petkovski, T.K., Scharf, B.W., Keyser, D., 2002. New and little known species of the genus Candona (Crustacea, Ostracoda) from Macedonia and other Balkan areas. Limnologica 32, 114-130.

Peyron, O., Guiot, J., Cheddadi, R., Tarasov, P., Reille, M., de Beaulieu, J.-L., Bottema, S., Andrieu, V., 1998. Climatic reconstruction in Europe for 18,000 yr B.P. from pollen data. Quaternary Research 49, 183-196.

Peyron, O., Goring, S., Dormoy, I., Kotthoff, U., Pross, J., de Beaulieu, J.L., de Beaulieu, J.-L., Drescher-Schneider, R., Vannière, B., Magny, M., 2011. Holocene seasonality changes in the central Mediterranean region reconstructed from the pollen sequences of Lake Accesa (Italy) and Tenaghi Philippon (Greece). The Holocene 21, 131-146.

Polunin, O., 1980. Flowers of Greece and the Balkans. A Field Guide. Oxford University Press, Oxford.

Popovska, C., Bonacci, O., 2007. Basic data on the hydrology of Lakes Ohrid and Prespa. Hydrological Processes 21, 658-664.

Pross, J., Kotthoff, U., Müller, U.C., Peyron, O., Dormoy, I., Schmiedl, G., Kalaitzidis, S., Smith, A.M., 2009. Massive perturbation in terrestrial ecosystems of the Eastern Mediterranean region associated with the 8.2 kyr B.P. climatic event. Geology 37, 887-890.

Punt, W., Clarke, G.C.S. (Eds.), 1980. The Northwest European Pollen Flora II. Elsevier Scientific Publishing Company, Amsterdam.

Punt, W., Blackmore, S. (Eds.), 1991. The Northwest European Pollen Flora VI. Elsevier Scientific Publishing Company, Amsterdam.

Reille, M., 1998. Pollen et spores d'Europe et d'Afrique du nord (Supplément 2). Laboratoire de Botanique Historique et Palynologie, Marseille.

Reille, M., 1999. Pollen et spores d'Europe et d'Afrique du nord. Laboratoire de Botanique Historique et Palynologie, Marseille.

Reimer, P.J., Baillie, M.G.L., Bard, E., Bayliss, A., Beck, J.W., Blackwell, P.G., Bronk Ramsey, C., Buck, C.E., Burr, G.S., Edwards, R.L., Friedrich, M., Grootes, P.M., Guilderson, T.P., Hajdas, I., Heaton, T.J., Hogg, A.G., Hughen, K.A., Kaiser, K.F., Kromer, B., McCormac, F.G., Manning, S.W., Reimer, R.W., Richards, D.A., Southon, J.R., Talamo, S., Turney, C.S.M., van der Plicht, J., Weyhenmeyer, C.E., 2009. IntCal09 and Marine09 radiocarbon age calibration curves, 0-50,000 years cal BP. Radiocarbon 51, 1111-1150.

Roberts, N., Jones, M.D., Benkaddour, A., Eastwood, W.J., Filippi, M.L., Frogley, M.R., Lamb, H.F., Leng, M.J., Reed, J.M., Stein, M., Stevens, L., Valero-Garcés, B., Zanchetta, G., 2008. Stable isotope records of Late Quaternary climate and hydrology from Mediterranean lakes: the ISOMED synthesis. Quaternary Science Reviews 27, 2426-2441.

Roberts, N., Eastwood, W., Kuzucuog!lu, C., Fiorentino, G., Caracuta, V., 2011. Climatic, vegetation and cultural change in the eastern Mediterranean during the mid- Holocene environmental transition. The Holocene 21, 147-162.

Rohling, E.J., Pälike, H., 2005. Centennial-scale climate cooling with a sudden cold event around 8,200 years ago. Nature 434, 975-979.

Rosi, M., Santacroce, R., 1983. The A.D. 472 'Pollena' eruption: volcanological and petrological data for this poorly-known, Plinian-type event at Vesuvius. Journal of Volcanology and Geothermal Research 17, 249-271.

Rosi, M., Sbrana, A., 1987. Phlegrean Fields. Consiglio Nazionale delle Ricerche, Roma.

Santacroce, R. (Ed.), 1987. Somma-Vesuvius. CNR (Consiglio Nazionale delle Ricer- che), Quaderni de la Ricerca Scientifica 114. Progetto Finalizzato Geodinamica. Monografie Finali 8 CNR, Rome.

Santacroce, R., Cioni, R., Marianelli, P., Sbrana, A., Sulpizio, R., Zanchetta, G., Donahue, D.J., Joron, J.L., 2008. Age and whole rock-glass compositions of proximal pyroclastics from the major explosive eruptions of Somma-Vesuvius: a review as a tool for distal tephrostratigraphy. Journal of Volcanology and Geothermal Research 177, 1-18.

Siani, G., Sulpizio, R., Paterne, M., Sbrana, A., 2004. Tephrostratigraphy study for the last 18,000 ^{14}C years in a deep-sea sediment sequence for the South Adriatic. Quaternary Science Reviews 23, 2485-2500.

Stankovic, S., 1960. The Balkan Lake Ohrid and Its Living World. In: Monographiae Biologicae IX. Dr. W. Junk, Den Haag, The Netherlands.

Sulpizio, R., Mele, D., Dellino, P., La Volpe, L., 2005. A complex, Subplinian-type eruption from low-viscosity, phonolitic to tephri-phonolitic magma: the AD 472 (Pollena) eruption of Somma-Vesuvius, Italy. Bulletin of Volcanology 67, 743-767.

Sulpizio, R., van Welden, A., Caron, B., Zanchetta, G., 2009. The Holocene tephrostratigraphic record of Lake Shkodra (Albania and Montenegro). Journal of Quaternary Science 25, 633-650.

Sulpizio, R., Zanchetta, G., D'Orazio, M., Vogel, H., Wagner, B., 2010. Tephrostratigraphy and tephrochronology of lakes Ohrid and Prespa, Balkans. Biogeosciences 7, 3273-3288.

Tzedakis, P.C., Lawson, I.T., Frogley, M.R., Hewitt, G.M., Preece, R.C., 2002. Buffered tree population changes in a Quaternary Refugium: evolutionary implications. Science 297, 2044-2047.

Vogel, H., Wagner, B., Zanchetta, G., Sulpizio, R., Rosén, P., 2010a. A paleoclimate record with tephrochronological age control for the last glacial-interglacial cycle from Lake Ohrid, Albania and Macedonia. Journal of Paleolimnology 44, 295-310.

Vogel, H., Zanchetta, G., Sulpizio, R., Wagner, B., Nowaczyk, N., 2010b. A tephrostratigraphic record for the last glacial-interglacial cycle from Lake Ohrid, Albania and Macedonia. Journal of Quaternary Science 25 (3), 320-338.

Wagner, B., Reicherter, K., Daut, G., Wessels, M., Matzinger, A., Schwalb, A., Spirkovski, Z., Sanxhaku, M., 2008. The potential of Lake Ohrid for long-term palaeoenvironmental reconstructions. Palaeogeography, Palaeoclimatology, Palaeoecology 259, 341-356.

Wagner, B., Lotter, A.F., Nowaczyk, N., Reed, J.M., Schwalb, A., Sulpizio, R., Valsecchi, V., Wessels, M., Zanchetta, G., 2009. A 40,000-year record of environmental change from ancient Lake Ohrid (Albania and Macedonia). Journal of Paleolimnology 41, 407-430.

Wagner, B., Vogel, H., Zanchetta, G., Sulpizio, R., 2010. Environmental changes on the Balkans recorded in the sediments from lakes Prespa and Ohrid. Biogeosciences 7, 3187-3198.

Wagner, B., Aufgebauer, A., Vogel, H., Zanchetta, G., Sulpizio, R., Damaschke, M., 2012. Late Pleistocene and Holocene contourite drift in Lake Prespa Albania/ F.Y.R. of Macedonia/Greece. Quaternary International 274, 112-121.

Wulf, S., Kraml, M., Brauer, A., Keller, J., Negendank, J.F.W., 2004. Tephrochronology of the 100 ka lacustrine sediment record of Lago Grande di Monticchio (southern Italy). Quaternary International 122, 7-30.

Zanchetta, G., Di Vito, M., Fallick, A.E., Sulpizio, R., 2000. Stable isotopes of pedogenic carbonates from the Somma-Vesuvius area southern Italy, over the past 18 kyr: palaeoclimatic implications. Journal of Quaternary Science 15, 813-824.

Zanchetta, G., Sulpizio, R., Roberts, N., Cioni, R., Eastwood, W.J., Siani, G., Paterne, M., Santacroce, R., 2011. Tephrostratigraphy, chronology and climatic events of the Mediterranean basin during the Holocene: an overview. The Holocene 21, 33-52.

III Vegetation and climate history of the Lake Prespa region since the Lateglacial*

Abstract

Pollen assemblages of a sediment sequence (Co1215) from Lake Prespa reveal substantial vegetational and environmental changes on a regional scale for the Lateglacial and Holocene. The age-depth model, based on radiocarbon dating and tephrochronology, indicates continuous sedimentation for the last c. 17 000 cal BP. An open landscape with prominent cold-resistant steppe vegetation and isolated tree patches (mainly *Pinus*) is inferred. The pollen data suggest the survival of numerous temperate deciduous trees in sheltered and favorable habitats despite the harsh climate conditions. The increase of *Pinus* and the subsequent drop in herb values point to the expansion of pines at higher elevations and/or the thickening of their stands during the Bølling/Allerød. The coeval rise of oak values and the increase of tree diversity imply rising temperatures and an increase in moisture availability. A reversal to stadial conditions, marked by *Artemisia* and Chenopodiaceae maxima, characterizes the Younger Dryas chronozone. Climate change during the Early Holocene resulted in the expansion and subsequent diversification of deciduous woodland. The continuous pollen curves of maquis constituents, such as *Pistacia* and *Phillyrea*, point to higher mean annual and winter temperatures. An abrupt short-lived reversal, associated with the 8.2 cooling event, was distinguished by a distinct peak of *Artemisia* percentages. After 7 900 cal BP arboreal percentages increased and the Prespa area underwent significant changes in floristic composition. The appearance of crop plant pollen and the increase of weed percentages suggest the intensification of agriculture and can be traced back to c. 2 000 cal BP.

Keywords: Lake Prespa, Balkans, pollen analysis, palaeoecology, palaeoclimate, human impact

* This chapter is based on Panagiotopoulos K., Aufgebauer A., Schäbitz F., Wagner B., 2013, Vegetation and climate history of Lake Prespa since the Lateglacial, Quaternary International 293, 157-169, dx.doi.org/10.1016/j.quaint.2012.05.048.

3.1 Introduction

The Balkan Peninsula, situated at the crossroads of several migration routes, is considered as a European biodiversity hotspot (e.g. Petit et al., 2003). Its proximity to Asia Minor and the wider Black Sea region and its heterogeneous topography contributed to a high degree of endemism of its fauna and flora (Griffiths et al., 2004). It has been suggested that during the Quaternary, when glaciation was limited locally to high mountains, plant species were able to migrate westwards across land bridges from Asia Minor, as well as the Pontic regions surrounding the Black Sea enriching the flora with drought tolerant oriental elements (evidence has been provided by recent palaeoecological studies e.g. Magyari et al., 2008). Migration occurred also eastwards (Alpine route) and southwards (Carpathian route) enriching the flora with representative central European and Mediterranean floristic elements (**Figure 3.1**). The Oriental and Pontic components contribute along with the Balkan endemics -including Neogene relicts- to the uniqueness of this old flora, which contains almost half of the 3 500 species endemic to Europe (cf. Turrill, 1929; Polunin, 1980).

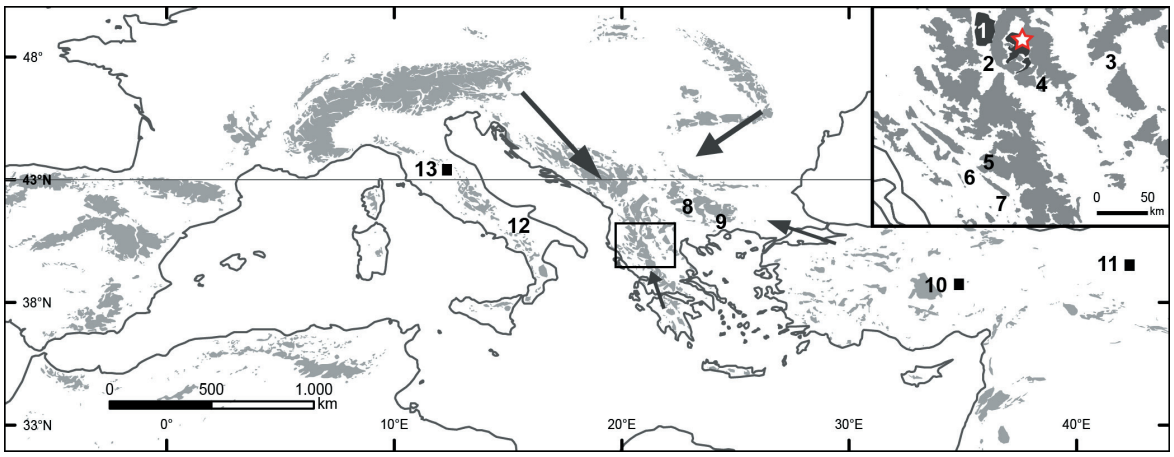

Figure 3.1: Locations of selected terrestrial pollen records and of Lake Prespa (star). Records with charcoal data are marked with a square, flora migration routes are indicated with arrows and highlands (above 1000 m a.s.l.) in gray: 1. Ohrid, 2. Maliq, 3. Nisi, 4. Kastoria, 5. Rezina, 6. Gramousti, 7. Ioannina, 8. Trilistnika, 9. Tenaghi Philippon, 10. Eski Acigöl, 11. Van, 12. Monticchio, 13. Accesa.

There has been an ongoing debate over the migration of temperate trees from southern glacial refugia to northern Europe (e.g. Bennett et al., 1991; Willis, 1994; Tzedakis et al., 2002) or their potential survival in situ (e.g. Willis and van Andel, 2004; Bhagwat and Willis, 2008; Birks and Willis, 2008). The latitudinal and altitudinal location of a site are critical parameters for their pursuit. The survival of tree communities, such as the five-needled Macedonian Pine (*Pinus peuce*) with a presumed Neogene origin, provides hard evidence for the importance of the Prespa region in this context during preceding climate oscillations.

Lake Prespa is presumed to be a remnant of an extensive lake system, consisting formerly of Lake Ohrid and the recently drained Lake Maliq (Hollis and Stevenson, 1997). Within the basin, which is enclosed by high mountains, lowlands represent nowadays a rather small stripe of land

along its banks (**Figure 3.2**). Signs of lakeside settlements in the vicinity of Prespa (Fouache et al., 2010; Karkanas et al., 2011) suggest a continuous occupation of the wider region since Neolithic times.

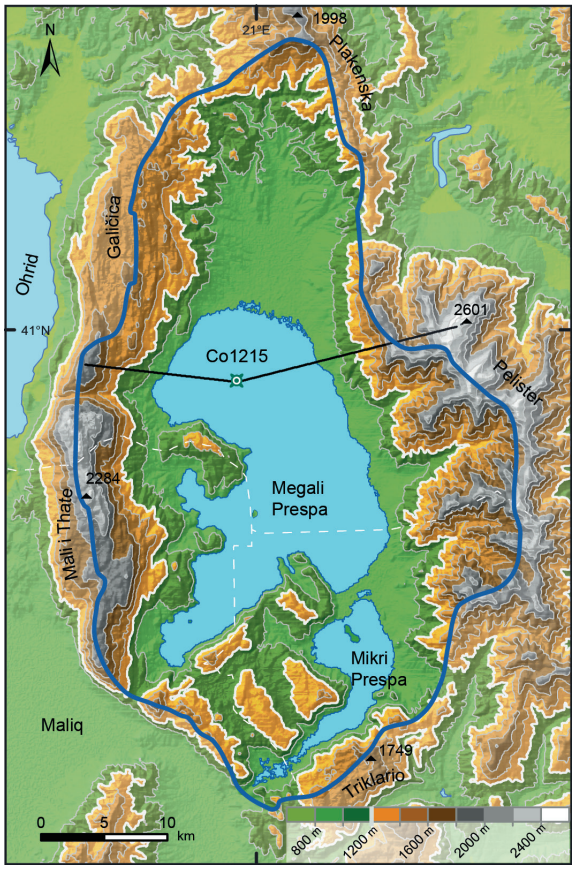

Figure 3.2: Topography of Lake Prespa. Lake catchment (blue line), core location (Co1215) and vegetation transects (black lines) are shown (SRTM Data: Jarvis et al., 2008).

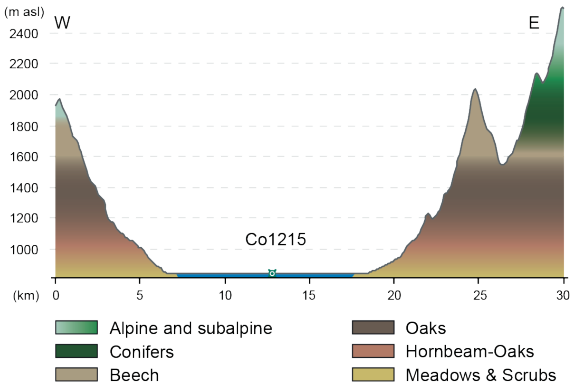

Figure 3.3: Simplified altitudinal vegetation belts on a transect of the Lake Prespa catchment (SRTM Data: Jarvis et al., 2008).

This study aims to reconstruct the vegetation and climate history of the region, on a centennial scale, based on palynomorph and microscopic charcoal data from Lake Prespa. Therefore, the role of intrinsic ecological factors, such as migration, competition and succession, is examined in an area that has sustained temperate tree populations over long time intervals. Consideration is also given to the role of humans in shaping the landscape on a local scale.

In comparison to other corners of the Balkans, a rather dense network of palaeorecords exists in the wider region (**Figure 3.1**). A selected number of these localities (especially sites containing fire and lake-level history) along with marine ones (e.g. Ariztegui et al., 2000; Gogou et al., 2007; Geraga et al., 2008; Kotthoff et al., 2008a) were used to reconstruct distinct patterns (e.g. seasonality shifts, precipitation gradients, deforestation) occurring at a greater spatial scale.

Sedimentological, geochemical and hydrological analyses that preceded (e.g. Matzinger et al., 2006; Wagner et al., 2010; Aufgebauer et al., 2012; Wagner et al., 2012) shed light to many aspects of this new site. It is noticeable, however, that the Younger Dryas, a major climatic event characterizing the end of the Pleistocene, remained undetected by the geochemical proxies already applied. This apparent discrepancy underlines the importance of multi-proxy investigations for the sound understanding of palaeorecords.

3.2 Study site

The transboundary Prespa catchment (c. 1300 km^2) comprises two lakes (**Figure 3.2**): Megali and Mikri Prespa, with an approximate surface area of 253.6 km^2 and 47.4 km^2 respectively (Hollis and Stevenson, 1997), separated by an alluvial isthmus located in the Greek side. The two lakes, which formed a single lake once, are nowadays connected through a man-made channel. Lake Megali Prespa, hereafter referred to as Lake Prespa, is situated at an altitude of 849 m a.s.l. and is surrounded by mountains with the highest peak at 2601 m a.s.l. (Pelister) to the east, and several other peaks around or above 2000 m a.s.l. to the west and the north (**Figure 3.2**).

Karstified dolomites and limestones dominate the western and southern part of the catchment, while metamorphic rocks and granites the eastern. Lake Prespa has no surface outflow, however, it is connected through karst channels traversing the Galičica Mountain to the neighboring Lake Ohrid standing at 693 m a.s.l. (Matzinger et al., 2006). It has a mean water depth of 14 m (48 m maximum) (Matzinger et al., 2006).

The climate of the area is transitional and can be classified as sub-Mediterranean with continental influences. Mean July and January temperatures in the lowlands are 21°C and 1°C respectively, with a mean annual temperature of 11°C. Precipitation peaks in winter (when snowfalls are frequent) and drops in summer. It varies from 750 mm in the lowlands to over 1200 mm in the mountains (Hollis and Stevenson, 1997). The diverse topography, the exposure of slopes and valleys, as well as the presence of a large water body create a complex patchwork of microclimates in the catchment that is also reflected in the vegetation.

It should be noted that the Prespa catchment has more than 1500 plant species (cf. Society for the Protection of Prespa, 2011). For instance, the flora of the National Park in the Greek side is composed of 1326 vascular plant species (Pavlides, 1997). Its location at a transitional climatic zone leads to a mixture of central European, Mediterranean and Balkan endemic species (Polunin, 1980). In the western part mixed deciduous woods of *Carpinus* (*C. betulus* and *C. orientalis*/*Ostrya carpinifolia*) with characteristic transitional Mediterranean elements (pseudo-maquis), such as deciduous *Pistacia terebinthus* and evergreen *Phillyrea latifolia*, can be found at lower elevations on rocky slopes. On the southern limestone hills a mixed evergreen-deciduous scrub, including the aforementioned maquis species as well as Greek and Stinking Juniper (*J. excelsa* and *J. foetidissima*), *Buxus sempervirens*, and *Quercus trojana*, is encountered. Another transitional plant community that characterizes the mountainous landscape in the eastern part is the distinctive climax communities of *Pinus peuce*, associated with *Pteridium aquilinum* or *Vaccinium myrtillus* (at higher elevations).

The modern vegetation was classified into a simplified zonation scheme on a transect (W-E) of the catchment presented in **Figure 3.3**. The major altitudinal formations encountered in this representative transect are the wet meadows and grasslands of the littoral zone, the mixed deciduous oak forests (dominated by *Q. trojana*, *Q. cerris*, *Q. frainetto*, *Q. pubesens*, *Q. petraea*, *Q. robur*) below 1600 m a.s.l., the montane deciduous forests (with *Fagus sylvatica* prominent) below 1800 m a.s.l., the montane conifer forests (*Abies borisii-regis*, *Pinus peuce*, *P. sylvestris*, *P. nigra*, *P. heldreichii*) below 2200 m a.s.l., and the subalpine and alpine meadows above the tree-line (Pavlides, 1997; Avramovski, 2006).

3.3 Materials and Methods

Here we present the upper 320 cm of the composite core Co1215 (40°57'50'' N, 20°58'41'' E), retrieved in November 2009, from a distal location at the northern part of Lake Prespa (14.5 m depth). The coring location was chosen based upon the results of a shallow hydro-acoustic survey (Wagner et al., 2012) that revealed relatively undisturbed sedimentation at the site. For core recovery, a floating platform equipped with a gravity corer for surface sediments and a percussion piston corer for deeper sediments (UWITEC Co, Austria) were used.

3.3.1 Chronology

The age model for the upper 320 cm of core Co1215 is based on accelerator mass spectrometry (AMS) ^{14}C dates measured at the ETH Laboratory in Zurich and tephra layers correlated to distinctive eruptions of Italian volcanoes (**Table 3.1**). A detailed discussion of the age model can be found in Aufgebauer et al. (2012, and references therein). Radiocarbon dates were calibrated into calendar years (cal BP) using the INTCAL09 calibration curve (Reimer et al., 2009) and for the uppermost sample using the Levin.14c dataset (Levin and Kromer, 2004). All ages presented in this paper are calibrated.

3.3.2 Sedimentological analyses

The methodology and equipment used for sedimentological analyses, performed in the laboratory of the Institute of Geology and Mineralogy of the University of Cologne, are described in detail by Aufgebauer et al. (2012). One core half was photographed, described, scanned with a XRF scanner at a resolution of 2 mm and then archived. The other core half was sampled continuously at 2 cm intervals and the samples were freeze-dried and ground. Subsamples were taken for geochemical (CNS, TC, TIC, TOC) and grain-size analyses.

3.3.3 Palaeontological analyses

Sixty sediment subsamples, with a dry weight of approximately 1 g, were taken at 2-8 cm intervals. After determining their volume, samples were sieved (112 μm) and then processed using standard palynological techniques including treatment with 10% HCl, 10% KOH, 40% HF, and acetolysis (Faegri et al., 2000). An exotic marker, i.e. *Lycopodium* tablets with a known amount of spores (Stockmarr, 1971), was added to each sample before treatment to enable calculation of pollen, spore and micro-charcoal concentrations. Identification of pollen and other palynomorphs was facilitated by their relatively good preservation and was performed with relevant keys and atlases (Beug, 2004; Moore et al., 1991; Reille, 1998; Reille, 1999; Punt and Clarke, 1980; Punt and Blackmore, 1991), as well as the reference collection of the Laboratory of Palynology of the University of Cologne, Seminar of Geography and Education. An average of 500 and a minimum of 300 terrestrial pollen grains were counted per sample. In addition, charcoal particles (>10 μm) were counted in the pollen slides. The average sample temporal resolution, derived from the presented age model, is c. 300 years. The relative percentages of the presented taxa are based upon the sum of terrestrial pollen (excluding Cyperaceae, obligate aquatics and spores). All diagrams were plotted using TILIA and TILIA Graph (Grimm, 1992).

Given the size of the catchment and its surface area, the source area of the pollen of Lake Prespa can be assumed to be mainly of regional origin (cf. Jacobson and Bradshaw, 1981; Davis, 2000). The selected taxa presented comprise trees, shrubs, vines, herbs, aquatics, ferns, algae and fungi. In addition, the terrestrial pollen accumulation rate (grains cm^{-2} $year^{-1}$) and the micro-charcoal particles influx (particles cm^{-2} $year^{-1}$) are plotted. The latter provides valuable insights concerning the duration and intensity of summer drought (cf. Vannière et al., 2011).

The taxonomic nomenclature follows Beug (2004). *Pinus* includes undifferentiated haploxylon (*P. peuce*) and diploxylon types (*P. heldreichii*, *P. sylvestris* and *P. nigra*). *Abies* grains belong to *A. borisii-regis*, a hybrid of *A. alba* and *A. chephalonica*. Single *Picea* grain occurrences recorded mainly during the Lateglacial are considered of extra-local origin. *Quercus* pollen is represented by several deciduous species, including endemics (e.g. semi-deciduous *Quercus trojana*). *Quercus* pollen was classified into two major groups, namely *Q. robur*-type and the thermophilous *Q. cerris*-type. Evergreen oak pollen grains were also encountered and probably originate from outside the Lake Prespa catchment, since they are not registered in modern local vegetation (Pavlides, 1997; Avramovski, 2006). They are grouped together with the thermophilous oak type. *Ephedra* consists of *E. fragilis* and *E. distachya*. *Carpinus* comprises *Carpinus betulus* and *Carpinus orientalis*/*Ostrya carpinifolia*, with the latter accounting for the majority of the grains counted. *Pistacia* grains belong to the deciduous *P. terebinthus*. The Asteroideae group includes the grains of *Anthemis*, *Senecio* and *Cirsium* types. Ericaceae belong to *Vaccinium* type. Other taxa of the Asteraceae family are presented separately, namely *Artemisia*, *Centaurea* and Cichorioideae. The *Plantago* group consists of *P. lanceolata*, *P. media*/*major* and undifferentiated other *Plantago* types. Cerealia consist of grasses with a pollen grain size greater than 40 μm, which might also include wild cereal types. *Pediastrum* comprises *P. boryanum* and *P. simplex*. *Botryococcus* includes *B. braunii* and *B. pila*. Ascospores belong mostly to *Sporormiella* sp.

3.4 Results

3.4.1 Age model

Fourteen AMS radiocarbon dates and four correlated tephra layers (**Table 3.1**) were used for the establishment of the chronology (**Figure 3.4**). Parallel dating of macrofossils and bulk in two horizons revealed a significant reservoir and/or hard-water effect that has/have not been constant over time. Aufgebauer et al. (2012) elaborate on the discrepancy between these offsets and on the choice of the AMS dates used in the age model. In addition, they present the composition of the identified tephra layers and discuss their correlation. According to the age-depth model, the base of the sediment sequence can be extrapolated to c. 17 ka cal BP.

Table 3.1: AMS dates and identified tephra layers in core Co1215.

Sample	Depth (cm)	Material	^{13}C (‰)	^{14}C Age (a BP)	Calendar Age (a cal BP [2σ]
ETH-40050	4 - 6	shell (*Dreissena presbensis*)	-0.8 ± 1.1	-1190 ± 30	(-15) ± 1
Col1030	42 - 44	plant (*Carex* sp.)	-16.5 ± 0.1	715 ± 28	630 ± 64
ETH-40051	74 - 76	plant (*Phragmites australis*)	-27.9 ± 1.1	2080 ± 35	2066 ± 80
ETH-40052	74 - 76	bulk organic matter	-26.9 ± 1.1	3095 ± 35	3312 ± 73
Col1031	104 - 108	bulk organic matter	-30.2 ± 0.1	6003 ± 28	6842 ± 90
ETH-40054	128 - 130	bulk organic matter	-28.3 ± 1.1	7055 ± 40	7892 ± 70
ETH-40055	146 - 147	bulk organic matter	-26.8 ± 1.1	8205 ± 40	9157 ± 127
ETH-40056	166 - 168	plant (*Phragmites australis*)	-26.2 ± 1.1	8755 ± 35	9752 ± 152
ETH-40057	166 - 168	bulk organic matter	-27.8 ± 1.1	9090 ± 35	10,244 ± 50
ETH-40059	184 - 186	bulk organic matter	-26.5 ± 1.1	9840 ± 35	11,241 ± 40
ETH-40060	212 - 214	fish remain	-12.5 ± 0.0	10,837 ± 132	12,815 ± 261
ETH-40062	214 - 216	fish remain	-17.1 ± 0.0	11,466 ± 121	13,358 ± 250
ETH-40063	214 - 216	bulk organic matter	-24.3 ± 1.1	11,005 ± 40	12,889 ± 187
Col1032	301 - 303	plant (aquatic)	-5.4 ± 0.1	14,056 ± 71	17,159 ± 301

Sample	Depth (cm)	Correlated to	Calendar Age (a cal BP)	Age Reference
PT0915-1	55.4 - 55.6	AD 472/512	1478/1438	Santacroce et al., 2008
PT0915-2	155.6 - 156.2	Mercato	8540 ± 50	Zanchetta et al., 2011
PT0915-3	265 - 267	LN1	14,697 ± 519	Siani et al., 2004
PT0915-4	287 - 289	LN2	15,551 ± 621	Siani et al., 2004

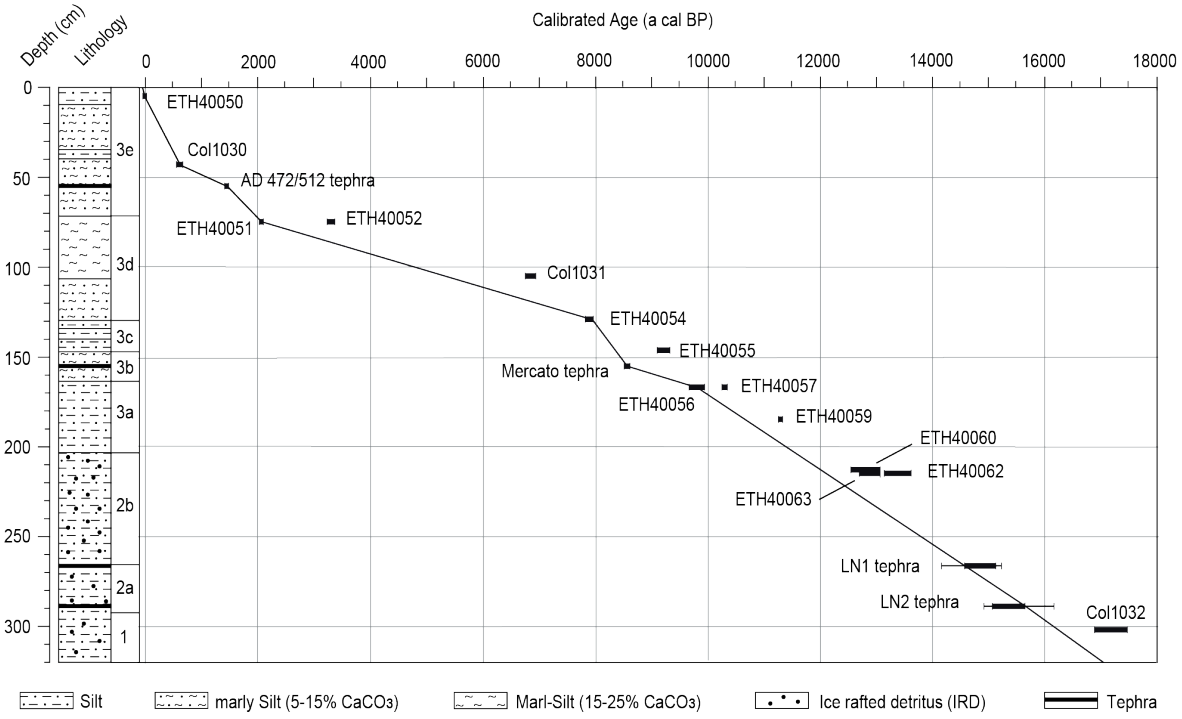

Figure 3.4: Age-depth model with lithology of core Co1215 (modified from Aufgebauer et al., 2012). Reliable age control points were interpolated on a linear basis.

3.4.2 Pollen Assemblage Zones

Two major pollen assemblage zones (P-1 and P-2) and several subzones were assigned based on visual inspection of the pollen record and supported by stratigraphically constrained incremental sum of squares analysis for terrestrial pollen taxa (>2%) as implemented in TILIA (Grimm, 1992). Zone numbers and letters were designated with ascending order from top to bottom. A summary of the pollen assemblage zones (PAZs) description along with changes in potassium (K) and total organic carbon (TOC) are given in **Table 3.2**.

Zone P-2 is characterized by high non-arboreal pollen (NAP) percentages (e.g. *Artemisia* (20%), Chenopodiaceae (10%), Poaceae (20%) and maximum percentages of other Asteraceae components). In subzone P-2c, *Pinus* reaches its maximum values (~60%), as well as *Juniperus*, *Hippophaë*, and *Ephedra*. Arboreal pollen (AP) percentages (and influx values) rise significantly in P-2b and distinct abrupt fluctuations are recorded mostly in *Pinus* percentages. *Pinus* values decline abruptly at the top of P-2b and recover partly in P-2a, but never reach percentages above 40% thereafter. In contrast, *Quercus* values expand gradually from P-2c to P-2a, while *Abies* retains low and rather stable values throughout this zone (P-2). *Ulmus*, *Corylus*, *Carpinus*, *Acer* and *Betula* are present in the spectrum intermittently in P-2c, but show continuous curves thereafter (P-2b and P-2a). Taxa excluded from the pollen sum, such as aquatics and fern spores, have relatively low and stable percentages throughout P-2, with some exceptions (e.g. Cyperaceae). Accumulation rates of green algae and microscopic charcoal particles are low, but with an increasing trend towards the top of the zone (P-2a).

Table 3.2: Synoptic description of pollen assemblage zones (PAZs).

	PAZs (cm, ka cal BP)	Lithology and Geochemistry	Palynomorphs and Micro-charcoal
Middle and Late Holocene	P-1a (0 - 38 cm, c. 0.5 - Present)	high (low) K (TOC)	Further tree pollen decrease, *Pinus* gradual increase and *Q. cerris*-type decrease, *Fagus* and *Juglans* maxima (10% and 3%), continuous *Buxus* and Ericaceae curve; Cerealia, *Plantago* and *Capsella* maxima; Cyperaceae and *Typha* increase; maximum influx values of *Pediastrum* and *Botryococcus*; charcoal peaks
	P-1b (38 - 70 cm, c. 1.9 - 0.5)	high (low) K (TOC)	Trees retract, *Q. cerris*-type and *Carpinus* maxima (25% and 15%); continuous *Juglans* curve; *Vitis* occurrences; Poaceae and Cerealia increase; influx decrease (trees and herbs)
	P-1c (70 - 132 cm, c. 7.9 - 1.9)	low (high) K (TOC)	*Carpinus*, *Corylus* and *Alnus* maxima (15%, 8% and 6%), gradual *Fagus* and *Pinus* expansion and decline of *Abies*; continuous *Phillyrea*, *Olea*, *Rumex*, *Plantago* and *Humulus* curves; rising tree influx values (*Pinus* maximum); continuous *Pediastrum* and Ascospores curves with maxima; charcoal peaks
8.2 event	P-1d (132 - 148 cm, c. 8.3 - 7.9)	abrupt K (TOC) increase (decrease)	Distinct *Artemisia* and Poaceae peaks (5% and 10%); oscillations in AP % and a total 10% decrease; *Myriophyllum* maximum; charcoal peaks; *Botryococcus* maximum; abrupt (AP + NAP) influx fluctuations with a decreasing trend

	PAZs (cm, ka cal BP)	Lithology and Geochemistry	Palynomorphs and Micro-charcoal
Early Holocene	P-1e (148 - 204 cm, c. 11.5 - 8.3)	K (TOC) decreases (increases) gradually	*Quercus* (up to 45%), expansion of thermophilous deciduous tree values, *Pinus* % decrease and *Abies* maximum (15%), *Betula* and *Ulmus* maximum and gradual retreat; *Hippophaë* and *Ephedra* decrease; Herbs retract; continuous *Pistacia* and *Fraxinus* curve; single occurrences of *Sanguisorba* minor and *Juglans* grains; *Typha* maximum (5%); maximum influx values
YD	P-2a (204 - 240 cm, c. 13.2 - 11.5)	K (TOC) constant; sporadic occurrence of IRD	Marked NAP (*Artemisia*, Chenopodiaceae percentage and influx maxima) expansion (60%); pronounced *Pinus* decrease (<40%), resurgence of *Hippophaë* and *Ephedra* values, *Betula* maximum (5%); *Sparganium* maximum (3%)
B/A	P-2b (240 - 277 cm, c. 15 - 13.2)	K (TOC) decreases (increases) gradually and plateaus; sporadic occurrence of IRD	*Pinus* maxima and distinct fluctuations (40% - 55%), *Quercus* values expansion; NAP % contract, Chenopodiaceae and *Artemisia* values decrease, Poaceae maximum; Ferns increase; influx values increase gradually (mainly *Pinus*)
LG/OD	P-2c (277 - 320 cm, c. 17 - 15)	high (low) K (TOC); sporadic occurrence of IRD	*Pinus* (>30%), several deciduous trees present (<10%); *Hippophaë* and *Ephedra* maxima; Herbs (mainly steppic taxa) dominant; Cyperaceae maximum; very low influx values (AP + NAP)

In zone P-1 arboreal percentages increase to 90% (P-1e), stabilize and decline towards the top of the sequence (P-1b, P-1a). P-1e is marked by the expansion of *Abies* percentages along with those of several deciduous trees and the parallel decline of *Pinus* and *Betula* percentages. Meanwhile, non-arboreal taxa (including shrubs and herbs) decrease gradually with minimum values at the end of this subzone (P-1e). Continuous curves of maquis vegetation components (e.g. *Pistacia* and *Phillyrea*) and sporadic occurrences of *Fagus*, *Olea* and *Juglans* pollen are recorded. The distinct peaks of *Artemisia* and Poaceae percentages coupled with the abrupt fluctuations of tree percentages (mainly conifers and oaks) characterize subzone P-1d. In addition, an abrupt drop of terrestrial pollen and green algae influx with a rather constant and high micro-charcoal influx are recorded. In P-1c, NAP percentages drop and several deciduous trees reach their maximum values (e.g. *Carpinus*, *Corylus*, *Alnus*). *Pinus* and *Q. cerris*-type percentages increase, while *Q. robur*-type, *Ulmus* and to a lesser extent *Abies* percentages decline. Maquis elements are continuously present, but with low values. A pronounced maximum in fungi spores is also recorded within this subzone. In P-1b, *Carpinus* and *Fagus* values increase, while conifer (notably *Pinus*) values decline. Crop plant pollen (*Cerealia*, *Juglans* and *Olea*) rises in the spectrum, accompanied by pollen of several other herbs (e.g. *Artemisia*, *Plantago*, *Rumex*, other Asteraceae). During this subzone, terrestrial pollen, green algae, and micro-charcoal accumulation rates decline in contrast to P1-a. A further expansion of herb and cultivar values, the decline of tree (except *Pinus*) values and the increase of shrub values are characterizing P-1a.

3.5 Discussion

3.5.1 Late Pleniglacial/Oldest Dryas (P-2c; c. 17 000 – 15 000 cal BP)

Pollen assemblages from subzone P-2c suggest a rather open landscape with prominent herbaceous steppe communities of *Artemisia* and Chenopodiaceae, along with grasses (Poaceae), Asteroideae, Cichorioideae and *Centaurea* (**Figure 3.6**). A relatively rich shrub component, containing mainly *Hippophaë*, *Juniperus* and *Ephedra*, is also registered in the pollen spectrum (**Figure 3.5**). A notable feature during the glacial is the almost even arboreal and non-arboreal percentages in the Prespa pollen record. In contrast to other neighboring sites, such as Maliq (Bordon et al., 2009), Ioannina (Lawson et al., 2004) and Tenaghi Philippon (Müller et al., 2011), arboreal percentages never drop below 40%. In most likelihood, this can be attributed to the influence of the local topography which fostered tree growth and contributed to the altitudinal distribution of diverse habitats within the basin. Despite the relative abundance of tree taxa, very low pollen influx values and high potassium counts (**Figure 3.7**), indicating fine clastic matter supply into the lake, confirm the notion of sparse vegetation within the catchment.

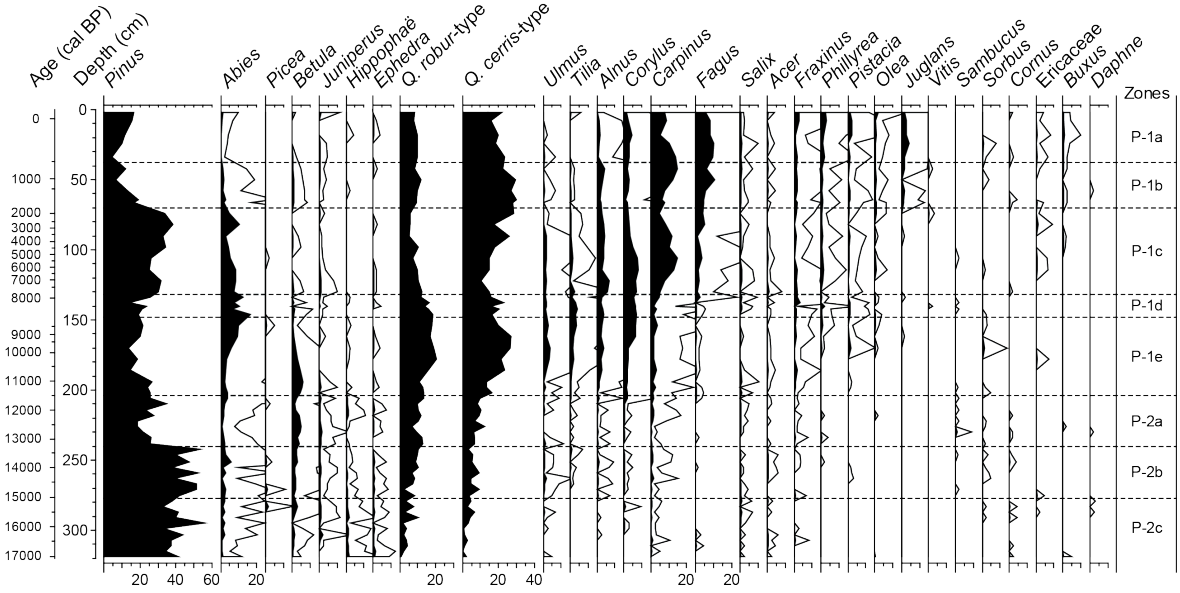

Figure 3.5: Pollen percentage diagram of core Co1215: selected trees, shrubs and vines (Exaggeration x 10).

There is, however, a remarkable diversity of tree pollen given the harsh climate conditions of the last glacial. Arboreal percentages are dominated by Pinus, including shrub (Krummholz) forms at higher elevations. The continuous *Abies* curve, despite its low values, implies its survival within the catchment of Lake Prespa. The isolated occurrence of *Picea* pollen (<2%) at the top of this subzone (P-2c) most likely indicates the presence of this taxon outside of the catchment, although spruce might be present locally at a site when pollen percentages are below 2% or even 1% (cf. Latałova and van der Knaap, 2006 and references therein). *Quercus* appears to be the most abundant arboreal taxon after *Pinus*. The presence of the former along with pollen of sev-

eral other temperate deciduous trees implies their existence in sheltered locations within the catchment area (with sufficient moisture and favorable temperature for growth). The existence of glacial refugia for temperate trees at mid-altitude locations in the Balkans has been discussed extensively elsewhere (e.g. Bennett et al., 1991; Willis, 1992; Willis, 1994; Tzedakis et al., 2002). The findings suggest that the Prespa region was such a glacial refugium.

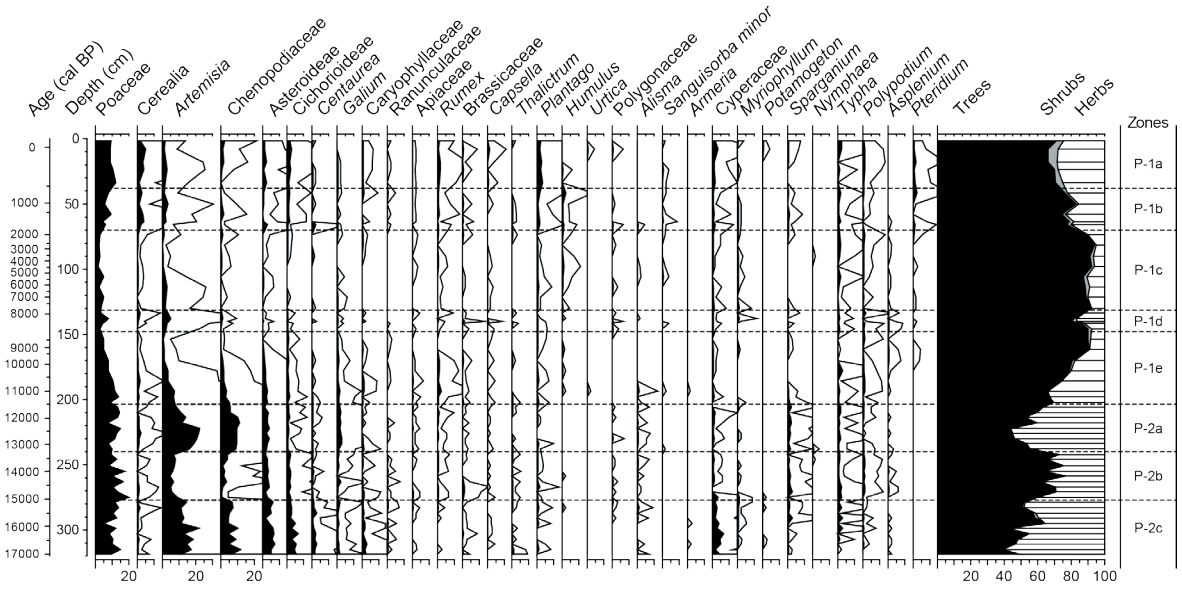

Figure 3.6: Pollen percentage diagram of core Co1215: selected herbs, aquatics and ferns (Exaggeration x 10).

The relatively high Cyperaceae percentages throughout this interval indicate rather well developed sedge communities, which usually thrive at seasonally flooded ground near the lake margin. This could be related to releases of melt water from local ice caps (Hughes et al., 2006a; , 2006b) resulting to local flooding events during late spring or summer. Alternatively, it can also be attributed to the melting of the lake ice cover. Aufgebauer et al. (2012) interpret the sporadic occurrence of coarse sand and gravel (>630 μm fraction) in this interval as ice rafted debris (IRD) and suggest at least partial ice cover of Lake Prespa in wintertime.

According to the age model, the subzone P-2c corresponding to the time interval between 17 000 and 15 000 cal BP can be linked climatostratigraphicaly to the Oldest Dryas/Heinrich 1 event (H1) or the Greenland Stadial 2a (GS-2a) in GICC05 (Lowe et al., 2008 and references therein). The pollen inferred palaeoclimate in the Prespa region seems to be in agreement with cores from the Ionian (Geraga et al., 2008) and the Adriatic Sea (Ariztegui et al., 2000) that point to cold and productive waters during this interval. Eastwards from Prespa, sea surface temperature (SST) reconstructed from planktic foraminifera and pollen reconstructed mean annual precipitation and temperature from a core retrieved from the Aegean Sea (Kotthoff et al., 2011), show particularly cold and dry conditions for this period culminating around 16 500 cal BP.

3.5.2 Bølling/Allerød Interstadial (P-2b; c. 15 000 – 13 200 cal BP)

The pollen record of Lake Prespa depicts distinct climate oscillations in this interval. Tree percentages expanded rapidly (70%) implying the colonization of new grounds at the expense of herb communities. The bulk of this expansion is due to *Pinus*, while *Quercus* seems to increase more gradually along with *Abies* and *Betula* percentages. The continuous curves of *Ulmus*, *Corylus*, *Carpinus*, *Alnus*, and the first appearance of *Tilia* pollen imply warmer and moister conditions (decreasing evapotranspiration). This shift in moisture availability is corroborated by the abrupt decrease of herbaceous steppe taxa relative abundances, notably *Artemisia* and Chenopodiaceae, and the concurrent increase of grasses. Assuming that moisture availability was the limiting factor during the preceding subzone, the occupation of new and/or higher elevation grounds by the hardy *Pinus* could be a possible explanation for its abundance. For instance, *Pinus peuce* has nowadays its optimum range at altitudes between 1500 and 2000 m. At this latitude, it is superior to spruce (*Picea*) due to its greater resistance to summer drought and its considerable capacity to grow at low temperatures (Bohn et al., 2004). *Picea* grains were also encountered in P-2b. Although spruce pollen morphology facilitates the dispersal of its grains over long distances, palaeoecological evidence (Latałova and van der Knaap, 2006) shows that *Picea* is not overrepresented in the pollen assemblages. Nevertheless, its irregular presence and low percentages (<1%) in the Lake Prespa record point to extra-local origin. Most probably, the Lake Prespa region was outside of the southern range limit of spruce, although the taxon must have been present in the vicinity of the catchment.

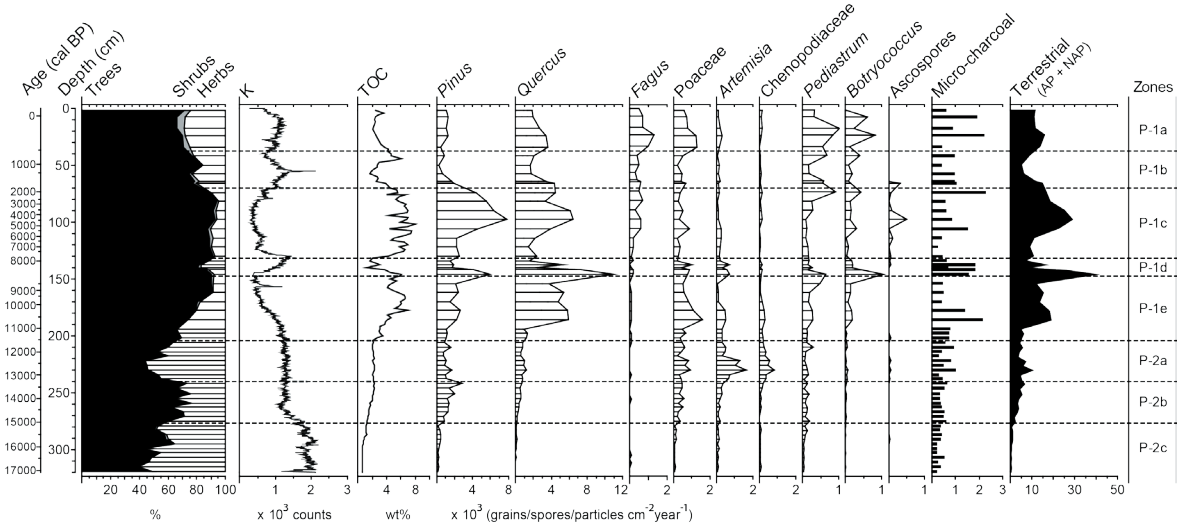

Figure 3.7: Composite diagram of core Co1215: pollen percentages of trees, shrubs and herbs; potassium counts; total organic carbon percentages; accumulation rates of selected pollen taxa, green algae, fungi, micro-charcoal and terrestrial pollen.

The ascending treeline most likely facilitated the parallel expansion of deciduous trees (mainly *Quercus*) reducing inter- and intraspecific competition. An alternative explanation could be the thickening of existing tree stands, with *Pinus* and *Betula* expanding on more challenging soils. It

seems plausible that both scenarios materialized, given the marked drop in soil erosion (inferred from decreasing potassium counts) and the gradual rise of TOC values suggesting increased productivity and/or less decomposition in the lake. However, the accumulation rates of *Pinus* and *Quercus* imply a rather gradual expansion and an open-woodland landscape. Sedgelands contracted in favor of shallow-water aquatic plants (e.g. *Sparganium*) suggesting more stable conditions in the littoral zone. This is in agreement with the ongoing deglaciation (Hughes et al., 2006a) and consequently with the reduced glacier melt-water supply and lower clastic input into the lake as it is suggested by decreasing K (Aufgebauer et al., 2012). Nevertheless, the occurrence of IRD implies that the lake was still covered with ice, at least partially, during winters.

The climatic signal inferred for this chronozone (corresponding to GI-1e-a cf. Lowe et al., 2008) can be traced across several Mediterranean sites (e.g. Dormoy et al., 2009; Watts et al., 1996), but it differs in its expression locally. For instance, in Monticchio (Watts et al., 1996), Accesa (Drescher-Schneider et al., 2007) and Ioannina (Lawson et al., 2004) the onset of the Bølling/Allerød is marked by the expansion of deciduous tree values (mostly *Quercus*) and in Bulgaria (e.g. lake Trilistnika Tonkov et al., 2008) by *Pinus*. In Maliq (Bordon et al., 2009), and Nisi (Lawson et al., 2005) a pattern similar to the one from Prespa can be observed.

3.5.3 Younger Dryas (P-2a; c. 13 200 – 11 500 cal BP)

An abrupt vegetation response with stadial-like characteristics marks PAZ P-2a. The expansion of *Artemisia* and Chenopodiaceae values, after their equally abrupt retreat in the preceding zone, suggests increasing aridity in the region. However, percentages of grasses and other non-steppe herbs (e.g. Asteroideae) remain relatively stable and are well represented. *Centaurea* and *Thalictrum* decrease and *Galium* reaches maximum values at this time. These shifts in the herbaceous vegetation, point to similar climatic conditions to zone P-2c, but also with distinct deviations, suggesting a cold and arid environment. The readvance of *Juniperus*, *Hippophaë* and *Ephedra* was favored by increasing aridity. The pronounced minimum in *Pinus* percentages around 12 500 cal BP indicates the abrupt opening of the landscape. *Betula* values continue to increase implying a colder climate, but with sufficient moisture available for growth. *Quercus* values show a similar trend with minor setbacks. Drought-sensitive deciduous trees seem to decrease at the bottom of P-2c or even disappear completely (e.g. *Ulmus*) and increase modestly towards its top. All of the above observations point to a major restructuring of the vegetation within the catchment. Terrain permitting colonization by *Pinus* during the preceding interval became unsuitable to sustain tree growth and consequently it was occupied by herbaceous steppe communities. This could be interpreted as the signature of a descending treeline. On the other hand, the established *Betula* and *Quercus* tree stands (in mid and/or low altitudes) remained relatively unaffected. Towards the top of the zone, pines gained traction and infiltrated the open deciduous tree stands, and steppe elements retreated once again signaling the termination of the Lateglacial.

The sporadic occurrence of IRD and the accumulation rates of trees and herbs support the notion of a cold climate and an open landscape with scattered tree stands. The rather constant potassium counts imply that the clastic input supply in the catchment remained similar to P-2b. In light of these observations, it seems plausible that the descending treeline, which affected

mostly pines, was responsible for the observed rise in steppic herbs and that the vegetation cover, at least in the lowlands, remained mostly unaffected. The unaltered abundance of shallow-water aquatics, namely *Sparganium* and *Typha*, suggest that the littoral zone was rather stable without excluding some seasonal flooding events, which can be inferred from the Cyperaceae peak towards the top of the zone.

The existence of Younger Dryas in several records across the eastern Mediterranean region was demonstrated by Rossignol-Strick (1995) and its expression was linked to a marked Chenopodiaceae and *Artemisia* peak, indicating a return to almost glacial conditions. The response of trees to this event, however, seems to differ substantially from site to site. For instance in Monticchio (Watts et al., 1996), where *Pinus* plays a limited role in the vegetation, the decline of *Quercus* is coupled with the parallel expansion of *Betula* values. Kotthoff et al. (2008a) documented a similar decrease in *Quercus* relative abundance from a marine core located at northern Aegean. In Bulgaria (Tonkov et al., 2008), where *Pinus* dominates the spectrum, the decline of *Pinus* is also combined with the expansion of *Betula*, but with very low total arboreal percentages due to the elevation of the site (2216 m a.s.l.).

Pollen records located in the vicinity of Prespa demonstrate a rather mixed reaction of the arboreal vegetation during the YD chronozone. In Maliq (Denèfle et al., 2000), low values and abrupt oscillations are detected in *Pinus*, *Quercus* and *Betula* values and an abrupt decline of annual temperature and precipitation is reconstructed (Bordon et al., 2009). In Nisi (Lawson et al., 2005) and Ioannina (Lawson et al., 2004), *Quercus* percentages are expanding gradually, as it is the case in Prespa, but *Pinus* percentages seem to remain relatively stable contrary to its pronounced minimum in Prespa. This could be tentatively attributed to the lower elevation of the sites (below 500 m a.s.l.), the limited role of *Pinus* in the pollen spectrum, as well as to differences in the pollen catchment size in comparison to Prespa.

In contrast to the rather subdued response of the vegetation at Ioannina, Wilson et al. (2008) demonstrated the unequivocal climatic signal of YD using diatoms. In a chironomid-based climate reconstruction from the southern Carpathians, Tóth et al. (2012) report a rather weak reconstructed summer temperature decline and show a noticeable YD vegetational signal implying significant cooling and decreasing moisture availability. Similarly, in Prespa, the apparent disparity between the different proxies (subdued geochemical/hydrological and strong vegetational response to YD, see also Aufgebauer et al., 2012) can be attributed to a large winter temperature decline and moisture deficit. This seems to be in agreement with regional climate model simulations (Rensen and Isarin, 2001) that suggest a negligible decline in summer temperatures in this region, but a significant winter temperature drop coupled with changes in the seasonality of precipitation. Bordon et al. (2009) based on pollen data reconstructions estimate a pronounced decline in annual temperatures (c. 10°C) and precipitation (c. 400 mm). The abrupt decline of annual temperature and precipitation across the Mediterranean is also inferred from marine cores (e.g. Gogou et al., 2007; Dormoy et al., 2009; Kotthoff et al., 2011).

3.5.4 Early Holocene (P-1e; c. 11 500 – 8 300 cal BP)

This period signals the expansion of trees at the expense of herbs in the Prespa catchment. This expansion is gradual and some of the arboreal taxa reach maximum values within the zone. *Quercus* formed closed forests as it is implied by its accumulation rates and relative abundances. An important component at the first phase of development of these forests appears to be *Betula*, a pioneer and light-demanding species, which attained maximum values around 11 000 cal BP. The continuous presence and gradual expansion of the percentages of thermophilous and drought-sensitive taxa (e.g. *Tilia*, *Fraxinus*, *Ulmus* and *Fagus*) imply rising temperatures during the growth season and increasing moisture availability (low evapotranspiration). The synchronous decline of *Pinus* and the expansion of *Abies* values is proof of an ongoing ecological succession in the surroundings of Lake Prespa. The initial expansion of pioneer and light-demanding species like *Pinus*, *Betula*, and *Quercus*, is followed by shade-tolerant species (e.g. *Abies*, *Ulmus*, *Tilia*). The sporadic occurrence of pollen of understory shrub species (e.g. *Sambucus*, *Sorbus*, and *Cornus*), in contrast to the previous zones, supports the notion of a relatively closed tree canopy. Hardy and drought-tolerant taxa, such as *Juniperus*, *Hippophaë* and *Ephedra*, are replaced gradually by *Pistacia* suggesting higher winter temperatures. Percentages of monolete fern spores are expanding and the first appearance of trilete spores (associated with the development of deciduous forests) is recorded towards the top of the zone.

Decreasing potassium counts suggest reduced soil erosion for this period reflecting the closing of the tree canopy in the basin. At the top of P-1e and the bottom of P-1d (c. 8 300 cal BP) the terrestrial pollen and green algae accumulation rates reach maxima of approximately 40 x 10^3 grains and 1 x 10^3 coenobia per cm^2 per year. These values register a substantial increase in primary production of the Prespa catchment and imply favorable conditions for plant growth within and outside of the lake ecosystem.

The distinct peaks of *Pinus* and *Betula* pollen, coeval with small setbacks in otherwise rising *Quercus* (*cerris*- and *robur*-type) percentages, dated at c. 11 000 cal BP can be tentatively correlated to the Preboreal Oscillation (PBO). The shifts above suggest a rather cold and dry centennial event that has been also reported in the Aegean (Kotthoff et al., 2011) and in Accesa (Drescher-Schneider et al., 2007). Magny et al. (2007) compared the hydrological signals of several European records and raised the hypothesis that mid-European sites witnessed wetter conditions during the PBO while southern and northern sites drier (**Figure 3.1**). The pollen record of Prespa appears to be in agreement with these observations.

Some marked fire events depicted as peaks of micro-charcoal particles per cm^2 per year can be observed at c. 10 600 and c. 10 200 cal BP. These can be attributed to a change in the seasonal distribution of precipitation, namely drier weather and higher evapotranspiration during summer. Increased micro-charcoal influx during the Early Holocene, coupled with the expansion of grasslands, are reported from high altitude sites in Turkey (e.g. Wick et al., 2003; Turner et al., 2008), as well as in Accesa, where deciduous oak forests replaced grasslands (Colombaroli et al., 2008; Vannière et al., 2008).

Reforestation in the Prespa catchment continues unabated, with the exception of a small plateau

at c. 10 000, which is preceded by increased fire activity. The subsequent expansion of *Corylus*, a species encountered at the early stages of ecological succession after a disturbance (Ellenberg, 2009), at c. 9 800 cal BP seems to be triggered by these events. In addition, the appearance of the continuous *Pistacia* curve, namely the summer-green *P. terebinthus*, dated at c. 10 000 cal BP confirms the gradual warming trend. The appearance and rise of *Pistacia* has been reported from several sites in the eastern Mediterranean and in some sites delimits the beginning of the Holocene (Bottema, 1974; Willis, 1994; Rossignol-Strick, 1995). *Pistacia* is an important constituent of maquis and along with other sclerophyllous species such as *Phillyrea* and *Olea* form characteristic shrub communities in areas with Mediterranean climate usually accompanied by evergreen *Quercus*. The main growing season for present-day maquis is during late winter and spring with the summer regarded as the hibernation period (Polunin, 1980). The establishment of these plant associations, even in low numbers, at the top of this zone suggests a change in the precipitation regime with wetter conditions during their growth season. Kotthoff et al. (2008b) report similar findings for reconstructed winter precipitation in the northern borderlands of the Aegean. The parallel expansion of *Abies* values, which appears to form climax communities outcompeting *Pinus* at the highlands of the catchment during the same period, apparently excludes the existence of a moisture deficit during springtime.

It could be argued that annual precipitation was more evenly distributed offering optimum growing conditions for different ecological groups in the Prespa region. This appears to be in agreement with the synchronous Sapropel (S1) formation in the eastern Mediterranean, which has been linked to warmer conditions and increased precipitation, dated between c. 9 800 and 7 000 cal BP in the Aegean (e.g. Gogou et al., 2007; Kotthoff et al., 2008b) and Ionian Sea (Geraga et al., 2008) and with a small time lag in the Adriatic at c. 9 000 (e.g. Ariztegui et al., 2000).

3.5.5 8.2 event (P-1d; c. 8 300 cal BP – 7 900 cal BP)

This short interval is characterized by a decline of arboreal percentages by approximately 10% coupled with the parallel increase of *Artemisia* and Poaceae percentages. The relative opening of the tree cover implies a perturbation that lasted a couple of centuries and can be related to a return to colder and drier climate conditions. It appears that the Prespa region underwent complex and partly contrasting changes at a sub-centennial scale, given the high temporal resolution (c. 50 years between samples). As the succession of events occurred rapidly and the lifespan of some trees (notably conifers) exceeded it, an expected lowering of the treeline should not have catastrophic impacts on established populations at high altitudes. *Juniperus*, *Hippophaë* and *Ephedra* reemerge although with low percentages resembling the shrub formations of the YD.

The sensitive response of the vegetation precedes the strong reaction of the geochemical proxies, particularly the potassium curve. A dramatic decrease in TOC and a subsequent increase of soil erosion imply substantial changes in the catchment (see also Aufgebauer et al., 2012). Accordingly, the accumulation rates of trees, herbs, green algae (notably *Botryococcus*) and micro-charcoal mirror the variations of TOC. The same trend is also detected in the percentages of aquatic plants. The reestablishment of shallow-water aquatics and a sharp decrease of green algae influx provide evidence of fluctuating lake levels and can be related to a decrease in precipitation and temperature.

Conifers recover at the end of this subzone and herbs retreat suggesting warmer and moister climate, however, oaks surprisingly decline. This points to the reorganization of arboreal vegetation, as it is evident from the subsequent rapid expansion of other thermophilous deciduous trees in the succeeding subzone. Human interference, although it can not be ruled out, seems unlikely as trees return shortly to percentages preceding the perturbation. An alternative but supplementary explanation for this apparent discrepancy can be sought in an intense fire episode recorded in the preceding sample. Drier climate conditions during summer (increased evapotranspiration) could account for fires at the oak forests probably in the lowlands as it is indicated by the mostly affected thermophilous oak type. Microscopic charcoal peaks, from c. 8 300 till c. 8 100 cal BP, are pronounced and corroborate the notion of increased aridity at Prespa. In Accesa, however, low fire frequency along with high lake-levels and evergreen oak percentages are reported (Colombaroli et al., 2008; Vannière et al., 2008). On the other hand, given the differences in fuel availability, the sites in Turkey show a decline in charcoal influx after c. 8 200 cal BP (Turner et al., 2008; Wick et al., 2003). A recent fire history review for the Mediterranean region (Vannière et al., 2011) provides evidence for a north-south gradient during this interval, which is in agreement with the data presented here.

In a regional context, most pollen records from southern sites, where the 8.2 event has been identified, imply similar climatic trends confirming the hypothesis of the hydrological tripartition of Europe (Magny et al., 2003; **Figure 3.1**). Quantitative climate reconstructions for Accesa and Tenaghi Philippon detect changes in seasonality with wet winters and summers for the former and dry winters and wet summers for the latter (Peyron et al., 2011). In contrast to Accesa, evergreen oak populations collapse at Tenaghi Philippon and the reconstructed winter temperature and annual precipitation show a much more pronounced drop in comparison to the former. Monticchio (Watts et al., 1996; Allen et al., 2002) displays a rather weak vegetation change (minor increase in *Abies* values), suggesting rather stable conditions. Bordon et al. (2009) report cool and dry conditions, especially in winter, from Maliq. In Ohrid (Wagner et al., 2009), increased values of *Artemisia* and a drop of the AP percentages mirror the signal of Prespa.

Consequently, a west-east precipitation gradient influenced strongly by local topography can be assumed. The interruption of the Sapropel S1, which is linked to increased ventilation and oxygenation of deep waters in the Mediterranean (Ariztegui et al., 2000; Gogou et al., 2007; Geraga et al., 2008), is concurrent with this subzone. In addition, reconstructed SST from the Aegean (Gogou et al., 2007; Marino et al., 2009) reveal a pronounced cooling during winter, which can be related to increased outbreaks of cold and dry air from higher latitudes (Siberian High) (Rohling et al., 2002; Gogou et al., 2007; Marino et al., 2009). These findings support the notion of a change in seasonality at Prespa between this and the preceding subzone.

3.5.6 Middle and Late Holocene (P-1c, P-1b, P-1a; c. 7 900 cal BP – present)

The reorganization of the dense forests within the Prespa basin manifested by the rapid expansion of several thermophilous trees characterizes the subzone P-1c; and the expansion of herbs and the appearance of crop species the subsequent subzones P-1b and P-1a. The Prespa data suggest a climate regime comparable to the ones preceding the 8.2 event, namely relative wet and

mild conditions throughout the year as it is suggested by the coexistence of Mediterranean and temperate plant associations. Accordingly, marine records report the continuation of Sapropel S1 formation (e.g. Ariztegui et al., 2000; Gogou et al., 2007; Marino et al., 2009). During this period of rather stable climate, natural processes such as migration, succession, competition and stability of woodland species can be distinguished and a parallel development of rich organic soils can be concluded.

The rather limited abundance of *Fagus*, a climax species of the montane zone, is puzzling as in the conditions described above it should be able to outgrow and finally outcompete most other trees in the montane zone. Apart from temperature constraints such as late frost, it is known that *Fagus* does not tolerate soils that are temporary waterlogged or flooded, in contrast to other species such as *Alnus*, *Betula*, *Fraxinus* and *Q. robur* (cf. Ellenberg, 2009). While a consistent presence (and maxima) of *Alnus* and *Fraxinus* pollen is recorded in P-1c (c. 7 900 to 1 900 cal BP), these species usually occupy stretches along the banks of streams and lakes. The decline of *Q. robur*-type percentages is consistent with the increase of *Fagus* percentages in P-1c, but both taxa appear to be in phase in P-1b and P-1a. Although waterlogged soils could have persisted locally at Prespa, there is no convincing evidence to support such a hypothesis. Selective anthropogenic pressure can not be ruled out, although the ensuing expansion of beech in P-1b and P-1a suggest that humans have not been limiting it during these subzones. *Fagus* is quite sensitive to dry conditions; nevertheless, it can survive at these habitats at higher elevations where orographic precipitation occurs. A possible interpretation, excluding edaphic and anthropogenic factors, could be the occurrence of prolonged and extreme summer droughts (increased evapotranspiration) coupled with fires. The micro-charcoal record, however, does not provide strong evidence for a rise of wildfires at the beginning of P-1c and maquis abundance experiences only a modest growth.

A plausible scenario for the relative scarcity of *Fagus* in the Prespa catchment in P-1c (c. 7 900 to 1 900 cal BP) is the restricted availability of habitats (altitudinal zone) where winter frost and summer drought were absent. High summer insolation in the Early Holocene likely disfavored *Fagus* at low elevation, while low winter insolation likely disfavored it in high altitude sites, where summer humidity was high but winter was too cold. Andrič (2007) documented in pollen records from lowland sites in Slovenia (< 200 m a.s.l.) a significant expansion of *Fagus* percentages (up to 20%) at c. 10 000 cal BP that imply suitable conditions for beech growth. The ecological optimum of *Fagus* must have been further north in the Early Holocene. A closer look at neighboring upland pollen sites (e.g. Ohrid, Maliq, Nisi and Rezina) unveils a similar picture of late expansion. A late migration of *Fagus* in the Prespa catchment seems to be a problematic but conceivable argument. However, Magri (2008) demonstrated using modern genetic data that refugial populations of *Fagus* in the Balkan Peninsula are distinguishable from other European populations (e.g. Slovenian) and have apparently experienced a very slow and modest growth. In light of the above, the findings suggest that *Fagus* was most likely present within or in the vicinity of the Lake Prespa catchment at least since the onset of the Holocene, but conditions became optimal for its growth only after c. 7 000 cal BP.

The pollen assemblages from the uppermost subzones (P-1b and P-1a) indicate an increasing role of humans in the shaping of the landscape at Prespa. The receding woodlands and the opening of the landscape at c. 2 000 cal BP permitted the development of rich shrub and herb layers manifested both in pollen percentages and accumulation rates. Increased soil erosion and lake sediments rich in organic material, as well as pronounced rises in green algae influx point to significant changes in the lake and its surroundings. Difficulties encountered in most pollen records while trying to disentangle natural from human impacts during the Late Holocene chronozone are common.

Ascospore accumulation rates (mostly spores of the coprophilous fungus *Sporormiella*) in P-1c (c. 7 900 to 1 900 cal BP) suggest the commencement of animal husbandry in the lowlands of Prespa almost at the bottom of the subzone and its intensification after c. 6 000 cal BP. Archaeological excavations from neighboring Maliq (Sovjan) provide evidence of an Early Neolithic culture and suggest the occupation of the site since c. 8 000 cal BP (Fouache et al., 2010 and references therein). Moreover, they report that farming and stock-breeding were developed since the beginning of the settlement's history. A lakeside settlement in Kastoria (approximately 20 km southern from Prespa) with intermittent occupation since the Middle Neolithic at c. 7 500 cal BP (Karkanas et al., 2011) leads us to the rather safe assumption that Prespa was also occupied around this period, although the footprint of its inhabitants seems rather limited in P-1c. Ascospores influx declined rapidly at the beginning of P-1b (c. 1 900 cal BP corresponding to the Roman Period). Excluding the complete abandonment of the Lake Prespa region, a relocation of animal husbandry to higher grounds can be invoked. Clearance of woodlands through human induced fire provides productive pastures suitable for grazing and has been one of the major factors forging the Mediterranean landscapes over millennia (e.g. Grove and Rackham, 2003). Increasing micro-charcoal accumulation rates, a dramatic drop in *Pinus* values, the resurgence of *Betula* and consistent percentages of *Corylus* are backing this interpretation.

An alternative but complementary explanation emerges from the first clear signs of farming activity. Cerealia and 'steppe' taxa (e.g. *Artemisia*, Chenopodiaceae, Cichorioideae) associated with agriculture, as well as crop trees (*Juglans* and *Olea*) increased substantially in P-1b and P-1a. Other pollen taxa indicative of disturbed or degraded landscapes with a causal relation to anthropogenic activity, such as *Plantago*, *Rumex*, *Capsella*, *Humulus*, *Urtica*, Ericaceae, *Pteridium* attained maximum percentages in these subzones (c. 1900 to present).

Despite the insufficient temporal resolution of Prespa during this interval, there are no unequivocal signs of substantial change in precipitation inferred from the vegetational history. Some of the shifts in woodland described could have been triggered by climate change, but anthropogenic activity and intrinsic ecological factors seem to override this signal. For instance, the decreasing abundance of climax *Abies* woodlands at high elevations and a modest rise of maquis components in the lowlands (P-1b,P-1a) could indicate drier conditions in the Prespa catchment. Intense fire events, natural or human induced, can affect severely fir forests, as its saplings can not withstand direct sunlight in contrast to *Pinus*. The percentages of the latter should normally surge under these conditions, but this is not the case (P-1b). In most likelihood, the grounds occupied formerly by *Abies* were colonized by *Fagus*. However, climate change does not appear to

account exclusively for the high frequency of extreme fires during this interval and the increase of maquis vegetation in the lowlands can also indicate human induced deforestation.

Neighboring records display decreasing diversity and/or a retreat of woodlands towards the Late Holocene recorded at upland and lowland sites alike. In the vicinity of Prespa, the decline of trees is modest or almost absent (e.g. Ohrid, Nisi, Maliq, Rezina). The same applies to upland locations in Bulgaria (e.g. Trilistnika) and Italy (e.g. Monticchio).

3.6 Conclusions

The Prespa pollen record shows centennial changes in the vegetation in response to climatic variability during the Lateglacial and Early Holocene. This period was punctuated by distinct climatic oscillations in the Northern Hemisphere and beyond, such as the Oldest Dryas, the Bølling/Allerød, the YD, the PBO and the 8.2 event. However, they are not always apparent at strict regional scales. Hence, the Prespa data attest to the sensitivity of this region and underline its potential as a powerful and continuous archive for palaeoclimate reconstructions.

The pronounced response of the vegetation to climate dynamics occurs rapidly and its signature can be traced without significant time lags (e.g. during the 8.2 event). Despite the sampling constraints in the Middle and Late Holocene, evidence of increasing anthropogenic activity can be found in several proxies. Human impact, however, renders the interpretation of concurrent climatic signals problematic.

- The wooded-steppe (with *Pinus* prominent) landscape of the Lateglacial, the presence of numerous deciduous trees and their subsequent expansion (without time lag) during the B/A confirm the existence of temperate tree refugia in the Prespa region. The warmer and moister climate conditions during B/A are clearly depicted in the expansion of woodland.
- The Younger Dryas climate reversal is pronounced and the findings suggest it mostly affected high elevation grounds within the catchment (e.g. *Pinus* populations contracted, treeline descended and herbaceous steppe vegetation spread). In the lowlands, however, deciduous trees continue to expand gradually.
- During the Early Holocene, the establishment of dense oak woods associated with thermophilous and drought-sensitive species points to a wet and mild climate, linked to the formation of the Sapropel S1 in the Mediterranean Sea.
- The 8.2 cooling event accounted for a short-lived advance of steppe elements, a rise of fire frequency, and signaled a shift in seasonality. The abrupt and subtle reaction of the vegetation at Prespa indicates the sensitivity of the site.
- Throughout the Middle and Late Holocene, woodlands at Prespa underwent substantial restructuring. The increase of anthropogenic activities, such as animal husbandry, clearances and agriculture, resulted in the opening of the landscape. Nevertheless, the site remained relatively wooded and provided a wide range of habitats that could sustain plant populations with contrasting requirements.

The diversity of modern flora at Prespa accentuates its potential as a refugium at greater time

scales. Systematic conservation efforts over the last decades will hopefully ensure the persistence of its unique and fragile ecosystems. Transitional communities, such as the Macedonian pine forests, are vulnerable to global warming and their survival can prove challenging. Notwithstanding, they confirm the capacity of the site to serve as a Holocene 'refugium'.

3.7 Acknowledgements

We are much obliged to our colleagues from the Seminar of Geography and Education and the Institute of Geology and Mineralogy at the University of Cologne for their valuable assistance during the field campaign and the processing of material in the laboratory. We thank the Hydrobiological Institute in Ohrid, the administration of Pelister and Galičica National Parks for logistic support. KP gratefully acknowledges Frederik von Reumont for help with cartography; Elena Marinova for providing pollen reference material; Jutta Meurers-Balke and Ingrid Kloss for help with pollen identification; the colleagues of the Department of Palynology and Climate Dynamics at the University of Göttingen, as well as Jean-Pierre Francois and Karsten Schittek for comments on the results. E. K. Magyari and U. C. Müller are acknowledged for providing constructive reviews. This study is part of Project B2 of the Collaborative Research Center 806 "Our Way to Europe" (http://www.sfb806.de) funded by the German Research Foundation (DFG).

3.8 References

Allen, J.R.M., Watts, W.A., McGee, E., Huntley, B., 2002. Holocene environmental variability - the record from Lago Grande di Monticchio, Italy. Quaternary International 88(1), 69-80.

Andrič, M., 2007. Holocene vegetation development in Bela krajina (Slovenia) and the impact of first farmers on the landscape. The Holocene 17(6), 763-776.

Ariztegui, D., Asioli, A., Lowe, J.J., Trincardi, F., Vigliotti, L., Tamburini, F., Chondrogianni, C., Accorsi, C.A., Bandini Mazzanti, M., Mercuri, A.M., van der Kaars, S., McKenzie, J.A., Oldfield, F., 2000. Palaeoclimate and the formation of sapropel S1: inferences from Late Quaternary lacustrine and marine sequences in the central Mediterranean region. Palaeogeography, Palaeoclimatology, Palaeoecology 158(3-4), 215-240.

Aufgebauer, A., Panagiotopoulos, K., Wagner, B., Schaebitz, F., Viehberg, F.A., Vogel, H., Zanchetta, G., Sulpizio, R., Leng, M.J., Damaschke, M., 2012. Climate and environmental change in the Balkans over the last 17 ka recorded in sediments from Lake Prespa (Albania/F.Y.R. of Macedonia/Greece). Quaternary International 274, 122-135.

Avramovski, O., 2006. Plan of Management for Pelister National Park and Supplement. Pelister National Park, Pelister Mountain Conservation Project, p. 179, Bitola.

Bennett, K.D., Tzedakis, P.C., Willis, K.J., 1991. Quaternary refugia of north European trees. Journal of Biogeography, 103-115.

Beug, H.J., 2004. Leitfaden der Pollenbestimmung für Mitteleuropa und angrenzende Gebiete. Pfeil, München.

Bhagwat, S.A., Willis, K.J., 2008. Species persistence in northerly glacial refugia of Europe: a matter of chance or biogeographical traits? Journal of Biogeography 35(3), 464-482.

Birks, H.J.B., Willis, K.J., 2008. Alpines, trees, and refugia in Europe. Plant Ecology & Diversity 1(2), 147-160.

Bohn, U., Gollub, G., Hettwer, C., Neuhäuslová, Z., Raus, T., Schlüter, H., Weber, H., 2004. Karte der natürlichen Vegetation Europas Map of the Natural Vegetation of Europe Maßstab/Scale 1:2 500 000.

Bundesamt für Naturschutz (BfN) Federal Agency for Nature Conservation, Bonn, Germany.

Bordon, A., Peyron, O., Lézine, A.M., Brewer, S., Fouache, E., 2009. Pollen-inferred Late-Glacial and Holocene climate in southern Balkans (Lake Maliq). Quaternary International 200, 19-30.

Bottema, S., 1974. Late Quaternary vegetation history of northwestern Greece. Ph.D Thesis, University of Groningen, Groningen.

Colombaroli, D., Vannière, B., Emmanuel, C., Magny, M., Tinner, W., 2008. Fire-vegetation interactions during the Mesolithic-Neolithic transition at Lago dell' Accesa, Tuscany, Italy. The Holocene 18(5), 679-692.

Davis, M.B., 2000. Palynology after Y2K - Understanding the source area of pollen in sediments. Annual Review of Earth and Planetary Sciences 28, 1-18.

Denèfle, M., Lézine, A., Fouache, E., Dufaure, J., 2000. A 12,000-year pollen record from Lake Maliq, Albania. Quaternary Research 54(3), 423-432.

Dormoy, I., Peyron, O., Nebout, N.C., Goring, S., Kotthoff, U., Magny, M., Pross, J., 2009. Terrestrial climate variability and seasonality changes in the Mediterranean region between 15 000 and 4000 years BP deduced from marine pollen records. Climate of the Past 5(4), 615-632.

Drescher-Schneider, R., De Beaulieu, J.L., Magny, M., Walter-Simonnet, A.V., Bossuet, G., Millet, L., Brugiapaglia, E., Drescher, A., 2007. Vegetation history, climate and human impact over the last 15,000 years at Lago dell' Accesa (Tuscany, Central Italy). Vegetation history and archaeobotany 16(4), 279-299.

Ellenberg, H., 2009. Vegetation Ecology of Central Europe. Cambridge University Press.

Faegri, K., Iversen, J., Kaland, P.E., Krzywinski, K., 2000. Textbook of Pollen Analysis. Blackburn Press.

Fouache, E., Desruelles, S., Magny, M., Bordon, A., Oberweiler, C., Coussot, C., Touchais, G., Lera, P., Lézine, A.M., Fadin, L., Roger, R., 2010. Palaeogeographical reconstructions of Lake Maliq (Korça Basin, Albania) between 14,000 BP and 2000 BP. Journal of Archeological Science 37, 525-535.

Geraga, M., Mylona, G., Tsaila-Monopoli, S., Papatheodorou, G., Ferentinos, G., 2008. Northeastern Ionian Sea: Palaeoceanographic variability over the last 22 ka. Journal of Marine Systems 74(1-2), 623-638.

Gogou, A., Bouloubassi, I., Lykousis, V., Arnaboldi, M., Gaitani, P., Meyers, P M., 2007. Organic geochemical evidence of Late Glacial-Holocene climate instability in the North Aegean Sea. Palaeogeography, Palaeoclimatology, Palaeoecology 256(1-2), 1-20.

Griffiths, H.I., Kryštufek, B., Reed, J.M. (Eds.), 2004. Balkan Biodiversity: Pattern and Process in the European Hotspot Kluwer Academic Publishers, Dodrecht, The Netherlands.

Grimm, E.C., 1992. TILIA and TILIA-graph: Pollen spreadsheet and graphics programs. Programs and Abstracts. Aix-en-Provence, France.

Grove, A.T., Rackham, O., 2003. The Nature of Mediterranean Europe - An Ecological History. Yale University Press, London.

Hollis, G., Stevenson, A., 1997. The physical basis of the Lake Mikri Prespa systems: geology, climate, hydrology and water quality. Hydrobiologia 351, 1-19.

Hughes, P.D., Woodward, J.C., Gibbard, P.L., 2006a. Late Pleistocene glaciers and climate in the Mediterranean. Global and Planetary Change 50(1-2), 83-98.

Hughes, P.D., Woodward, J.C., Gibbard, P.L., 2006b. The last glaciers of Greece. Zeitschrift für Geomorphologie 50(1), 37-61.

Jacobson, G.L., Bradshaw, R.H., 1981. The selection of asites for paleovegetational studies. Quaternary Research 16(1), 80-96.

Jarvis, A., Reuter H.I., Nelson A., Guevara E., 2008. Hole-filled SRTM for the globe Version 4, available from the CGIAR-CSI SRTM 90m Database, retrieved 27.11.2011, from http://srtm.csi.cgiar.org.

Karkanas, P., Pavlopoulos, K., Kouli, K., Ntinou, M., Tsartsidou, G., Facorellis, Y., Tsourou, T., 2011. Palaeoenvironments and site formation processes at the Neolithic lakeside settlement of Dispilio, Kastoria, Northern Greece. Geoarchaeology 26(1), 83-117.

Kotthoff, U., Muller, U., Pross, J., Schmiedl, G., Lawson, I., van De Schootbrugge, B., Schulz, H., 2008a. Lateglacial and Holocene vegetation dynamics in the Aegean region: an integrated view based on pollen data from marine and terrestrial archives. The Holocene 18(7), 1019.

Kotthoff, U., Pross, J., Müller, U.C., Peyron, O., Schmiedl, G., Schulz, H., Bordon, A., 2008b. Climate dynamics in the borderlands of the Aegean Sea during formation of sapropel S1 deduced from a marine pollen record. Quaternary Science Reviews 27(7-8), 832-845.

Kotthoff, U., Koutsodendris, A., Pross, J., Schmiedl, G., Bornemann, A., Kaul, C., Marino, G., Peyron, O., Schiebel, R., 2011. Impact of Lateglacial cold events on the northern Aegean region reconstructed from marine and terrestrial proxy data. Journal of Quaternary Science. 26(1), 86-96.

Latałowa, M., Van Der Knaap, W.O., 2006. Late Quaternary expansion of Norway spruce Picea abies (L.) Karst. in Europe according to pollen data. Quaternary Science Reviews 25(21-22), 2780-2805.

Lawson, I., Frogley, M., Bryant, C., Preece, R., Tzedakis, P., 2004. The Lateglacial and Holocene environmental history of the Ioannina basin, north-west Greece. Quaternary Science Reviews 23(14-15), 1599-1625.

Lawson, I., Al-Omari, S., Tzedakis, P., Bryant, C., Christanis, K., 2005. Lateglacial and Holocene vegetation history at Nisi Fen and the Boras mountains, northern Greece. The Holocene 15(6), 873- 887.

Levin, I., Kromer, B., 2004. The tropospheric $^{14}CO_2$ level in mid-latitudes of the Northern Hemisphere (1959-2003). Radiocarbon 46(3), 1261-1272.

Lowe, J.J., Rasmussen, S.O., Björck, S., Hoek, W.Z., Steffensen, J.P., Walker, M.J.C., Yu, Z.C., the INTIMATE group, 2008. Synchronisation of palaeoenvironmental events in the North Atlantic region during the Last Termination: a revised protocol recommended by the INTIMATE group. Quaternary Science Reviews 27(1-2), 6-17.

Magny, M., Bégeot, C., Guiot, J., Peyron, O., 2003. Contrasting patterns of hydrological changes in Europe in response to Holocene climate cooling phases. Quaternary Science Reviews 22(15-17), 1589-1596.

Magny, M., Vannière, B., De Beaulieu, J.L., Bégeot, C., Heiri, O., Millet, L., Peyron, O., Walter-Simonnet, A.V., 2007. Early-Holocene climatic oscillations recorded by lake-level fluctuations in west-central Europe and in central Italy. Quaternary Science Reviews 26(15-16), 1951-1964.

Magri, D., 2008. Patterns of post-glacial spread and the extent of glacial refugia of European beech (Fagus sylvatica). Journal of Biogeography 35(3), 450-463.

Magyari, E., Chapman, J., Gaydarska, B., Marinova, E., Deli, T., Huntley, J., Allen, J., Huntley, B., 2008. The 'oriental' component of the Balkan flora: evidence of presence on the Thracian Plain during the Weichselian late-glacial. Journal of Biogeography 35(5), 865-883.

Marino, G., Rohling, E.J., Sangiorgi, F., Hayes, A., Casford, J.L., Lotter, A.F., Kucera, M., Brinkhuis, H., 2009. Early and middle Holocene in the Aegean Sea: interplay between high and low latitude climate variability. Quaternary Science Reviews 28(27-28), 3246-3262.

Matzinger, A., Jordanoski, M., Veljanoska-Sarafiloska, E., Sturm, M., Müller, B., Wüest, A., 2006. Is Lake Prespa jeopardizing the ecosystem of ancient Lake Ohrid? Hydrobiologia 553(1), 89-109.

Moore, P.D., Webb, J.A., Collinson, M.E., 1991. Pollen Analysis. Blackwell Scientific Publications, Oxford.

Müller, U.C., Pross, J., Tzedakis, P.C., Gamble, C., Kotthoff, U., Schmiedl, G., Wulf, S., Christanis, K., 2011. The role of climate in the spread of modern humans into Europe. Quaternary Science Reviews 30(3-4), 273-279.

Pavlides, G., 1997. The flora of Prespa National Park with emphasis on species of conservation interest. Hydrobiologia 351(1), 35-40.

Petit, R., Aguinagalde, I., De Beaulieu, J.L., Bittkau, C., Brewer, S., Cheddadi, R., Ennos, R., Fineschi, S., Grivet, D., Lascoux, M., Mohanty, A., Müller-Starck, G., Demesure-Musch, B., Palmé, A., Martín, J.P., Rendell, S., Vendramin, G.G., 2003. Glacial refugia: hotspots but not melting pots of genetic diversity. Science 300(5625), 1563-1565.

Peyron, O., Goring, S., Dormoy, I., Kotthoff, U., Pross, J., De Beaulieu, J.L., Drescher-Schneider, R., Vannière, B., Magny, M., 2011. Holocene seasonality changes in the central Mediterranean region reconstructed from the pollen sequences of Lake Accesa (Italy) and Tenaghi Philippon (Greece). The Holocene 21(1), 131-146.

Polunin, O., 1980. Flowers of Greece and the Balkans - A Field Guide. Oxford University Press, Oxford.

Punt, W., Clarke, G.C.S. (Eds.), 1980. The Northwest European Pollen Flora (II). Elsevier, Amsterdam.

Punt, W., Blackmore, S. (Eds.), 1991. The Northwest European Pollen Flora (VI). Elsevier, Amsterdam.

Reille, M., 1998. Pollen et Spores d' Europe et d' Afrique du nord. (Supplement 2). Laboratoire de Botanique Historique et Palynologie, Marseille.

Reille, M., 1999. Pollen et Spores d' Europe et d' Afrique du nord. Laboratoire de Botanique Historique et Palynologie, Marseille.

Reimer, P.J., Baillie, M.G.L., Bard, E., Bayliss, A., Beck, J.W., Blackwell, P.G., Bronk Ramsey, C., Buck, C.E., Burr, G.S., Edwards, R.L., Friedrich, M., Grootes, P.M., Guilderson, T.P., Hajdas, I., Heaton, T.J., Hogg, A.G., Hughen, K.A., Kaiser, K.F., Kromer, B., Mccormac, F.G., Manning, S.W., Reimer, R.W., Richards, D.A., Southon, J.R., Talamo, S., Turney, C.S.M., Van Der Plicht, J.W., C.E., 2009. IntCal09 and Marine09 Radiocarbon Age Calibration Curves, 0 - 50,000 years cal BP. Radiocarbon 51, 1111-1150.

Renssen, H., Isarin, R., 2001. The two major warming phases of the last deglaciation at similar to 14.7 and similar to 11.5 ka cal BP in Europe: climate reconstructions and AGCM experiments. Global Planet Change 30(1-2), 117-153.

Rohling, E.J., Mayewski, P.A., Abu-Zied, R.H., Casford, J.S.L., Hayes, A., 2002. Holocene atmosphere-ocean interactions: records from Greenland and the Aegean Sea. Climate Dynamics 18(7), 587-593.

Rossignol-Strick, M., 1995. Sea-land correlation of pollen records in the Eastern Mediterranean for the glacial-interglacial transition: biostratigraphy versus radiometric time-scale. Quaternary Science Reviews 14(9), 893-915.

Santacroce, R., Cioni, R., Marianelli, P., Sbrana, A., Sulpizio, R., Zanchetta, G., Donahue, D.J., Joron, J.L., 2008. Age and whole rock-glass compositions of proximal pyroclastics from the major explosive eruptions of Somma-Vesuvius: a review as a tool for distal tephrostratigraphy. Journal of Volcanology Geothermal Research 177, 1–18.

Siani, G., Sulpizio, R., Paterne, M., Sbrana, A., 2004. Tephrostratigraphy study for the last 18,000 ^{14}C years in a deep-sea sediment sequence for the South Adriatic. Quaternary Science Reviews 23, 2485–2500.

Society for the Protection of Prespa, SPP, 2011. Number of species, retrieved 27.11.2011, from http://www.spp.gr/spp/species%20chart_en.pdf.

Stockmarr, J., 1971. Tablets with spores used in absolute pollen analysis. Pollen et spores.

Tonkov, S., Bozilova, E., Possnert, G., Velčev, A., 2008. A contribution to the postglacial vegetation history of the Rila Mountains, Bulgaria: The pollen record of Lake Trilistnika. Quaternary International 190(1), 58-70.

Tóth, M., Magyari, E.K., Brooks, S.J., Braun, M., Buczkó, K., Bálint, M., Heiri, O., 2012. A chironomid-based reconstruction of late glacial summer temperatures in the southern Carpathians (Romania). Quaternary Research 77(1), 122-131.

Turner, R., Roberts, N., Jones, M.D., 2008. Climatic pacing of Mediterranean fire histories from lake sedimentary microcharcoal. Global and Planetary Change 63(4), 317-324.

Turrill, W.B., 1929. The plant-life of the Balkan Peninsula: a phytogeographical study. Clarendon Press, Oxford.

Tzedakis, P., Lawson, I., Frogley, M., Hewitt, G., Preece, R., 2002. Buffered tree population changes in a quaternary refugium: evolutionary implications. Science 297(5589), 2044-2047.

Vannière, B., Colombaroli, D., Chapron, E., Leroux, A., Tinner, W., Magny, M., 2008. Climate versus human-driven fire regimes in Mediterranean landscapes: the Holocene record of Lago dell' Accesa (Tuscany, Italy). Quaternary Science Reviews 27(11-12), 1181-1196.

Vannière, B., Power, M.J., Roberts, N., Tinner, W., Carrión, J., Magny, M., Bartlein, P., Colombaroli, D., Daniau, A.L., Finsinger, W., Gil-Romera, G., Kaltenrieder, P., Pini, R., Sadori, L., Turner, R., Valsecchi, V., Vescovi, E., 2011. Circum-Mediterranean fire activity and climate changes during the mid-Holocene environmental transition (8500-2500 cal. BP). The Holocene 21(1), 53-73.

Wagner, B., Lotter, A., Nowaczyk, N., Reed, J., Schwalb, A., Sulpizio, R., Valsecchi, V., Wessels, M., Zanchetta, G., 2009. A 40,000-year record of environmental change from ancient Lake Ohrid (Albania and Macedonia). Journal of Paleolimnology 41(3), 407-430.

Wagner, B., Vogel, H., Zanchetta, G., Sulpizio, R., 2010. Environmental change within the Balkan region during the past ca. 50 ka recorded in the sediments from lakes Prespa and Ohrid. Biogeosciences 7, 3187-3198.

Wagner, B., Aufgebauer, A., Vogel, H., Zanchetta, G., Sulpizio, R., Damaschke, M., 2012. Late Pleistocene to Holocene re-organization of sedimentation patterns in Lake Prespa (Albania/F.Y.R. of Macedonia/Greece). Quaternary International 274, 112-121.

Watts, W.A., Allen, J.R.M., Huntley, B., Fritz, S.C., 1996. Vegetation history and climate of the last 15,000 years at Laghi di Monticchio, southern Italy. Quaternary Science Reviews 15(2-3), 113-132.

Wick, L., Lemcke, G., Sturm, M., 2003. Evidence of Lateglacial and Holocene climatic change and human impact in eastern Anatolia: high-resolution pollen, charcoal, isotopic and geochemical records from the laminated sediments of Lake Van, Turkey. The Holocene 13(5), 665-675.

Willis, K.J., 1992. The late Quaternary vegetational history of northwest Greece III. A comparative study of two contrasting sites. New Phytologist 121, 139-155.

Willis, K.J., 1994. The vegetation history of the Balkans. Quaternary Science Reviews 13, 769-788.

Willis, K., Van Andel, T.H., 2004. Trees or no trees? The environments of central and eastern Europe during the Last Glaciation. Quaternary Science Reviews 23, 2369-2387.

Wilson, G.P., Reed, J.M., Lawson, I.T., Frogley, M.R., Preece, R.C., Tzedakis, P.C., 2008. Diatom response to the Last Glacial-Interglacial Transition in the Ioannina basin, northwest Greece: implications for Mediterranean palaeoclimate reconstruction. Quaternary Science Reviews 27(3-4), 428-440.

Zanchetta, G., Sulpizio, R., Roberts, N., Cioni, R., Eastwood, W.J., Siani, G., Paterne, M., Santacroce, R., 2011. Tephrostratigraphy, chronology and climatic events of the Mediterranean basin during the Holocene: an overview. The Holocene 21, 33-52.

IV Understanding past climatic and hydrological variability in the Mediterranean from Lake Prespa sediment isotope and geochemical record over the Last Glacial cycle*

Abstract

Here we present stable isotope and geochemical data from Lake Prespa (Macedonia/Albania border) over the Last Glacial cycle (Marine Isotope Stages 5-1) and discuss past lake hydrology and climate (TIC, oxygen and carbon isotopes), as well as responses to climate of terrestrial and aquatic vegetation (TOC, Rock Eval pyrolysis, carbon isotopes, pollen). The Lake Prespa sediments broadly fall into 5 zones based on their sedimentology, geochemistry, palynology and the existing chronology. The Glacial sediments suggest low supply of carbon to the lake, but high summer productivity; intermittent siderite layers suggest that although the lake was likely to have mixed regularly leading to enhanced oxidation of organic matter, there must have been within sediment reducing conditions and methanogenesis. MIS 5 and 1 sediments suggest much more productivity, higher rates of organic material preservation possibly due to more limited mixing with longer periods of oxygen-depleted bottom waters. We also calculated lakewater $\delta^{18}O$ from siderite (authigenic/Glacial) and calcite (endogenic/Holocene) and show much lower lakewater $\delta^{18}O$ values in the Glacial when compared to the Holocene, suggesting the lake was less evaporative in the Glacial, probably as a consequence of cooler summers and longer winter ice cover. In the Holocene the oxygen isotope data suggests general humidity, with just 2 marked arid phases, features observed in other Eastern and Central Mediterranean lakes.

Keywords: Late Quaternary, Mediterranean, lake, stable isotopes, Rock Eval pyrolysis, geochemistry

* This chapter is based on Leng, M.J., Wagner, B., Boehm, A., Panagiotopoulos, K., Vane, C.H., Snelling, A., Haidon, C., Woodley, E., Vogel, H., Zanchetta, G., and Baneschi, I., 2013, Understanding past climatic and hydrological variability in the Mediterranean from Lake Prespa sediment isotope and geochemical record over the Last Glacial cycle, Quaternary Science Reviews 66, 123-136, dx.doi.org/10.1016/j.quascirev.2012.07.015.

4.1 Introduction

Understanding past climatic (including hydrological) variability is a particular issue in the Mediterranean region because there is an acute link between water resource and socio-economic impacts (e.g. Bolle, 2003; Lionello et al., 2006). Also for future predictions it is necessary to investigate the past response of the region to global climate fluctuations. Today's effective management of groundwater and lake catchment areas, as well as the need to understand and monitor human-induced trends affecting water resources, can be helped by understanding how past variations in climate impact lakewater resources (Roberts et al., 2008). Stable isotope data from lacustrine carbonates and organic matter through time can define local climatic and hydrological change (e.g., Leng and Marshall, 2004) and when lake records are combined across regions these data can be used to assess the spatial coherency of climate and hydrology (Roberts et al., 2008). There are numerous lacustrine carbonate stable isotope records from the Mediterranean (Leng et al., 1999; Frogley et al., 2001; Roberts et al., 2008), including in the Balkans, Lake Prespa (described here) and the neighboring Lake Ohrid (Leng et al., 2010). The former records are mainly limited to a few tens of thousands of years, and all have imperfect chronologies. The previous lake isotope records from Prespa and Ohrid are at low resolution and given their mostly relatively long time spans (back to 130 ka) also have significant chronological issues. Here, we discuss new stable isotope and geochemical data from Lake Prespa through the last 4 or 5 Marine Isotope Stages (MIS) and discuss past lake hydrology and climate (TIC, oxygen and carbon isotopes), as well as responses to climate of terrestrial and aquatic vegetation (TOC, Rock Eval pyrolysis, carbon isotopes, pollen).

4.2 General setting

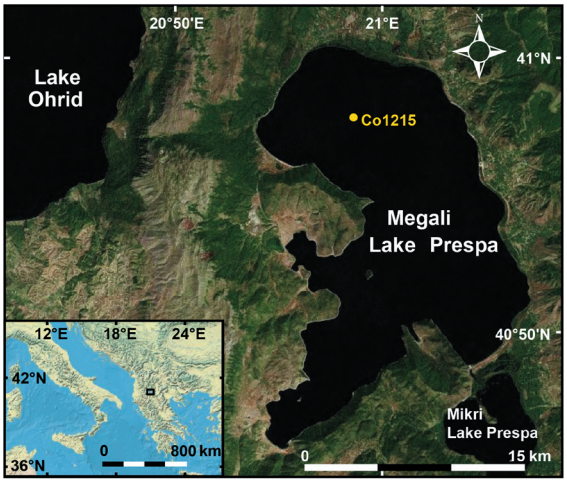

Figure 4.1: Lake Prespa in SE Europe, situated between Albania, Macedonia and Greece. Coring location of Co1215 is marked.

Lake Prespa is situated in SE Europe between Albania, Macedonia and Greece (**Figure 4.1**). The lake drains into the larger Lake Ohrid through a karst system within the Mali Thate (2287 m above sea level (m a.s.l.) and Galičica (2262 m a.s.l.) mountains, which form the topographical divide between the two lakes. The lake is thought to have been formed within a tectonic graben during the Alpine Orogeny in the Pliocene (Aliaj et al., 2001). Owing to the lakes position within the rain shadow of the surrounding mountains and the proximity to the Adriatic Sea, the lake catchment is under the influence of a sub-Mediterranean climate with continental influences (Watzin et al., 2002). Mean July and January temperatures are + 21 °C and + 1 °C respectively, with a mean annual temperature of + 11 °C. Precipitation

peaks in winter (when snowfalls are frequent) and drops in summer, varying from 750 mm in the lowlands to over 1200 mm on the mountains (Hollis and Stevenson, 1997). The diverse topography, the exposure of slopes and valleys, as well as the presence of a large water body create a complex patchwork of microclimates in the catchment that is also reflected in the vegetation (Panagiotopoulos et al., 2013). As such we expect that Mediterranean type changes seen across the circum-Mediterranean will also be recorded in Lake Prespa (Roberts et al., 2008).

Table 4.1: Characteristics of Lake Prespa (data from Matzinger et al., 2006a; Wilke et al., 2010).

Property	Prespa
Altitude (m a.s.l.)	849
Catchment area (km^2)	1300
Lake area (km^2)	254
Mean lake depth (m)	14-19
Volume (km^3)	3.6
pH (surface/bottom)	8.4-7.3

Lake Prespa (Megali Prespa) is located at 849 m a.s.l., ca 150 m above Lake Ohrid, and has a volume of ca 3.6 km^3 (see **Table 4.1**). To the south, the lake is connected to a smaller lake, called Mikri Prespa, by a controllable man-made channel with a current hydraulic head of 3 m (Hollis and Stevenson, 1997). The total inflow into Lake Prespa is estimated to be 16.9 $m^3 s^{-1}$, with 56% originating from river runoff from numerous small streams, 35% from direct precipitation, and 9% from Mikri Prespa to the south (Matzinger et al., 2006b). Lake Prespa has no natural surface outlet, water loss is through evaporation (52%), irrigation (2%) and outflow through the karst aquifer (46%); the latter leading to springs, some of which flow into Lake Ohrid (Matzinger et al., 2006b). The lakewater residence time in Lake Prespa is estimated to be ca 11 years. Significant lake level lowering in response to climate and exploitation for human use has been recorded in the past (Popovska and Bonacci, 2007; Stefouli et al., 2008). As Lake Prespa is relatively shallow with respect to the large surface area, wind-induced mixing leads to a complete destratification of the water column from autumn to spring (Matzinger et al., 2006b), meaning that the isotope composition of the lakewater will be fairly homogeneous and at steady state on a decadal time scale. Summer bottom water anoxia and an average total phosphorus concentration of 31 mg m^{-3} in the water column characterize the modern lake as mesotrophic, although previous work has shown that the lake has been more oligotrophic in the past (Wagner et al., 2010).

4.3 Material and methods

The sediment core described here from Lake Prespa was retrieved using a floating platform, gravity and piston corers (UWITEC Corp. Austria). The coring site is an area of flat lying, largely undisturbed sediment, identified during a hydroacoustic survey (Wagner et al., 2012). Core composite records were obtained by correlation of individual 3 m long core sections using a variety of methods including visual inspection of the sediment composition, as well as aligning optical, magnetic and geochemical marker horizons (Wagner et al., 2012). The sediment record (core Co1215) forms the best dated and longest sediment record from Lake Prespa to date. Detailed core descriptions, chronology and geochemical measurements back to 17 000 years (except stable isotopes) are discussed in Aufgebauer et al. (2012), while the full record is described in

Wagner et al. (2012). The core was sampled continuously at 2 cm intervals (correlated core depth = 1575 cm), a sample aliquot from each level was freeze-dried and homogenized to <63 mm using an agate ball mill. Total carbon (TC) and total inorganic carbon (TIC) concentrations were determined with a DIMATOC 200 (DIMATEC Co.). Concentrations of total carbon (TC) and total nitrogen (N) were measured with a VARIO MICROCUBE elemental analyzer. Total organic carbon (TOC) was quantified from the difference between total carbon (TC) and total inorganic carbon (TIC), which were measured with a DIMATOC 200 (DIMATEC Co.).

Here we present: new stable isotope data from the modern waters ($\delta^{18}O$, δD, $\delta^{13}C$ from NIGL); stable isotope data from organic matter ($\delta^{13}C$, from IGG) supported by %TOC and %N (from which we calculate TOC/N, Cologne), Rock Eval data (BGS), pollen data (Cologne); and stable isotope data from carbonates ($\delta^{18}O$ and $\delta^{13}C$ from both calcite and siderite, from NIGL). The combined data set within the existing chronology are used to interpret the past environment and climate and some comparisons are made with lakes on a more regional basis.

4.3.1 Stable isotope analysis of modern waters

Water isotope data include data from a monitoring period between 1984 and 2000 published by Anovski et al. (1992) and Anovski (2001) and data from waters reported in Matzinger et al. (2006a), data collected between August 2008-October 2009 (Leng et al., 2010), and new data from June 2011 (**Figure 4.2** a). The new data (June 2011) were measured at NIGL, the waters were equilibrated with CO_2 using an Isoprep 18 device for oxygen isotope analysis with mass spectrometry using a VG SIRA. For hydrogen isotope analysis, an on-line Cr reduction method was used with a EuroPyrOH-3110 system coupled to a Micromass Isoprime mass spectrometer. Isotopic ratios ($^{18}O/^{16}O$ and $^{2}H/^{1}H$) are expressed in delta units, $\delta^{18}O$ and δD (‰, parts per mille), and defined in relation to the international standard, VSMOW (Vienna Standard Mean Ocean Water). Analytical precision is typically <0.2‰ for $\delta^{18}O$ and ±1.0‰ for δD.

Total dissolved inorganic carbonate (TDIC) was precipitated from the June 2011 water collection (**Figure 4.2** b), c. 85 ml of water was reacted with c. 15 ml of NaOH-$BaCl_2$ solution soon after collection. The resultant barium carbonate was filtered in the laboratory under N_2, and rinsed with deionised water. The carbon isotope analysis ($\delta^{13}C$TDIC) followed the method described below for the sedimentary calcite.

4.3.2 Stable isotope and Rock Eval analysis of organic matter

The core from Lake Prespa was sampled for carbon isotopes on organic matter at 2 cm intervals from the surface to a correlated depth of 168 cm, and c. 10 cm from 170 cm to the base at 1575 cm. The samples were dried at 40 °C and powdered. The powders were treated with 10% HCl to remove calcite, washed several times with distilled water to neutral pH, and then dried again at 40 °C. CO_2 was evolved by combustion using a Carlo Erba 1108 elemental analyzer, interfaced to a Finnigan DeltaPlusXL via the Finnigan MAT Conflo II interface. Organic carbon isotope values ($\delta^{13}C$org) are reported as per mille (‰) deviations of the isotopic ratios ($^{13}C/^{12}C$) calculated to the VPDB scale using a within-run laboratory standards (graphite and ANU-sucrose) and international NBS standards. Overall analytical reproducibility for the standards was <0.1‰ for $\delta^{13}C$. Note that any siderite (see Section **4.3.4**) present

below 168 cm would not be removed with 10% HCl. In any case, the TIC spikes seen in the TIC data do not correspond to spikes in the $\delta^{13}C_{org}$ data, the calculated 1-2% of siderite with an $\delta^{13}C$ composition of c. +10‰ changes the $\delta^{13}C_{org}$ data by <1‰, and within the high frequency (not interpreted) variability of the $\delta^{13}C_{org}$ record (**Figure 4.3**).

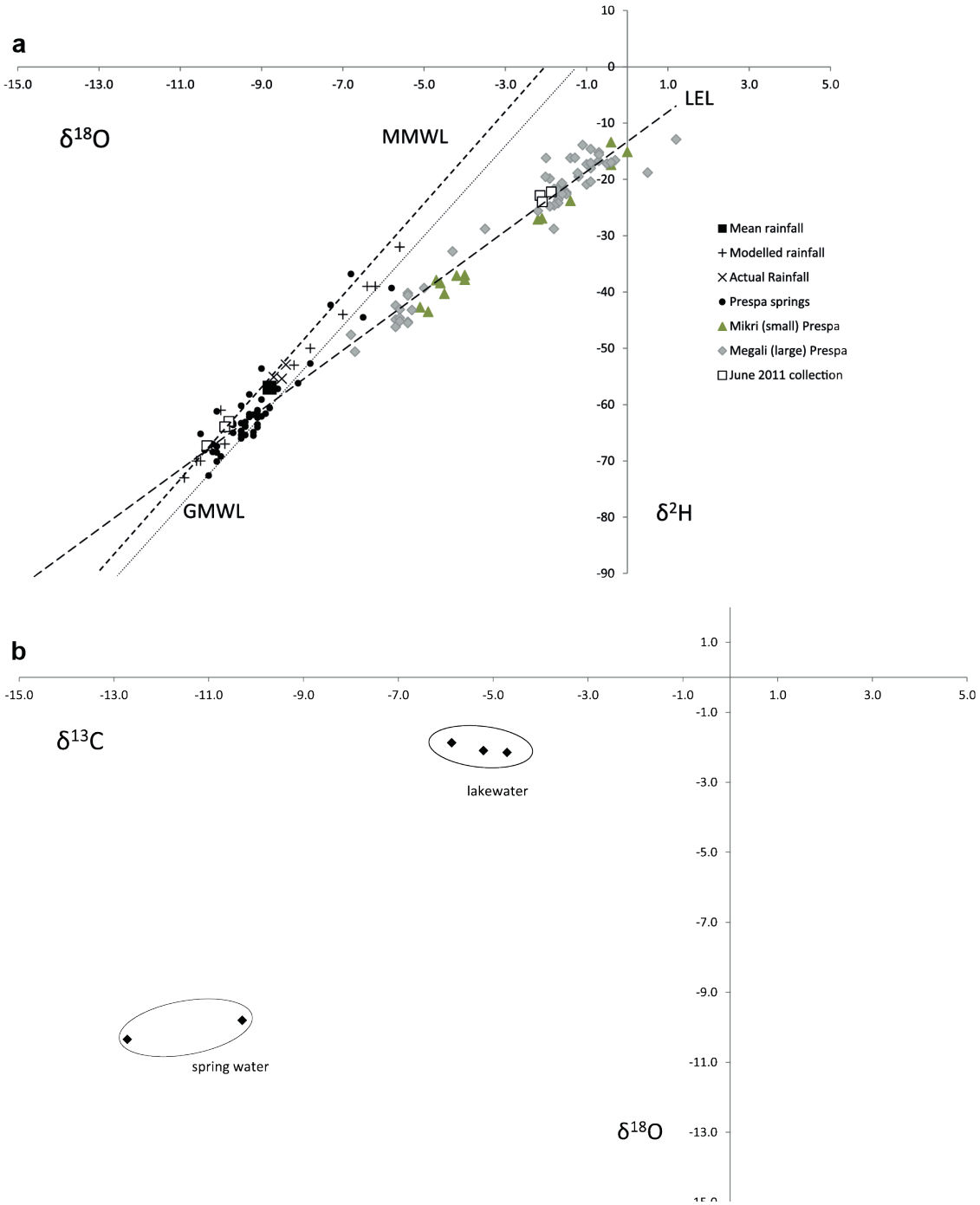

Figure 4.2: The isotopic (a: $\delta^{18}O$ and δD; b: $\delta^{13}C$TDIC and $\delta^{18}O$) composition of present day waters from Lake Prespa and springs. The Global Meteoric Water Line (GMWL) and the Mediterranean Meteoric Water Line (MMWL) (cf. Anovski et al. (1991) and Eftimi and Zoto (1997)) are also given on (a) with the calculated Local Evaporation Line (LEL). All but the June 2011 data are from data compiled in Leng et al. (2010).

Samples for Rock Eval analysis were selected at 5 cm resolution from correlated depths ranging from 10 to 1563 cm. Pyrolysis was performed on approximately 60 mg of powdered sediment (dry/wt) using a Rock-Eval 6 analyzer (Vinci Technologies) in standard configuration (pyrolysis and oxidation as a serial process). Samples were heated from 300 ˚C to 650 ˚C at 25 ˚C/min in an inert atmosphere of N_2. The residual carbon was then oxidized at 300 ˚C - 850 ˚C at 20 ˚C/min (hold 5 min). Hydrocarbons released during the two stage pyrolysis were measured using a flame ionization detector. The CO and CO_2 released during thermal cracking of the bound organic matter (OM) were monitored using an IR cell. The performance of the instrument was checked every 10 samples against the accepted values of Institut Français du Pétrole (IFP) standard (IFP 160 000, S/N1 5-081840). Classical Rock-Eval parameters were calculated by integration of the amounts of HC (Thermo-vaporized free hydrocarbons) expressed in mg/HC/g rock (S1) and hydrocarbons released from cracking of bound OM expressed in mg/HC/g rock (S2) as well as CO and CO_2. During analysis thirteen acquisition parameters are determined from integration of the amounts of OM, CO and CO_2. Here the data presented are the Hydrogen Index (HI) calculated from S2 x 100/ TOC and the Oxygen Index (OI), S3 x 100/TOC (**Figure 4.3** and **Figure 4.4**).

4.3.3 Pollen data

For pollen analysis 139 subsamples taken at 2-16 cm (average = 10 cm) intervals, and prepared using standard palynological techniques (Fægri et al., 2000). An exotic spike (*Lycopodium* tablets; Stockmarr, 1971) was added to each subsample of a known volume before processing them in order to calculate concentrations. Identification of pollen and other palynomorphs was per- formed with relevant keys and atlases, as well as the reference collection of the Laboratory of Palynology of the University of Cologne (Panagiotopoulos et al., 2013; and references therein). The relative percentages of the presented taxa are based upon the sum of terrestrial pollen (excluding obligate aquatics, spores and algae). An average of 500 terrestrial pollen grains were counted per sample (**Figure 4.5**).

4.3.4 Stable isotope and XRD analysis of carbonates

The core from Lake Prespa was sampled for oxygen and carbon isotopes on carbonate at 2 cm intervals from the surface to a correlated depth of 168 cm, where after carbonate content becomes negligible, although small (0.5-2%) TIC spikes occur (**Figure 4.3**). The identification of carbonate species was undertaken using X-Ray Diffraction (XRD) using a Bruker D8 Advance powder diffractometer equipped with a LynxEye linear position sensitive detector and using CuKa radiation over the scan range 4-90˚2θ. The step size was 0.015˚2θ, with 0.8 s per step. Phase identification (calcite and siderite) was performed using Bruker DIFFRACplus EVA search/match software interfaced with the PDF-4+ database from the International Centre for Diffraction Data (ICDD). The Ca-, Mg-substituted siderite pattern 04-009-7660 (Heiss, 1988) offers a better match than pure siderite. Calcite is the only carbonate mineral present above 168 cm, thereafter the carbonate is substituted siderite, except for a layer at depth 1458-1463 cm which contains shelly fragments (and no siderite).

1 cm^3 subsamples (from 0 to 168 cm and from the TIC spikes below 168 cm) were disaggregated in 5% sodium hypochlorite solution for 24 h to oxidize reactive organic material. Samples were then washed three times in distilled water and sieved at 85 mm to remove any potential biogenic carbonate. The <85 mm fraction was filtered, washed with deionized water and dried at 40 °C and ground in agate. Prior to the carbonate isotope analysis, the form of the carbonate was investigated using SEM. Calcite crystals in Lake Prespa are of mixed form, some fragments are platy while others are in the form of fine (partially redissolved) calcite rhombs. The siderite crystals were not found using SEM. For the calcite isotope analysis (0-168 cm and 1462 cm) the CO_2 was evolved by reaction with anhydrous phosphoric acid within a vacuum overnight at a constant 25 °C. For the siderite isotope analysis (TIC spikes between 170 and 1575 cm, except 1462 cm) the CO_2 was evolved by reaction with anhydrous phosphoric acid within a vacuum for 72 h at 90 °C. For both the calcite and siderite, the CO_2 was cryogenically separated from water vapor under vacuum and collected for analysis using a VG Optima dual inlet mass spectrometer. The mineral-gas fractionation factors for calcite and siderite used were 1.01025 and 1.01006 (derived from Rosenbaum and Sheppard, 1986). Carbon and oxygen isotope values ($\delta^{13}C_{calcite/siderite}$, $\delta^{18}O_{calcite/siderite}$) are reported as per mille (‰) deviations of the isotopic ratios ($^{13}C/^{12}C$, $^{18}O/^{16}O$) calculated to the VPDB scale using within- run laboratory standards (calcite = MCS, siderite = CHH8) and international NBS standards. Overall analytical reproducibility for MCS and CHH8 was <0.1‰ for $\delta^{13}C$ and $\delta^{18}O$.

4.4 Chronology

Radiocarbon, tephrochronology and ESR dating have all been used to obtain chronological information for the core Co1215 (**Figure 4.3**). The chronological tie points are presented and discussed in detail in Aufgebauer et al. (2012) and Wagner et al. (2012). The chronology of the lower part of the core is poorly constrained. ESR dating of a shell layer at 1458-1463 cm depth provides a minimum age of 73.9 ± 11.4 ka BP, suggesting deposition at the end of the marine isotope stage (MIS) 5 (cf. Bassinot et al., 1994), which is supported by relatively high, but decreasing organic matter content (**Figure 4.3**). Above the shell horizon, tephras at 1079 and 901 cm depth are difficult to correlate with known tephras, but those at 856, 844, 770, 692, and 617 cm depth have been correlated with the Y-6, SMP1a, Y-5, Codola(?), and Y-3 tephras (Wagner et al., 2012). The tephrostratigraphy, radiocarbon ages, and the characteristics of the sediments (gray color, high clastic matter, high K, low TOC, low TIC and spikes in Mn; cf. Wagner et al., 2010), indicate that this part of the core (>292 cm) was deposited during the Last Glacial (Wagner et al., 2012). Above a transition between ca 292 and 204 cm, radiocarbon ages, tephras, and the sediments (browner, lack of coarse grains, gradual increase of TOC and TIC, and the decreasing K) indicate that the topmost part (204 cm) was deposited during the Holocene. Based on these sedimentological and geochemical variations we suggest that core Co1215 covers MIS 5 to 1, from here on we describe these zones within the MIS framework (**Figure 4.3**).

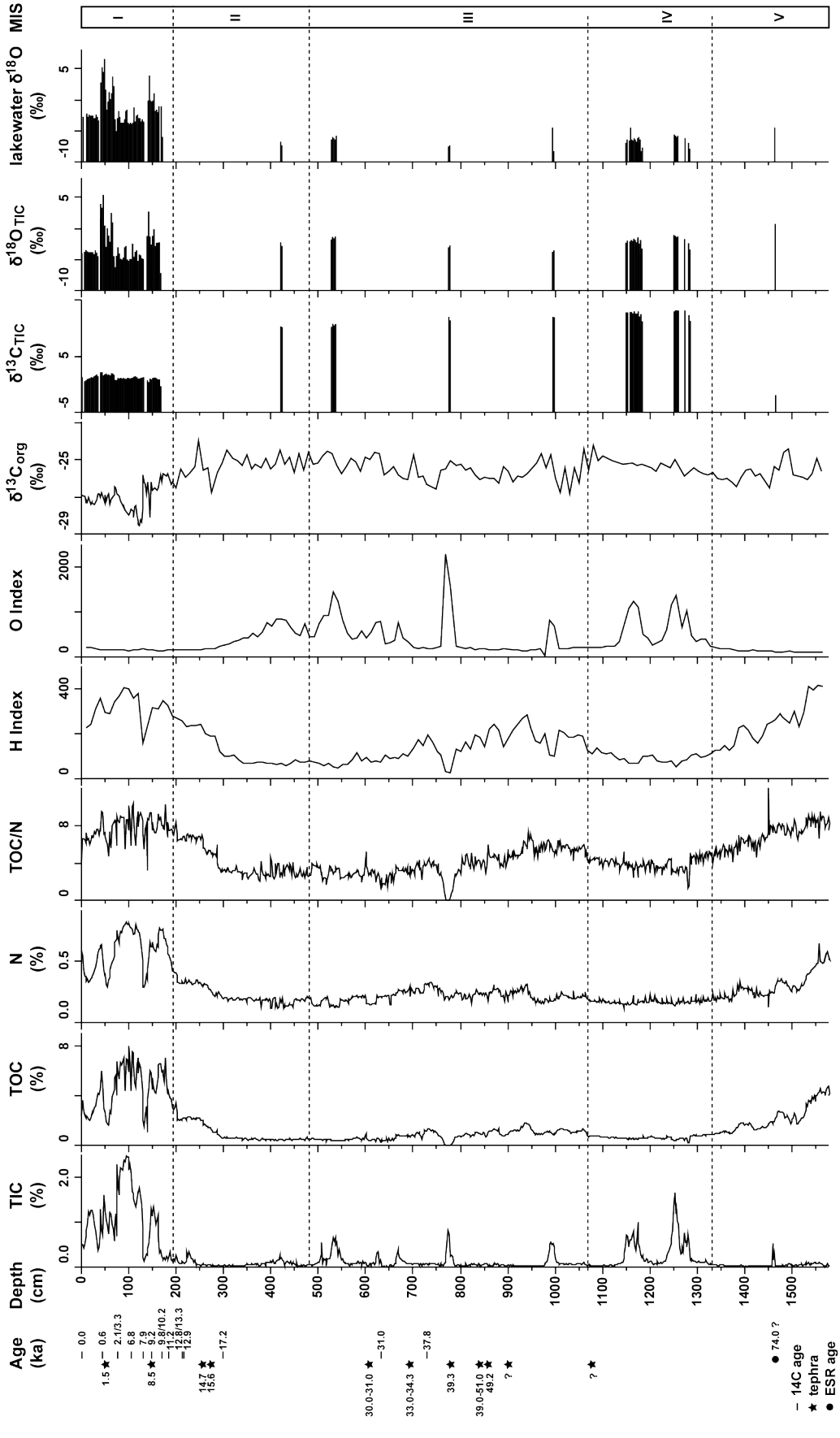

Figure 4.3: Multi-proxy data from Lake Prespa core Co1215. The data fall into zones which roughly equate to Marine Isotope Stages which are marked. The chronology is based on published dates given on the left hand side of the figure. (The oxygen isotope composition of carbonate was obtained from calcite in MIS 1 and siderite in all other zones).

4.5 Results

4.5.1 Modern waters

The oxygen and hydrogen isotope composition of present day waters from a variety of springs around Lakes' Prespa (Mikri and Megali), as well as the lakes themselves are given in **Figure 4.2**a (alongside the Global Meteoric Water Line (GMWL) and Mediterranean Meteoric Water Line (MMWL)). In addition there are 3 spot rainfall samples which fall on or close to the MMWL. These data are from samples taken between 1984 and 2009 (described in Leng et al., 2010), and new data (from springs/rivers entering Lake Prespa as well as the lake itself) from June 2011. Also plotted are monthly modeled rainfall isotope compositions (using 41.17°N, 20.75°E, average altitude of precipitation 1500 m) and mean weighted annual rainfall isotope composition (from G.J. Bowen's online calculator at Waterisotopes.org; Bowen et al., 2005) and 3 spot rainfall samples from around Lake Prespa.

The range in spring/river $\delta^{18}O$ and δD overlaps with the calculated isotope composition of monthly precipitation, although most of the measured spring water isotope data concentrate in the lower isotope range. The calculated mean weighted annual isotope composition of precipitation is $\delta^{18}O$ -8.8‰ and δD -57‰ (Bowen et al., 2005) and is above the vast majority of the spring/river data. Therefore the data suggests that the springs/rivers are likely to be recharged by higher altitude and/or cold season snow/rainfall around the calculated winter rainfall isotope composition (November to March). As such the recharge of the springs/rivers by winter precipitation is very important to the lake levels and the isotope composition of the Prespa lakes (cf. Hollis and Stevenson, 1997).

The isotopic composition of the present day lakewaters fall on a Local Evaporation Line (LEL) away from both the GMWL and the MMWL between -10.9 and +1.2‰ for $\delta^{18}O$ and -69.4 and -12.9‰ for δD. Both Megali and Mikri Prespa are evaporated and the intersection of the LEL with the MMWL at around $\delta^{18}O$ = -8.8‰ and δD = -60.6‰, is c. 2‰ in $\delta^{18}O$ lower than the mean rainfall value, confirming the dominantly spring water recharge (from high altitude and/or cold season snow/rain).

4.5.2 Prespa core Co1215 data

Although the chronology is currently limited and does not allow the establishment of a robust age-depth model, the chronological, sedimentological, palynology and geochemical data allows broad palaeoenvironmental information in comparison with Marine Isotope Stages (**Figure 4.3** and **Figure 4.5**). In general, the MIS 5 sediments are brown, have relatively high TOC, TOC/N, HI while TIC, OI, are low. Arboreal pollen dominates during MIS 5. The Glacial sediments (MIS 4 to 2) are greyish in color, contain low TOC and TOC/N (except for a slight increase around 45-55 ka), and high $\delta^{13}C_{organic}$ (possibly MIS 3). Through this period there are spikes in TIC and OI. The TIC spikes were identified as siderite and measured for their isotope composition; both $\delta^{13}C_{siderite}$ and $\delta^{18}O_{siderite}$ are generally high in comparison to the majority of calcite $\delta^{13}C$ and $\delta^{18}O$. During MIS 4-2 several individual peaks of AP values exceed 70%, pollen from aquatic macrophytes and algae are present but in low numbers. The Pleistocene/Holocene

transition is likely between 292 and 204 cm based on dating and a change in the proxies, i.e. a return to brown sediments, increasing HI, TOC, TOC/N, TIC, and decreasing OI, $\delta^{13}C_{organic}$. The Holocene (MIS 1) sediments in the upper 204 cm have high HI, TOC, TOC/N, TIC and low OI, $\delta^{13}C_{organic}$. High TIC is due to calcite precipitation, $\delta^{13}C$ is consistent around +1.1 ± 0.4‰, while $\delta^{18}O$ is generally low (-4.6 ± 0.8‰) except for two high phases in the early and late Holocene. Arboreal pollen as well as aquatic macrophytes and algae dominate in the Holocene.

4.6 Discussion

4.6.1 Modern water oxygen and hydrogen isotope composition

Over the lakewater collection period (1984-2011) the two Prespa lakes (Megali and Mikri Prespa) had an almost identical range in water isotope composition ($\delta^{18}O$ c. -7 to +1‰; δD c. -47 to -13‰). $\delta^{18}O$ and δD fall on a Local Evaporation Line (LEL) and as such are evaporated (compared to spring waters), the similarity in the isotope data for the two lakes reflects their hydrological connection (**Figure 4.2** a). The range in isotope data for the lakes suggests that the Prespa lakes are very sensitive to moisture balance (winter precipitation versus summer evaporation) and as such respond dramatically too seasonally (i.e. their isotope composition changes through the season due to winter recharge and summer evaporation). However, large seasonal ranges in lake level (up to 1.5 m) have been recorded (Hollis and Stevenson, 1997), so another explanation is that the samples with the intermediary isotope compositions were collected close to rivers or subaqueous springs that flow into the lake (Matzinger et al., 2006a). We know from Lake Ohrid that subaqueous springs result in lake waters with intermediary isotope compositions (Leng et al., 2010), and that lakes at steady state change very gradually in their isotope composition based on successive, seasonally averaged, either dry or wet conditions at time scales longer than the residence time of the lakewater. In addition, Megali Prespa has no surface outlet, although there is subaqueous water outflow through the karst aquifer into Lake Ohrid (Matzinger et al., 2006b). The isotope composition of Lake Ohrid which is very stable with $\delta^{18}O$ and δD values around -4 and -32‰ since 1989 (Leng et al., 2010). The difference in the isotope composition of Ohrid and Prespa lakewater is probably a function of lake size. The volumetrically much larger Lake Ohrid (55.4 km^3 compared to 3.6 km^3 of Lake Prespa, Matzinger et al., 2006a) with its longer residence time (70 and 11 years respectively, Matzinger et al., 2006a) makes Lake Ohrid much better buffered and less responsive (on a decadal scale) against high frequency hydrological change compared to Lake Prespa. Overall, in terms of understanding past lakewater balance from the oxygen isotope composition of lacustrine carbonates, the modern water isotope data suggest that we should interpret $\delta^{18}O$ variation in Lake Prespa as mainly representing changes of the amount of winter rainfall water contribution (recharge), winter ice cover (reducing winter evaporation), summer aridity (enhancing evaporation), and changes in lakewater residence time at a decadal resolution.

4.6.2 Modern water carbon isotope composition

$\delta^{13}C_{TDIC}$ of bicarbonate from the Lake Prespa springs, inflowing rivers, and lakewaters taken in June 2011 provide a range in $\delta^{13}C_{TDIC}$ values between -15.7‰ and -4.7‰ (**Figure 4.2** b). Dissolved bicarbonate is derived from dissolution and weathering of catchment rocks, soils and atmospheric CO_2. The geology around Prespa is largely old basement rocks and Triassic limestones although there are large areas with Quaternary Glacial and volcanic deposits (Aufgebauer et al., 2012). Geological sources of bicarbonate tend to have high $\delta^{13}C$ (Andrews et al., 1993, 1997; Hammarlund, 1993) and so are not likely the major source of the isotopically light ion in the springs and rivers. In contrast organic derived C has $\delta^{13}C$ values generally between -25 and -35‰ (higher up to -16‰ where there is a greater contribution from C4 taxa). Isotopically light CO_2 liberated by decay of terrestrial organic matter in the soil infiltrates springs and rivers by shallow groundwater flow. Under alkaline conditions, and mid range annual temperatures (+10 ˚C), HCO_3^- derived solely from soil CO_2 with $\delta^{13}C_{organic}$ of c. -25‰ should have $\delta^{13}C_{TDIC}$ of ~ -15‰. This is remarkably consistent with the measured spring and river water $\delta^{13}C$ (-15.7‰, see also Leng et al., 1999), although once the bicarbonate enters rivers and lakes other processes change $\delta^{13}C$. Prespa lakewater has high $\delta^{13}C_{TDIC}$ (**Figure 4.2** b). High $\delta^{13}C_{TDIC}$ is common in lakes which do not have a surface outlet (so called closed lakes) where dissolved bicarbonate has time to exchange with atmospheric CO_2 (Leng and Marshall, 2004) or in lakes with a large biomass, so long as there is sedimentation of organic matter (i.e. removal of ^{12}C, and not recycling of ^{12}C) (Meyers and Teranes, 2001). Both processes (exchange and productivity) are likely in Lake Prespa.

4.6.3 Sources of organic matter in the Lake Prespa sedimentary record

Several measurements through the core profile show similar fluctuations in the organic matter (HI, TOC, N, TOC/N) (**Figure 4.3**) while others (OI and $\delta^{13}C_{TOC}$) have an almost inverse relationship being high when the other organic proxies are mostly low. These broad changes in the organic matter broadly fall within zones, which approximate to MIS 5 to MIS 1 (**Figure 4.3**) based on our limited chronology. In general, the amount of organic matter in lake sediments is a function of changes in organic production in the lake, catchment vegetation changes and transfer of terrestrial particulate and dissolved organic matter to the lake, loss processes, and dilution effects (by varying inorganic inputs). These processes can sometimes be disentangled by a combination of organic proxy data (Meyers and Teranes, 2001). Sources of organic matter can be estimated from their TOC/N ratio as well as HI versus OI. Organic nitrogen occurs preferentially in proteins and nucleic acids which are relatively abundant in aquatic plants (Talbot and Johannessen, 1992). Here we assume that the term aquatic plants refers both to macrophytes and phytoplankton; in Lake Prespa the aquatic plants mainly comprise green algae (eg. *Pediastrum*, *Botryococcus*) and Dinoflagellates.

Phytoplankton have low TOC/N, typically ~<10 (Meyers and Teranes, 2001) whereas vascular (cellulose rich) plants tend to have high TOC/N, usually greatly in excess of 10, macrophytes generally sit in between. In Co1215, the TOC/N fluctuates but overall the mean TOC/N = 4.9 (SD = 2.0), varying between 1.3 and 10.4. This range in TOC/N would be interpreted

as organic material mostly from plankton, although very low values ≤6 suggest that there are decompositional processes (cf. Meyers and Ishiwatari, 1995), so the ratio is not unequivocal and needs supporting evidence.

The van Krevelen-type HI-OI diagram distinguishes three main types of organic matter (Types I, II, III) but also can provide information on the amount of oxidation and diagenetic alteration of the organic matter (Talbot and Livingstone, 1989). The data from Lake Prespa shows both Type II and Type III organic matter, which is either a source function or an oxidation artefact (**Figure 4.4**). Type II organic matter corresponds to moderately rich hydrocarbons, and suggests that the sedimentary organic matter is predominantly derived from algae, whereas Type III is poor in hydrocarbon- generating materials and more typical of woody plant material. However, the data fall on a curve of changing OI suggesting that the organic matter has undergone differential amounts of oxidation (which is climate or hydrology related and not time dependent). The down core HI, TOC and N data show that Lake Prespa sediments have changed in their Rock Eval and elemental characteristics through time. Type II sediments with high HI are more typical of the sediments from the Holocene, MIS 3 and MIS 5; whereas Type III with low HI are more common in MIS 2 and 4.

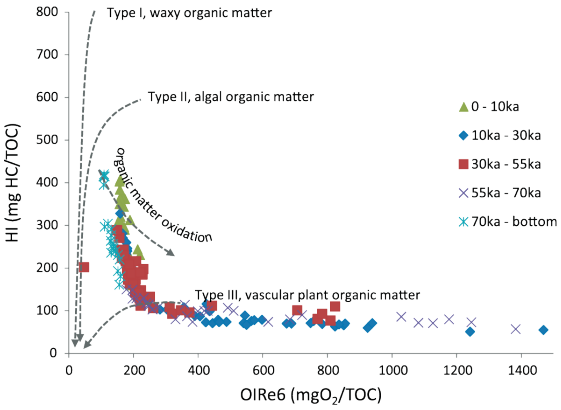

Figure 4.4: Lake Prespa organic matter on a van Krevelen-type discrimination plot (after Meyers and Lallier-Vergès, 1999).

At the end of MIS 5, initial high HI values decrease towards MIS 4, commensurate with a decrease in TOC and low OI and suggest initially high but declining lacustrine productivity. In MIS 4 (and MIS 2) relatively low HI and TOC are more typical of vascular plant organic material (kerogen Type III) although the variable OI values suggests that the organic matter has undergone more extensive oxidation, this is supported by the very low TOC/N perhaps being more likely a function of degradation than source (Talbot and Livingstone, 1989). High rates of oxidation and reduced TOC are more likely in a lake with dimictic or polymictic conditions, although Type III organic matter and high organic oxidation can be found in degraded woody tissues mediated by various types of fungi which cause abiotic diagenetic alterations (Vane and Abbott, 1999; Vane et al., 2003).

In MIS 3, HI and TOC are intermediary between MIS 1 and 2/4, while OI is generally low apart from some spikes. The most likely explanation of the intermediary values is that of a mixed source (samples from this interval also span the kerogen Type II and III boundary), likely being partially altered terrestrial plant matter but also containing a component of aquatic organic matter which is reflected in the rise in TOC and TOC/N. In MIS 1, HI, and TOC peak, and suggest lake sediments containing significant amounts of aquatic organic material (Jacob et al., 2004; Hetényi et al., 2005; Lojka et al., 2009). High algal productivity is indicated by high TIC,

which is fine grained calcium carbonate. Similar <30 mm idiomorphic calcite crystals occur in Lake Ohrid and are typical of photosynthetic phytoplankton endogenic precipitation (Leng et al., 2010; Matter et al., 2010). The high rates of organic material preservation suggest more limited mixing with longer periods of O-depleted bottom waters and might imply less seasonal (i.e. from dimictic to monomictic) overturning. Within MIS 1 there are spikes to lower HI, TOC, TIC (i.e. at 140 cm) which might suggest short perturbations back to cold conditions and better lake mixing. The highest TOC/N ratios of the entire profile occur in MIS 1 (up to 9) but are still suggestive of aquatic productivity and perhaps less decomposition/degradation.

4.6.4 Carbon isotope composition of organic matter from Lake Prespa

It is possible that most of the organic matter in Lake Prespa is planktonic in origin as high summer water temperatures and the large surface area of the lake promote algal activity. Moreover, there are only a few inlets to Lake Prespa and those that do occur have relatively low discharge. Therefore the carbon isotope signal should act as a tracer for past changes in the aquatic carbon cycle. Even if the sediments have undergone some selective diagenesis the primary isotope signature of organic matter incorporated during burial is often not significantly altered and most importantly relative isotope variations are often preserved (Hodell and Schelske, 1998; Meyers and Lalier-Vergès, 1999). Lacustrine algae utilise dissolved HCO_3^- in hard water lakes so variations in the isotope composition of the dissolved HCO_3^- and changes in $\delta^{13}C$ related to productivity and nutrient supply are both possible. The modern TDIC data suggest that the main source of carbon ions to the lakes is soil derived CO_2. The ion will be utilized by the plants growing in the lake. Phytoplankton tend to have $\delta^{13}C$ that is 20‰ lower than the $\delta^{13}C$ of the bicarbonate ion (Leng et al., 2005). In Lake Prespa $\delta^{13}C_{org}$ is consistent around -25‰ and so could be derived from $\delta^{13}C_{TDIC}$ with a value similar to the modern lake (of c. -4.7‰) through MIS 5, 4, 3, 2. These stages also have low TOC, except MIS 5. In contrast the Holocene has lower $\delta^{13}C_{org}$ (-28‰) and high TOC relative to the other stages. The higher $\delta^{13}C_{org}$ in the pre-Holocene sediments suggests high productivity, but in the presence of low TOC suggests productivity under a more limited carbon input, possibly due to more limited recharge of soil-CO_2 leached from the catchment. If soil development is critical that it would follow that the lower $\delta^{13}C$ in the Holocene could just be a function of greater supply of soil derived CO_2 and an improving climate. Pollen evidence suggests well developed soils during the Holocene infer- red from rising amounts of AP pollen types and increasing total pollen concentration values culminating during the Middle and Late Holocene (**Figure 4.5**; Panagiotopoulos et al., 2013). Other pollen data from the region suggest a cold climate during MIS 4 and 2 (e.g. Allen et al., 1999, 2000; Wagner et al., 2009; Lézine et al., 2010). During MIS 5 (and to a lesser extend during MIS 3) the total pollen concentration and percentages of AP suggest favorable climate conditions for plant growth (warmer and/or sufficient moisture).

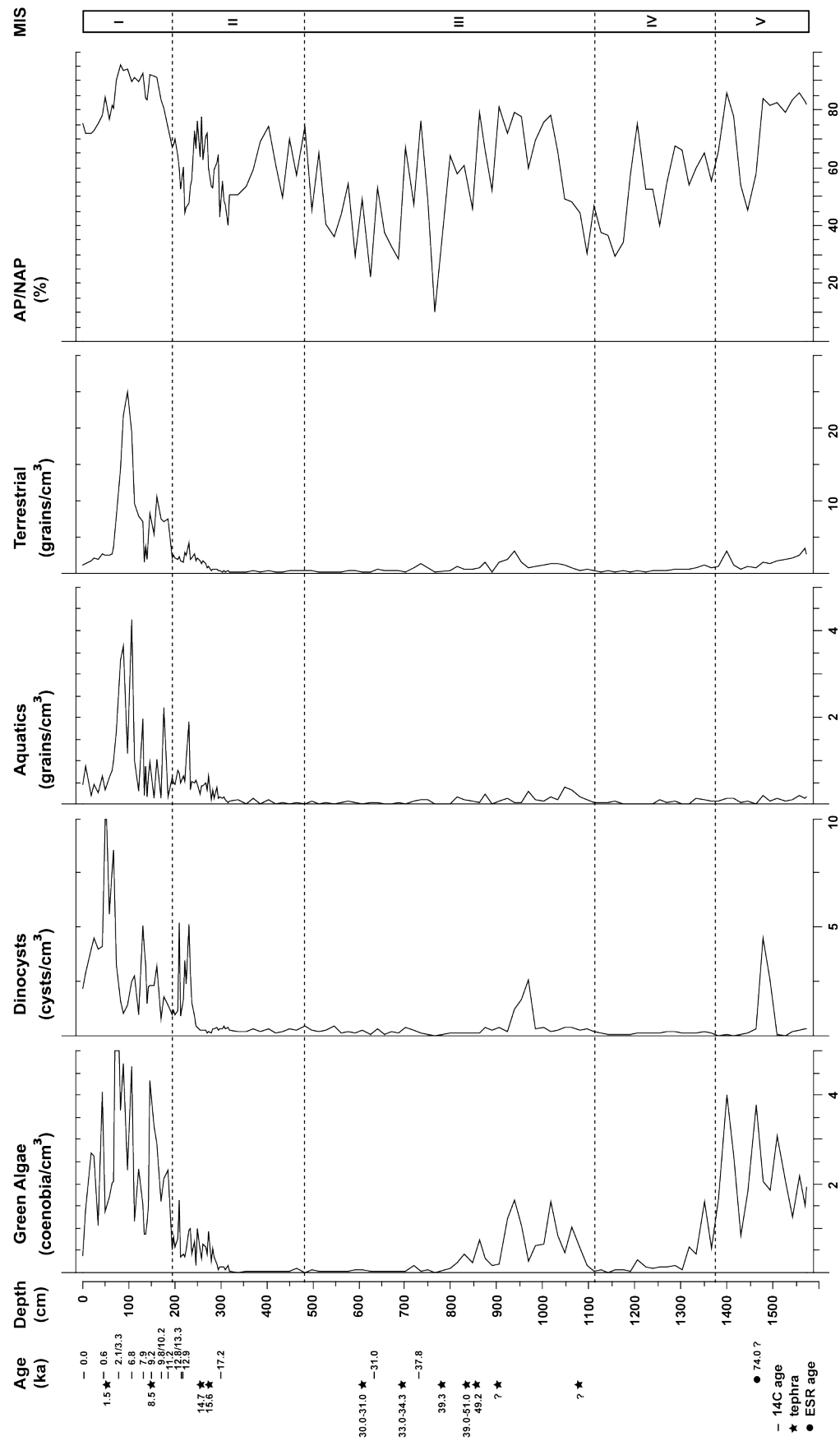

Figure 4.5: A composite pollen diagram including concentration curves of green algae (*Pediastrum* and *Botryococcus*), dinocysts, aquatics (macrophytes) total pollen (including fern spores) and percentage curve of arboreal (AP) versus non-arboreal pollen (NAP).

4.6.5 Oxygen and carbon isotope composition of carbonate from Lake Prespa: MIS 5-1

The TIC spike at 1458-1463 cm is calcite, and investigation of the sediments revealed small (<0.5 mm) shelly fragments of *Dreissena* sp. (Wagner et al., 2012), no siderite was evident from the XRD analysis. This is the only shelly layer in Co1215 and has been interpreted as a period of low lake level although macrophyte remains were not recovered suggesting the shells may have transported by wave action rather than representing a desiccation horizon (Wagner et al., 2012). The $\delta^{13}C$ from the shell fragments is low (-2.0‰) while the $\delta^{18}O$ is high (+0.6‰) in comparison to the isotope composition of the endogenic calcites in the Holocene. Low $\delta^{13}C$ in shell calcite is common as a result of mollusc diet and their microenvironments. Molluscs tend to be most abundant in highly vegetative parts of lakes where there may be greater recycling of ^{12}C (Leng and Marshall, 2004). High $\delta^{18}O$ supports the conclusion that lake levels were low driven by a significant arid phase (similar to the $\delta^{18}O$ highs seen on the Holocene). This arid phase is also recorded in the hydro-acoustic data from Lake Prespa (Wagner et al., 2012) and as a decrease in total pollen concentration and a rise in NAP pollen values. Interestingly though there is no endogenic calcite at this level.

The modern water isotope composition of Lake Prespa shows that the lake is sensitive to the winter recharge (input) versus the summer evaporation ratio (I/E). We assume that the oxygen isotope composition of the lakewater is captured in the carbonates that are precipitated within the lake (Leng and Marshall, 2004). The TIC spikes through MIS 4-2 comprise siderite. Siderite is a common early diagenetic mineral in many lake sediments, forming in porewaters close to the sediment-water interface (Giresse et al., 1991), its geochemistry is often used as an indicator of sediment water redox. Siderite precipitation usually occurs under reducing conditions (Berner, 1971) in slightly to strongly reducing methanogenic zones because of relatively low sulfate and high organic carbon concentrations (Coleman, 1985). We do not know why the siderite only occurs sporadically, although the siderite spikes correlate with highs in the OI and low values in the HI, so perhaps the siderite forms under particular environmental conditions, likely involving a more acidic environment where oxides and hydroxyl ferric-oxides are dissolved (Giresse et al., 1991). The formation of siderite over other carbonates suggests low Ca and Mg. The mean $\delta^{13}C$ value for the Prespa siderites is +11.9‰. Similar high $\delta^{13}C$ values have been reported elsewhere for other lake carbonates (Mozley and Wersin, 1992) and their formation is described as a function of low sulfate concentrations being consumed at shallower levels in the sediments fairly rapidly leaving a greater quantity of organic matter for decomposition by methanogenic bacteria. The heavy $\delta^{13}C$ forms as a result of ^{13}C enriched bicarbonate derived from methanogenesis (Berner, 1980). Indeed methane and/or CO_2 gas occur trapped within the Lake Prespa sediments because when the cores were retrieved there was core swelling due to gas expansion and release. There is no evidence to support other causes of high $\delta^{13}C$, for example ^{13}C-enriched volcanic gas, dissolution of ^{13}C enriched carbonate, and high planktonic productivity (Bahrig, 1988).

The $\delta^{18}O$ of the Prespa siderites is, like calcite, a function of lakewater (input vs. evaporation; I/E) and temperature. However calcite $\delta^{18}O$ cannot be directly compared to siderite $\delta^{18}O$ because of the different equilibration fractionations between the two minerals. The temperature dependent mineral-water fractionation for calcite has been extensively investigated (Epstein et al., 1953;

Craig, 1965; O'Neil et al., 1969 etc.) while there are less empirical studies on the siderite-water fractionation (Carothers et al., 1988; Zhang et al., 2001). To compare the two carbonate minerals and their $\delta^{18}O$ composition we have to use specific mineral fractionation equations and estimate the temperature at the time of the mineral precipitation. For the Holocene aged calcite we use the equation of O'Neil et al. (1969), and assume that the calcite precipitated in the photic zone during the spring and summer months and that the average temperature during these months in the photic zone is c. 21 °C (maximum summer temperature of surface waters can be 27 °C; Kocev et al., 2010). For those periods containing siderites (in the Glacial) we use the equation of Zhang et al. (2001). The estimation of formation temperature for siderite is more difficult, but assuming it is an early diagenetic mineral formed within the sediment during the Glacial period then we might assume cold bottom water temperatures of 4 °C minimum. The calculated $\delta^{18}O$ of the lakewater using the different minerals-formation temperatures are given in **Figure 4.3**. Just comparing the Glacial-Holocene shows much lower modelled lakewater $\delta^{18}O$ values in the Glacial when compared to the Holocene. Even allowing for lower Glacial $\delta^{18}O$ precipitation it seems likely that the lake was less evaporative in the Glacial, probably as a consequence of cooler summers and longer winter ice cover.

Within the Holocene we assume that the mechanism for calcite precipitation is likely the same as described for Ohrid whereby phytoplankton productivity assimilate CO_2 as long as there is a supply of bicarbonate (Matzinger et al., 2006b) which will be replenished via surface run-off into the lake and concentrated by evaporation. There is likely some seasonal dissolution of calcite in the bottom waters triggered by aerobic decomposition of organic matter, higher CO_2 and lower pH (Vogel et al., 2010b). Indeed, Löffle et al. (1998) have shown that pH in the surface waters (pH = 8.3) is generally higher than at depth (pH = 7.3). Endogenic calcite preservation is coincident with high organic matter and suggests high primary productivity likely as a result of the transition from the former Glacial to interglacial together with more ion input due to soil development and weathering. In addition the OI, HI and TOC/N suggest better preservation of organic matter possibly due to less lakewater mixing and due to longer periods of bottom water anoxia.

Overall, the $\delta^{18}O_{calcite}$ data are low (mean = -3.1‰) except for 2 significant $\delta^{18}O_{calcite}$ high phases between 10-8 ka and 2-0.5 ka. If we interpret these highs in $\delta^{18}O_{calcite}$ as a function of hydrological balance (less winter rainfall, greater summer aridity) as suggested by the modern data, then these changes should be also seen in the other Lake Prespa and Lake Ohrid cores, within the limitations of the dating. However, generally high amounts of AP between 10 and 8 ka indicate a positive water balance (sufficient annual precipitation) and forest growth in the catchment of lake Prespa. There is only one exception visible in the pollen data: during the 8.2 ka event. During the last 2 ka human impact has masked possible climatic interpretation of the vegetational proxies. Although we would expect any change should be significantly damped in the Lake Ohrid due to its greater size and residence time.

Lake Prespa $\delta^{18}O_{calcite}$ shows similarities to $\delta^{18}O_{calcite}$ from Lake Ohrid cores (Leng et al., 2010). The basal portions of Co1215 from Prespa and Co1202 from Ohrid show higher values, although the highest values in Prespa between 10 and 8 ka are not evident in Co1202. From ca

6 ka the Ohrid cores show a general trend toward higher $\delta^{18}O$, although Lake Prespa has low and fairly consistent $\delta^{18}O$ between 8 and 2 ka. High $\delta^{18}O$ between 2 and 0.5 ka appear in both cores although the magnitude of variation is significantly different. Prespa $\delta^{18}O_{calcite}$ range is -7 to +6‰, while Ohrid is -7 to -3‰. The enhanced response to lakes level changes in Lake Prespa is not surprising given the difference in water volumes and residence between the lakes.

Lakes that are sensitive to moisture balance (I/E) often have some hydrological closure and/or longer residence time and precipitate carbonates with high $\delta^{13}C_{calcite}$, despite having much more ^{12}C-enriched inflowing waters (Andrews et al., 1993). Evaporating lakes tend to have a covariant relationship between $\delta^{13}C_{calcite}$ and $\delta^{18}O_{calcite}$ (Talbot, 1990; Leng and Marshall, 2004), this is not the case for Lake Prespa ($r^2 = 0.25$). $\delta^{13}C_{calcite}$ values in Prespa will reflect $\delta^{13}C_{TDIC}$ at the time of calcite formation, and like the composition of aquatic organic material the $\delta^{13}C_{TDIC}$ is likely a function of equilibration of the bicarbonate ion with atmospheric CO_2. High algal productivity is unlikely to explain these values because during MIS 2-4 the algae peaks in our diagram are not synchronous with peaks in TIC (**Figure 4.3** and **Figure 4.5**). However, during MIS 1 and 5 algal and TIC peaks are synchronous. Isotopic equilibrium with atmospheric CO_2 will result in lakewater $\delta^{13}C$ having values between +1 and +3‰ (Usdowski and Hoefs, 1990), values similar to the core values within Lake Prespa ($\delta^{13}C_{calcite}$ values through the Holocene = +1.1‰ ± 0.4‰) perhaps suggesting the bicarbonate has reached a steady state due to the long water residence time. One explanation for the lack of a co-variation between $\delta^{13}C_{calcite}$ and $\delta^{18}O_{calcite}$ is perhaps low bicarbonate concentration, unlike changes in $\delta^{18}O$ which will be driven by hydrological balance.

4.6.6 Comparison of $\delta^{18}O$ between Prespa, Ohrid and other lakes in the region from 15 ka

4.6.6.1 Late Glacial to Holocene transition

The Late Glacial to Holocene transition in Prespa Co1215 initiates at c. 15 ka (**Figure 4.3**) with a gradual increase in organic matter content (interpreted as increased productivity; Aufgebauer et al., 2012), increased TOC/N (less decomposition). There is little or poor evidence that a similar change occurs in the existing Lake Ohrid cores. This gradual transition to the Younger Dryas is often marked in Mediterranean lake records by an increase in $\delta^{18}O_{calcite}$ (Roberts et al., 2008), this phase and other Pleistocene carbonate isotopic enrichment events seen in Mediterranean lakes may be linked to the North Atlantic Heinrich cold events (Roberts et al., 2008), although chronological imprecision means this suggestion is currently not verifiable. In Lake Prespa the low carbonate content prior to 10 ka cannot confirm this transition from the isotope perspective (the carbonate is too low to analyze for isotopes), although the absence of significant amounts of carbonate perhaps implies a lake with low evaporation. Within this transition, immediately post the harsh climate of the Late Glacial/Oldest Dryas, the pollen show a retreat of steppe herb communities (eg. *Artemisia* and Chenopodiaceae) coupled with a gradual rise of pine and oak suggest rising moisture availability within the Prespa catchment. This trend is interrupted by an abrupt millennial vegetational setback (likely the Younger Dryas chronozone) which is characterized by increasing aridity and lower temperatures. Around Prespa this is marked by

a major restructuring of the vegetation including a descending treeline and/or a thinning of existing tree stands (Panagiotopoulos et al., 2013).

4.6.6.2 Early Holocene

In the early Holocene, Lake Prespa shows a small peak in $\delta^{18}O_{calcite}$ between 10 and 8 ka while Lake Ohrid shows a small $\delta^{18}O_{calcite}$ peak between 10 and 9 ka. Other lakes in the Eastern and Central Mediterranean show that the early Holocene carbonates are isotopically depleted at this time (Roberts et al., 2008; their **Figure 4.5** and **Figure 4.6**). The magnitude of evaporative enrichment in Lake Prespa during the early Holocene is less than the later Holocene (see below). It is difficult to compare directly the $\delta^{18}O_{calcite}$ from the early and late Holocene because there are isotope complications, for example, the source composition of precipitation would have likely been different partly because of changes in the Mediterranean Sea at that time. Other lakes around the Eastern Mediterranean show an early Holocene oxygen isotope depletion, which Roberts et al. (2008) ascribe as most likely a function of regional water balance and a difference in the source isotope composition of precipitation due to the formation of sapropel in the Mediterranean Sea. The sapropel formation was thought to be initiated by increased rainfall and runoff from the Nile into the Eastern Mediterranean Sea, which would have contributed significantly to the creation of a freshwater lid and subsequently bottom water anoxia between 9.5 ka and 6.5 ka (Rohling, 1994; Ariztegui et al., 2000). The pollen record shows the gradual formation of closed oak forests and their diversification, with the establishment of thermophilous

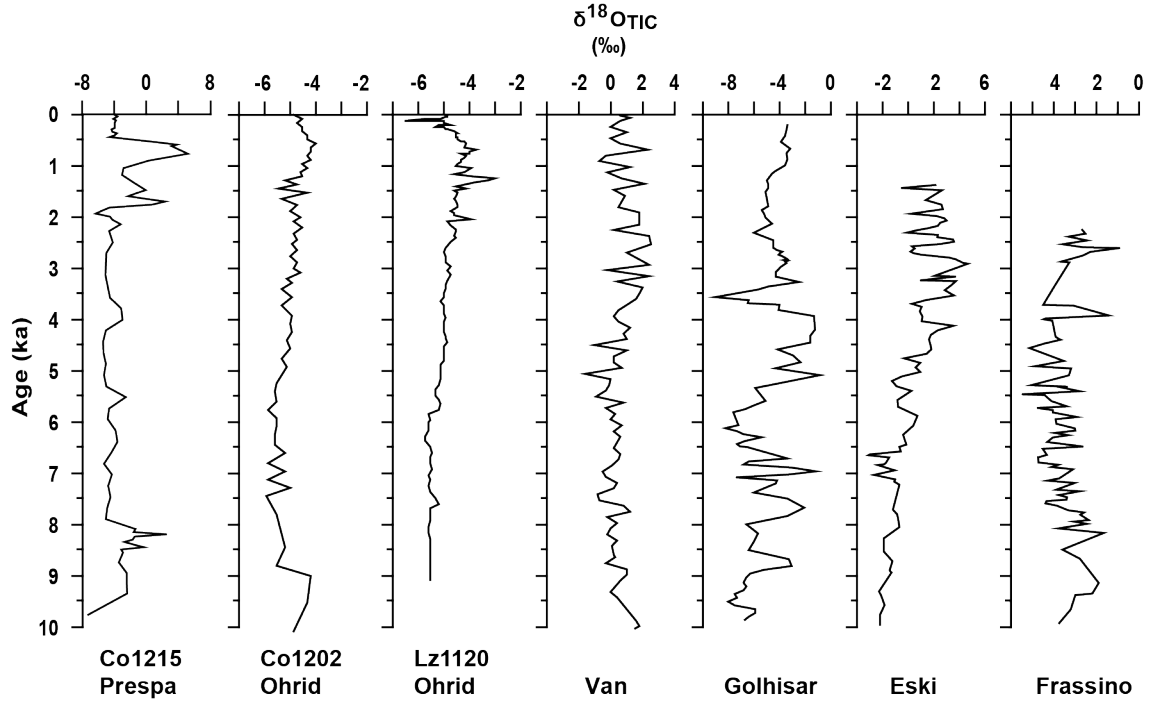

Figure 4.6: Comparison of oxygen isotope profiles form Lake Prespa core Co1215, to cores from Lake Ohrid and other lakes from around the Mediterranean over the Holocene where carbonate data can be compared (data in Roberts et al., 2008 and references therein).

and drought-sensitive trees after approximately 10 ka which suggests the absence of summer droughts and thus confirms sufficient precipitation for forest growth during this period. Moreover, the parallel appearance and establishment of important maquis constituents exclude the existence of intense late winter and spring droughts. In light of the above, the pollen record suggests a rather even distribution of annual precipitation, which appears to be in agreement with the sapropel formation in the eastern Mediterranean (Panagiotopoulos et al., 2013).

4.6.6.3 Middle Holocene humidity

Lake Prespa records the lowest $\delta^{18}O_{calcite}$ values for the period (8-2 ka), while Lake Ohrid clearly shows a progressive enrichment in $\delta^{18}O_{calcite}$ over this time interval (**Figure 4.6**). This difference could be a function of hydrology and the different lake sizes. Recharge into Lake Prespa was presumably sufficient to counter summer evaporation, whereas in Ohrid with its much larger lakewater volume to surface area in comparison to catchment area may mean that Lake Ohrid may be less responsive to winter recharge. The pollen records from the two sites (Wagner et al., 2009; Panagiotopoulos et al., 2013) are almost identical during the Holocene implying similar climate regimes in both catchments. Overall, the low and stable $\delta^{18}O$ values in both Prespa and Ohrid through the middle Holocene is a general feature observed in other eastern and central Mediterranean lakes and speleothems (Bar-Matthews et al., 2000; Zanchetta et al., 2007b; Roberts et al., 2008; Develle et al., 2010), although not always over exactly the same time periods notwithstanding dating issues. Lakes Van and Frassino have a low and stable $\delta^{18}O$ period from 9 to 4 ka (Baroni et al., 2006), while Eski is low only till about 6 ka (Roberts et al., 2001). The much smaller Golhisar Golu appears to respond very rapidly to moisture balance although values are generally low between 7 and 5 ka (Eastwood et al., 2007, **Figure 4.6**). This mid-Holocene humidity has been interpreted in different ways, for example it has been attributed to increased amounts of precipitation related to an increase in winter precipitation of Atlantic origin (Zanchetta et al., 2007; Zhornyak et al., 2011) or a significant (especially for eastern Mediterranean) freshening of surface marine water of the eastern Mediterranean at that time resulting in lower $\delta^{18}O$ of precipitation (e.g., Kolodny et al., 2005; Develle et al., 2010). The Middle Holocene Prespa pollen record suggests similar climatic and environmental conditions to the early Holocene.

4.6.6.4 Late Holocene

The higher $\delta^{18}O_{calcite}$ in Lake Prespa (and Lake Ohrid) from 2 ka suggests drier conditions, and probably a significant lake level drop in Prespa, as $\delta^{18}O_{calcite}$ values are the highest of the entire record. Over this time there is a general trend towards higher $\delta^{18}O_{calcite}$ in many other Mediterranean isotopic records both in lakes (e.g. Roberts et al., 2008; Develle et al., 2010) and in speleothems (e.g. Bar-Matthews et al., 2000; Zanchetta et al., 2007b; Verheyden et al., 2008). Lake Van, Eski and Frassino show consistently high values from 4 ka (the latter 2 showing hiati from between 2 and 1 ka; **Figure 4.6**). In Golhisar Golu there are high values also from 4 ka but the hydrology likely changes around 3 ka with the effect of the Santorini tephra on the lake catchment (Eastwood et al., 2007; **Figure 4.6**). This regional drying has previously been described as

related to progressive reduction in moisture advection from the Atlantic linked to a reduction in summer insolation, which also resulted in a decrease in monsoon activity on tropical Africa and progressive aridification of the Sahara (e.g. Gasse, 2000). Isotopically this increase could also be related to progressive increase in isotopic composition in the Mediterranean Sea (Emeis et al., 2000) and the related effect on rainfall amount. Very low lake levels (and highest $\delta^{18}O_{calcite}$) at Lake Prespa occur around c. 1 ka and are thought to correspond with the occurrence of ruins of several buildings at 840-842 m a.s.l. (Sibinoviç, 1987). These buildings were constructed at the end of the 10th/beginning of the 11th century AD and it is unlikely that they were formed in the water. There is a rapid reversal in the last 500 years as $\delta^{18}O_{calcite}$ declines to some of the lowest values (-7‰) in the most recent sediments (also seen in Ohrid core Lz1120; Leng et al., 2010; **Figure 4.6**). Why Co1215 shows a consistent wet phase (low $\delta^{18}O$) in the last 500 years is unclear but there is some evidence in Lake Ohrid for very recent (apparent) freshening driven by anthropogenic change including the Roman and recent forest clearance (Wagner et al., 2009).

Finally, in the modern lakewater, assuming peak precipitation of calcite occurs during the warmer summer months when mean monthly temperatures are high (summer temperatures between 2001 and 2004 averaged between + 20 and + 22 ˚C, Matzinger et al., 2007), calcite precipitating in Lake Prespa with a lakewater value of -1‰ will have a $\delta^{18}O_{calcite}$ of around -2‰, i.e. an oxygen isotope composition that is higher than most of the Holocene calcite $\delta^{18}O$ except for the early and late Holocene arid phases. However, the isotopic composition of modern lakewater is perhaps as much to do with anthropogenic activities as climate. Indeed the recent receding woodlands and the development of agriculture (cereals and crop trees) occurring alongside the increased accumulation rates of algae suggests that Lake Prespa is undergoing substantial changes that point to intensive anthropogenic activities (Panagiotopoulos et al., 2013). In Lake Prespa as with many other lakes disentangling natural from human impact over the very recent past is challenging.

4.7 Conclusions

The current Lake Prespa waters are evaporated compared to the inflowing spring waters. The hydrological balance in Lake Prespa is a function of summer aridity and winter precipitation, on a decadal scale. The spring water bicarbonate ion is likely derived from soil CO_2 which once incorporated into the lakewater likely equilibrates with atmospheric CO_2.

The Lake Prespa sediments broadly fall into zones based on their sedimentology, geochemistry, palynology and the existing chronology; these zones roughly equate to Marine Isotope Stages 5 to 1. The Glacial sediments are grey, contain low TOC and TOC/N and high $\delta^{13}C_{organic}$ suggesting low supply of carbon to the lake, but high summer productivity. Through this period there are spikes in OI and siderite, which suggest that although the lake was likely to have mixed regularly leading to enhanced oxidation of organic matter, there must have been within sediment reducing conditions and methanogenesis. In contrast the MIS 5 sediments have relatively high TOC, TOC/N, HI while TIC, OI, and $\delta^{13}C_{org}$ are low, similar to MIS 1 although the Holocene sediments contain high calcite. MIS 5 and 1 sediments suggest much more productivity, higher rates of organic material preservation possibly due to more limited mixing with longer periods of O-depleted bottom waters.

The $\delta^{18}O$ of the Glacial siderites is, like calcite, a function of lakewater input: evaporation balance and temperature. However calcite $\delta^{18}O$ cannot be directly compared to siderite $\delta^{18}O$ because of the different equilibration fractionations between the two minerals. Here we recalculate lakewater $\delta^{18}O$ from siderite and calcite, estimating the temperature of formation. The calculated $\delta^{18}O$ of the lakewater using the different minerals shows much lower modeled lakewater $\delta^{18}O$ values in the Glacial when compared to the Holocene. Even allowing for lower Glacial $\delta^{18}O_{precipitation}$ it seems likely that the lake was less evaporative in the Glacial, probably as a consequence of cooler summers and longer winter ice cover.

The oxygen isotope composition of calcites and palynology from the Holocene show a generally humid Holocene, a feature observed in other Eastern and Central Mediterranean lakes and speleothems and can be attributed to increased amounts of precipitation related to an increase in winter precipitation of Atlantic origin together with a freshening of the surface of the Mediterranean Sea (lower $\delta^{18}O$ in rainfall) at that time. Ours and other pollen records and climate reconstructions from this region indicate the importance of seasonality in precipitation regime during the Holocene (Panagiotopoulos et al., 2013 and references therein). Regional drying in the late Holocene has been ascribed to progressive reduction in moisture advection from the Atlantic linked to a reduction in summer insolation, a decrease in monsoon activity on tropical Africa and progressive aridification of the Sahara leading to regional aridity and an increase in isotopic composition in the Mediterranean Sea (Emeis et al., 2000).

4.8 Acknowledgements

We would like to thank the logistic support from the Hydrobiological Institute in Ohrid and the Police Station in Stenje. The overall project is funded by the German Research Foundation (DFG) within the scope of the CRC 806 “Our way to Europe”. The isotope project was funded by the British Geological Survey. Leng and Wagner undertook the main interpretation of all the data sets. Boehm provided the geochemical concentration data (and intellectually via Aufgebauer et al. 2012). Panagiotopoulos provided the pollen data and interpretation of the pollen (and intellectually via Panagiotopoulos et al., 2013). Vane provided the Rock Eval data and interpretation. Snelling, Haidon, Woodley and Baneschi provided the isotope and mineralogy data. Vogel and Zanchetta contributed intellectually to the discussions of the data.

4.9 References

Aliaj, S.H., Baldassarre, G., Shkupi, D., 2001. Quaternary subsidence zones in Albania: some case studies. Bulletin of Engineering Geology and the Environment 59, 313-318.

Allen, J.R.M., Huntley, B., 2000. Weichselian palynological records from southern Europe: correlation and chronology. Quaternary International 73, 111-125.

Allen, J.R.M., Brandt, U., Brauer, A., Hubberten, H.-W., Huntley, B., Keller, J., Kraml, M., Mackensen, A., Mingram, J., Negendank, J.F.W., Nowaczyk, N.R., Oberhänsli, H., Watts, W.A., Wulf, S., Zolitschka, B., 1999. Rapid environmental changes in southern Europe during the Last Glacial period. Nature 400, 740-743.

Andrews, J.E., Riding, R., Dennis, P.F., 1993. Stable isotope compositions of recent freshwater cyanobacterial carbonates from the British Isles: local and regional environmental controls. Sedimentology 40, 303-314.

Andrews, J.E., Riding, R., Dennis, P.F., 1997. The stable isotope record of environmental and climatic signals in modern terrestrial microbial carbonates from Europe. Palaeogeography, Palaeoclimatology, Palaeoecology 129, 171-189.

Anovski, T. (Ed.), 2001. Progress in the Study of Prespa Lake Using Nuclear and Related Techniques, Project Report. IAEA Regional Project RER/8/008, ISBN 9989-650-21-7. Skopje, Macedonia.

Anovski, T., Andonovski, B., Minceva, B., 1991. Study of the hydrological relationship between lakes Ohrid and Prespa. In: Proceedings of an IAEA International Symposium, IAEA-SM-Vienna, 11-15 March 1991, 319, pp. 62.

Anovski, T., Andonovski, B., Minceva, B., 1992. Study of the hydrological relationship between Lake Ohrid and Prespa. In: Proceedings of Symposium on Isotope Techniques in Water Resources Development. IAEA, Vienna, Austria.

Ariztegui, D., Asioli, A., Lowe, J.J., Trincardi, F., Vigliotti, L., Tamburini, F., Chondrogianni, C., Accorsi, C.A., Mazzanti, M.B., Mercuri, A.M., van der Kaars, S., McKenzie, J.A., Oldfield, F., 2000. Palaeoclimate and the formation of sapropel S1: inferences from Late Quaternary lacustrine and marine sequences in the central Mediterranean region. Palaeogeography, Palaeoclimatology, Palaeoecology 158, 215-240.

Aufgebauer, A., Panagiatopoulos, K., Wagner, B., Schäbitz, F., Viehberg, F.A., Vogel, H., Zanchetta, G., Sulpizio, R., Leng, M.J., Damaschke, M., 2012. Climate and environmental change in the Balkans over the last 17 ka recorded in sediments from Lake Prespa (Albania/F.Y.R. of Macedonia/Greece). Quaternary International 274, 122-135.

Bahrig, B., 1988. Palaeo-environment Information from Deep Water Siderite (Lake of Laach, West Germany). In: Geological Society London, Special Publications, vol. 40, pp. 153-158.

Bar-Matthews, M., Ayalon, A., Kaufman, A., 2000. Timing and hydrological conditions of Sapropel events in the Eastern Mediterranean, as evident from speleothems, Soreq Cave, Israel. Chemical Geology 169, 145-156.

Baroni, C., Zanchetta, G., Fallick, A.E., Longinelli, A., 2006. Mollusca stable isotope record of a core from Lake Frassino, northern Italy: hydrological and climatic changes during the last 14 ka. The Holocene 16, 827-837.

Bassinot, F.C., Labeyrie, L.D., Vincent, E., Quidelleur, X., Shackleton, N.J., Lancelot, Y., 1994. The astronomical theory of climate and the age of the Brunhes-Matuyama magnetic reversal. Earth and Planetary Science Letters 126, 91-108.

Berner, R.A., 1971. Principals of Sedimentology. McGraw-Hill, New York, p. 240.

Berner, R.A., 1980. Early Diagenesis: a Theoretical Approach. Princeton University Press, Princeton, New Jersey, p. 241.

Bolle, H.J., 2003. Mediterranean Climate. In: Variability and Trends. Springer, Berlin.

Bowen, G.J., Wassenaar, L.I., Hobson, K.A., 2005. Global application of stable hydrogen and oxygen isotopes to wildlife forensics. Oecologia 143, 337-348.

Carothers, W.W., Adami, L.H., Rosenbauer, R.J., 1988. Experimental oxygen isotope fractionation between siderite-water and phosphoric acid liberated CO_2-siderite. Geochimica et Cosmochimica Acta 52, 2445-2450.

Coleman, M.L., 1985. Geochemistry of diagenetic non-silicate minerals: kinetic considerations. In: Eglington, G., et al. (Eds.), Geochemistry of Buried Sediments. London, Royal Society, pp. 39-54.

Craig, H., 1965. The measurement of oxygen isotope palaeotemperatures. In: Tongiorgi, E. (Ed.), Stable Isotopes in Oceanographic Studies and Palaeotemperatures. Consiglio Nazionale delle Ricerche Laboratorio di Geologia Nucleare, Pisa, pp. 161-182.

Develle, A.L., Herreros, J., Vidal, L., Sursock, A., Gasse, F., 2010. Controlling factors on paleolake oxygen isotope record (Yammouneh, Lebanon) since the Last Glacial Maximum. Quaternary Science Reviews 29, 865-886.

Eastwood, W.J., Leng, M.J., Roberts, N., Davis, B., 2007. Holocene climate change in the eastern Mediterranean region: a comparison of stable isotope and pollen data from a lake record in southwest Turkey. Journal of Quaternary Science 22, 327-341.

Eftimi, R., Zoto, J., 1997. Isotope study of the connection of Ohrid and Prespa lakes. In: International Symposium "Towards Integrated Conservation and Sustainable Development of Transboundary Macro and Micro Prespa Lakes", Korcha, Albania.

Emeis, K.C., Struck, U., Schulz, H.M., Rosenberg, R., Bernasconi, S., Erlenkeuser, H., Sakamoto, T., Martinez-Ruiz, F., 2000. Temperature and salinity variations of Mediterranean Sea surface waters over the last 16,000 years from records of planktonic stable oxygen isotopes and alkenone unsaturation ratios. Palaeogeography, Palaeoclimatology, Palaeoecology 158, 259-280.

Epstein, S., Buchsbaum, R., Lowenstam, H.A., Urey, H.C., 1953. Revised carbonate- water isotopic temperature scale. Geological Society of America Bulletin 64, 1315-1325.

Frogley, M.R., Griffiths, H.I., Heaton, T.H.E., 2001. Historical biogeography and Late Quaternary environmental change of Lake Pamvotis, Ioannina (north-western Greece): evidence from ostracods. Journal of Biogeography 28, 745-756.

Fægri, K., Iversen, J., Kaland, P.E., Krzywinski, K., 2000. Textbook of Pollen Analysis, fourth ed. Blackburn Press, Caldwell, p. 340.

Gasse, F., 2000. Hydrological changes in the African tropics since the Last Glacial Maximum. Quaternary Science Reviews 19, 189-211.

Giresse, P., Maley, J., Kelts, K., 1991. Sedimentation and palaeoenvironment in crater lake Barombi Mbo, Cameroon, during the last 25,000 years. Sedimentary Geology 71, 151-175.

Hammarlund, D., 1993. A distinct d13C decline in organic lake sediments at the Pleistocene-Holocene transition in southern Sweden. Boreas 22, 236-243. Heiss, G., 1988. Crystal structure refinement of a synthetic Fe-Mg-Ca-carbonate phase. Zeitschrift fur Kristallographie 185, 604.

Hetényi, M., Nyilas, T., Tóth, T., 2005. Stepwise rock-eval pyrolysis as a tool for typing heterogeneous organic matter in soils. Journal of Analytical and Applied Pyrolysis 74, 45-54.

Hodell, D.A., Schelske, C.L., 1998. Production, sedimentation and isotopic composition of organic matter in Lake Ontario. Limnology and Oceanography 43, 200-214.

Hollis, G.E., Stevenson, A.C., 1997. The physical basis of the lake Mikri Prespa systems: geology, climate, hydrology and water quality. Hydrobiologia 351, 1-19.

Jacob, J., Disnar, J.-R., Boussafir, M., Sifeddine, A., Turcq, B., Spadano Albuquerque, A.L., 2004. Major environmental changes recorded by lacustrine sedimentary organic matter since the Last Glacial maximum near the equator (Lagoa do Caçó, NE Brazil). Palaeogeography, Palaeoclimatology, Palaeoecology 205, 183-197.

Kocev, D., Naumoski, A., Mitreski, K., Krstic, S., Dzeroski, S., 2010. Learning habitat models for the diatom community in Lake Prespa. Ecological Modelling 221, 330-337.

Kolodny, Y., Stein, M., Machlus, M., 2005. Seaerainelake relation in the Last Glacial East Mediterranean revealed by $\delta^{18}O$-$\delta^{13}C$ Lake Lisan aragonites. Geochimica et Cosmochimica Acta 69, 4045-4060.

Leng, M.J., Marshall, J.D., 2004. Palaeoclimate interpretation of stable isotope data from lake sediment archives. Quaternary Science Reviews 23, 811-831.

Leng, M.J., Roberts, N., Reed, J.M., Sloane, H.J., 1999. Late Quaternary climatic and limnological variations based on carbon and oxygen isotope data from authigenic and ostracod carbonate in the Konya Basin, Turkey. Journal of Paleo- limnology 22, 187-204.

Leng, M.J., Lamb, A.L., Heaton, T.H.E., Marshall, J.D., Wolfe, B.B., Jones, M.D., Holmes, J.A., Arrowsmith, C., 2005. Isotopes in lake sediments. In: Leng, M.J. (Ed.), Isotopes in Palaeoenvironmental Research. Springer, Dordrecht, The Netherlands, pp. 148-176.

Leng, M.J., Baneschi, I., Zanchetta, G., Jex, C.N., Wagner, B., Vogel, H., 2010. Late Quaternary palaeoenvironmental reconstruction from Lakes Ohrid and Prespa (Macedonia/Albania border) using stable isotopes. Biogeosciences 7, 3109-3122.

Lézine, A.-M., von Grafenstein, U., Andersen, N., Belmecheri, S., Bordon, A., Caron, B., Cazet, J.P., Erlenkeuser, H., Fouache, E., Grenier, C., Huntsman-Mapila, P., Hur-eau-Mazaudier, D., Manelli, D., Mazaud, A., Robert, C., Sulpizio, R., Tiercelin, J.J., Zanchetta, G., Zeqollari, Z., 2010. Lake Ohrid, Albania, provides an exceptional multi-proxy record of environmental changes during the Last Glacial-interglacial cycle. Palaeogeography, Palaeoclimatology, Palaeoecology 287, 116-127.

Lionello, P., Malanotte-Rizzoli, P., Boscolo, R., 2006. Mediterranean Climate Variability. Elsevier, The Netherlands.

Löffle, H., Schiller, E., Kusel, E., Kraill, H., 1998. Lake Prespa, a European natural monument, endangered by irrigation and eutrophication? Hydrobiologia 384, 69-74.

Lojka, R., Drábková, J., Zajíc, J., Sýkorová, I., Franc#u, J., Bláhová, A., Grygar, T., 2009. Climate variability in the Stephanian B based on environmental record of the Msec Lake deposits (Kladno-Rakovník Basin, Czech Republic). Palaeogeography, Palaeoclimatology, Palaeoecology 280, 78-93.

Matter, M., Anselmetti, F.S., Jordanoska, B., Wagner, B., Wessels, M., Wüest, A., 2010. Carbonate sedimentation and effects of eutrophication observed at the Kalista subaquatic springs in Lake Ohrid (Mazedonia). Biogeosciences 7, 3755-3767.

Matzinger, A., Jordanoski, M., Veljanoska-Sarafiloska, E., Sturm, M., Müller, B., Wüest, A., 2006a. Is Lake Prespa jeopardizing the ecosystem of ancient Lake Ohrid? Hydrobiology 553, 89-109.

Matzinger, A., Spirkovski, Z., Patceva, S., Wüest, A., 2006b. Sensitivity of ancient Lake Ohrid to local anthropogenic impacts and global warming. Journal of Great Lakes Research 32, 158-179.

Matzinger, A., Schmid, M., Veljanoska-Sarafiloska, E., Patceva, S., Guseska, D., Wagner, B., Müller, B., Sturm, M., Wüest, A., 2007. Eutrophication of ancient Lake Ohrid: global warming amplifies detrimental effects of increased nutrient inputs. Limnology and Oceanography 52, 338-353.

Meyers, P.A., Ishiwatari, R., 1995. Organic matter accumulation records in lake sediments. In: Lerman, A., Imboden, D.M., Gat, J.R. (Eds.), Physics and Chemistry of Lakes. Springer Verlag Berlin, Heidelberg, New York, pp. 279-328.

Meyers, P.A., Lallier-Vergès, E., 1999. Lacustrine sedimentary organic matter records of late Quaternary paleoclimates. Journal of Paleolimnology 21, 345-372.

Meyers, P.A., Teranes, J.L., 2001. Sediment organic matter. In: Last, W.M., Smol, J.P. (Eds.), Developments in Paleoenvironmental Research. Tracking Environmental Change Using Lake Sediments, vol. 2. Kliwer Academic Publishers, Dordrecht, pp. 239-269.

Mozley, P.S., Wersin, P., 1992. Isotopic composition of siderite as an indicator of depositional environment. Geology 20, 817-820.

O'Neil, J.R., Clayton, R.N., Mayeda, T.K., 1969. Oxygen isotope fractionation in diva- lent metal carbonates. Journal of Chemical Physics 51, 5547-5558.

Panagiotopoulos, K., Aufgebauer, A., Schäbitz, F., Wagner, B., 2013 Vegetation and climate history of the Lake Prespa region since the Lateglacial. Quaternary International 293, 157-169.

Popovska, C., Bonacci, O., 2007. Basic data on the hydrology of Lakes Ohrid and Prespa. Hydrological Processes 21, 658-664.

Roberts, N., Reed, J., Leng, M.J., Kuzucuoglu, C., Fontugne, M., Bertaux, J., Woldring, H., Bottema, S., Black, S., Hunt, E., Karabıyıkoglu, M., 2001. The tempo of Holocene climatic change in the eastern Mediterranean region: new high-resolution crater-lake sediment data from central Turkey. The Holocene 11, 721-736.

Roberts, N., Jones, M.D., Benkaddour, A., Eastwood, W.J., Filippi, M.L., Frogley, M.R., Lamb, H.F., Leng, M.J., Reed, J.M., Stein, M., Stevens, L., Valero-Garcés, B., Zanchetta, G., 2008. Stable isotope records of Late Quaternary climate and hydrology from Mediterranean lakes: the ISOMED synthesis. Quaternary Science Reviews 27, 2426-2441.

Rohling, E.J., 1994. Review and new aspects concerning the formation of eastern Mediterranean sapropels. Marine Geology 122, 1-28.

Rosenbaum, J., Sheppard, S.M.F., 1986. An isotopic study of siderites, dolomites and ankerites at high temperatures. Geochimica et Cosmochimica Acta 50, 1147-1150.

Sibinoviç, M., 1987. Ezera Prespansko i Ohridsko. The SRC & Agency of Water Resources of R. of Macedonia, Skopje (in Macedonian).

Stefouli, M., Kouraev, A., Charou, E., 2008. In: Proceedings of the 2nd MERIS/(A) ATSR User Workshop, Frascati, Italy, 22-26 September 2008.

Stockmarr, J., 1971. Tablets with spores used in absolute pollen analysis. Pollen et Spores 13, 615-621.

Talbot, M.R., 1990. A review of the palaeohydrological interpretation of carbon and oxygen isotopic ratios in primary lacustrine carbonates. Chemical Geology 80, 261-279.

Talbot, M.R., Johannessen, T., 1992. A high resolution palaeoclimatic record for the last 27 500 years in tropical West Africa from the carbon and nitrogen isotopic composition of lacustrine organic matter. Earth and Planetary Science Letters 110, 23-37.

Talbot, M.R., Livingstone, D.A., 1989. Hydrogen index and carbon isotopes of lacustrine organic matter as lake level indicators. Palaeogeography, Palaeoclimatology, Palaeoecology 70, 121-137.

Usdowski, E., Hoefs, J., 1990. Kinetic C-13 C-12 and O-18 O-16 effects upon dissolution and outgassing of CO_2 in the system CO_2-H_2O. Chemical Geology 80, 109-118.

Vane, C.H., Abbott, G.D., 1999. Proxies for land plant biomass: closed system pyrolysis of some methoxyphenols. Organic Geochemistry 30, 1535-1541. Vane, C.H., Drage, T.C., Snape, C.E., 2003. Biodegradation of Oak (*Quercus alba*) wood during growth of the shiitake mushroom (*Lentinula edodes*): a molecular approach. Journal of Agricultural and Food Chemistry 51, 947-956.

Verheyden, S., Nader, F.H., Cheng, H.J., Edwards, L.R., Swennen, R., 2008. Paleoclimate reconstruction in the Levant region from geochemistry of a Holocene stalagmite from Jeita Cave, Lebanon. Quaternary Research 70, 368-381.

Vogel, H., Wagner, B., Zanchetta, G., Sulpizio, R., Rosén, P., 2010. A paleoclimate record with tephrochronological age control for the Last Glacial-interglacial cycle from Lake Ohrid, Albania and Macedonia. Journal of Paleolimnology 44, 295-310.

Wagner, B., Lotter, A.F., Nowaczyk, N., Reed, J.M., Schwalb, A., Sulpizio, R., Valsecchi, V., Wessels, M., Zanchetta, G., 2009. A 40,000-year record of environmental change from ancient Lake Ohrid (Albania and Macedonia). Journal of Paleolimnology 41, 407-430.

Wagner, B., Vogel, H., Zanchetta, G., Sulpizio, R., 2010. Environmental changes on the Balkans recorded in the sediments from Lakes Prespa and Ohrid. Biogeosciences 7, 3187-3198.

Wagner, B., Aufgebauer, A., Vogel, H., Zanchetta, G., Sulpizio, R., Damaschke, M., 2012. Late Pleistocene and Holocene contourite drift in Lake Prespa (Albania/F.Y.R. of Macedonia/Greece). Quaternary International 274, 112-121.

Watzin, M.C., Puka, V., Naumoski, T.B. (Eds.), 2002. Lake Ohrid and its Watershed, State of the Environment Report. Lake Ohrid Conservation Project, Tirana, Albania and Ohrid, Macedonia, pp. 134.

Wilke, T., Schultheiß, R., Albrecht, C., Bornmann, N., Trajanovski, S., Kevrekidis, T., 2010. Native Dreissena freshwater mussels in the Balkans: in and out of ancient lakes. Biogeosciences 7, 3051-3065.

Zanchetta, G., Drysdale, R.N., Hellstrom, J.C., Fallick, A.E., Isola, I., Gagan, M.K., Pareschi, M.T., 2007. Enhanced rainfall in the Western Mediterranean during deposition of sapropel S1: stalagmite evidence from Corchia cave (Central Italy). Quaternary Science Reviews 26, 279-286.

Zhang, C.L., Horita, J., Cole, D.R., Zhou, J., Lovley, D.R., Phelps, T.J., 2001. Temperature-dependent oxygen and carbon isotope fractionations of biogenic siderite. Geochimica et Cosmochimica Acta 65, 2257-2271.

Zhornyak, L.V., Zanchetta, G., Drysdale, R.N., Hellstrom, J.C., Isola, I., Regattieri, E., Piccini, L., Baneschi, I., 2011. Stratigraphic evidence for a "pluvial phase" between ca. 8200-7100 ka from Renella Cave (Central Italy). Quaternary Science Reviews 30, 409-417.

V Climate variability since MIS 5 in SW Balkans inferred from multiproxy analysis of Lake Prespa sediments*

Abstract

The transboundary Lake Prespa (AL/FYROM/GR) has been recognized as a conservation priority wetland. The catchment area has a remarkably diverse flora that points to its refugial properties. A lake sediment core retrieved from a coring location in the northern part of the lake was investigated through geophysical, sedimentological, geochemical, and palynological analyses. Based on tephrochronology, radiocarbon and electron spin resonance (ESR) dating, and cross correlation with other Northern Hemisphere records, the age model suggests that the basal part of core Co1215 reaches back to 92 ka cal BP. Here we present the response of this mid-altitude site (849 m a.s.l.) to climate oscillations during this interval and assess its sensitivity to millennial-scale variability. Endogenic calcite precipitation occurred in Marine Isotope Stages (MIS) 5 and 1 and is synchronous with periods of increased primary production (terrestrial and/or lacustrine). Periods of pronounced phytoplankton blooms (inferred from green algae and dinoflagellate concentrations) are recorded in MIS 5 and MIS 1 and suggest that the trophic state and lake levels underwent substantial fluctuations. Three major phases of vegetation development are distinguished: the forested phases of MIS 5 and MIS 1 dominated by deciduous trees with higher temperatures and moisture availability, the open landscapes of MIS 3 with significant presence of temperate trees, and the pine dominated open landscapes of MIS 4 and MIS 2 with lower temperatures and moisture availability. Forest dynamics, cover and density are discussed in an altitudinal context and the existence of temperate tree refugia is examined.

Keywords: paleoclimate, pollen analysis, paleolimnology, lake-level changes, last glacial, Mediterranean, modern humans

* This chapter is based on Panagiotopoulos, K., Böhm, A., Leng, M. J., Wagner, B., Schäbitz, F., 2013b, Climate variability since MIS 5 in SW Balkans inferred from multiproxy analysis of Lake Prespa sediments, Climate of the Past Discussions, dx.doi.org/10.5194/cpd-9-1321-2013.

5.1 Introduction

The Balkan Peninsula is currently very heterogeneous in terms of its landscapes, climate and habitats (Grove and Rackham, 2003). This heterogeneity has shaped the fauna and flora through time and accounts for the impressive floral and faunal biodiversity, also found on the Iberian and Italian peninsulas (Blondel et al., 2010). These three Mediterranean peninsulas, in particular the Balkans, are thought to have provided shelter for species over recurring glacial-interglacial cycles (Griffiths et al., 2004).

A recent review of the vegetational response in Europe during the last glacial (Fletcher et al., 2010) demonstrated that millennial-scale events, such as Dansgaard-Oeschger (D-O) cycles and Heinrich (H) events are clearly identifiable in both terrestrial and marine pollen diagrams. Two features are apparent from this regional review of MIS 4 to MIS 2. Firstly, long and continuous sequences registering millennial-scale variability during this period are located almost exclusively within the Mediterranean region. Indeed, owing to its latitudinal location, this region has provided exceptional records that span several glacial cycles such as the renowned pollen sequence of Tenaghi Philippon (Wijmstra, 1969). The second feature is the limited number of glacial records originating from the Balkans in comparison with sites from the Italian and Iberian peninsulas. Several long and continuous pollen sequences encompassing multiple glacial cycles have been obtained from Greece (Wijmstra, 1969; Okuda et al., 2001; Tzedakis et al., 2002). Some of them confirm the notion of glacial refugia for temperate trees (e.g. the Ioannina basin located in northwestern Greece). There are no pollen records covering the Last Glacial cycle outside Greece with the exception of Lake Ohrid (Lézine et al., 2010). However, most cores retrieved from the latter reveal disruptions in the sedimentation patterns (Vogel et al., 2010; Lézine et al., 2010).

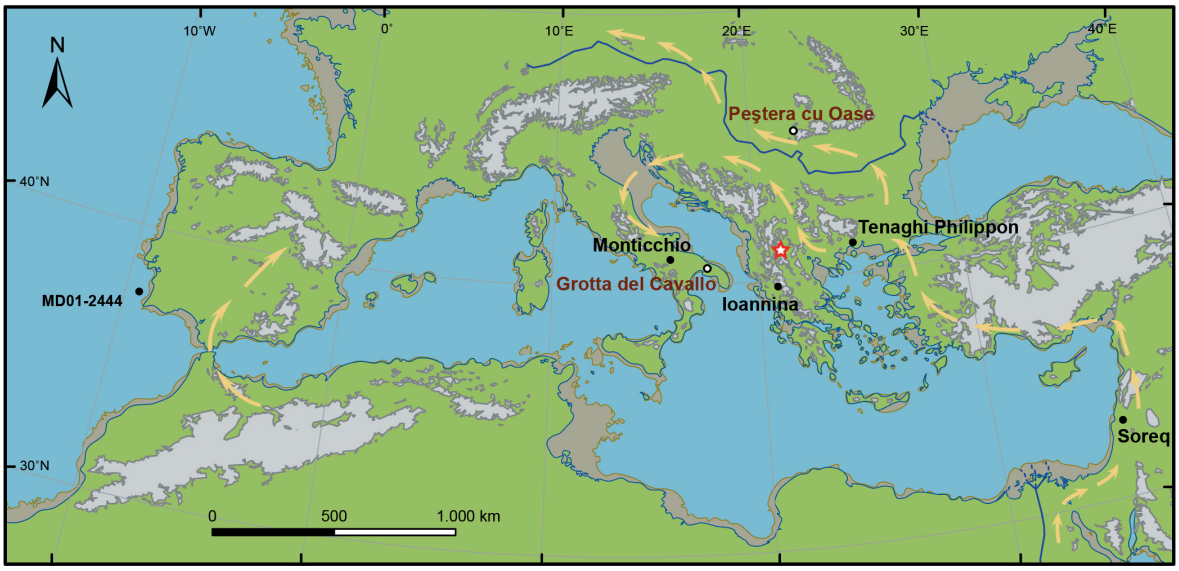

Figure 5.1: Locations of selected records discussed and of Lake Prespa (star); archaeological sites are marked with an open circle. Note the paleocoastline at 100 m (in brown) and possible dispersal routes of modern humans (arrows).

The Lateglacial pollen record from neighboring Lake Prespa (**Figure 5.1**) provides insights into the vegetation and climate conditions at a centennial-scale from an altitude of 849 m a.s.l. (Aufgebauer et al., 2012; Panagiotopoulos et al., 2013). Ensuing isotopic and hydrological studies on a c. 16 m core (Co1215) confirmed the sensitivity of the site to climate variability (Wagner et al., 2012; Leng et al., 2013) and a recent lithological and tephrostratigraphical study on a c. 18 m long core (Co1215) indicates that the sediment accumulation in the central northern part of the lake is undisturbed and covers the last c. 92 ka cal BP (Damaschke et al., 2013).

Here we present sedimentological, geochemical and palynological data of core Co1215 with a focus on biological proxies and ecological processes. Our multi-proxy approach aims at understanding the complex responses of the Lake Prespa catchment to climate variability during the Last Glacial. In order to assess the impacts of orbital- and suborbital-scale variability we first examine the response of the study area on a local level, and then compare it to selected regional and global reference archives. Finally, we discuss implications of the climate reconstruction for modern human dispersal into Europe and other environmental constraints posed on hominid migrations/populations.

5.2 Physical setting

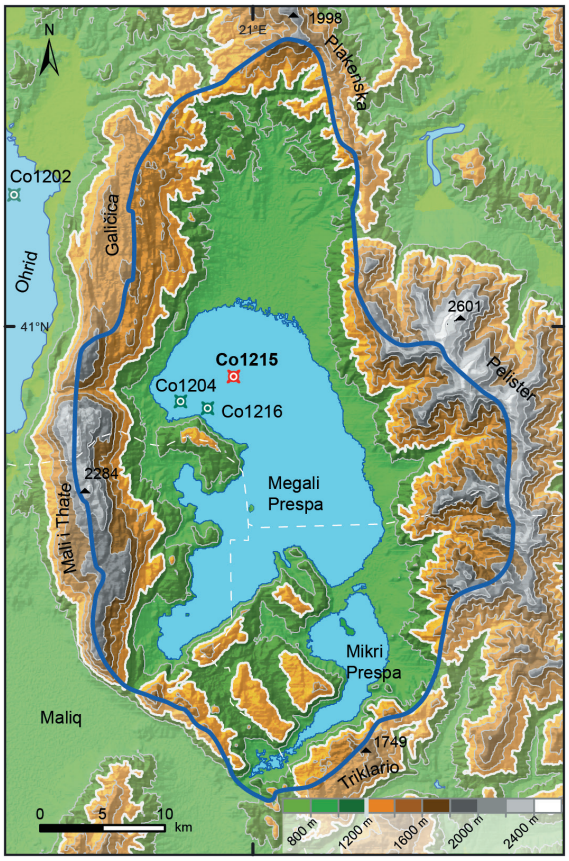

Figure 5.2: Topography of Lake Prespa. Lake catchment (blue line) and core locations (Co1215, this study) are shown (SRTM Data: Jarvis et al., 2008).

The Prespa Lakes (Megali and Mikri Prespa) and the surrounding streams and springs, enveloped by mountains forming several peaks around or above 2000 m a.s.l., are shared between Albania, the Former Yugoslav Republic of Macedonia, and Greece (**Figure 5.2**). Lake Megali Prespa, hereafter referred to as Lake Prespa, has no surface outflow and is separated by an alluvial isthmus from Lake Mikri Prespa. The lake has a catchment area of 1300 km^2, a mean water depth of 14 m (48 m maximum), and a surface area of 254 km^2 (Matzinger et al., 2006). Lake Prespa is situated at 849 m a.s.l. and drains through karst channels traversing the Galičica and Mali Tate mountains into Lake Ohrid standing at 693 m a.s.l. Hence, it belongs hydrologically to the Adriatic drainage region, although recent faunal studies suggested a closer biogeographical affiliation with lakes eastwards belonging to the Aegean drainage region (Wilke et al., 2010).

The geology of the area mainly comprises Mesozoic limestones and granites. The climate is transitional and can be classified as sub-Mediterranean with continental influences. Mean July and January temperatures in the lowlands are 21 ˚C and 1 ˚C respectively, with a mean annual temperature of 11 ˚C. Precipitation varies from 750 mm in the lowlands to over 1200 mm in the mountains and peaks in winter when snowfalls are frequent (Hollis and Stevenson, 1997). Consequently, streams and springs are fed by late spring snowmelt resulting in peak lake levels in May and June. Total inflow comprises stream and spring discharge (56%), direct precipitation (35%) and Mikri Prespa inflow (9%). In the absence of natural surface outlet, water from Lake Prespa is mostly evaporated (52%), fed through the karst aquifer (46%) to Ohrid springs, and 2% is used for irrigation (Matzinger et al., 2006). Increasing anthropogenic pressure combined with precipitation patterns and the closed nature of the watershed account for the annual lake level change and an estimated residence time of 11 years (Matzinger et al., 2006). Apart from seasonal variations, lake levels have oscillated historically (up to several meters) as evidenced by existing national records and inundated settlement ruins from the 11th century (Wagner et al., 2012). Level fluctuations of Lake Prespa are expected to influence the sedimentation regime given the shallow water depth with reference to the large surface area. At present, Lake Prespa is a mesotrophic lake and overturning of the water column has been documented to occur between fall and spring, while thermal summer stratification results in dissolved oxygen depletion below 15 m (Matzinger et al., 2006). However, the lake underwent substantial changes in its trophic, mixing and level status in the past (Aufgebauer et al., 2012). The presence of gyres on the surface of Lake Prespa is assumed to propagate currents in the water column leading, in concert with geostrophic effects, to the formation of a contourite drift (Wagner et al., 2012).

The diverse topography of the Lake Prespa catchment and its location at a transitional climate zone gave rise to an assemblage of central European, Mediterranean and Balkan endemic plant species (Polunin, 1980). Panagiotopoulos et al. (2013) described the diversity and origin of the modern flora found at Prespa and discussed the refugial character of the study site.

5.3 Material and Methods

Here we present a dataset of core Co1215 (40°57'50'' N, 20°58'41'' E) with a composite length of 1776 cm recovered from a location at the northern part of Lake Prespa (14.5 m water depth) in November 2009 and June 2011 (**Figure 5.2**). The coring location displays relatively undisturbed sedimentation, revealed after a shallow hydro-acoustic survey (Wagner et al., 2012). The core was recovered from a floating platform equipped with a gravity corer for surface sediments and a 3 m long percussion piston corer for deeper sediments (UWITEC Co. Austria). One core half was used for non-destructive analyses (e.g. XRF scanning) and then archived at the Institute of Geology and Mineralogy at the University of Cologne; the other half was subsampled at 2 cm intervals and the samples were freeze-dried and homogenized using an agate ball mill.

5.3.1 Geochemical analyses

X-ray fluorescence (XRF) scanning was performed at 2 mm steps with an analysis time of 10 s per measurement using an ITRAX core scanner (COX Ltd. Sweden). The count rates of individual

elements presented here were used as semi-quantitative estimates of their relative concentrations (for more details see Aufgebauer et al. 2012). Total carbon (TC) and total inorganic carbon (TIC) were measured with a DIMATOC 200 (DIMATEC Co. UK) and total organic carbon (TOC) was calculated by subtracting TIC from TC. The identification of carbonate types (e.g. calcite, siderite) was determined by X-ray diffraction (XRD) analysis (Leng et al., 2013).

5.3.2 Palynological analyses

Palynological analyses were performed on 170 subsamples taken at 2-16 cm intervals. After measuring their volume, samples were sieved (112 μm), Lycopodium tablets (Stockmarr, 1971) were added in order to calculate concentrations, and subsequently they were processed using standard palynological techniques. Identification of palynomorphs was performed with relevant keys and atlases, as well as the reference collection of the Laboratory of Palynology of the Seminar of Geography and Education at the University of Cologne (Panagiotopoulos et al., 2013; and references therein). An average of 500 (with a minimum of 300) terrestrial pollen grains were counted per sample (with the exception of two samples at 546 cm and 890 cm with a pollen sum of 171 and 177 respectively). The average temporal resolution between pollen samples, derived from the presented age model, is c. 500 years (ranging between 50 and 1250 years). Relative percentages were based on the sum of terrestrial pollen (excluding aquatics and spores). The term aquatics (or aquatic vegetation) in this study comprises vascular plants (macrophytes); and phytoplankton comprising green algae and dinoflagellates. The latter are presented in concentrations and the former both in concentrations and percentages based on a pollen sum including the main pollen sum and aquatics. Nomenclature and taxa group terminology follows Panagiotopoulos et al. (2013). Apart from *Artemisia*, which is plotted separately, the Asteraceae curve comprises differentiated Asteroideae, Cichorioideae and *Centaurea* pollen percentages. Poaceae groups together Poaceae (wild types) and Cerealia (cultivars > 40 μm). Although *Phragmites* pollen grains were not differentiated, the modern vegetation of Prespa suggests that *Phragmites* grains must form part of the Poaceae (wild type) group. *Quercus* comprises differentiated deciduous (*Quercus robur*-type and *Quercus cerris*-type) and evergreen types.

The *Pediastrum* species encountered (*P. boryanum* spp., *P. simplex*) are freshwater planktic green algae, which have a cosmopolitan distribution and wide ecological tolerance (Komárek and Jankovská, 2001). Both species are dominant in eutrophic lakes under temperate climates, although the latter is also commonly found in tropical regions (Komárek and Jankovská, 2001). *Botryococcus* species are dominated by *B. braunii* mostly in association with *B. neglectus* and *B. pila*. The synchronous occurrence of *Pediastrum* and *Botryococcus* species is characteristic of large eutrophic lakes with open water surface and extensive submerged and littoral vegetation typical for climatic optima (Jankovská and Komárek, 2000).

Dinoflagellate cysts were counted from the pollen slides and can be attributed tentatively to *Gonyaulux*-type. Two morphotypes were distinguished; a dominant one with pronounced and protruding ornamentation present throughout the core and one with very limited or absent ornamentation and intermittent presence. Further studies (including SEM imaging; see Appendix A) are needed to determine the species. Kouli et al. (2001) reported the presence of

two identified freshwater dinoflagellates (*Gonyaulux apiculata* and *Spiniferites cruciformis*) from Lake Kastoria. As this lake is situated 20 km southwards from Lake Prespa, it is assumed the dinoflagellates encountered at Prespa (*Gonyaulux*-type) belong to *G. apiculata*.

5.3.3 Chronology

The age model of core Co1215 is based on accelerator mass spectrometry (AMS) 14C dates, tephrochronology, electron spin resonance (ESR) dating and cross correlation with the NGRIP ice core record and described in detail in Damaschke et al. 2013 (**Figure 5.3**). Radiocarbon dates were calibrated into calendar years (a cal BP) using the INTCAL09 calibration curve (Reimer et al., 2009) and for the uppermost sample using the Levin14c dataset (Levin and Kromer, 2004). All ages presented in this paper are calendar ages. Aufgebauer et al. (2012), Wagner et al. (2012) and Damaschke et al. (2013) elaborate on the composition and correlation of the identified tephra layers, as well as on the ESR dating of a shell horizon at 1458 - 1463 cm. The ESR dating provided the only independent chronological tie-point below 858 cm (representing the last identified tephra layer) in core Co1215. Two additional tie points demarcating the maximum age of the lowermost part of the core were fixed by tuning two TOC peaks to Dansgaard-Oeschger (D-O) warming events 21 and 22 of the NGRIP GICC05modelext (Damaschke et al., 2013). According to the proposed age model, the base of the sediment sequence can be extrapolated to c. 92 ka cal BP.

Figure 5.3: Age model of core Co1215 with lithology. Reliable age control points were interpolated on a linear basis.

5.4 Results

The upper 320 cm of core Co1215, spanning the past 17 ka, were described with respect to lithology, geochemistry and chronology in Aufgebauer et al. (2012) and with respect to palynological and microscopic charcoal data in Panagiotopoulos et al. (2013). Wagner et al. (2012) and Leng et al. (2013) presented sedimentological and geochemical data for the upper 1576 cm and provided some first age estimations of the sequence. This study presents sedimentological, palynological, geophysical, and geochemical parameters for the longest (1776 cm) composite core to date, after the addition of 2 m recovered during fieldwork in June 2011.

Considering the distinct and overlapping lithological and palynological units, the ensuing discussion utilizes the marine isotope stages (MIS) chronological framework (Lisiecki and Raymo, 2005) to facilitate comparison between different proxies as well as other regional or global archives.

5.4.1 Lithology and Geochemistry

Three lithofacies (L3, L2, L1) occur in Co1215, and have been distinguished based on color, grain-size composition and chemistry (**Figure 5.3**). Lithofacies 3 (1776-1516 and 204-0 cm) sediments are characterized by olive-brown colored bioturbated silt, relatively high organic matter and calcium carbonate (calcite) and low to intermediate clastic content. Lithofacies 2 (1516-1380, 1066-662, and 292-204 cm) has gray-olive, non-laminated silts with intermediate organic content, and generally low carbonate content but with distinct TIC (calcite and siderite) and Fe spikes. Sporadic occurrence of sand and gravel was recorded in L2. Lithofacies 1 (662-292 and 1380-1066 cm) sediments are gray, bioturbated, dominated by silt and with very low organic conent. Conspicuous TIC (siderite) and (Fe) spikes are present between 1380 and 1066 cm, and an irregular black-greenish lamination associated with black spots and high Fe and Mn (between 662 and 292 cm). Coarse sand and gravel were present intermittently throughout L1.

5.4.2 Pollen Assemblage Zones (PAZs)

Ten local pollen assemblage zones (P-1 to P-10) and several subzones were delimited based on visual inspection of the pollen record and supported by CONISS analysis for pollen taxa (>2%) included in the pollen sum as implemented in TILIA (Grimm, 1992). Zone numbers and letters were assigned with ascending order from top to bottom (**Figure 5.4**).

Arboreal pollen (AP) percentages above 80% with a significant deciduous-tree component (20% *Quercus*, 10% *Carpinus* and 10% *Fagus*) are recorded in zone P-10 (1776-1680 cm). In P-9 (1680-1580 cm), non-arboreal pollen (NAP) percentages rise up to 60% abruptly (30% *Artemisia*, 15% Poaceae and 10% Chenopodiaceae), while tree values (mostly conifers) contract (AP <40%) and recover at the top of the zone (~ 80%). Aquatic pollen percentages (excluded from the main pollen sum) and phytoplankton concentrations reach maximum values in zone P-9 forming prominent peaks. The ensuing P-8 (1580-1390 cm) marks the last consecutive zone with AP percentages crossing the 80% threshold. P-8b (1580-1480 cm) is characterized by high arboreal values (>80%) and a gradual transition to conifer-dominated pollen spectra (from 20%

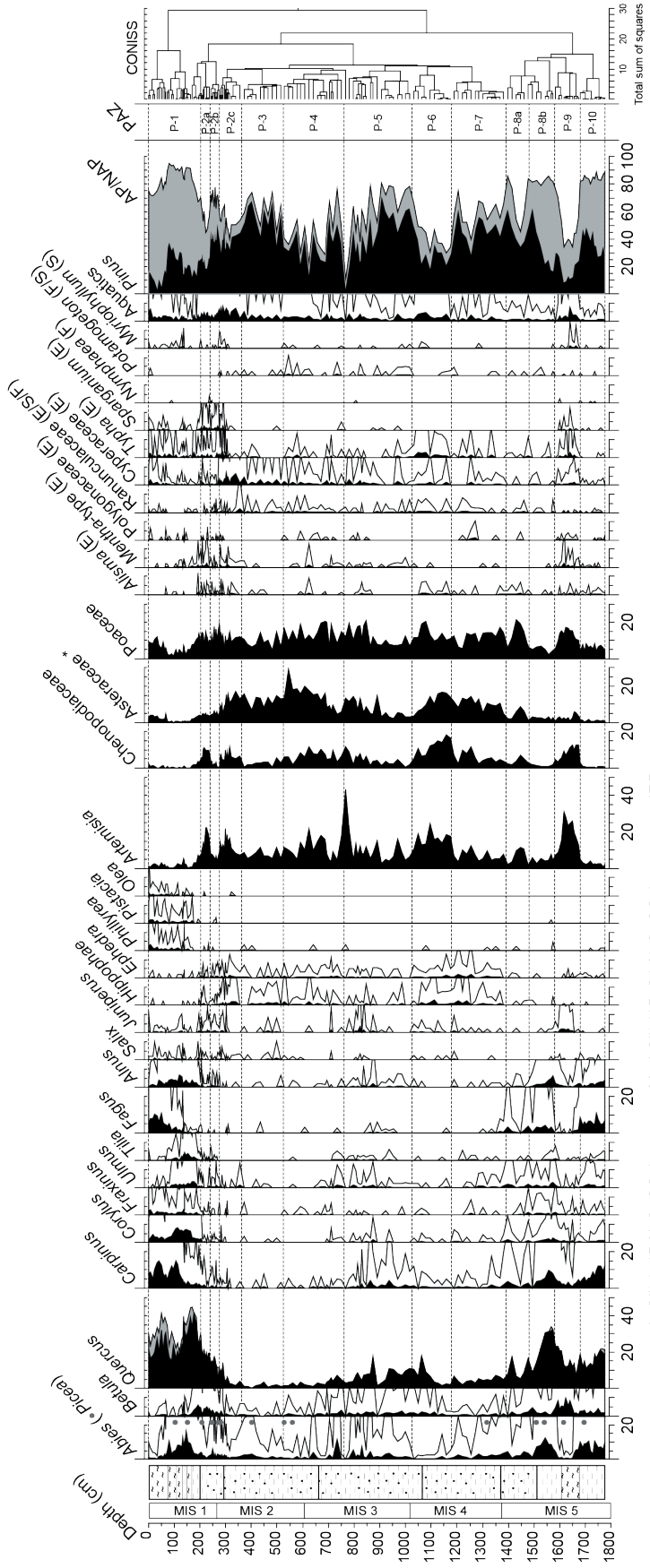

Figure 5.4: Pollen percentage diagram of core Co1215: selected trees, shrubs, herbs, and aquatics. Evergreen *Quercus* is presented in gray; Asteracae* does not include *Artemisia*; emergent (E), submerged (S) and floating (F) aquatic plants are marked. Lithology, marine isotope stages (MIS), pollen assemblage zones (PAZ), and CONISS are shown. (Exaggeration x10)

to 60% *Pinus*). An abrupt expansion of NAP percentages (21% Poaceae and 10% *Artemisia*) and a subsequent contraction occur in P-8a (1480-1390 cm). *Pinus* dominance (up to 60%) continues in P-7 (1390-1180 cm), while NAP rise above 50% towards the top of the zone. In P-6 (1180-1027 cm) the *Pinus*-dominated AP percentages decline and NAP percentages stay above 50% throughout the zone (*Artemisia*, Chenopodiaceae and Poaceae values mostly above 10%). *Pinus* and *Quercus* percentages rise towards the top of the zone (peaking at 18%) in parallel with Poaceae (peaking at 20%) and Aquatics (*Typha* reaches absolute maximum values of 3% within P-6). In P-5 (1027-760 cm), several peaks above 70% are recorded in AP percentages and an absolute maximum of NAP values (NAP = 90% comprising 43% *Artemisia*) at the top of the zone. AP percentages are dominated by *Pinus* (up to 60%), however a significant *Quercus* component is present (peaking at 19% and contracting down to 2%) and several other deciduous trees are almost continuously present despite very low values (e.g. *Carpinus* and *Ulmus*). Conspicuous NAP spikes (mostly *Artemisia*) are characterizing P-5 and the succeeding P-4 (760-525 cm). In P-4, AP values show abrupt fluctuations and decline (below 50%) at the top of the zone. Asteraceae percentages peak (27%) towards the top of the zone, whereas deciduous tree values decline. In P-3 (525-364 cm), *Quercus* percentages contract further and absolute minima (<1%) are recorded at the top of the zone. Abrupt fluctuations of *Pinus* values, continuous *Hippophae* presence and increasing Aquatics percentages characterize zone P-3. The ensuing zone, P-2 (364-240 cm), marks the gradual expansion of deciduous tree percentages and the parallel decline of *Pinus*. Two conspicuous *Artemisia* and Chenopodiaceae peaks are registered in P-2c (364-277 cm) and P-2a (240-204 cm) separated by a subzone, P-2b (277-240 cm), with relatively high AP percentages (>65%). Zone P-1 (204-0 cm) is characterized by high AP percentages (up to 95%) that decrease (70%) at the top of the record. Abies and several deciduous trees percentages rise above 10% (e.g. *Quercus*, *Carpinus*, *Corylus* and *Fagus*), while *Pinus* declines substantially (min 5%). Mediterranean taxa (e.g. *Phillyrea*, *Pistacia* and *Olea*) are continuously present in this zone. Aquatics and phytoplankton concentrations peak within P-1.

5.5 Discussion

5.5.1 The Prespa paleoarchive

5.5.1.1 Vegetational and limnological feedbacks to climate variability at a local scale

The pollen record (**Figure 5.4**) reveals two distinct phases (P-10 and P-8b) of high and sustained arboreal pollen percentages (AP>70%) at the base and one (P-1) at the top of core Co1215. During these intervals, deciduous trees dominated the pollen spectra and displaced *Pinus* suggesting warmer and moister conditions. According to the age model, P-10 and P-8b correspond to MIS 5 and P-1 to the Holocene. The forested landscape inferred is substantiated by relatively high arboreal pollen concentration (proportional to tree population density) and low to intermediate Ti counts which indicate fluctuating allochthonous clastic material input (i.e. Ti; **Figure 5.5** a, d). In contrast, in P-7, P-6, P-4 (upper part), P-3 and P-2c AP percentages stay below the 70% boundary suggesting these time periods represent an open landscape and glacial conditions. As

pollen percentages are dependant of each pollen type included in the pollen sum, some taxa such as *Pinus* with its exceptional pollen productivity and dispersal properties are over-represented in the relatively open landscapes encountered during full glacial conditions. These pollen zones, corresponding to MIS 4 (P-7 to P-6) and MIS 2 (P-4 to P-2c), contain extremely low arboreal pollen concentrations (below 200 000 grains cm^{-3}) and have a high clastic content. Arboreal relative percentages (reflecting mostly forest composition) were dominated by *Pinus* during MIS 4 and MIS 2. Although *Quercus* pollen is present throughout the record, pointing to the refugial properties of the area, distinct minima occur within zones P-6, P-5 and P-3. A prolonged phase of moderate *Quercus* percentages occurs between P-6 and P-4 and correlates with MIS 3. During this interval of abrupt AP percentage fluctuations, total tree abundance (percentages and concentrations) was high in comparison with the preceding (MIS 4) and ensuing (MIS 2) intervals.

It is apparent that climate oscillations control the response of vegetation within the Prespa watershed influencing spatial patterns and floristic composition through time. However, there are other environmental parameters, such as geomorphology, slope exposure, soil formation, lake level, pH and nutrient availability, which determine vegetation development in the terrestrial and aquatic ecosystems. Semi-aquatic and aquatic vascular plant pollen percentages in Prespa (**Figure 5.4**) can be employed as a proxy to infer fluctuations in lake levels (e.g. Harrison and Digerfeldt, 1993). Poaceae percentages are assumed to contain a portion of grassland (upland) and reed-bed taxa (e.g. *Phragmites* sp.) growing at the littoral zone. In Co1215, Poaceae maxima are synchronous with *Artemisia* peaks (a proxy of increasing aridity) throughout the core. At first sight, this appears to be contradictory as grasslands usually expand with increasing precipitation. Hence, we assume that *Phragmites* sp. contribute a significant percentage to Poaceae expansions during these zones and consequently these abrupt expansions are estimated to be synchronous to fluctuating lake levels. Along with peaking *Typha* and *Cyperaceae* percentages, Poaceae percentages are used to infer intervals of spreading reed beds and sedgelands. At this point, it should be underlined that changes inferred from aquatic pollen are relative and indicative of trends (e.g. a lowering of the lake level). They do not necessarily coincide with low or high stands of Lake Prespa (namely with actual water depth). In fact, the concomitant occurrence of *Nymphaea*, *Sparganium*, *Myriophyllum* and *Potamogeton* pollen suggest rather deep waters (>6 m) at the coring site (Harrison and Digerfeldt, 1993) throughout the study period. Therefore, different lines of evidence (i.e. sedimentological, seismic, geochemical, geophysical and isotopic data) are compiled to infer changes in the littoral and aquatic environment of Lake Prespa through time.

Green algae and dinoflagellate concentrations (**Figure 5.5** d, e) are considered to represent periods when frequent phytoplankton blooms occurred. Rising temperatures and light intensity, nutrient availability, and the onset of lake stratification constitute the major parameters controlling (springtime) phytoplankton blooms (Wetzel, 2001). In mesotrophic and eutrophic lakes, diatoms and cyanobacteria (blue-green algae) account for dense blooms as a result of excess nutrient accumulation, notably phosphorus. On an annual basis, phytoplankton blooms are usually terminated with the gradual depletion of soluble nutrients (e.g. phosphorus, nitrogen, silicon) available for algae growth in the epilimnion (Wetzel, 2001). In Co1215, high plankton concentrations occur in MIS 5, MIS 3 and MIS 1. In general, these intervals coincide with

increased forest cover suggesting higher moisture availability and/or temperatures in the catchment. However, absolute maximum values occurred during a short interval in MIS 5 concurrent with an abrupt arboreal retreat (P-9). Matzinger et al. (2006) discussed the dramatic impact of changes in lake volume on the concentration of dissolved nutrients (in particular the focusing on phosphorus) considering the relatively shallow depth of Lake Prespa with respect to its surface area. In the presence of low lake-levels, increased wave and current activity and thus enhanced mixing and oxygenation are expected. In addition, increased nutrients (e.g. phosphorus) and oxygenation could lead to high lake productivity and extensive blooms.

The lake productivity proxies in Co1215 (**Figure 5.4** and **Figure 5.5** d, e) comprise green algae (*Pediastrum* and *Botryococcus* species), dinoflagellates (*Gonyalux*-type) and aquatic vascular plants (emerged, submerged and floating; **Figure 5.4**). Along with terrestrial pollen (**Figure 5.5** a, d), they are assumed to indicate changes in organic matter (OM) sources within the Prespa catchment. Atomic C/N values between 4 and 10 imply that sedimentary OM in Co1215 originated from non-vascular plants and is probably affected by decomposition (Meyers, 1994). The synchronous C/N, TOC, AP/NAP and plankton fluctuations (**Figure 5.5** a, c, f) downcore and peak C/N values corresponding to forested intervals (i.e. MIS 5 and MIS 1) suggest that diagenesis did not alter significantly the source signal of OM for the past 92 ka. Indeed, Rock Eval analysis of the Prespa sediments confirmed that although oxidation did play an active role, the source of OM was found to be a function of climate/hydrology (Leng et al., 2013). High rates of OM oxidation are mostly found during MIS 4 and MIS 2 and coincide with phases of open catchment vegetation, low primary production and siderite precipitation in the lake sediments (Leng et al., 2013).

Carbonate minerals formed intermittently in Lake Prespa throughout the period examined (**Figure 5.5** g). Calcite precipitation occurred sporadically in MIS 5 and continuously in MIS 1 (Holocene). Calcite precipitation is often controlled by pH shifts induced by photosynthesis (higher pH and removal of carbon dioxide causing precipitation). Subsequent respiration and decomposition of OM lower the pH releasing CO_2 and thus promote $CaCO_3$ dissolution. Usually, most of the autochthonous precipitated calcite is dissolved in the anoxic and more acidic hypolimnion (Cohen, 2003). Dittrich and Koschel (2002) have shown that sedimentation of phosphorus and calcite precipitation are closely linked; and that artificial addition of $Ca(OH)_2$ in the hypolimnion during summer in a stratified hardwater lake intensified calcite precipitation and lowered the trophic state enhancing the internal phosphorus sink. The absence of calcium carbonate in the Glacial is assumed to be a result of low trophic status, dissolution due to aerobic decomposition of organic matter and inhibited ion supply from the catchment (Aufgebauer et al., 2012). However, siderite ($FeCO_3$) peaks in Co1215 are scattered within the Last Glacial. The TIC peaks throughout MIS 4 to MIS 2 occur alongside Fe peaks and suggest changing redox conditions and burial processes, such as proposed for peaks in Mn (Wagner et al., 2010).

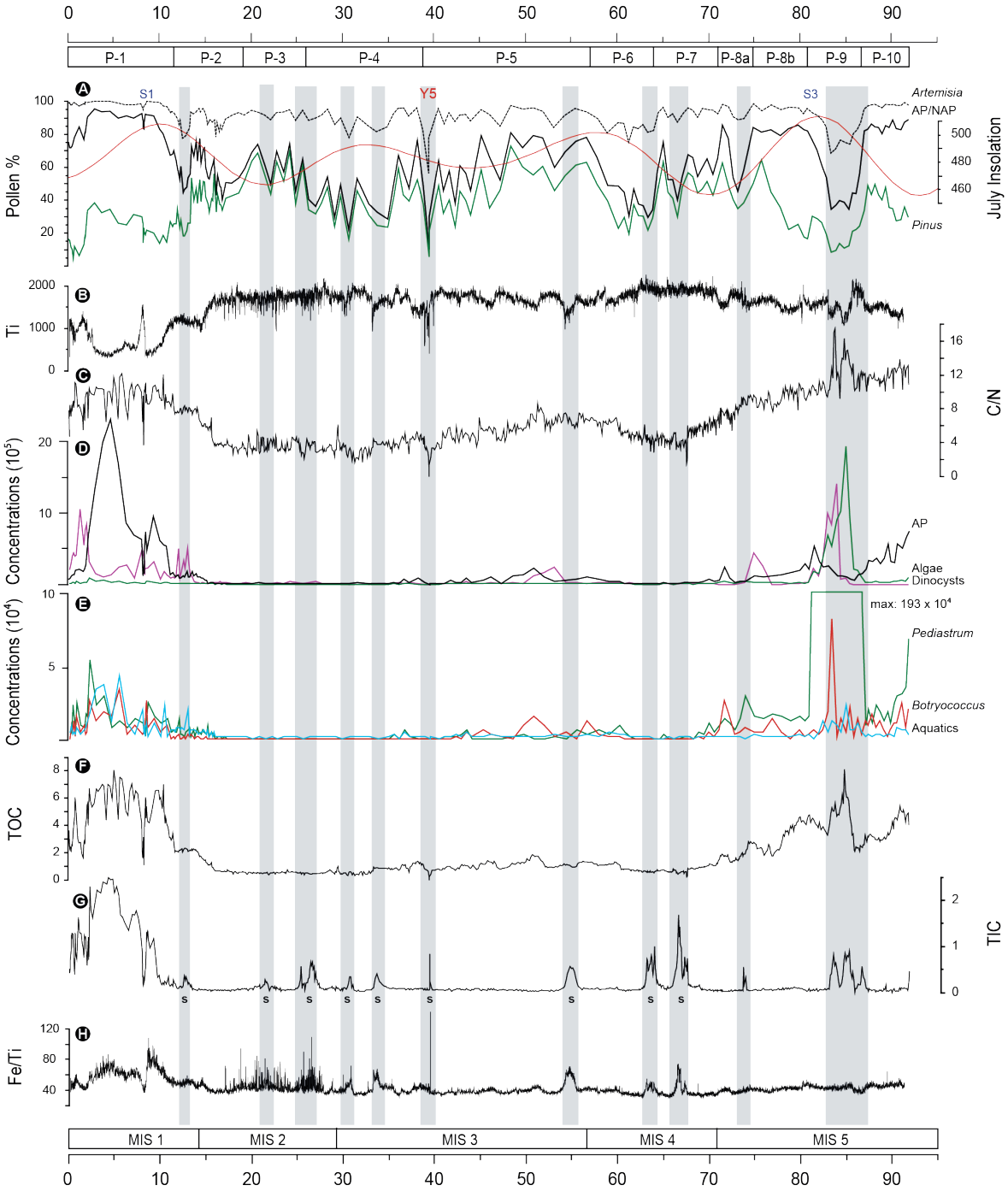

Figure 5.5: Selected biological, geophysical and geochemical proxies from Lake Prespa (core Co1215) plotted against age. (a) *Artemisia* (dashed line), AP/NAP (black), and *Pinus* (green) pollen percentages; mean July insolation at 40 °N (W/m^2; red); sapropels (S1, S3); and Y5 tephra layer, (b) Titanium (Ti) counts, (c) Atomic C/N, (d) Concentrations (x 10^5) of arboreal pollen (AP; black), green algae (green) and dinoflagellates (purple), (e) Concentrations (x 10^4) of aquatics (blue), *Botryococcus* (red) and *Pediastrum* (green). Note the difference in scale, (f) Total organic carbon (wt %) and siderite (s) peaks are marked, (g) Total inorganic carbon (wt %), (h) Iron/titanium (Fe/Ti). Shaded intervals correspond to carbonate peaks precipitated in Lake Prespa during the Last Glacial.

5.5.1.2 Temporal and spatial development of local ecosystems

MIS 5 (c. 92 – 71 ka cal BP; P-10 to P-8)

In terms of forest dynamics within the Prespa catchment, the AP/NAP curve (**Figure 5.5** a) outlines the rather limited duration of closed-canopy phases in Co1215. High percentages of *Abies* along with *Quercus*, *Carpinus*, *Fagus*, and other deciduous trees point to sufficient moisture availability and temperatures for growth in P-10 (c. 92-87 ka cal BP). However, the conspicuous absence or appearances of isolated grains of Mediterranean taxa suggest that (winter) temperatures were not favorable for their survival/expansion. A similar picture of advancing temperate forest and absence of sclerophyllous species occurs within P-8 (c. 81-71 ka cal BP). Continuous presence of the latter is confined to P-1 (Holocene) and marks in effect the warmest interval in the core. Two periods (P-9 and P-8a) of rapid herb expansion interrupt forest continuity at the base of Co1215. The collapse of conifer populations, the relative stable *Quercus* and rising *Betula* percentages and pronounced peaks of *Artemisia* and Chenopodiaceae attest to increased aridity, dropping temperatures and a descending treeline in P-9 (c. 87-81 ka cal BP). A parallel AP concentration decrease supports the notion of thinning tree stands. A similar arboreal (mainly *Pinus*) response with maximum Poaceae (**Figure 5.4**) percentages is evident in P-8a (c. 75-71 ka cal BP). In both zones, pollen spectra resemble the ones belonging to Younger Dryas (P-2a) discussed extensively elsewhere (Panagiotopoulos et al., 2013). Calcite precipitation during MIS 5 is mostly confined to a short interval between 87-82 ka cal BP and two isolated peaks at 91 and 74 ka cal BP. High and fluctuating TOC throughout MIS 5 implies high catchment productivity. The apparent decoupling of organic and inorganic carbon preserved in Lake Prespa sediments points to increased accumulation and/or deposition of organic matter and intensified dissolution respectively. The first TIC peak at the base of Co1215 is the only interval in MIS 5 coincident with a forested watershed phase (high AP percentages and concentrations) and relatively high green algae content (*Pediastrum*) suggesting high temperatures, limited decomposition and seasonal bottom water anoxia. Between 87 and 82 ka cal BP, three distinct TIC (calcite) peaks are expressed concurrently in fluctuating C/N and TOC. However, the TIC peaks between 87-82 and 74 ka cal BP occur during periods of declining tree cover and apparently lower lake levels.

MIS 4 (c. 71 – 57 ka cal BP; P-7 and P-6)

Pinus dominance established in zone P-8a continues in P-7 (c. 71-64 ka cal BP), and deciduous tree and Abies percentages decline gradually reaching minimums within the subsequent zone (P-6; c. 64-57 ka cal BP). AP concentrations are very low and the relatively stable Ti values suggest limited clastic material input in contrast to MIS 5. IRD, first recorded at the end of MIS 5 (P-a), is present throughout this interval and suggest ice-floe transport. Chenopodiaceae, *Artemisia* and Poaceae values culminate in this order upcore in P-6. The declining TOC and C/N ratio suggest retreating catchment vegetation and/or increased degradation of OM due to enhanced mixing promoted by a colder climate and/or a lower lake level. The synchronous *Typha* and Poaceae maxima at the top of P-6 point to a lake level lowering. Two pronounced siderite peaks concomitant to Fe peaks indicate changes in the redox front conditions and correspond

to distinct minima in AP percentages (at 66 and 63 ka cal BP). The apparent opening of the landscape and/or lowering of treeline imply a cold climate regime and a deficit in moisture required for tree growth within the catchment. Trees (mostly hardy pines) were restricted to favorable habitats provided by the diverse topography of the Prespa area. The ensuing decline of herb percentages and a notable *Quercus* peak mark the top of P-6.

MIS 3 (c. 57 – 29 ka cal BP; P-5 and partly P-4)

The onset of MIS 3 is characterized by the expansion of deciduous tree percentages (primarily *Quercus*). The parallel increase of AP concentrations points to a rise in primary production in the Prespa catchment. Relatively high C/N values (above 6) up to c. 50 ka cal BP imply an increased input of terrestrial OM and/or inhibited decomposition. The siderite and Fe peak at c. 55 ka cal BP corresponds to a period of decreasing AP abundance and clastic content suggesting enhanced mixing of the water column. The presence of IRD, which is continuous throughout MIS 3, indicates the occurrence of (at least partial) ice cover at Prespa. Although pines constitute the majority of trees at Prespa, the continuous *Abies*, *Betula*, *Quercus* and *Carpinus* curves along with intermittent presence of others (e.g. *Alnus*, *Corylus*, *Ulmus*, *Tilia*) suggest their likely survival within the catchment. A pronounced minimum in AP percentages at the top of P-5 (at 39 ka cal BP) coincides with the deposition of the substantial (19 cm) Y5 tephra layer. Following this abrupt event, trees return briefly to values preceding the perturbation (at the base of P-4) and decline significantly (down to 20%) thereafter. From c. 40 ka cal BP till the end of MIS 3, the geochemical proxies and the AP percentages show abrupt fluctuations. AP minima and siderite precipitation are accompanied by changes in the redox conditions and the mixing regime of Lake Prespa. The low TOC and C/N values (below 6) during this period suggest that primary productivity declined and/or decomposition of OM increased. At c. 31 ka cal BP *Artemisia* and Chenopodiaceae peak while a synchronous siderite precipitation event marks the end of MIS 3.

MIS 2 (c. 29 – 14 ka cal BP; partly P-4 to P-2c)

At the top of P-4, Asteraceae (excluding *Artemisia*) reach maximum values, ensuing the distinct *Artemisia* and Chenopodiaceae peaks. Arboreal pollen concentrations show minimum values and resemble conditions similar to MIS 4. The relatively high tree percentages in P-3 comprise mostly pines. *Abies* and *Quercus* are the only other trees in the catchment with most likely continuous presence, but with very limited abundances. *Quercus* absolute minima (<1%) are recorded at the top of this zone (P-3) suggesting cold and dry conditions. The synchronous *Pinus* and *Abies* peaks point to the critical role of extremely low temperatures rather than moisture availability, in light of no significant peak in steppe elements (i.e. *Artemisia* and Chenopodiaceae). In P-2c (c. 19-15 ka cal BP), distinct peaks of *Artemisia* and Chenopodiaceae indicate periods of increased aridity. The very low TOC content and C/N values imply retreating tree cover in the surroundings of Lake Prespa and a high decomposition of OM. The TIC peaks are concurrent with AP percentage minima, as well as increased and abruptly fluctuating iron counts, suggesting abrupt shifts in temperatures, moisture availability, redox conditions at the hypolimnion. In addition, the very low phytoplankton concentrations point to restricting temperatures and/or nutrient availability for their growth.

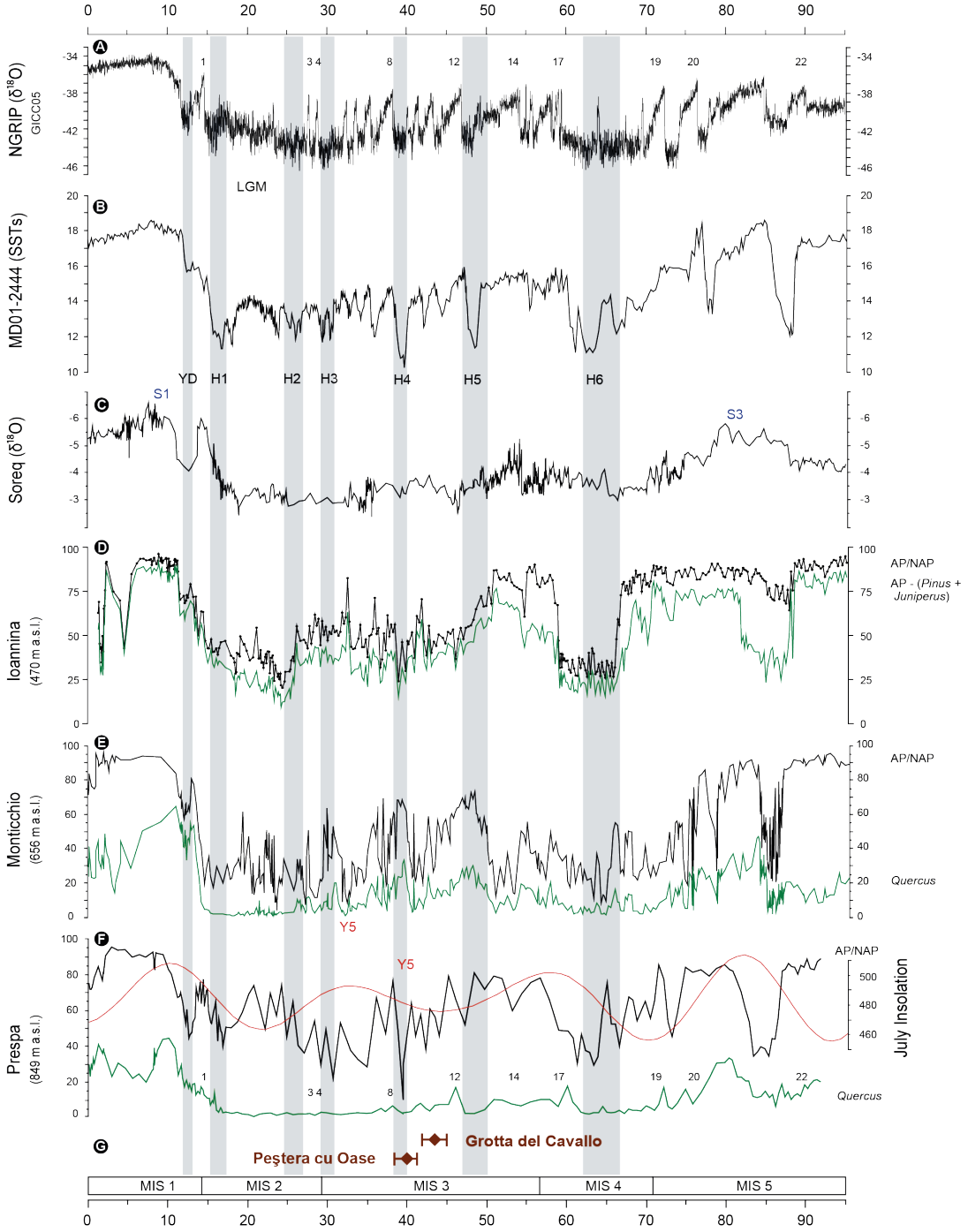

Figure 5.6: Comparison of Prespa proxies with regional and global records. (a) Ice oxygen isotopes (‰) measured in NGRIP (GICC05) with Dansgaard-Oeschger (D-O) warming events/Greenland interstadials (GI) numbered; Last Glacial Maximum is indicated, (b) Alkenone derived ($U^{k'}_{37}$) sea surface temperatures (SSTs) measured in core MD01-2444 from the Atlantic Ocean, (c) Oxygen isotopes (‰) measured in speleothems from Soreq cave (Israel) and sapropel depositions (S1, S2) in the eastern Mediterranean Sea, (d) AP/NAP (black) and AP minus *Pinus* and *Juniperus* (green) pollen percentages in I-284 from Lake Ioannina (Greece), (e) AP/NAP (black) and *Quercus* (green) pollen percentages from Lago Grande di Monticchio (Italy), (f) AP/NAP (black) and *Quercus* (green) pollen percentages from Lake Prespa; mean July insolation at 40 °N (W/m²; red), (g) Calibrated radiocarbon ages from neighboring sites with modern human remains. Gray bars correspond to Heinrich events in MD01-2444.

MIS 1 (c. 15 ka cal BP to Present; partly P-2b to P-1)

The Lateglacial transition and the onset of the Holocene marked the termination of the last glacial and the return to interglacial conditions at Prespa. During MIS 1, the Prespa catchment underwent substantial changes in floristic composition as forests expanded (ascending treeline) and diversified. The restricted erosion activity, inferred from decreasing titanium counts, and maximum AP concentrations of (absolute max of 23 x 10^5 grains cm^{-3}) suggest the closing of the tree canopy within the catchment. High macrophytes concentration indicates fluctuating lake levels during the Lateglacial and the Holocene. Aufgebauer et al. (2012) and Panagiotopoulos et al. (2013) describe in detail the vegetational and limnological response to climate change during this interval. Holocene sediments with high TOC content suggest high primary production in the Prespa watershed, as well as enhanced deposition of OM and thus seasonal stratification and hypolimnion anoxia. Relatively high phytoplankton (green algae and dinoflagellates) concentrations during this interval imply increased nutrient accumulation and/or higher temperatures. This increase in lake productivity was coincident with forest expansion (P-1 in **Figure 5.4**) and decreasing allochthonous input. High and synchronous TIC content was attributed to authigenic calcite precipitation corresponding to higher temperatures and productivity in the lake (Aufgebauer et al., 2012). However, during the Early Holocene TIC values (**Figure 5.6** g) remained low implying that increased dissolution of calcium carbonates occurred with seasonal stratification.

5.5.1.3 Understanding ecological processes, triggers and thresholds

Three noteworthy events involving lentic organisms are encountered in the Prespa sequence (phytoplankton blooms, dinoflagellate migration and formation of a shell horizon) and their potential ecological-indicator value is assessed.

The *Pediastrum* and subsequent dinoflagellate peaks at 85 ka and 84 ka cal BP (1648 and 1624 cm) are the only recorded incidents of planktonic population expansion of this order (maxima of 19 x 10^5 coenobia cm^{-3} and 14 x 10^5 dinoflagellates cm^{-3} respectively). Calcite peaks between 87 and 82 ka cal BP, an abrupt opening of the landscape (AP, Ti) and peaking macrophyte (e.g. *Typha* and Cyperaceae) and plankton percentages suggest that the catchment underwent dramatic changes within this interval. The descending treeline left large areas of the surrounding limestone slopes barren and exposed to chemical weathering and erosion. Rising percentages of emergent aquatic vegetation point to fluctuating lake levels and frequent flooding of the littoral zone. Increased aridity and lower annual temperatures inferred from corresponding pollen spectra suggest that these flooding events can be related to seasonal releases of snowmelt from local ice caps (Woodward and Hughes, 2011). Owing to bedrock composition of the Prespa catchment, lake-water likely became supersaturated with respect to calcium during these events. Pronounced calcium peaks concurrent with TIC peaks back this interpretation. Moreover, relative high fine-sand content (up to 14 vol% at 1578 cm) corroborates the notion of increased wave and current activity indicating lowering lake levels and/or increased aeolian activity. Therefore, the expansion of sedgelands (Cyperaceae) and reed beds (e.g *Phragmites* and *Typha*) attest to lower lake levels and most likely also accounted for increasing OM accumulation allowing ripar-

ian trees (i.e. *Salix* and *Alnus*) to reclaim land and in effect pushing the reed beds further into the lake. It should also be noted that during this period summer insolation and light intensity were increasing (**Figure 5.5** a). This could imply that aridity promoted by enhanced seasonality (rather than lower temperatures) was the decisive parameter controlling the aforementioned environmental response. However, the conspicuous absence of Mediterranean taxa pollen points to a rather dry and cold climate regime similar to the one inferred during the Lateglacial to Holocene transition (Panagiotopoulos et al., 2013).

The acceleration of calcium ion accumulation and generally enriched nutrient concentrations caused by a presumed lower stand of Lake Prespa provided ideal conditions for algal growth (see 5.5.1.1). The unprecedented phytoplankton blooms (inferred by peaking Pediastrum and dinoflagellates concentrations) were in turn instrumental in triggering the formation of calcite (nucleation) and thus catalyzed its precipitation. The concomitant double TOC peak and low terrestrial productivity suggest that phytoplankton was the major source of OM deposited. Considering that both planktonic species preserved in pollen slides are composed of robust sporopollenin and cellulose (for green algae and dinoflagellates respectively), the relative high C/N ratio (above 12) can be partly attributed to these properties and due to restricted decomposition of OM. Increased macrophyte biomass (**Figure 5.5** e) within this interval probably accounted for the high C/N ratio as terrestrial biomass retreated substantially. Indeed, relatively high macrophyte percentages (e.g. *Typha*, Cyperaceae and *Sparganium*) and concentrations are registered between c. 87-81 ka cal BP (P-9; **Figure 5.4**).

In contrast to green algae, dinoflagellates are not found in the period prior to 87 ka cal BP (1672 cm). Thus, it is postulated that they were most likely introduced (reintroduced?) into the lake by migrating (avian) fauna. In fact, Wilke et al. (2010) reported the appearance of bivalves (*Dreissena* spp.) in artificial water reservoirs -constructed during the last decades in Greece- implying the occurrence of such re/introduction events on a regular basis. The third event accounts for the TIC peak (calcite) at 74 ka cal BP comprising a horizon of *Dreissena* (*presbensis*) fragments and was tentatively attributed to low lake levels (Wagner et al., 2012).

A *Dreissena* shell layer (1463-1458 cm) formed at 74 ka cal BP and corresponds to the last calcite peak in MIS 5. *Dreissena* spp. are native to several Balkan lakes (Albrecht et al., 2007) and in contrast to their infamous relative, namely the invasive zebra-mussel (*D. polymorpha*), form an integral and vital link in the trophic chain of these ecosystems. These freshwater bivalves exhibit a similar feeding strategy to their marine counterparts (i.e. filtering particles suspended in the water column) and preferably attach to solid substrates (Griffiths et al., 2004). Sparse *Dreissena* fragments were also encountered and dated in the uppermost centimeters of Co1215. Considering the current water depth and distance to the shore, these fragments were most likely transferred to the coring location with waves and currents. A similar transfer mechanism and lower lake levels can be invoked to explain the formation of the mollusk horizon. Wagner et al. (2012) interpreted the undulating reflections found in hydro-acoustic profiles from Lake Prespa during this interval as the result of intensified wave/current activity and low lake levels. Accordingly, the opening of catchment vegetation and decreasing percentages of deciduous trees in P-8a (c. 75-71 ka cal BP) point to a moisture deficit and dropping temperatures. In general, aquatic

vegetation abundance is rather low with the exception of a pronounced Poaceae maximum that could indicate a high *Phragmites* percentage (see **5.5.1.1**). In addition, measured phytoplankton concentrations are peaking within this zone (P-8a). It seems plausible that the expansion of the littoral zone caused by a lake-level lowering is responsible for the population growth of *Dreissena* providing suitable habitats and nourishment. Based on genetic and mismatch analyses, Wilke et al. (2010) modeled the spatial and demographic expansion of *Dreissena* at Prespa and reported estimated ages of 72 ka and 113 ka for these expansions respectively. It can be argued that demographic expansion of *D. presbensis* at Prespa is related to the unprecedented event of 74 ka cal BP marking the end of MIS 5.

5.5.2 Comparison with regional and global records

5.5.2.1 Mediterranean records

On a regional scale, the Prespa pollen record is probably best compared to the Monticchio (Allen et al., 1999) and Ioannina (Tzedakis et al., 2002) pollen archives (**Figure 5.6**), as both records have a similar climate (sub-Mediterranean), elevation (middle-altitude, located at 656 m a.s.l. and 470 m a.s.l. respectively), sedimentation regime (absence of hiatus), sample resolution (detecting millennial-scale variability), and timescale (reaching back to MIS 5). Despite the differences in elevation, topography, sedimentation, chronology and plant composition some general conclusions can be drawn from the comparison between the three pollen records. It should be noted that the Monticchio sequence features an independent chronology based on tephrostratigraphy and varve counting. Whereas, orbital tuning was applied beyond the range of radiocarbon dating in core I-284 (Ioannina), which differs from the tuning procedure for the basal part of Co1215. As evidenced in section **5.5.1**, pollen relative percentages can be misleading in respect to the actual forest coverage of the examined paleolandscapes. Consequently, the ensuing discussion focuses on prominent features that can be traced across several proxies and/or archives.

Further regional records include the oxygen stable isotopes measured in speleothems from Soreq cave (Bar-Matthews et al., 2000) and the Alkenone-derived SST curve from core MD01-2444 at the Iberian margin (Martrat et al., 2007).

The temperate tree (AP - *Juniperus*+*Pinus*, mostly *Quercus*) curve of I-284 (**Figure 5.6** d), the site with the lowest altitude, provides a closer match to the AP curves of Prespa and Monticchio. This is partly due to the rather limited role of *Pinus* at the Ioannina basin and the dominance of deciduous *Quercus* in the pollen spectra (Tzedakis et al., 2002). A similar picture emerges from Monticchio (Allen et al., 2000), where *Pinus* relative abundance is limited and attains maximum values only around the LGM (>40%) while *Quercus* percentages dominate pollen spectra (i.e. MIS 5, MIS 3 and MIS 1). In comparison, core Co1215 has the highest (lowest) *Pinus* (*Quercus*) percentages.

Among other factors, it has been suggested that mid-altitude sites were better suited in sustaining refugial temperate tree populations due to the effect of orographic precipitation (Bennett et al., 1991). Tzedakis et al. (2004) studied three pollen records from contrasting bioclimatic areas in Greece and demonstrated the importance of local topography and ecological thresholds

in controlling the response of the vegetation to climate variability. The Lake Prespa catchment sustained temperate tree populations throughout the Last Glacial (**Figure 5.4**). However, the intermittent appearance and very low values of some drought-sensitive taxa, such as *Fagus*, *Ulmus* and *Tilia*, during MIS 4 to MIS 2 imply that environmental conditions were challenging for growth at an altitude of 849 m a.s.l. (minimum). Taking into account the individual characteristics of each record examined here, it can be argued that the Lake Prespa catchment at 849 m a.s.l. seems to form roughly the upper distribution limit of drought-sensitive trees at these latitudes in Mediterranean mountains.

The *Quercus* curve of Co1215, although continuous, registers very low oak values in particular in MIS 4 and MIS 2 (**Figure 5.6** f). These intervals show the maximum contraction of *Quercus* percentages in all three pollen records, suggesting cold and dry conditions, and a rather open landscape (Fig. 5 D). The $\delta^{18}O$ record from Israel is in agreement with pollen records, and depicts pluvial conditions in MIS 5 and MIS 1 (**Figure 5.6** c). As precipitation in that area originated from the Mediterranean Sea (Bar-Matthews et al., 2003), and given its independent ^{230}Th-U dating, it appears that the conditions described above were synchronously prevalent across the (central and eastern) Mediterranean.

The deposition of two Sapropel layers (S3 and S1) in the eastern Mediterranean coincided with peaks in the speleothem oxygen-isotope record and AP percentage maxima in all pollen records (implying a notable increase in rainfall). It was originally proposed that these organic rich layers, which formed under anoxic conditions in the eastern Mediterranean basin, originated during periods of increased Nile River runoff fed by enhanced monsoon intensity (Rossignol-Strick, 1985). It was demonstrated that increased Nile discharge was not the exclusive cause of sapropel formation (Rohling and Hilgen, 1991). However, Rossignol-Strick (1985) described first the temporal connection between sapropel formation and orbital forcing. Hilgen (1991) correlated sapropels to precession minima (when perihelion occurs in boreal summer and aphelion in boreal winter) and eccentricity maxima. With this orbital configuration, the seasonal insolation contrast (enhanced summer and subdued winter insolation) is greater and thus it affects atmospheric and oceanic circulation (e.g. monsoonal intensification). At Prespa, increased lake and catchment primary production are associated with June insolation maxima during MIS 5, MIS 3 and MIS 1 (**Figure 5.5**). AP percentage maxima concurrent with sapropel deposition are preceded by pronounced retractions (GS 22 and YD) of trees evident in all records presented.

5.5.2.2 Global records

Millennial-scale climate variability was expressed in the North Atlantic during the Last Glacial at a suborbital scale. Events of extreme iceberg discharges from the Laurentide Ice Sheet to the Hudson Strait occurred during this period and are detected as distinct layers of ice-rafted debris (IRD) in marine cores from the North Atlantic (Heinrich, 1988). Bond et al. (1993) recognized six Heinrich events (H1-H6) and additional ones were also proposed (Hodell et al., 2008). Dansgaard-Oeschger (D-O) cycles, characterized by a rapid warming and subsequent cooling, are another type of millennial-scale climate oscillations first recorded in Greenland ice cores spanning the last glacial period (Dansgaard et al., 1984).

Numerous investigations around the globe have detected the imprint of these short-lived climate oscillations in different proxies in the marine as well as in the terrestrial realm (Dansgaard et al., 1984). Marine cores from the Iberian continental margin have been instrumental in establishing the link between ice and other terrestrial records showing the synchronous response of European vegetation to Greenland climate oscillations (Cacho et al., 1999; Sánchez Goñi et al., 2000). Allen et al. (1999) associated millennial-scale variability at Monticchio with the one observed in Greenland ice-cores and argued that the Mediterranean region responded to changes in North Atlantic climate rapidly. At Ioannina, Tzedakis et al. (2002) suggested that AP absolute minima should correlate to Heinrich events recorded in marine cores from the Iberian margin.

At Prespa, Wagner et al. (2010) correlated peaks in Mn and Zr/Ti from cores Co1202 and Co1204 (retrieved from Prespa and Ohrid respectively; **Figure 5.2**) with cold intervals associated with Heinrich events in the North Atlantic. Sediments of the longest core from Lake Prespa to date (Co1215) react sensitively to suborbital climate oscillations and capture these global signals in different proxies. Synchronous peaks in Fe and TIC correlate well with H6, H4, H3, and H2, but there are absent during H5 and H1 implying the complex interplay between climate and environmental parameters and limnological processes. Despite the resolution constraints, the Quercus curve picks up several D-O warming events (**Figure 5.6** f), while Heinrich events are imprinted as distinct minima in AP percentages. Heinrich event 4, which is concurrent with the deposition of the Y5 tephra layer (de Vivo et al., 2001; Lowe et al., 2012), had the greatest impact (AP percentages absolute minimum) on the vegetation at the Lake Prespa catchment. This observation is in agreement with the SST record from the Iberian margin (**Figure 5.6** b), which was associated with the lowest sea surface temperatures (~10 °C) within the period studied. Consequently, the Campanian/Ignimbrite eruption was not solely responsible for the conditions experienced downwind, but probably enhanced the impacts experienced by local ecosystems. The combined effect of H4 and the volcanic ash also affected the other two pollen sites as registered by significant declines of AP percentages.

5.5.3 Environmental constraints posed on hominid populations

Modern human colonization of Europe is in the spotlight for researchers from a variety of disciplines. Genetic studies (involving mitochondrial and Y-chromosome DNA) confirmed the African origin of modern humans and estimated their dispersal out of the continent between c. 80 and 60 ka BP (Mellars, 2006). Although skeletal remains from Skhul and Qafzeh caves in Israel indicate an early and apparently short-lived colonization of the Levant in MIS 5 (c. 100 ka BP), there are no signs of dispersal at such an early stage into Europe (Mellars, 2011; Richter et al., 2012).

The Aurignacian technocomplex, associated with many distinctive features of 'modern' cultural behavior, took place at c. 40 ka (Upper Paleolithic) according to the archaeological record and has been traditionally linked with the dispersal of modern humans into Europe (Mellars, 2011; Richter et al., 2012). This period differs considerably from the preceding Middle Paleolithic that is considered to be formed of Neanderthal communities (Mellars, 2011). Mellars (2004) pointed out that major constraints in the process of unraveling these migration trajectories have been the quality of dated material and the implicit limitations of radiocarbon dating and calibra-

tion techniques at the time. Despite the continuous advances in ^{14}C calibration (Reimer et al., 2009), the selection and treatment of dated material (e.g. shell, bone) is critical and can bias the acquired ages.

One well-established migration route for subsequent modern human dispersals westwards into Europe is considered to be the Danube River valley (Conard, 2002; Conard and Bolus, 2003; Mellars, 2004; Zilhão et al., 2007). The Peştera cu Oase site located in close proximity to the Danube in the southwestern Carpathians (**Figure 5.1**) yielded one of the oldest directly dated human finds in the Balkans with an age of c. 40 ka cal BP (Trinkhaus et al., 2003; Zilhão et al., 2007). Recent evidence from a site in the United Kingdom (Higham et al., 2011) provided estimates of a human maxilla with an age of c. 43 ka cal BP making it the oldest known modern human fossil in northwestern Europe to date. Assuming that one of the primary dispersal routes crossed the Balkan peninsula, it should be expected that modern human finds in this and surrounding areas should be at least of the same age. Indeed, deciduous molars of modern human origin from Grotta del Cavallo (associated with the Uluzzian industry) were dated indirectly at c. 44 ka cal BP (Benazzi et al., 2011). The only known sites associated with this technology outside of the Italian peninsula are located in the Peloponnese, Greece (layer V at Klissoura, Cave 1; Koumouzelis et al., 2001; Lowe et al., 2012), and consequently a Levantine origin can be assumed (Mellars, 2011), although the Uluzzian is absent in the Near East.

The pollen record from Lake Prespa reveals a period of relative high AP and *Quercus* percentages between 60 and 35 ka cal BP that are interpreted as the signature of increased precipitation and higher temperatures (**Figure 5.6** g). The oxygen isotope record from Israel registers a concurrent increase in precipitation at the Levant that coincides with the onset of MIS 3 (**Figure 5.6** c). These findings, apparent in regional and global archives, suggest that climatic conditions were favorable for sustained forest growth within this interval at Prespa. Müller et al. (2011) argued that the summer insolation maximum at c. 58 ka cal BP resulted in a northward displacement of the Intertropical Convergence Zone (associated with increased rainfall in northern Africa) and thus facilitated modern human dispersal out of the continent during the period between 55 to 50 ka cal BP (GI 14-13). Based on a collapse of AP percentages at the Tenaghi Philippon record concurrent with Heinrich event 5 (**Figure 5.6** b), the authors suggested that modern human populations entered Europe taking advantage of the demographic vacuum left by retreating Neanderthals during this centennial event.

The impact of the H5 event (c. 48 ka cal BP) at Prespa, as is the case for Ioannina, was apparently less severe on arboreal vegetation given the dating and sampling constraints. As a consequence, the climatic and environmental conditions across the southwestern part of the Balkan Peninsula remained favorable for modern human occupation during most of the MIS 3. A precipitation gradient between western and eastern Greece exists today and was present during the last glacial as it was demonstrated in pollen archives from Greece (Tzedakis et al., 2004). Differences in local parameters, such as topography and plant composition, can therefore hamper the comparison between different records and proxies (even within similar climate regimes). Thus, the need of a dense network of paleorecords from a region is critical for the accurate reconstruction of climatic and environmental conditions along potential corridors of human migration.

It should also be noted, that ice accumulation during glacial times was a major factor in shaping coastal planes and determining the paleocoastline (Waelbroeck et al., 2002). Sea-level fluctuations (of up to 100m, see contour line marked in **Figure 5.1**) were reconstructed during MIS 3, exposing large areas of the continental self during the last glacial period (Siddall et al., 2003). In most certainty, several of these were used for the dispersal of our ancestors into Europe.

5.6 Conclusions

The Lateglacial pollen record of Co1215 hints to the refugial properties of the Prespa watershed during the Last Glacial period. This study confirms the survival of several deciduous temperate trees in the catchment since MIS 5. At an altitude of 849 m a.s.l., the study area formed most likely the upper limit of their glacial distribution at these latitudes within the Mediterranean region. The middle-altitude, the diverse topography and the relative proximity to the Adriatic Sea were decisive factors in shaping Prespa's microclimate throughout this interval.

These topographical characteristics in concert with the relative shallow morphology of Lake Prespa enabled the registration of centennial- to millennial-scale climate oscillations. The ecosystems of Lake Prespa and its watershed respond sensitively to D-O cycles and Heinrich events occurring in the North Atlantic and propagated into the Mediterranean through atmospheric and ocean circulation. Our multi-proxy approach captures the imprint of climatic signals in biotic as well as abiotic components of the local environment.

Three major phases of vegetation development closely following climate variability are distinguished for the last 92 ka cal BP. The wooded phases of MIS 5 and MIS 1 dominated by deciduous trees with higher temperatures and moisture availability, the rather open but wooded landscape with significant temperate-tree presence of MIS 3 and the pine dominated wooded-steppe (open landscape) of MIS 4 and MIS 2 when temperatures and moisture availability declined. The succession of the forest density in the catchment is also depicted in geophysical and geochemical parameters, such as the titanium and total organic carbon curves, that follow closely the landscape evolution. Periods of reduced forest cover or a retreating treeline (MIS 4 and MIS 2) resulted in enhanced erosional activity in the catchment and restricted lake productivity. Siderite formation occurs sporadically throughout the glacial and signified substantial changes in lake mixing and redox conditions. Several of these peaks depicted in the TIC curve are concurrent with short lived cold events and probably represent far field responses to the North Atlantic events. During periods of enhanced lake productivity (MIS 5 and MIS 1) calcite is precipitated in the lake and the lake-mixing regime is altered.

The Lake Prespa record appears to be in good agreement with regional and global archives depicting orbital and suborbital climate variability. Despite the limitations of the age model of Co1215 (i.e. tuning with NGRIP curve at the basal part), major climate events are in phase with other archives in the eastern Mediterranean featuring independent chronologies (e.g. speleothem record). The Prespa record as well as other reference archives from the Mediterranean point to a time window encompassing MIS 3 when the climate conditions were likely favorable for modern human dispersal from the Levant into Europe.

5.7 Acknowledgements

We are much obliged to our colleagues from the Seminar of Geography and Education and the Institute of Geology and Mineralogy at the University of Cologne for their valuable assistance during the field campaign and the processing of material in the laboratory. We thank the Hydrobiological Institute in Ohrid, the administration of Pelister and Galičica National Parks for logistic support. KP gratefully acknowledges Frederik von Reumont for help with cartography, as well as Valery Sitlivy, Jean-Pierre Francois and Karsten Schittek for comments on results and previous versions of the manuscript. This study is part of Project B2 of the Collaborative Research Center 806 "Our Way to Europe" funded by the German Research Foundation (DFG).

5.8 References

Albrecht, C., Schultheiß, R., Kevrekidis, T., Streit, B., and Wilke, T.: Invaders or endemics? Molecular phylogenetics, biogeography and systematics of *Dreissena* in the Balkans, Freshwater Biol., 52, 1525-1536, doi:10.1111/fwb.2007.52.issue-8, 2007.

Allen, J.R.M., Brandt, U., Brauer, A., Hubberten, H.W., and Huntley, B.: Rapid environmental changes in southern Europe during the last glacial period, Nature, 400, 740-743, 1999.

Allen, J.R.M., Watts, W.A., and Huntley, B.: Weichselian palynostratigraphy, palaeovegetation and palaeoenvironment; the record from Lago Grande di Monticchio, southern Italy, Quatern. Int., 73-4, 91-110, 2000.

Aufgebauer, A., Panagiotopoulos, K., Wagner, B., Schaebitz, F., Viehberg, F.A., Vogel, H., Zanchetta, G., Sulpizio, R., Leng, M.J., and Damaschke, M.: Climate and environmental change in the Balkans over the last 17 ka recorded in sediments from Lake Prespa (Albania/F.Y.R. of Macedonia/Greece), Quatern. Int., 274, 122-135, doi:10.1016/j.quaint.2012.02.015, 2012.

Bar-Matthews, M., Ayalon, A., and Kaufman, A.: Timing and hydrological conditions of Sapropel events in the Eastern Mediterranean, as evident from speleothems, Soreq cave, Israel, Chem. Geol., 169, 145-156, 2000.

Bar-Matthews, M., Ayalon, A., Gilmour, M., Matthews, A., and Hawkesworth, C.J.: Sea-land oxygen isotopic relationships from planktonic foraminifera and speleothems in the Eastern Mediterranean region and their implication for paleorainfall during interglacial intervals, Geochim. Cosmochim. Ac., 67, 3181-3199, 2003.

Benazzi, S., Douka, K., Fornai, C., Bauer, C.C., Kullmer, O., Svoboda, J., Pap, I., Mallegni, F., Bayle, P., Coquerelle, M., Condemi, S., Ronchitelli, A., Harvati, K., and Weber, G.W.: Early dispersal of modern humans in Europe and implications for Neanderthal behaviour, Nature, 479, 525-528, doi:10.1038/nature10617, 2011.

Bennett, K.D., Tzedakis, P.C., and Willis, K.J.: Quaternary refugia of north European trees, J Biogeogr., 18, 103-115, 1991.

Blondel, J., Aronson, J., Bodiou, J.-Y., and Boef, G.: The Mediterranean Region. Biological Diversity in Space and Time, Second Edition, Oxford University Press, Oxford, 2010.

Bond, G., Broecker, W., Johnsen, S., McManus, J., Labeyrie, L., Jouzel, J., and Bonani, G.: Correlations between climate records from North Atlantic sediments and Greenland ice, Nature, 365, 143-147, 1993.

Cacho, I., Grimalt, J.O., Pelejero, C., Canals, M., Sierro, F.J., Flores, J.A., and Shackleton, N.: Dansgaard-Oeschger and Heinrich event imprints in Alboran Sea paleotemperatures, Paleoceanography, 14, 698-705, 1999.

Cohen, A.S.: Paleolimnology, The History and Evolution of Lake Ecosystems, Oxford University Press, Oxford, pp. 500, 2003.

Conard, N.J.: The timing of cultural innovations and the dispersal of modern humans in Europe, Terra nostra, 2002/6, 82-94, 2002.

Conard, N.J., and Bolus, M.: Radiocarbon dating the appearance of modern humans and timing of cultural innovations in Europe: new results and new challenges, J. Hum. Evol., 44, 331-371, doi:10.1016/S0047-2484(02)00202-6, 2003.

Damaschke, M., Sulpizio, R., Zanchetta, G., Wagner, B., Böhm, A., Nowaczyk, N., Rethemeyer, J., and Hilgers, A.: Tephrostratigraphic studies on a sediment core from Lake Prespa in the Balkans, Clim. Past, 9, 267-287, doi:10.5194/cp-9-267-2013, 2013.

Dansgaard, W., Johnsen, S., Clausen, H.B., Dahl-Jensen, D., Gundestrup, N., Hammer, C.U., and Oeschger, H.: North Atlantic climatic oscillations revealed by deep Greenland ice cores, Hansen, J.E., and Takahashi, T. (Eds.), American Geophysical Union, Washington DC, 288-298, 1984.

De Vivo, B., Rolandi, G., Gans, P.B., Calvert, A., Bohrson, W.A., Spera, F.J., and Belkin, H.E.: New constraints on the pyroclastic eruptive history of the Campanian volcanic Plain (Italy), Miner. Petrol., 73, 47-65, 2001.

Dittrich, M., and Koschel, R.: Interactions between calcite precipitation (natural and artificial) and phosphorus cycle in the hardwater lake, Hydrobiologia, 469, 49-57, 2002.

Fletcher, W.J., Sánchez Goñi, M.F., Allen, J.R.M., Cheddadi, R., Coumbourieu-Nebout, N., Huntley, B., Lawson, I.T., Londeix, L., Magri, D., Margari, V., Müller, U.C., Naughton, F., Novenko, E., Roucoux, K.H., and Tzedakis, P.C.: Millennial-scale variability during the last glacial in vegetation records from Europe, Quaternary Sci. Rev., 29, 2839-2864, 2010.

Griffiths, H.I., Kryštufek, B., and Reed, J.M. (Eds.): Balkan Biodiversity: Pattern and Process in the European Hotspot, Kluwer Academic Publishers, Dodrecht, The Netherlands, pp. 357, 2004.

Grimm, E.C.: TILIA and TILIA-graph: Pollen spreadsheet and graphics programs. Programs and Abstracts, 8th International Palynological Congress, Aix-en-Provence, France, pp. 56, 1992.

Grove, A.T., and Rackham, O.: The Nature of Mediterranean Europe - An Ecological History, Yale University Press, London, pp. 384, 2003.

Harrison, S.P., and Digerfeldt, G.: European lakes as palaeohydrological and palaeoclimatic indicators, Quaternary Sci. Rev., 12, 233-248, 1993.

Heinrich, H.: Origin and consequences of cyclic ice rafting in the northeast Atlantic Ocean during the past 130,000 years, Quaternary Res., 29, 142-152, 1988.

Higham, T., Compton, T., Stringer, C., Jacobi, R., Shapiro, B., Trinkaus, E., Chandler, B., Groning, F., Collins, C., Hillson, S., O'Higgins, P., FitzGerald, C., and Fagan, M.: The earliest evidence for anatomically modern humans in northwestern Europe, Nature, 479, 521-524, doi:10.1038/nature10484, 2011.

Hilgen, F.J.: Astronomical calibration of Gauss to Matuyama sapropels in the Mediterranean and implication for the geomagnetic polarity time scale, Earth Planet. Sc. Lett., 104, 226-244, 1991.

Hodell, D.A., Channell, J.E.T., Curtis, J.H., Romero, O.E., and Röhl, U.: Onset of "Hudson Strait" Heinrich events in the eastern North Atlantic at the end of the middle Pleistocene transition (~640 ka)?, Paleoceanography, 23, PA4218, doi:10.1029/2008PA001591, 2008.

Hollis, G.E., and Stevenson, A.C.: The physical basis of the Lake Mikri Prespa systems: geology, climate, hydrology and water quality, Hydrobiologia, 351, 1-19, 1997.

Jankovská, V., and Komárek, J.: Indicative value of *Pediastrum* and other coccal green algae in paleoecology, Folia Geobot., 35, 59-82, 2000.

Jarvis, A, Reuter, H I, Nelson, A, and Guevara, E: Hole-filled SRTM for the globe Version 4, available from the CGIAR-CSI SRTM 90m Database, last access: 27.11.2011, available at: http://srtm.csi.cgiar.org,

Komárek, J., and Jankovská, V.: Review of the Green Algal Genus *Pediastrum*; Implication for Pollen-analytical Research, Bibliotheca Phycologica, 108, J. Cramer, Berlin ; Stuttgart, pp. 127, 2001.

Kouli, K., Brinkhuis, H., and Dale, B.: *Spiniferites cruciformis*: a fresh water dinoflagellate cyst?, Rev. Palaeobot. Palyno., 113, 273-286, 2001.

Koumouzelis, M., Kozlowski, J.K., Escutenaire, C., Sitlivy, V., Sobczyk, K., Valladas, H., Tisnerat-Laborde, N., Wojtal, P., and Ginter, B.: La fin du Paléolithique moyen et le début du Paléolithique supérieur en Grece: la séquence de la Grotte 1 de Klissoura, L'Anthropologie, 105, 469-504, 2001.

Leng, M.J., Wagner, B., Boehm, A., Panagiotopoulos, K., Vane, C.H., Snelling, A., Haidon, C., Woodley, E., Vogel, H., Zanchetta, G., and Baneschi, I.: Understanding past climatic and hydrological variability in the Mediterranean from Lake Prespa sediment isotope and geochemical record over the Last Glacial cycle, Quaternary Sci. Rev., 66, 123-136, doi:10.1016/j.quascirev.2012.07.015, 2013.

Levin, I., and Kromer, B.: The tropospheric 14CO2 level in mid-latitudes of the Northern Hemisphere (1959-2003), Radiocarbon, 46, 1261-1272, 2004.

Lézine, A.M., von Grafenstein, U., Andersen, N., Belmecheri, S., Bordon, A., Caron, B., Cazet, J.P., Erlenkeuser, H., Fouache, E., and Grenier, C.: Lake Ohrid, Albania, provides an exceptional multi-proxy record of environmental changes during the last glacial–interglacial cycle, Palaeogeography, Palaeoclimatology, Palaeoecology, 287, 116-127, doi:10.1016/j.palaeo.2010.01.016, 2010.

Lisiecki, L.E., and Raymo, M.E.: A Pliocene-Pleistocene stack of 57 globally distributed benthic δ18O records, Paleoceanography, 20, PA1003, doi:10.1029/2004PA001071, 2005.

Lowe, J., Barton, N., Blockley, S., Ramsey, C.B., Cullen, V.L., Davies, W., Gamble, C., Grant, K., Hardiman, M., Housley, R., Lane, C.S., Lee, S., Lewis, M., MacLeod, A., Menzies, M., Muller, W., Pollard, M., Price, C., Roberts, A.P., Rohling, E.J., Satow, C., Smith, V.C., Stringer, C.B., Tomlinson, E.L., White, D., Albert, P., Arienzo, I., Barker, G., Boric, D., Carandente, A., Civetta, L., Ferrier, C., Guadelli, J.L., Karkanas, P., Koumouzelis, M., Müller, U.C., Orsi, G., Pross, J., Rosi, M., Shalamanov-Korobar, L., Sirakov, N., and Tzedakis, P.C.: Volcanic ash layers illuminate the resilience of Neanderthals and early modern humans to natural hazards, Proc Natl Acad Sci U S A, 109, 13532-13537, doi:10.1073/pnas.1204579109, 2012.

Martrat, B., Grimalt, J.O., Shackleton, N.J., de Abreu, L., Hutterli, M.A., and Stocker, T.F.: Four climate cycles of recurring deep and surface water stabilizations on the Iberian margin, Science, 317, 502-507, doi:10.1126/science.1142964, 2007.

Matzinger, A., Jordanoski, M., Veljanoska-Sarafiloska, E., Sturm, M., Müller, B., and Wüest, A.: Is Lake Prespa jeopardizing the ecosystem of ancient Lake Ohrid?, Hydrobiologia, 553, 89-109, doi:10.1007/s10750-005-6427-9, 2006.

Mellars, P.: Neanderthals and the modern human colonization of Europe, Nature, 432, 461-465, doi:10.1038/nature03103, 2004.

Mellars, P.: Why did modern human populations disperse from Africa ca. 60,000 years ago? A new model, P. Natl. Acad. Sci. USA, 103, 9381-9386, 2006.

Mellars, P.: Palaeoanthropology: The earliest modern humans in Europe, Nature, 479, 483-485, 2011.

Meyers, P.A.: Preservation of source identification of sedimentary organic matter during and after deposition, Chem. Geol., 144, 289-302, 1994.

Müller, U.C., Pross, J., Tzedakis, P.C., Gamble, C., Kotthoff, U., Schmiedl, G., Wulf, S., and Christanis, K.: The role of climate in the spread of modern humans into Europe, Quaternary Sci. Rev., 30, 273-279, doi:10.1016/j.quascirev.2010.11.016, 2011.

NGRIP Members.: High-resolution record of Northern Hemisphere climate extending into the last interglacial period, Nature, 431, 147-151, 2004.

Okuda, M., Yasuda, Y., and Setoguchi, T.: Middle to Late Pleistocene vegetation history and climatic changes at Lake Kopais, Southeast Greece, Boreas, 30, 73-82, doi:10.1111/j.1502-3885.2001.tb00990.x, 2001.

Panagiotopoulos, K., Aufgebauer, A., Schäbitz, F., and Wagner, B.: Vegetation and climate history of the Lake Prespa region since the Lateglacial, Quatern. Int., 293, 157-169, doi:10.1016/j.quaint.2012.05.048, 2013.

Polunin, O.: Flowers of Greece and the Balkans - A Field Guide, Oxford University Press, Oxford, pp. 692, 1980.

Reimer, P.J., Baillie, M.G.L., Bard, E., Bayliss, A., Beck, J.W., Blackwell, P.G., Bronk Ramsey, C., Buck, C.E., Burr, G.S., Edwards, R.L., Friedrich, M., Grootes, P.M., Guilderson, T.P., Hajdas, I., Heaton, T.J., Hogg, A.G., Hughen, K.A., Kaiser, K.F., Kromer, B., McCormac, F.G., Manning, S.W., Reimer, R.W., Richards, D.A., Southon, J.R., Talamo, S., Turney, C.S.M., van der Plicht, J., and Weyhenmeyer, C. E.: IntCal09 and Marine09 Radiocarbon Age Calibration Curves, 0 - 50,000 years cal BP, Radiocarbon, 51, 1111-1150, 2009.

Richter, J., Hauck, T., Vogelsang, R., Widlok, T., Le Tensorer, J.-M., and Schmid, P.: "Contextual areas" of early Homo sapiens and their significance for human dispersal from Africa into Eurasia between 200 ka and 70 ka, Quatern. Int., 274, 5-24, doi:10.1016/j.quaint.2012.04.017, 2012.

Rohling, E.J., and Hilgen, F.J.: The eastern Mediterranean climate at times of sapropel formation: a review, Geol. Mijnbouw, 70, 253-264, 1991.

Rossignol-Strick, M.: Mediterranean Quaternary sapropels, an immediate response of the African monsoon to variation of insolation, Palaeogeography, palaeoclimatology, palaeoecology, 49, 237-263, 1985.

Sánchez Goñi, M.F., Turon, J.-L., Eynaud, F., and Gendreau, S.: European Climatic Response to Millennial-Scale Changes in the Atmosphere-Ocean System during the Last Glacial Period, Quaternary Res., 54, 394-403, doi:10.1006/qres.2000.2176, 2000.

Siddall, M., Rohling, E.J., Almogi-Labin, A., Hemleben, C., Meischner, D., Schmelzer, I., and Smeed, D.A.: Sea-level fluctuations during the last glacial cycle, Nature, 423, 853-858, doi:10.1038/nature01687, 2003.

Stockmarr, J.: Tablets with spores used in absolute pollen analysis, Pollen et spores, 13, 615-621, 1971.

Tzedakis, P.C., Lawson, I.T., Frogley, M.R., Hewitt, G.M., and Preece, R.C.: Buffered tree population changes in a quaternary refugium: evolutionary implications, Science, 297, 2044-2047, doi:10.1126/science.1073083, 2002.

Tzedakis, P.C., Frogley, M.R., Lawson, I.T., Preece, R.C., Cacho, I., and de Abreu, L.: Ecological thresholds and patterns of millennial-scale climate variability: The response of vegetation in Greece during the last glacial period, Geol, 32, 109-112, doi:10.1130/G20118.1, 2004.

Vogel, H., Wagner, B., Zanchetta, G., Sulpizio, R., and Rosén, P.: A paleoclimate record with tephrochronological age control for the last glacial-interglacial cycle from Lake Ohrid, Albania and Macedonia, J. Paleolimnol., 44, 295-310, doi:10.1007/s10933-009-9404-x, 2010.

Waelbroeck, C., Labeyrie, L., Michel, E., Duplessy, J.C., McManus, J.F., Lambeck, K., Balbon, E., and Labracherie, M.: Sea-level and deep water temperature changes derived from benthic foraminifera isotopic records, Quaternary Sci. Rev., 21, 295-305, 2002.

Wagner, B., Vogel, H., Zanchetta, G., and Sulpizio, R.: Environmental change within the Balkan region during the past ca. 50 ka recorded in the sediments from lakes Prespa and Ohrid, Biogeosciences, 7, 3187-3198, doi:10.5194/bg-7-3187-2010, 2010.

Wagner, B., Aufgebauer, A., Vogel, H., Zanchetta, G., Sulpizio, R., and Damaschke, M.: Late Pleistocene and Holocene contourite drift in Lake Prespa (Albania/F.Y.R. of Macedonia/Greece), Quatern. Int., 274, 112-121, doi:10.1016/j.quaint.2012.02.016, 2012.

Wetzel, R.G.: Limnology, Lake and River Ecosystems, Third Edition, Academic Press, pp. 1006, 2001.

Wijmstra, T.A.: Palynology of the first 30 meters of a 120 m deep section in northern Greece, Acta Bot. Neerl., 18, 511-527, 1969.

Wilke, T., Schultheiß, R., Albrecht, C., Bornmann, N., Trajanovski, S., and Kevrekidis, T.: Native *Dreissena* freshwater mussels in the Balkans: in and out of ancient lakes, Biogeosciences, 7, 3051-3065, doi:10.5194/bg-7-3051-2010, 2010.

Woodward, J.C., and Hughes, P.D.: Glaciation in Greece: A New Record of Cold Stage Environments in the Mediterranean, in: Quaternary Glaciations - Extent and Chronology, Ehlers, J., Gibbard, P.L., and Hughes, P.D. (Eds.), Elsevier, Amsterdam, 175-198, 2011.

Zilhão, J., Trinkaus, E., Constantin, S., Milota, S., Gherase, M., Sarcina, L., Danciu, A., Rougier, H., Ouilès, J., and Rodrigo, R.: The Peştera cu Oase People, Europe's Earliest Modern Humans, in: Rethinking the Human Revolution, Mellars, P., Boyle, K., Bar-Yosef, O., and Stringer, C. (Eds.), McDonald Institute for Archaeological Research, Cambridge, 249-262, 2007.

VI Towards a theoretical framework for analyzing integrated socio-environmental systems*

Abstract

This article addresses two major challenges for an integrated analysis of socio-environmental systems, namely the diversity of contributing disciplines and the wide spectrum of temporal and spatial scales. Archaeology, the geosciences and socio-cultural anthropology provide information relating to a diversity of specific time series and spatial distribution maps in order to answer questions relating to the impact of environmental and anthropogenic factors in population growth and migration processes. A model based on the key idea of adaptive cycles as it was initially developed in resilience research can be productively employed to bridge the diversity of disciplines and to integrate the diversity of data that they provide. This article outlines first steps towards recognizing similar patterns across a wide spectrum of empirical observations. It is exploratory in its attempt to trace these patterns across different layers of understanding the complexity of human-environment interaction.

The case material considered relates to (1) observable ethnographic data on forager mobility and its simulation, (2) the demography of the Central European Neolithic, (3) the palaeodemography of foragers during the Late Upper Palaeolithic, (4) the societal reorganization by Palaeolithic foragers under climate instability, (5) the palaeoenvironmental study of lake Prespa in the Balkans, and (6) environmental responses to agricultural land use practices in relation to sediment flux in hillslope systems. With reference to these cases, an adaptive cycle model is outlined, with phases of growth, conservation, distortion and reorganization. The model helps to infer internal dynamics in the diverse environmental and social domains without reducing one domain to another while still connecting evidence from a host of different sources. More generally, such a model could help in understanding features of non-linearity, multifactoral relations, scale dependency and time-lags which seem to be typical for the complex dynamics of integrated socio-environmental systems.

* This chapter is based on Widlok, T., Aufgebauer, A., Bradtmöller, M., Dikau, R., Hoffmann, T., Kretschmer, I., Panagiotopoulos, K., Pastoors, A., Peters, R., Schäbitz, F., Schlummer, M., Solich, M., Wagner, B., Weniger, G.-C., Zimmermann, A., 2012: Towards a theoretical framework for analyzing integrated socio-environmental systems. Quaternary International 274, 259-272, dx.doi.org/10.1016/j.quaint.2012.01.020.

6.1 Introduction

The objectives of the Collaborative Research Centre (CRC), "Our way to Europe: Culture-Environment Interaction and Human Mobility in the Late Quaternary", are succinctly summarized in three principal themes (expansion into Europe, retreat and repopulation, mobility patterns) which are investigated through the integration of data relating to climate, environment and culture. The key questions relate to the problem of how to conceive of culture-environment relations in terms of integrated systems. The same topic also plays a key role in another forum of international researchers dealing with the complexity of socio-ecological systems in different temporal and spatial scales who base their work on the concepts resilience, adaptive cycles and panarchy (Gunderson and Holling, 2002; Resilience Alliance, 2011).

The goals of this paper are (1) to introduce some of the theoretical considerations emerging from the panarchy group that are relevant for an understanding of socio-ecological systems, (2) to present case studies from different CRC projects that attempt to integrate the social dimension of migrating Homo sapiens with the environmental contexts of the migration corridors in time and space, and (3) to encourage further contributions to this emerging discussion. The authors are convinced that the shared research goal of outlining culture-environment interaction requires seriously considering existing approaches that can help to integrate data and ideas across disciplines and case studies. Human social processes and environmental processes are linked, and this link is characterized by complex feedbacks on different spatial and temporal scales which demand a coherent and comprehensive theoretical framework.

This paper hopes to contribute to a research perspective that integrates human agency and environmental parameters in a single explanatory model. To date, the disciplinary division of labor and entrenched theoretical assumptions led to a situation whereby humanity and the natural environment are investigated independently, so that human-environment interaction appears to be an afterthought and a topic for investigation at some distant point in the future. However, there are many indications that the two are in fact mutually constitutive in that human agency is more than a passive adaptation to a given framework and in that what constitutes a relevant environmental frame is not simply given but has to be demonstrated to be systematically linked to human behavior. The approach is to strive for a framework which allows demonstration of how dynamic relationships can be described that involve human agents as much as environmental conditions without the need to subsume one under the other and without drawing a sharp line between the two as separate systems.

6.2 The theory of resilience and adaptive cycles (according to Gunderson and Holling)

Socio-ecological systems are characterized by different degrees of resilience, which is defined by their capacity to adjust to perturbations. If a society has lost much of its resilience capacity it may be vulnerable to internal or external impacts, to challenges or changes. Resilience theory is based on the hypothesis that the stability of an integrated socio-ecological system (SES) is related to multiple, stable states maintaining their primary functional relationships. Four assumptions are being made (following Gunderson and Holling, 2002).

(1) Changes in an integrated SES are sometimes chaotic and not gradual or continuous but show rather episodic behavior. Time periods of slow accumulation of natural resources are punctuated by sudden release and reorganization. Examples are the interactions between fast variables (e.g. river floods or droughts) and slow variables (e.g. the increasing vulnerability of the food production system caused by decreasing soil fertility from overcropping).

(2) The spatial and temporal properties of the system are not scale invariant or uniform. The system components (processes, patterns) may be discontinuous at all scales. Up-scaling methods cannot be based on simple aggregation (e.g. by mean values of subscale attributes).

(3) SESs have multiple equilibria on functionally different levels. Stabilizing forces maintain productivity, fixed capital and social memory of a society while destabilizing forces are important to maintain diversity, flexibility and opportunity.

(4) If a society is to achieve constant yields (e.g. a sustainable yield of wood) but does not consider scales of system behavior and the changing SES context (e.g. changing soil moisture) in its policies and management rules (e.g. in crop production) the resilience of the system is decreasing. Such systems can then suddenly breakdown after a disturbance.

There are a number of different definitions of resilience depending on the discipline and the methodological background of the scientists involved. Gunderson and Holling (2002) define resilience in two different ways (see Redman et al., 2007, p. 118): Engineering resilience is a state of system stability approaching a steady state of equilibrium, "where resistance to disturbance and speed of return to the equilibrium are used to measure the property" of the system. The second definition refers to ecosystem resilience, and is related to systems that are far from equilibrium steady state, "where instabilities can flip a system into another regime of behavior", e.g. to another stability domain. Here, resilience is measured by "the magnitude of the disturbance that can be absorbed before the system changes its structure by changing the variables and processes that control behavior". The authors present a number of examples for the dynamics and management of such systems, e.g. freshwater systems, forests or semi-arid grasslands.

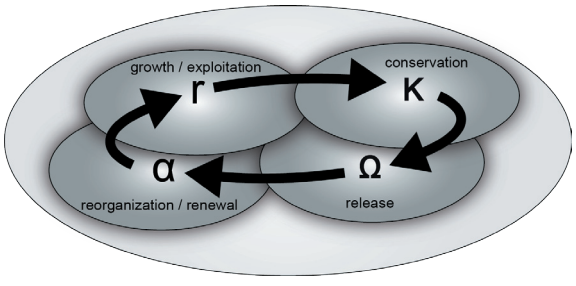

Figure 6.1: Adaptive cycle model (adapted from Resilience Alliance, 2011).

The general framework for describing the development and change of ecosystems as developed by Gunderson and Holling (2002) is centered around the concept of adaptive cycles. This concept defines four ecosystem functions (r, K, U, a) and the "flow of events" between them (**Figure 6.1** for a simplified representations of the adaptive cycle model). Flow means the spatio-temporal trajectory of the system development (e.g. a forest). The r- and K-phases are well known from ecology, they refer to growth/exploitation and to conservation respectively. The two additional functions U and a are adapted from economy. In the U-phase of the system (e.g. a forest) accumulation of

biomass and nutrients leads to an increasingly over-connected and fragile status, so that already small perturbations can release the system (e.g. a forest fire). The second additional function is the a-phase of the system, in which reorganization occurs, for instance the appearance of pioneer organisms in the environment after a forest fire. The resilience of an ecological system is not fixed for the whole system. It is expanding and contracting within the cycle.

The second feature of the concept of adaptive cycle is related to the hierarchical structure of the components within the cycle as well as between adaptive cycles on different scales. Gunderson and Holling (2002) argue that the term "hierarchy" is "burdened by the rigid, top-down nature" of its common meaning, so that they prefer the term "panarchy" to "capture the adaptive and evolutionary nature of adaptive cycles that are nested one within the other across space and time scales" (Gunderson and Holling, 2002, p. 73). A panarchy system is thus a nested set of adaptive cycles on different space and time scales with distinct connections between different levels. The model allows envisaging that a critical change in a small and fast cycle cascades up during the low-resilience phase of the larger and slower system (the "revolt connection" according to Gunderson and Holling, 2002, p. 75). In this fragile stage of the larger system (e.g. a forest with low resilience in terms of accumulated dry biomass) a small ground fire can lead to the collapse of the forest. The downward-connection indicates properties of the larger cycle system (e.g. seeds, physical structure, surviving species) contributing to the reorganization (a-phase) of the middle size system (the "remember connection" according to Gunderson and Holling, 2002, p. 75).

The theoretical concepts outlined above have also been applied in the IHOPE project (Integrated History and Future of People on Earth) which models long-term historical time scales of integrated ancient systems and their dynamics (Constanza et al., 2007; Dearing, 2008). The basic conclusions are:

- The research focus should move away from simple cause-and- effect paradigms to complex, adaptive, integrated socio-ecological systems.
- Resilience theory and the focus on adaptive cycles including "risk spirals" are important.
- Further topics are the conflicts and the trade-offs between short-term production and long-term resilience or sustain- ability of the integrated system.
- The role of feedback processes is crucial in complex socio-ecological systems.

Further topics include:

- Temporal dynamics, rates of change in critical phenomena as thresholds, nonlinearities, abrupt or extreme events in the human and the natural parts of the system.
- Contingencies and legacies from the past.
- The phenomenon of "collapse".

6.3 Case studies

In the following section, case studies from a number of different CRC projects are presented which range from seasonal cycles of one year in small areas to processes at a continental scale

covering several thousand years (**Figure 6.2**). A model of nested cycles can accommodate such a diversity of cases and promises to link data from such a diversity of temporal and spatial scales into one integrated model.

6.3.1 The small scale of observable human-environment interaction and its simulation in forager studies (TW, MS - project E3)

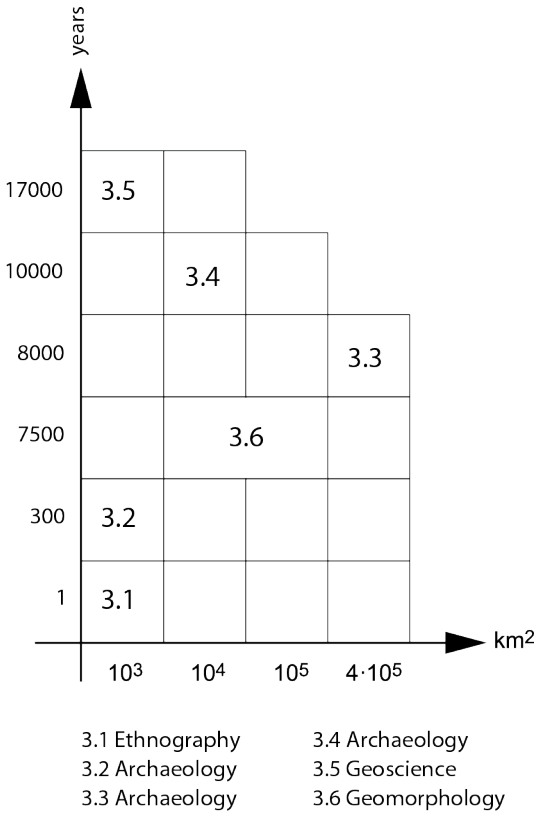

Figure 6.2: Spatial and temporal scales of case studies dealt within Sections 6.3.1 - 6.3.6.

The empirical ethnographic data on forager mobility shows, above all, that there is great variability in hunter-gatherer responses to environmental changes (see Barnard, 1992; Kelly, 1995). Not only are there different mobilities (patterns of mobility) but mobility itself is only one of the means developed by foragers to buffer the effects of environmental change on human life e other important ones being changes in diet, reproductive control, and changes in social networks including networks of exchange for risk reduction (see Kelly, 1995). Foragers not only move in a variety of ways but the degree to which mobility is complemented or substituted by other strategies may also vary. Human mobility, in the sense of migration, is therefore not only the result of relevant environmental and anthropogenic factors but mobility, in the sense of cultivated patterns of movement, is in itself one aspect within such a larger bundle of anthropogenic factors involved in human-environment interaction. As mobility allows changes in population size beyond the demographic factors of reproduction, it also affects relevant population growth (or shrinkage) in a relevant segment of space and time. These are complex interaction and feedback cycles and not isolated single effects that can be paired with single results in a unilinear fashion.

The empirical record based on ethnography does, therefore, not support any environmental or climatic deterministic view but suggests that any predictions will have to include both, environmental and social aspects. This article illustrates this point with regard to the Kalahari "San" foragers during the 20th century and with regard to attempts to extrapolate by means of simulation from this specific ethnographic record. Kalahari foragers, even under similar environmental conditions, have developed diverse cultural patterns (including patterns of mobility) and one cannot predict in any simple way the occurrence of a particular cultural form by referring back

to environmental conditions. While these conditions are clearly limiting factors, a more complex model is needed to explain how environmental and anthropogenic factors are linked. Correspondences and causalities may be elicited when looking not at the empirical data at face value but when analyzing the patterns that link a number of observations in the domain of cultural strategies and in the domain of environmental changes (as well as links between the two). Patterns emerge already at the low- resolution level of seasonal changes. The ethnographic record (summarized in Kelly, 1995 and Binford, 2001) suggests that a regular movement occurs between smaller groups (often called bands, with around 25 members) and larger groups (often called band clusters with up to 500 members). There is also evidence for the ecological consequences that this has had. For instance, the movements of small bands in Australia and their use of fire has been instrumental in creating a patchwork of (more or less recently) burnt and unburnt patches of land with differing states of re-growth and the corresponding plant and animal communities (Widlok, 2008). With the ban of forager mobility during colonization the system became susceptible for large-scale destructive bushfires as large amounts of fuel accumulated and the patchwork had disappeared as mobility was reduced. This illustrates the dynamic relation between environmental situations and cultural strategies.

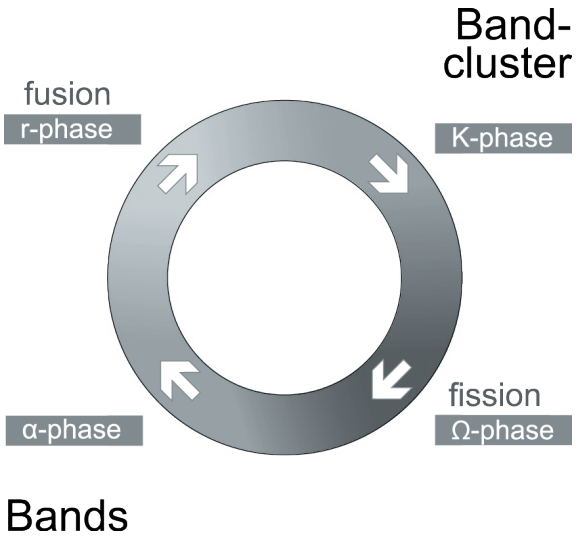

Figure 6.3: Band dynamics in terms of adaptive cycle phases.

In the case of the Kalahari San (Barnard, 1992, p. 231) increasing aridity in the dry season may lead to fusion (e.g. among the foragers of the central Kalahari who have a very limited number of water sources during that season) or to fission (e.g. among the foragers of the northwestern Kalahari who have numerous but small water sources at their disposal). Moreover, the trans- formation between the two states of aggregation and dispersal is typically gradual so that not only the end products (band and band cluster) are distinguished, but also the two processes that lead to them (fission and fusion) which are also subject to social dynamics of creating social distance and closeness and subject to cultural practices of sharing that allow individuals to cope, in this case, with long distances to the nearest water source. In the fusion phase, there is increasing cooperation and contact between individuals and existing groups whereas in the fission phase, there is a decreasing interaction and coordination between individuals and groups. All these observable characteristics of forager social organization over time allow description of them as features of a more comprehensive human-environment system of recurring cycles relating to the band (cluster) with four phases as outlined in the adaptive cycle model (see above) whereby "the band" corresponds to the alpha phase, "band-cluster" to the K-phase, "fission" to the omega phase and "fusion" to the r-phase (**Figure 6.3**). In other words, it does not need to be assumed that these

groups switch between cultures or that one form of organization is more typical or representative than another. Instead, it is the combination of anthropogenic and environmental aspects that generate the dynamic system and it is the dynamics of the system that regularly reproduces certain forms of San social organization and that also helps to shape the Kalahari environment over time.

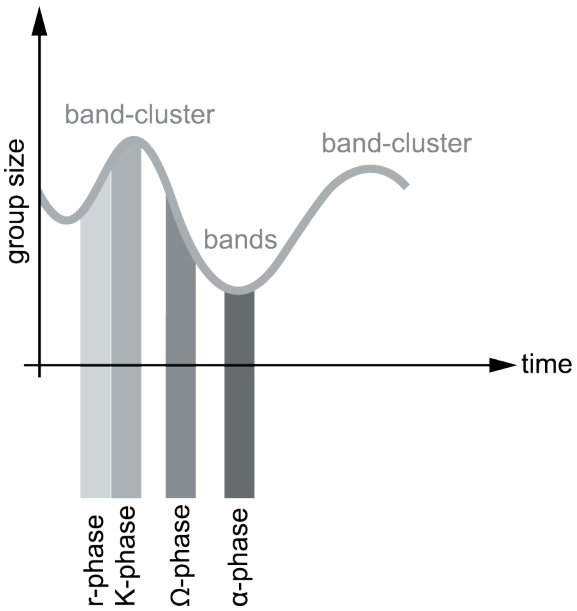

Figure 6.4: Phases of fission and fusion in longitudinal perspective.

When moving from a merely descriptive model of cycles to an explanatory or even predictive model the directly observable data do not suffice. In each ethnographic case, there is a host of ecological and anthropogenic factors involved. The reasons for fusion may be ecological (a seasonal rich resource) or socio-cultural (a ritual or group alliance event). Similarly, reasons for fission may be ecological (depletion of sources or increase of disease) or socio-cultural (conflicts) or a combination of the two. Moreover, the ethnographic record suggests that often agents may highlight ecological factors (pollution) to avoid discussing social conflicts and that the processes of fission and fusion are set off not by unbearable ecological pressure but by apparently minor changes in the environment or the social setup. At this point, a simulation of forager interaction with their environment (and with each other) promises some headway because it allows isolation and manipulation of some of these factors and to read off their effects in a longitudinal perspective (**Figure 6.4**).

In its simplest version, the simulation maps the distribution of foragers in an area of resources that continually re-grow over time but which are, of course, also depleted by the foragers themselves. The scenario can then be altered by adding different resources (with differing properties of re-growth) and different properties of foragers (depleting resources at different rates, moving at different rates etc.). The first step in increasing complexity that brings the simulation substantially closer to a realistic setting is when foragers become interactive and the simulation is designed as a multi-agent simulation

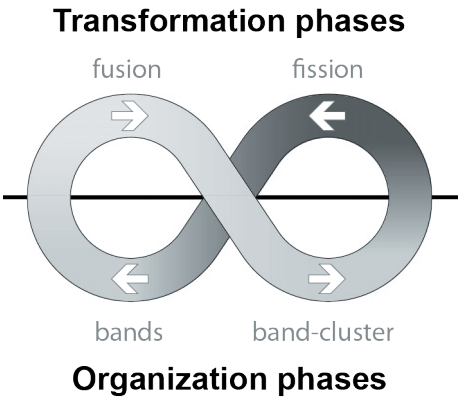

Figure 6.5: Transformation and organization phases of a cyclical model of forager mobility.

in which the action of one agent has repercussions for those of the others, not only in terms of attraction or avoidance of resource patches but also because the agents are systematically linked with one another as cooperative or competitive agents. The challenge is to integrate into the simulation the communication between agents and their particular cultural attributes and preferences. As both the simulated social and the ecological system become more realistic (i.e. with more attributes), the explanatory power of a cycle model of integrated socio-ecological systems is revealed. It allows recognition of how small changes in the overall setup may lead e over time e to considerable effects and how changes in one set of factors (for instance social factors or with regard to the climate) may have larger or smaller effects depending on the stage of the cycle in which they become effective.

Furthermore, in beginning to connect the ethnography of a forager mobility with simulation and a cyclic model, new productive questions for future research emerge that link environmental and cultural factors, such as: What are the natural changes that may trigger, or contribute to, the fission of band clusters (the omega phase)? How many places, and of what sorts, are there in a region that can afford bands (in the alpha phase)? How big is the continuous region that allows for a growing cooperation and integration of bands (in the r-phase)? What are the conditions that would link the transformation and organization phases into a cycle (**Figure 6.5**) rather than an open spiral or a simple alternation between the two ends of a spectrum?

6.3.2 Demographic cycles in the Central European Neolithic (RP, AZ - project D2)

Another application of the socio-ecological concept of adaptive cycles is being made to gain a better understanding of demographic developments in the Central European Neolithic. The study aims at investigating the interrelation between population dynamics and change in the material culture of the first farmers at different social scales.

The approach centers on the Linearbandkeramik Culture (5300-4950 cal BC) in the Lower Rhine Basin. The spatial scope is some 100-1000 km^2 and the temporal scale a few hundred years. Regarding the research questions of the CRC, the projects aim is to contribute to the questions concerning changes in population density and to the social and cultural background of migrations.

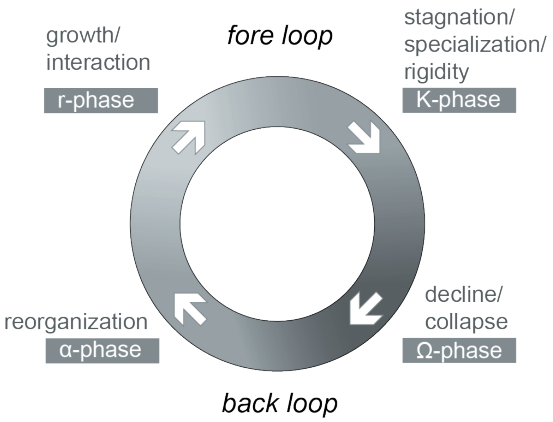

Figure 6.6: Fore loop (r- and K-phases) and back loop (a- and U-phases) of the adaptive cycle.

In this case study, the adaptive cycle concept is operationalized to describe the dynamics of an archaeological culture. Concerning the regional scale, it is suggested that the cycle fore loop is characterized by demographic growth and decreasing interaction as well as increasing specialization and rigidity at the local scale (**Figure 6.6**).

The development of the Linearbandkeramik (LBK) in the Lower Rhine Basin is summarized in

Figure 6.7. The connection between the cultural features (material culture and household size) and the concept of adaptive cycles is the reconstructed demographic trend. The demography is the independent variable against which the evolution of material culture (dependent variables) is being compared. The number of discovered longhouses per pottery style phase (1-15) is used as a demographic proxy (Zimmermann et al., 2009). Each stylistic phase corresponds to approximately 25 years. The demographic trend shows an increase in population followed by a phase of stagnation and finally a population decrease (**Figure 6.7** a).

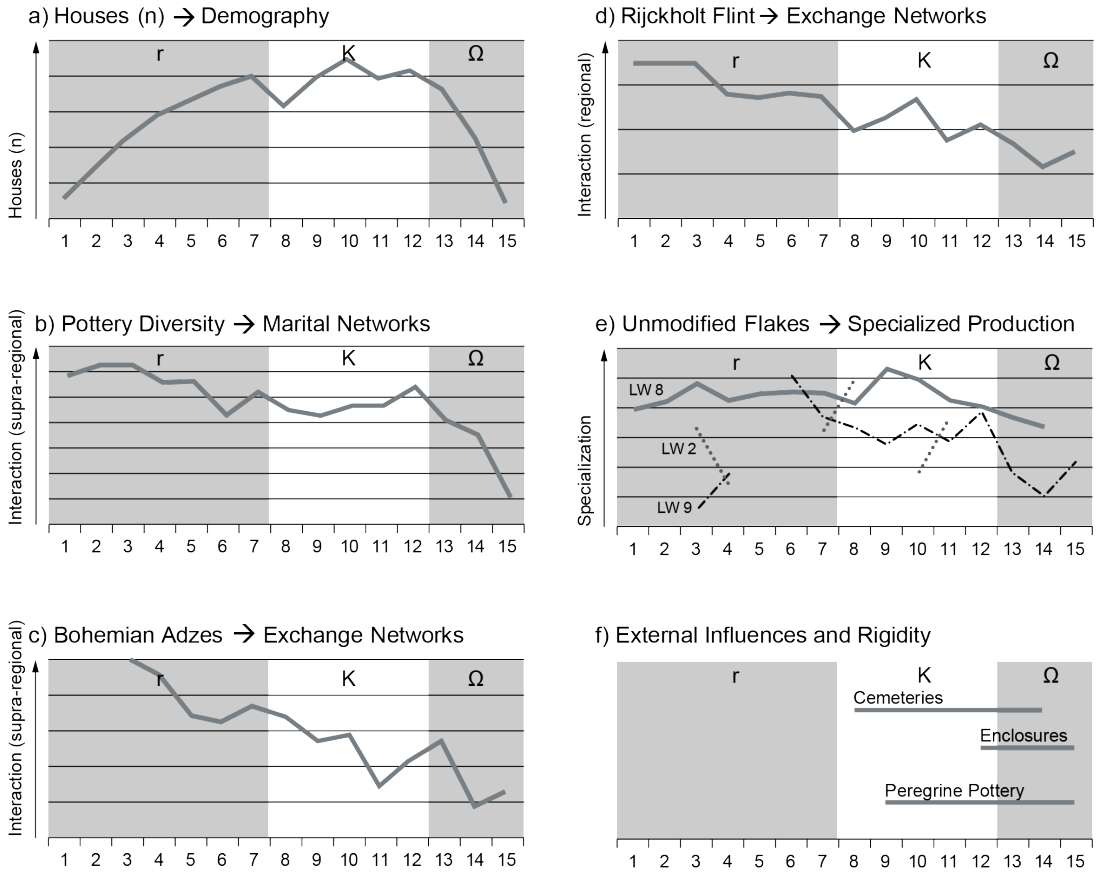

Figure 6.7: The Linearbandkeramik culture as a dynamic system passing through the growth, conservation and disturbance phases of the adaptive cycle. (a) Number of houses per pottery style phase (Zimmermann et al., 2009, Figure 6); (b) Pottery ornamentation diversity; (c) Percentage of Bohemian adzes (Nowak, 2008); (d) Percentage of Rijckholt flint in the settlement Erkelenz-Kückhoven (Mischka, 2004); (e) Percentage of unmodified flakes (Mischka, 2004); (f) Occurrence of cemeteries, ditched enclosures and peregrine pottery.

The regional diversity of pottery ornamentation can be used as a measure for the range of marital networks. Generally, it is assumed that women make the pottery and that the major mode of diffusion of pottery styles is marriage. Homogeneity is therefore an indicator for large marital networks and much interaction (under the condition of patrilocal residence as established through isotopic analysis, aDNA analyses, flint production techniques, and the distribution patterns of ceramic ornamentation). In the first phase, homogeneous pottery corresponds with a low population density and large networks. With growing population size the network size

decreases as does the pottery homogeneity. One reason could be that marital networks became smaller in this phase. But in the last phase, pottery becomes even more diverse (**Figure 6.7** b) although the population is declining.

A comparable development can be observed concerning the numbers of amphibolite adzes from Bohemia (Nowak, 2008). In the first part of the LBK these adzes are abundant (**Figure 6.7** c). They can be seen as a material indicator for communication across large distances. Then the population size increases while the number of adzes declines. Even in the last phase, when there is a population decrease and larger networks of communication would be expected, the percentage of adzes further declines. These deviations from the model concerning the pottery ornamentation and the raw material networks indicate a "collapse" or "release" in LBK society. This corresponds to what is seen in changing perspective from supraregional to regional networks. The LBK settlements are supplied with flint from Rijckholt (35-60 km distance) by an exchange network. At the end of the Linearbandkeramik, less and less Rijckholt flint is brought into the settlements (Mischka, 2004) (**Figure 6.7** d). The exchange network breaks down.

The waste of the stone artifact production is a proxy for production intensity and specialization of single settlements. In phases nine and ten, the large settlement Langweiler 8 (LW 8) produces a lot of artifacts (**Figure 6.7** e), supplying the smaller hamlets with these. In fact supraregional exchange, networks became less important in this phase. This kind of specialization occurs only in the middle of the LBK. Parallel to the developments described above, other phenomena are noticed. In the second part of the LBK for the first time cemeteries do occur (**Figure 6.7** f). Some scholars interpret them as a kind of land claim. At the end of the LBK ditched enclosures, communal monuments, are being built. The enclosures and cemeteries can be interpreted as indicator for increasing rigidity. Pottery from other archaeological cultures is also found in LBK context. Apparently, the interaction with other cultural groups is increasing again.

To conclude, the development of the Linearbandkeramik in the Lower Rhine Basin can be seen as a dynamic system that passes through different stages. Analogue to the concept of adaptive cycles, a growth, conservation and disturbance phase can be identified.

The observations of Pfyn settlement patterns at Lake Constance (3870-3500 cal BC) that are much better dated due to dendrochronological data will be interpreted in a similar way.

6.3.3 Analysis of the palaeodemography of hunters and gatherers during the Late Upper Palaeolithic in Europe (IK, AZ - project E1)

This case study investigates the demography of Upper Pleistocene hunter and gatherer populations. It is focused on the time period of the Late Upper Palaeolithic, when Europe was repopulated after the Last Glacial Maximum (20,000-12,000 cal BC). The database comprises around 1800 sites from the Magdalenian, Hamburgian, Creswellian and Epigravettian (e.g. Bocquet-Appel et al., 2005; Maier, 2012). The high-scaled level of this study deals with an area which contains from three to four million square kilometers of the European continent. A method based on GIS techniques is used to upscale archaeological data from key sites and key regions to culturally homogeneous contextual areas at larger scale (see Richter in Zimmermann

et al., 2004). The results are then related to ethnographic parameters and to ecological factors, especially the procurement of raw materials. Regarding the research questions of the CRC, the aim of the project is to investigate temporal and spatial changes in population densities and to point out the environmental factors (palaeogeography, climate, flora and fauna), which are relevant for migration processes.

The applied method is based on the GIS-calculated spatial density of sites (Thiessen Polygons, Largest Empty Circle, Interpolation with Kriging) which has already been used for the estimations of population densities of sedentary societies (Zimmermann et al., 2004). The GIS-calculated isolines enclose regions with a defined average density of sites and are taken as indicators for settlement regions. Furthermore, the procurement of raw material is a very important parameter for understanding Palaeolithic hunters and gatherers. The mapping of basic raw material catchments of single sites indicates the minimal size of seasonal or annual settlement areas, which has been used by a specific group of foragers. The settlement areas divided by the single site catchment areas result in the number of groups settled in a region (assuming a high degree of territoriality). The first analyses suggest that there are diverse settlement areas in different regions of Europe (**Figure 6.8**). For instance, in southwestern France with average distances of non-local raw material less than 100 km (e.g. Demars, 1998; Chollet and Dujardin, 2005) small and numerous single site catchments are reconstructed. This is in contrast to northwestern and Central Europe with raw material distances up to 250 km and more than 300 km, respectively (Rensink et al., 1991; Féblot-Augustins, 1997) where few and wide associated single site catchments are simulated. The different key regions are characterized by different settlement patterns and group sizes.

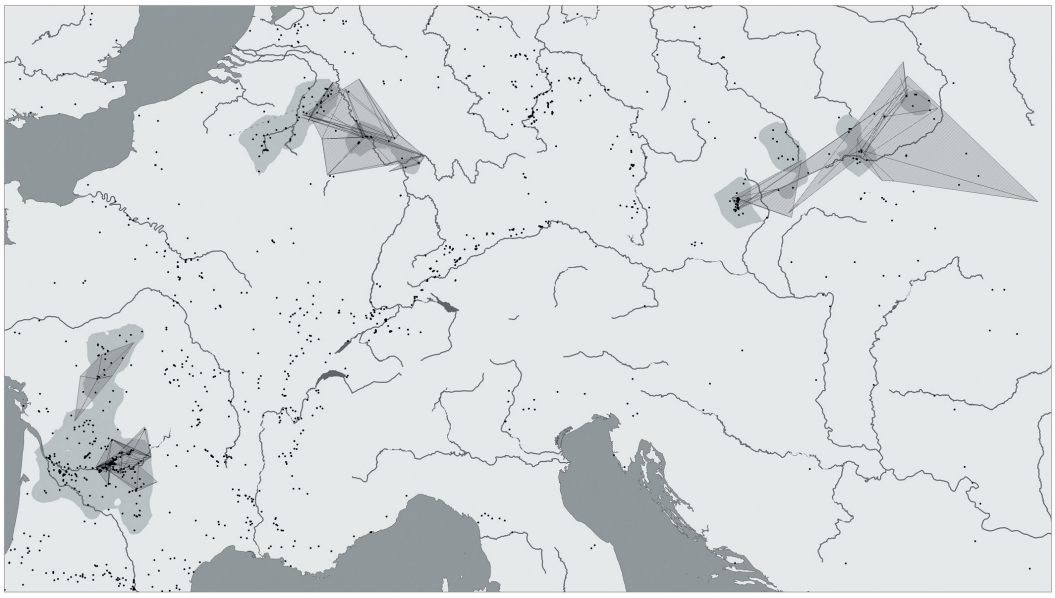

Figure 6.8: Sizes of settlement areas in different European settlement regions (settlement areas - gray polygons; raw material catchments - hatched polygons). The settlement regions of the Rhine-Meuse area and Central Europe comprise both around 20,000 km^2, southwestern France more than 45,000 km^2. The settlement region of Southwestern France comprises multiple times the number of minimal settlement areas found in Northwestern or Central Europe.

These findings can be related to data from the ethnographic record on group sizes and dynamics in hunter-gatherer societies, such as the detailed database of more than 300 hunter and gatherer groups of Binford (2001). On the basis of this accumulated ethnographic data, it seems that a band cluster mode of aggregation and a high population density can be expected for southwestern France, contrary to a lower population density to be expected for the Rhine-Meuse area and Central Europe. With reference to the concept of adaptive cycles, the situation in Central Europe shows patterns of a phase which is still in reorganization after the Glacial maximum, whereas the hunter-gatherer groups in south-western France already are at the stage of growth or conservation, so each region would represent a different phase in the adaptive cycle model (**Figure 6.9**). This leads to the question which factors are relevant for the diversity of settlement patterns in Europe. For instance, climatic parameters (continental or maritime climate), flora and fauna, the distribution of raw materials and the topography of landscape should play a role for the differences. Further- more, the time span of migration processes could possibly explain the diversity of settlement patterns in those regions.

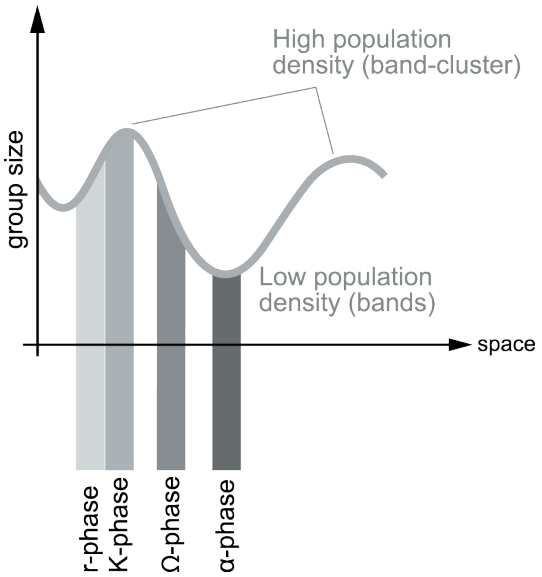

Figure 6.9: Population dynamics in terms of adaptive cycle phases.

6.3.4 The cascade model - societal reorganization by Palaeolithic hunter-gatherers as a reaction of climatic instability (MB, AP, GCW - project C1)

The cascade model introduced here and outlined in more detail elsewhere (Bradtmöller et al., 2012; **Figure 6.10**) is a concrete example of applying the idea of multiple nested adaptive cycles to an archaeological case study from the Late Pleistocene (Holling and Gunderson, 2002, p. 65). It represents the hierarchic succession of different modes of system (re-)organization (x-axis), each of which is described in terms of climatic variability (y-axis).

In this model, external agents in the form of different level of environmental instability (release impacts) are leading to vital distur-

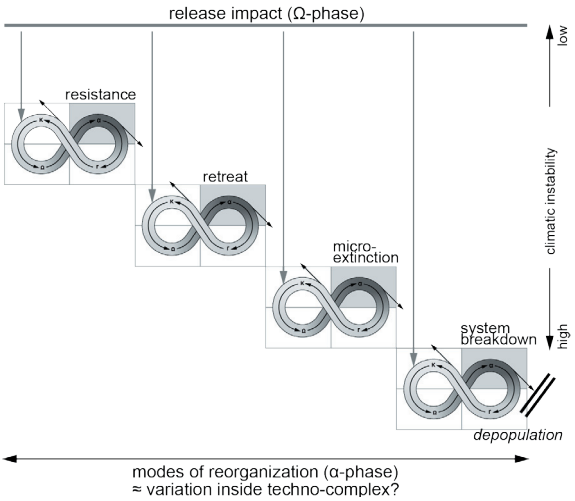

Figure 6.10: Archaeological cascade model; the adaptive cycle was mirrored along the vertical axis to underline the hierarchic succession of the modes of reorganization (adapted from Bradtmöller et al., 2012).

bances in the socio-ecological system. This climatic instability and hence the restricted tolerance of the system towards climatic stress is used as the basic release factor. As Redman and Kinzig (2003, p. 7) stated: "... we see in archaeological and historical records many cases in which a society has undergone a minor adjustment or reorganization to maintain itself. One interpretation could be that each one of these adjustments represents an entire adaptive cycle; the other is that this is an expected part of the transition to the K conservation phase or of effort to maintain the system within the K-phase".

This model, following their first interpretation, subdivided the different reactions of a social system towards increasingly extreme climates in four modes of reorganization: resistance, retreat, micro- extinction, and system breakdown. The primary mode of reorganization as reaction to climate change is here termed resistance. Basically, the subsistence patterns can be described as a cultural adjustment within the same territory. Minor disturbances can be understood as components of the normal development of the system, considering the plausible assumption that "periods of gradual change and periods of rapid transition coexist and complement one another" (Folke, 2006, p. 258). In this version of the model, it is the optimal ability to react on climatic instability. In a second step increasing environmental changes can lead to a local retreat, which corresponds to the observation that human groups may occasionally only abandon certain parts of their settlement area. Following accelerated climatic forces, the next reaction would be the micro-extinction of peripheral groups. This mode of reaction has been described by various researchers (e.g. Stiner and Kuhn, 2006; Hublin and Roebroeks, 2009). In a last step of "adaptation", the social system ends in a breakdown of the meta-population and their macro-extinction corresponding to the complete collapse of the cultural system and their underlying "remember cycle" (Redman and Kinzig, 2003).

It is important to remark here, that in each mode of reorganization the adaptive cycle is open to change in both directions (down and upwards) and is therefore able to react towards increasing as well as decreasing climatic instability, except for the irreversible breakdown of population. Changes in social structure, settlement pattern, mobility or technology are indeed highly probable as reactions towards climatic change, e.g. during Green- land stadial/interstadial transitions. One main problem in applying the research model outlined here is the limited archaeological visibility of these changes. Only a very few items in the fragmentary and coarse grained Late Pleistocene archaeological archives will be sufficiently sensitive to the climatic changes to allow the necessary model testing. The majority of Palaeolithic archives have only very low potential for detection of cultural changes. Nevertheless, there is the possibility that the different modes of reorganization may be identifiable as variations inside the established techno-complexes. Under this assumption, which remains to be tested (Schmidt et al., 2012), a complete change in techno-complex would be indicative for a complete population breakdown (e.g. Blackwell and Buck, 2003).

6.3.5 Adaptive cycles: the lake Prespa case study (FS, KP, AA, BW - project B2)

Lake Prespa, situated at 849 m a.s.l. at the border between Albania, F.Y.R. of Macedonia and Greece, is one of the oldest and largest lakes of the Balkans. The sedimentological and palynological composition of a 15 m long core taken from its central northern part was studied in order to reconstruct palaeoenvironments. Different proxies are presented by Aufgebauer et al. (2012) for the uppermost 3.2 m of core Co1215 covering roughly the last 17 ka cal BP. Titanium (Ti), as is the case with Potassium (K), is identified as a proxy of surface erosion in the catchment and clastic input into Lake Prespa. Ti is correlated to non-arboreal pollen (NAP) percentages as shown in **Figure 6.11**. Apparently, the opening of the vegetation cover intensifies soil erosion and leads to higher amounts of Ti accumulation in lake sediments. During the Late Glacial a rather open vegetation with high NAP percentages (35 to >60%) dominated in the catchment area resulting in higher erosional activity on the adjacent slopes and the accumulation of Ti rich sediments (1300-1900 XRF-counts) in the lake. During the Bölling/Alleröd interstadial a shift of the treeline and/or the thickening of forest patches are expressed as a coeval drop of NAP values to 20-30% and Ti values to 900-1300 counts. The lowering of the treeline and/or decreasing forest cover during the Younger Dryas suggest colder climate conditions. Subsequently, forest cover increases steadily in the Early Holocene until the occurrence of the 8.2 ka cooling event. The rapid and substantial increase of Ti values is accompanied by a moderate increase of NAP percentages during this 200-year cooling event. The data points to a considerable reduction of arboreal vegetation in the upper mountain belts suggesting lower annual temperatures. Mid-Holocene is characterized by significant and sustained forest expansion and a remarkable consolidation of the slopes (NAP <10%; Ti 300-700). At c. 2.7 ka cal BP, anthropogenic activity in the catchment area likely intensified leading to higher NAP percentages (around 20%) and triggering intensive soil erosion (**Figure 6.11**).

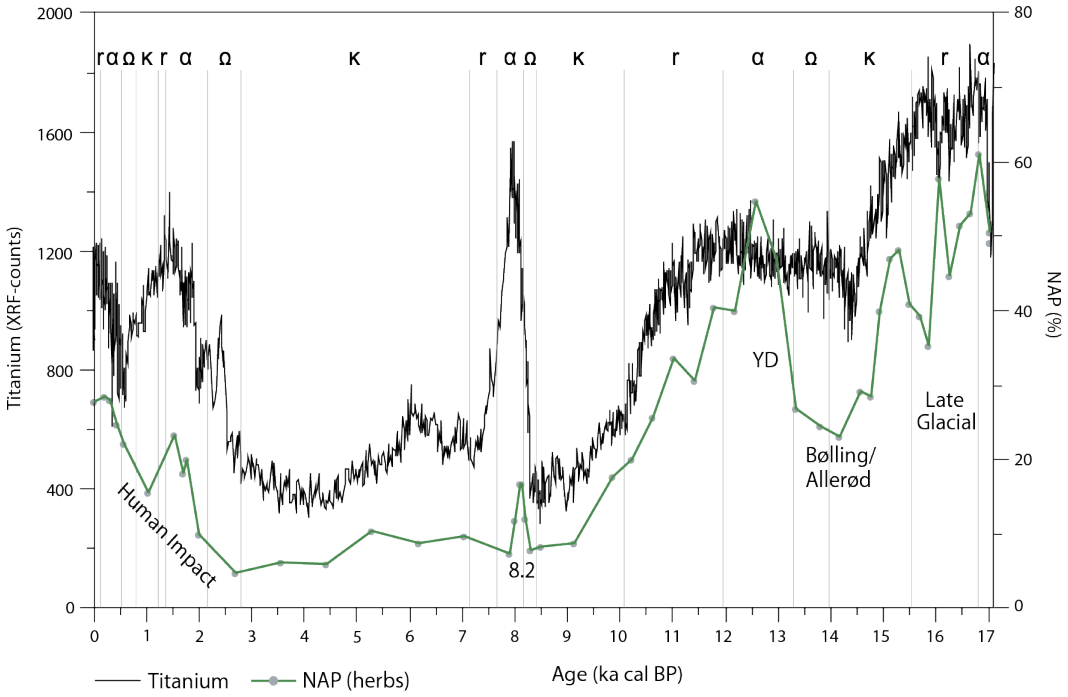

Figure 6.11: Titanium counts and non-arboreal pollen (NAP) in % of Lake Prespa.

With respect to the "adaptive cycles" (**Figure 6.1**), one could state for the Prespa catchment that there was a "steady degraded" situation (a-phase) due to the cold climate of the Late Glacial (**Figure 6.11**). A first transition (T1) to a somewhat denser vegetation cover is similar to the other transitions T2 and T3 with a very high level of clastic input still accumulating into the lake. The Holocene transitions (T4 and T5 natural driven, T6 due to human impact) produced relatively moderate amounts of soil erosion except for the 8.2 cooling event.

When human impact is limited, periods characterized by relatively open landscapes are succeeded by periods of dense forests (steady non-degraded state) following climate oscillations. In ecology, this is known as a succession cycle towards a climax under a given climate setting. Plant taxa composition of different climax states may vary, but vegetation cover is generally dense, preventing soil erosion (non-degraded state). In the adaptive cycle model this corresponds to the K-phase (**Figure 6.11**), which at Prespa for example corresponds to the period between 7 and 2.7 ka cal BP. This interval is preceded by a rapid growth phase (r), which corresponds to the transition (T5, **Figure 6.12**) from the 8.2 cooling event (a-phase) back to a relative denser forest cover. However, expansion of agricultural land following deforestation at the end of the K-phase results in increasing erosional activity impacting the lake surroundings from 2.7 ka cal BP onwards (U-phase). Soil erosion increases until about 1.5 ka cal BP (a-phase), when Ti values start to decline after the re-expansion of the forest (r-phase).

At least four complete cycles of this type can be identified for the last 17 ka cal BP in the sediments of Lake Prespa. The oldest one is incomplete starting with an a-phase, while the youngest one did not reach a K-phase yet.

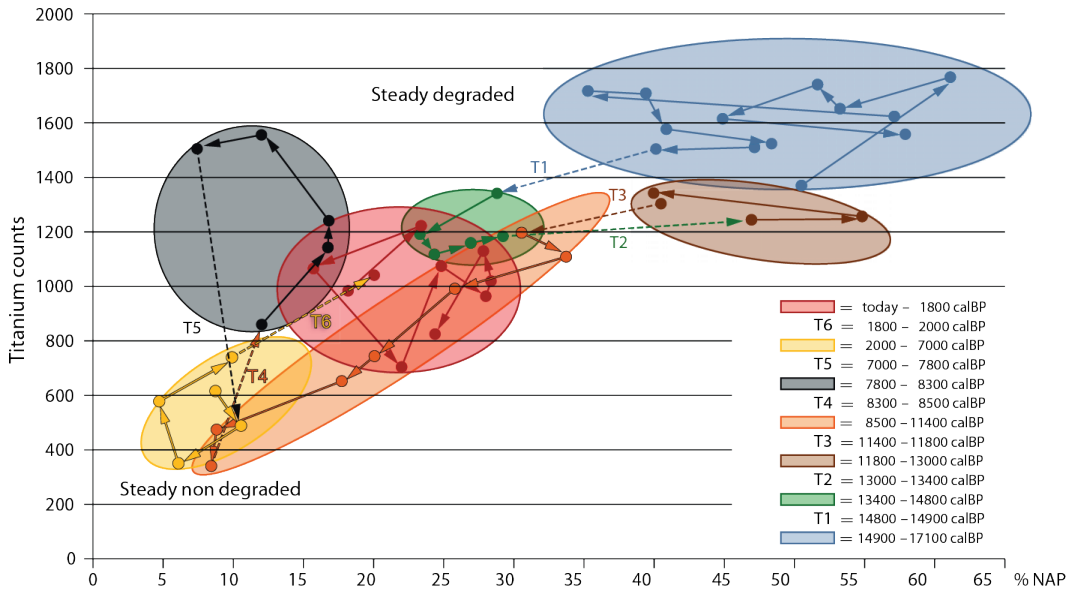

Figure 6.12: Phase diagram of erosion and disturbed land in the catchment of Lake Prespa (Titanium counts versus non-arboreal pollen in %).

6.3.6 Environmental response to agricultural land use practices in relation to sediment flux and storage in hillslope systems (MSch, TH, RD - project D3)

Archaeological and geomorphological evidences indicate a long history of human-environmental interaction throughout the Holocene. Soil degradation and soil erosion has been a central link that connects agricultural land use and sediment fluxes in geomorphological systems. However, only a few attempts have been made to apply the concepts of "resilience" and "adaptive cycles" to integrated human-geomorphological systems on Holocene time scales. In this respect, the most profound analysis of socio-ecological interactions has been accomplished by Dearing (2008) in the Erhai lake-catchment in Yunnan, SW China. Palaeoenvironmental proxy records on monsoon intensity and disturbed land (understood as external driving factors) as well as on surface soil erosion, gully erosion and flood intensity (understood as response variables) derived from lake sediments has been analyzed to understand the systems trajectory over the last 3000 years. Thresholds, alternative steady states, hysteresis and linked fast and slow processes in the lake-catchment dynamics are evident across the time scales of decennia and millennia and suggest the application of the concept of adaptive cycles to assess the socio-ecological development of the lake Erhai catchment. Based on phase diagrams Dearing (2008) identifies a macro-scale land use-erosion adaptive cycle covering the last 3000 years.

Similar to the catchments of the Erhai lake and lake Prespa, hillslope systems in Central Europe are components of socio-environmental systems on millennial time scales: Since 7500 cal BP, hillslope dynamics are affected by deforestation and agricultural land use with strong interactive and feedback mechanisms between human societies and soil resources. However, the expansion of agriculture throughout Central Europe did not occur continuously, but according to population dynamics in phases of expansion and regression of deforestation and arable land. Human disturbances therefore impacted hillslope systems in a discontinuous way.

Lake sediments provide an integrated, but buffered signal of the sediment dynamic in their associated catchments. Internal sediment redistribution along the sediment cascade from the hillslope to the lake inlet is not detectable in the lake sediment archive. Thus, colluvial sediments that are deposited in close proximity to their sources provide a more direct link between soil erosion and human impact in terms of cyclic land use phases.

An aim is to evaluate the theoretical approach presented by Dearing (2008) with respect to erosion and deposition in hillslope systems. Therefore, the focus is on colluvial deposits in Central Europe resulting from land use induced soil erosion processes since the Neolithic and stored in sediment sinks along the hillslope cascade. Temporal trajectories of soil erosion and colluviation are modeled and validated on local scales considering available data on colluvial deposits (local sediment depths, ages and volumes) and historical land use practices. The local scale model will be transferred to larger scales to quantify colluvial sediment storages in catchments of 104-105 km^2.

Four basic questions arise concerning cyclicity in sediment cascades and fluxes:

(1) What does "cyclicity" mean with respect to sediment cascades and fluxes?

(2) If hillslope sediment dynamics bear their own cyclicity, on which time scales does this cyclicity operate?

(3) Are sediment dynamics (the response variable) superimposed by the cyclicity of the land use and/or the climate system dynamics (the external driving force variable)?

(4) Do colluvial sediment storage records reveal the cyclic behavior of sedimentation, which might reflect a cyclic behavior of the land use or is the geomorphic system response complex and nonlinear (CND, complex nonlinear dynamics according to Phillips, 2003), so that sediment records cannot unequivocally be interpreted in terms of external system driving forces?

In sediment systems, the processes of reworking and removal are inherent to the hillslope systems causing sediment sinks to be recurrently (cyclically?) filled and (partially) depleted. Colluvial deposits therefore are likely to be reworked in succeeding erosion events, to be conveyed to the next sediment sink or even to be yielded to the fluvial system (Lang and Hönscheidt, 1999). As the probability of reworking increases with increasing sediment age (Telfer et al., 2010, see also "taphonomic bias" in Surovell and Brantingham, 2007; Surovell et al., 2009) the interpretation of the sediment record may underestimate external driving forces, especially those occurring in older periods (e.g. Neolithic land use). The recurrent reworking of sediments or "cyclicity" in the sediment system may thus leave a stratigraphical record concealing the magnitude and frequency of external driving forces.

In a previous study Hoffmann et al. (2008) analyzed available empirical data on colluvial, alluvial and channel bed ages from the Rhine catchment. Relative probability functions of the sediment ages should reveal phases of increased geomorphic activity on a regional scale (**Figure 6.13**). Comparison with independent palaeohydrological indicators and population data yields a changing significance of climate and population dynamics in terms of external driving forces of the fluvial system. The time series in **Figure 6.13** raises the question whether the sequence of geomorphic activity and stability follows a system trajectory which can be explained in terms of adaptive cycles and thus represents a kind of cyclicity in the geomorphic system that can be related to cyclic changes in the socio-cultural system.

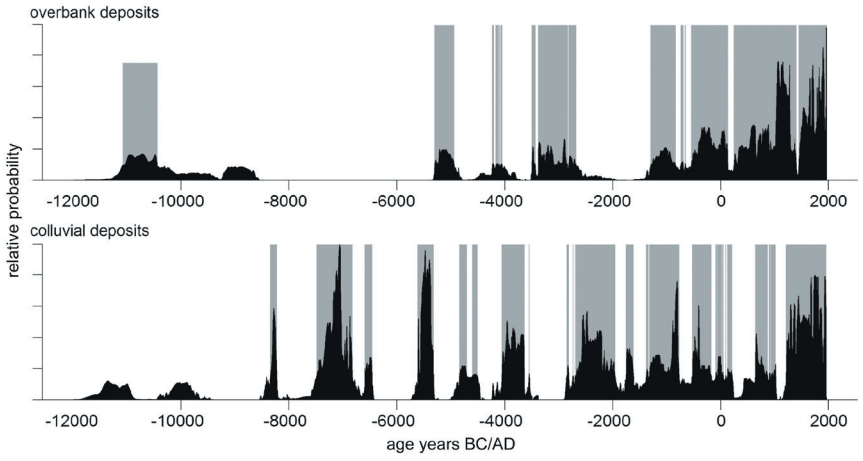

Figure 6.13: Cumulative Probability Functions (CPF) of ^{14}C ages. 51 overbank ages (top) and 62 slope ages (below) reflecting differential activities of overflow sedimentation and sediment flux at the hillslope scale. Gray shaded areas mark phases where the CPF is larger than the mean probability of the corresponding CPF (modified after Hoffmann et al., 2008).

Cyclicity in a coupled hillslope-land use system in Central Europe on a time scale of a cultural period is suggested in a simplified form in **Figure 6.14**. Beginning colonization of the hillslope and soils is associated with forest clearing, first agricultural land use and soil erosion (r-phase). The resilience of the hillslope/soils is assumed to be high in this stage as soils are still well developed and the extension of cultivated areas is low. Increasing population densities necessitates intensification of land use and cultivated areas are extended causing an increase of soil erosion rates and soil degradation (K-phase). During this phase the resilience of the hillslope/soils is reduced expressed by degrading soil profiles, low nutrient status and wide spread open land. Severe storm events and/or gradually progressing soil erosion may exceed thresholds that are associated with severe soil degradation (U-phase). The depletion of the soil resources may result in a collapse of the cultural period, land abandonment and subsequent reforestation and restabilization of hillslopes and soils (a-phase) until a new colonization phase begins.

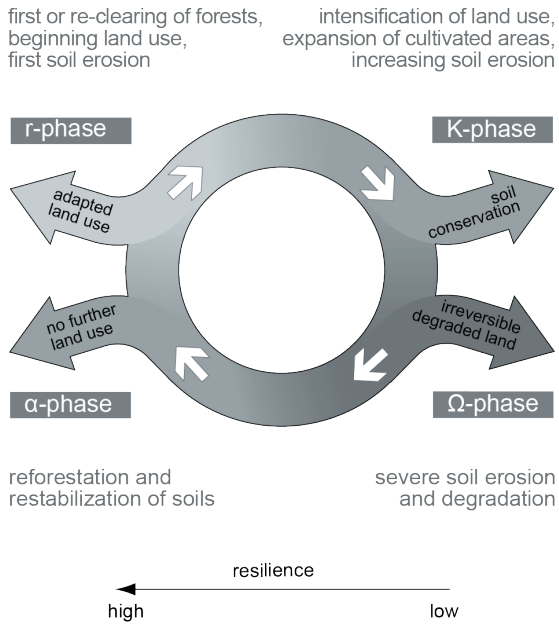

Figure 6.14: Hypothetical adaptive cycle of the coupled hillslope-land use system in terms of hillslope and soil stability, and resilience.

In fact, different exits are conceivable, which allow a transition to an alternative cycle. Another cycle might be entered by adapted land use (e.g. soil conservation) or an irreversible soil degradation (gully erosion), which is not arable anymore even after reforestation. An alternative exit might be that hillslopes are simply not recolonized after reforestation because of cultural reasons.

While this adaptive cycle is applicable to single cultural periods spanning approximately 500-1500 years (meso-scale), a macro- scale cycle might be identified on a Quaternary time scale. This long-term cycle may have been started approximately 130,000 years ago (r-phase) and currently reached the K-phase with an ever increasing pressure of human land use activity and associated degradation of the world soils. Understanding short-term cycles of single cultural periods may help to predict possible future scenarios of this long-term cycle (collapse or sustainable soil use). Thus it needs to be tested if cyclicity is present in the hillslope dynamic at least on a macro- and meso-time scale. Therefore a quantification of soil erosion and the reconstruction of the colluviation for different cultural periods during the Holocene is urgently needed.

Several studies (Lang and Wagner, 1996; Dreibrodt and Bork, 2005; Fuchs et al., 2010; Tinapp et al., 2008; Reiß et al., 2009; Fischer, 2010, etc.) dated colluvial layers to the Neolithic period by ^{14}C or OSL-dating methods. Disregarding possible dating uncertainties these sediment ages indicate that soil erosion already occurred under the influence of Neolithic land use practices.

With respect to the resilience concept it has to be asked whether the colluvial deposits dated to the Neolithic period as well as the Neolithic peak of the relative probability of colluvial ages (**Figure 6.13**) give evidence for an already low-resilient state of the hillslope systems during initial agricultural impacts. The problem is then whether early land use impacts already forced threshold transgression for marked soil erosion processes.

The intensity of prehistoric soil erosion has not been quantified so far and the cumulative probability function curves only represent relative changes of sedimentation without information about absolute soil erosion or sedimentation rates. However, the quantification of prehistoric soil erosion under consideration of reworking processes and a critical assessment of sediment ages will be one valuable step towards developing and testing hypotheses about the dynamic of hillslope systems in Central Europe in terms of integrated socio-ecological systems and adaptive cyclicity.

6.4 Time series, spatial scales and models

6.4.1 Where do we come from?

Disciplinary work of the last century could be characterized reductionistically (and somewhat mischievously) in the following way:

- Archaeologists have been working mostly descriptive, driven by a fascination for dating.
- Geoscientists have been crude environmental determinists, driven by a fascination for simple causalities.
- Anthropologists have been idiographically describing special cases, driven by a fascination for variability.

These caricatured approaches cannot answer key questions of the CRC. Questions such as "Which role did the social, cultural, and technical development play for migration?" and "What relevance do environmental and anthropogenic factors have for the population growth and migration processes in space and time?" clearly demands a more integrative approach.

Researchers in each CRC project continue to collect data specific for their respective disciplines: Some collect high resolution time series of proxies for climatic developments, some produce evidence which will appear as dated points at large-scale distribution maps, and others present large-scale distribution maps where points are already transformed into areas. Interdisciplinary discussions deal with issues such as who produces which proxies and for which area and time these are representative, and which intentions of interpretation inform the compilation of these databases. While this is the necessary groundwork for any joint enterprise, Collaborative Research Centres by their nature provide the opportunity to go beyond these basics.

6.4.2 Where are we heading to?

For the future, therefore, it is important to begin early on with exchanges about how to correlate disciplinary data relating to specific time series, point distribution maps, and area distribution

maps. This is critical for getting closer to answering the questions concerning the way in which culture-environment interaction is integrated, questions that the CRC has set for itself and that are at the cross-roads of a number of disciplines. Models are needed for understanding migration and mobility that integrate information from different scales. For archaeologists and anthropologists it is not sufficient to argue in terms of an idealized typology of logistic and residential mobility since these refer to processes in a scale of a few hundred square kilometers only whereas the dispersal of man out of Africa is a process of a much larger scale. Inland migration during the Neolithic is a process on yet another scale. For geographers, geologists and climatologists it is not sufficient to argue in terms of very long-term changes or very short-term changes since these often allow no recognition of human impact and human response whereas the dispersal of man out of Africa or within one of the possible migration corridors was not an automatic process where choice and agency played no role.

This paper has suggested one possibility to develop a comprehensive model, adopting ideas from the literature about adaptive cycles which hold some attraction in this regard. At this stage, there is a promising route ahead and future work will show how productive this path turns out to be. The authors expect that this model will prove to be the most useful one for an interdisciplinary approach that can help to answer key questions of the CRC and beyond. There may also be possibilities of combining the adaptive cycle model with other existing models. Here are two examples of existing models where we can already see how including the adaptive cycle model would yield considerable conceptual advantages:

The "internal African frontier model" was developed to explain the spread and reproduction of African agropastoralist polities before colonization, both sub-continental dispersions such as the Bantu expansion as well as local movements (Kopytoff, 1987, p. 7). It is problematic to extrapolate this model into the forager past because this would mean making some unwarranted assumptions about the socio-cultural dynamics behind these movements. There is nothing to indicate that early humans did have the plan to occupy Europe or that they had the sense of a moving frontier of occupation "out of Africa" found in other, later processes of human migration. While "the internal African frontier" like other frontier notions of gradual exploration suggests that subjects themselves conceptualize and plan their movement in terms of occupying new land, current foragers (and Palaeolithic foragers probably even less so) are not driven by a map-like representation of their movements as occupying two- dimensional space. Rather, their movements are informed by the perception of attractive (or repulsive) qualities of the landscape in close relation to the way in which the social group and the individual body is perceived as gaining or losing strength, as expanding or diminishing in volume, and not as expanding across a flat surface. While their own conception is not one of nature versus culture or of the need to overcome distance in order to get from one place to another, their movements still have effects that can be detected through map-like models, at least in part. There are indications, therefore, that only a model that allows description of partially independent dynamics that are at the same time nested in one another will be appropriate for dealing with the systemic complexities.

The "wave of advance model", as a second example, was developed to explain the expansion of the Neolithic from the Middle East to Europe (Ammerman and Cavalli-Sforza, 1971). It

is not advisable to apply this model to the dispersal of humans out of Africa because it would include some unwarranted assumptions about climatic determinism. The model is applicable for the Neolithic at a continental scale considering several thousand years. After formation of the Neolithic in the Near East something happens and the wave of farming economy advances slowly with a speed of one or 2 km per year. After some time in the whole of Europe, a Neolithic economy was adopted. At a continental scale (some million square kilometers), the model seems to be sufficiently valid. However, at another scale of some hundred thousand square kilometers, which allows distinguishing for example Southeast and Central Europe, two important deviations from the model emerge. Firstly, the expansion of the Neolithic economy is no continuous process at this scale. After exceeding a threshold value in an area already settled for some hundred years, many small new areas extending some hundred kilometers are settled apparently at one and the same moment in time. Secondly, not all suitable areas are used in this stretch of land, neither at the beginning nor in the end of the farming economy. Instead, land use seems to oscillate in cycles between small areas. One possible explanation could be that in selected areas demographic growth at the beginning exceeds carrying capacity causing abandonment during the next period. Only after some hundred years of oscillations, a threshold value is once again reached and a new expansion phase begins. In order to simplify the existing model, consider the threshold value as a limit in population density and of carrying capacity as a limit of food producing capacity e however, it might be more complicated than that. The existing wave of advance model is not suited for accounting for a host of different situations varying along the scales of time and spatial expansion.

It is for these reasons that the adaptive cycle model seems particularly attractive. Nested cycles with their phases of growth, conservation, distortion and reorganization that characterize the adaptive cycle model are a pattern that is sufficiently general to be found in archaeological and ethnological observations at different scales without being limited to regions in the frontier region of Neolithic expansion or indeed to the notion of a frontier region at all. The adaptive cycle model, in its adaptation as outlined in this paper, is attractive in particular because it allows introduction of the internal dynamics of one domain, for example of the social domain, into an analysis that covers very different domains and different data sets without reducing one domain to the other. For example, emigration is a typical feature of the U (release)-phase of the adaptive cycle while immigration is encountered in the a- or r-phase. The model allows incorporating the environmental and cultural dimensions of "Culture-Environment Interaction and Human Mobility in the Late Quaternary" without falling back into determinism and without being paralyzed by a host of disconnected details.

6.5 Conclusion

This article has brought together results which are rarely, if ever, treated together in a single perspective: the ethnography of forager decisions on moving camp that considers different settlements and groups not as "types" but as instances of a larger dynamic of fission and fusion (Section 6.3.1), the archaeology of demography, exchange and marital networks in Linearbandkeramik and Pfyn settlements in the Central European Neolithic that show a succession of

phases of growth, conservation and disturbance (Section 6.3.2), the palaeodemography of the Late Upper Palaeolithic that suggests that two patterns found in different parts of Europe may in fact be considered to be different phases of an underlying dynamic model (Section 6.3.3), the archaeological synopsis of palaeolithic archives as representing different modes of reorganization that may be variations explained in terms of nested developmental cycles with different outcomes depending on the way they are interlocked in any particular setting (Section 6.3.4), the palaeoenvironmental record of Lake Prespa in the Balkans which can be read in terms of an adaptive cycle model of land use practices and the corresponding environmental responses (Section 6.3.5), and finally geomorphological evidence on colluviation which suggests a long-term cyclical dynamic that involves both anthropogenic and environmental factors within a single system (Section 6.3.6). Despite the huge spread in terms of spatial and temporal scales, all these case studies can be successfully read in terms of an adaptive cycle model as it was initially suggested by Gunderson and Holling (2002) and as it has been enriched further in this paper. Moreover, the application of the model allows connection of the data from these cases that were hitherto disconnected. It promises a comprehensive picture whereby data from very diverse sources (ethnography, Palaeolithic, Neolithic, palaeodemography, palaeoenvironment and geomorphology) can be pooled and tied into a unified model understanding processes of human-environment interaction and (in due course) working towards a better picture of human mobility more generally and the human expansion out of Africa more specifically. It should be emphasized that this unified model does not require ranking or weighting different factors across all scales, as the model allows (and in fact presupposes) that different factors may have different impacts at different scales and in different phases of what constitutes a large complex system.

All models of systems, including adaptive cycle models, face the problem of defining the boundaries of the system under consideration, the "environment" that conceptually provides the system with its boundedness. An adaptive cycle model as it is suggested here does not solve this general problem of systemic representations but it, nevertheless, provides two major advances: Firstly, the adaptive cycle model does not require a strict separation of "the natural system" from "the cultural system", which has increasingly been criticized as an unproductive and even distortive separation. Instead, it is understood as a "hybrid system" integrating social and environmental aspects (Weichhart, 2007, p. 948). For instance, in the first case study above (see Section 6.3.1) the system is not "the Kalahari environment" or "the San culture" but the integrated human-environment interaction that involves both. Secondly, the adaptive cycle model explicitly is a scale model with levels being mutually constitutive. These various scale levels (ecosystem levels, cultural populations and their subgroups) have sufficient continuity across phases of a cycle (even though not remaining the same) to identify them as constituting a system. However, the model does not require establishing unchanging system boundaries at the onset of research. Instead, it allows redrawing of boundaries of systems as patterns emerge that integrate entities that were previously considered to be set apart.

It is unrealistic that this model, or any other particular model, will allow an understanding of human behavior in every individual complex case. Features such as non-linearity, multifactorial relations, scale dependency, and time-lags before effects become visible make the analysis much

more difficult. However, what the model could help to achieve is an ability to distinguish those features and processes that are predictable from those that require other and new methods for tackling the complexity of individual cases.

In other words, the model proposed here is not so much a "spitting image", a model of human-environment interaction and of human mobility, a simple summary of the evidence. Rather, it is a model for understanding the processes for which evidence is found in very different archives (be they ethnographic, artifactual or sedimentary) but evidence that requires a model for reconstructing the dynamic that produced it in the first place. It is in the nature of such an enterprise that the model will change as more evidence is collected, but from the start, and even though it may initially be incomplete, it can play a critical role in recognizing relevant evidence and in directing efforts to collect further data. Consequently, the dynamic model of adaptive cycles as applied here is considered, not as the consummation of research, but as a much needed stimulus for multidisciplinary enterprises directed at some of the most complex research questions that are currently being investigated.

6.6 Acknowledgments

This article is the result of research and cooperation within the Collaborative Research Centre 806 (Sonderforschungsbereich 806) funded by the Deutsche Forschungsgemeinschaft (DFG, German Research Council). All authors would like to thank the DFG for funding this research. Individual authors and projects that relate to the various case studies are indicated with abbreviations in the parenthesis that follow the respective sub-headings. An overview of the CRC research projects can be gained by consulting the webpage www.sfb806.uni-koeln.de.

6.7 References

Ammerman, A.J., Cavalli-Sforza, L.L., 1971. Measuring the rate of spread of early farming in Europe. Man 6, 674-688.

Aufgebauer, A., Panagiotopoulos, K., Wagner, B., Schaebitz, F., Viehberg, F.A., Vogel, H., Zanchetta, G., Sulpizio, R., Leng, M.J., Damaschke, M., 2012. Climate and environmental change in the Balkans over the last 17 ka recorded in sediments from Lake Prespa (Albania/F.Y.R. of Macedonia/Greece). Quaternary International 274, 122-135.

Barnard, A., 1992. Hunters and Herders of Southern Africa. A Comparative Ethnography of the Khoisan Peoples. Cambridge University Press, Cambridge.

Binford, L.R., 2001. Constructing Frames of Reference. An Analytical Method for Archaeological Theory Building Using Hunter-gatherer and Environmental Data Sets. University of California Press, Berkeley, Los Angeles.

Blackwell, P.G., Buck, C.E., 2003. The Late Glacial human reoccupation of north-western Europe: new approaches to space-time modeling. Antiquity 77, 232-240.

Bocquet-Appel, J.-P., Demars, P.-Y., Noiret, L., Dobrowsky, D., 2005. Estimates of Upper Palaeolithic meta-population size in Europe from archaeological data. Journal of Archaeological Science 32, 1656-1668.

Bradtmöller, M., Pastoors, A., Weninger, B., Weniger, G.-Ch., 2012. The repeated replacement model - rapid climate change and population dynamics in Upper Pleistocene Europe. Quaternary International 247, 38-49.

Chollet, A., Dujardin, V., 2005. La grotte du Bois-Ragot à Gouex (Vienne). Mag- dalénien et Azilien. Essais sur les hommes et leur environnement. In: Mémoires de la Société Préhistorique Française, vol. 38. La Simarre, Joué-lès-Tours.

Constanza, R., Graumlich, L.J., Steffen, W. (Eds.), 2007. Sustainability or Collapse? An Integrated History and Future of People on Earth. Dahlem Workshop Report 96. MIT Press, Cambridge, MA.

Dearing, J.A., 2008. Landscape change and resilience theory: a palaeoenvironmental assessment from Yunnan, SW China. The Holocene 18 (1), 117-127.

Demars, P.-Y., 1998. Circulation des silex dans le nord de l'Aquitaine au Paléolithique Supérieur. L'occupation de l'espace par les derniers chasseurs-cueilluers. Gallia Préhistoire 40, 1-28.

Dreibrodt, S., Bork, H.-R., 2005. Historical soil erosion and landscape development at Lake Belau (North Germany) - a comparison of colluvial deposits and lake sediments. Zeitschrift für Geomorphologie NF (Suppl. 139), 101-128.

Féblot-Augustins, J., 1997. La circulation des matières premières au Paléolithique. In: Etudes et recherches archéologiques de l'Université de Liège (ERAUL), vol. 75. Université de Liège, Liège.

Fischer, P., 2010. Zur mittel- und jungquartären Relief- und Bodenentwicklung der nordwestlichen Kölner Bucht - Detailuntersuchungen der lössbedeckten Mittelterrassenlandschaft. Ph.D. Thesis, University of Cologne, Germany.

Folke, C., 2006. Resilience: the emergence of a perspective for social-ecological systems analyses. Global Environmental Change 16, 253-267.

Fuchs, M., Fischer, M., Raverman, R., 2010. Colluvial and alluvial sediment archives temporally resolved by OSL dating: implications for reconstructing soil erosion. Quaternary Geochronology 5, 269-273.

Gunderson, L.H., Holling, C.S., 2002. Panarchy. Understanding Transformations in Human and Natural Systems. Island Press, Washington, D.C.

Hoffmann, T., Lang, A., Dikau, R., 2008. Holocene river activity: analysing 14C-dated fluvial and colluvial sediments from Germany. Quaternary Science Reviews 27, 2031-2040.

Holling, C.S., Gunderson, L.H., 2002. Resilience and adaptive cycles. In: Gunderson, L.H., Holling, C.S. (Eds.), Panarchy: Understanding Transformations in Human and Natural Systems. Island Press, Washington, D.C.

Hublin, J.J., Roebroeks, W., 2009. Ebb and flow or regional extinctions? On the character of Neandertal occupation of northern environments. Comptes Rendus Palevol 8, 503-509.

Kelly, R.L., 1995. The Foraging Spectrum. Diversity in Hunter-gatherer Lifeways. Smithsonian Institution Press, Washington.

Kopytoff, I. (Ed.), 1987. The African Frontier. The reproduction of Traditional African Societies Bloomington.

Lang, A., Hönscheidt, S., 1999. Age and source of colluvial sediments at Vaihingen-Enz, Germany. Catena 38, 89-107.

Lang, A., Wagner, G.A., 1996. Infrared stimulated luminescence dating of archaeosediments. Archaeometry 38 (1), 129-141.

Maier, A., 2012. Variability and regional diversity in the Central European Magdalenian. Doctoral Thesis, Institute of Prehistoric Archaeology, University of Cologne.

Mischka, D., 2004. Zentraler Ort oder Nebensiedlung? Die Feinchronologie der Grundformspektren des bandkeramischen Fundplatzes Kückhoven im Vergleich. In: Der bandkeramische Siedlungsplatz von Erkelenz-Kückhoven I. Untersuchungen zum bandkeramischen Siedlungsplatz Erkelenz-Kückhoven, Kreis Heinsberg (Grabungskampagnen 1989e1994). Rheinische Ausgrabungen 54. Verlag Philipp von Zabern, Mainz, pp. 537-594.

Nowak, K., 2008. Zur räumlichen Verteilung von Dechselklingen aus Aktinolith- Hornblendschiefer in der Linearbandkeramik. Archäologische Informationen 31 (1&2), 25-32.

Phillips, J.D., 2003. Sources of nonlinearity and complexity in geomorphic systems. Progress in Physical Geography 27 (1), 1-23.

Redman, C.L., Kinzig, A.P., 2003. Resilience of past landscapes: resilience theory, society, and longue durée. Conservation Ecology 7 (1), 14.

Redman, C.L., Crumley, C.L., Hassan, F.A., Hole, F., Morais, J., Riedel, F., Scarborough, V.L., Tainter, J.A., Turchin, P., Yasuda, Y., 2007. Group report: millennial perspectives on the dynamic interaction of climate, people, and resources. In: Costanza, R., Graumlich, L.J., Steffen, W. (Eds.), Sustainability or Collapse? An Integrated History and Future of People on Earth. MIT Press, Cambridge, MA, London, pp. 115-148.

Reiß, S., Dreibrodt, S., Lubos, C.C.M., Bork, H.-R., 2009. Land use history and historical soil erosion at Albersdorf (northern Germany) e ceased agricultural land use after the pre-historical period. Catena 77, 107-118.

Rensink, E., Kolen, J., Spieksma, A., 1991. Patterns of raw material distribution in the Upper Pleistocene of Northwestern and Central Europe. In: Montet-White, A., Holen, S. (Eds.), Raw Material Economies Among Prehistoric Hunter-Gatherers. Publications in Anthropology 19. University of Kansas Library, Lawrence, pp. 141-159.

Resilience Alliance, 2011. Retrieved 21.06.11 from http://www.resalliance.org/index.php/adaptive_cycle.

Schmidt, I., Bradtmöller, M., Kehl, M., Pastoors, A., Tafelmaier, Y., Weninger, B., Weniger, G.-C., 2012. Rapid climate change and variability of settlement patterns in Iberia during the Late Pleistocene. Quaternary International 274, 179-204.

Stiner, M.C., Kuhn, S.L., 2006. Changes in the 'connectedness' and resilience of Paleolithic societies in Mediterranean ecosystems. Human Ecology 34, 693-712.

Surovell, T.A., Brantingham, P.J., 2007. A note on the use of temporal frequency distributions in studies of prehistoric demography. Journal of Archaeological Science 34, 1868-1877.

Surovell, T.A., Finley, J.B., Smith, G.M., Brantingham, P.J., Kelly, R., 2009. Correcting temporal frequency distributions for taphonomic bias. Journal of Archaeological Science 36, 1715-1724.

Telfer, M.W., Bailey, R.M., Burrough, S.L., Stone, A.E.S., Thomas, D.S.G., Wiggs, G.S.F., 2010. Understanding linear dune chronologies: insights from a simple accumulation model. Geomorphology 120, 195-208.

Tinapp, C., Meller, H., Baumhauer, R., 2008. Holocene accumulation of colluvial and alluvial sediments in the Weiße Elster river valley in Saxony, Germany. Archaeometry 50 (4), 696-709.

Weichhart, P., 2007. Humanökologie. In: Gebhardt, H., Glaser, R., Radtke, U., Reuber, P. (Eds.), Geographie. Physische Geographie und Humangeographie. Elsvier GmbH, Spektrum Akademischer Verlag, München, pp. 941-949.

Widlok, T., 2008. Local experts - expert locals: a comparative perspective on biodiversity and environmental knowledge systems in Australia and Namibia. In: Casimir, M. (Ed.), Culture and the Changing Environment. Berghahn Books, New York, Oxford, pp. 351-381.

Zimmermann, A., Richter, J., Frank, Th., Wendt, K.P., 2004. Landschaftsarchäologie II - Überlegungen zu Prinzipien einer Landschaftsarchäologie. Bericht der Römisch-Germanischen Kommission 85, 37-95.

Zimmermann, A., Hilpert, J., Wendt, K.P., 2009. Estimations of population density for selected periods between the Neolithic and AD 1800. In: Steel, J., Shennan, S. (Eds.), Demography and Cultural Macroevolution. Special Issue Human Biology, vol. 81, pp. 357-380.

VII Exploratory analyses and microcharcoal results

7.1 Microscopic Charcoal

Charred particles with a length greater than 10 µm were counted in pollen slides. Microscopic charcoal concentrations were calculated with the addition of *Lycopodium* tablets with a known amount of spores (Stockmarr, 1971). The microscopic charcoal concentration curve (**Figure 7.1**) shows relatively stable and low values throughout the Last Glacial with some peaks recorded in MIS 5 (P-9, P-8b) and a gradual increase of microcharcoal values during the Lateglacial transition (P-2). In comparison, elevated concentrations (and accumulation rates) and some pronounced charcoal peaks are registered within the Holocene. Microscopic charcoal accumulation rates over the last 17 ka are presented and discussed in Section **3.5** (see also **Figure 3.7**).

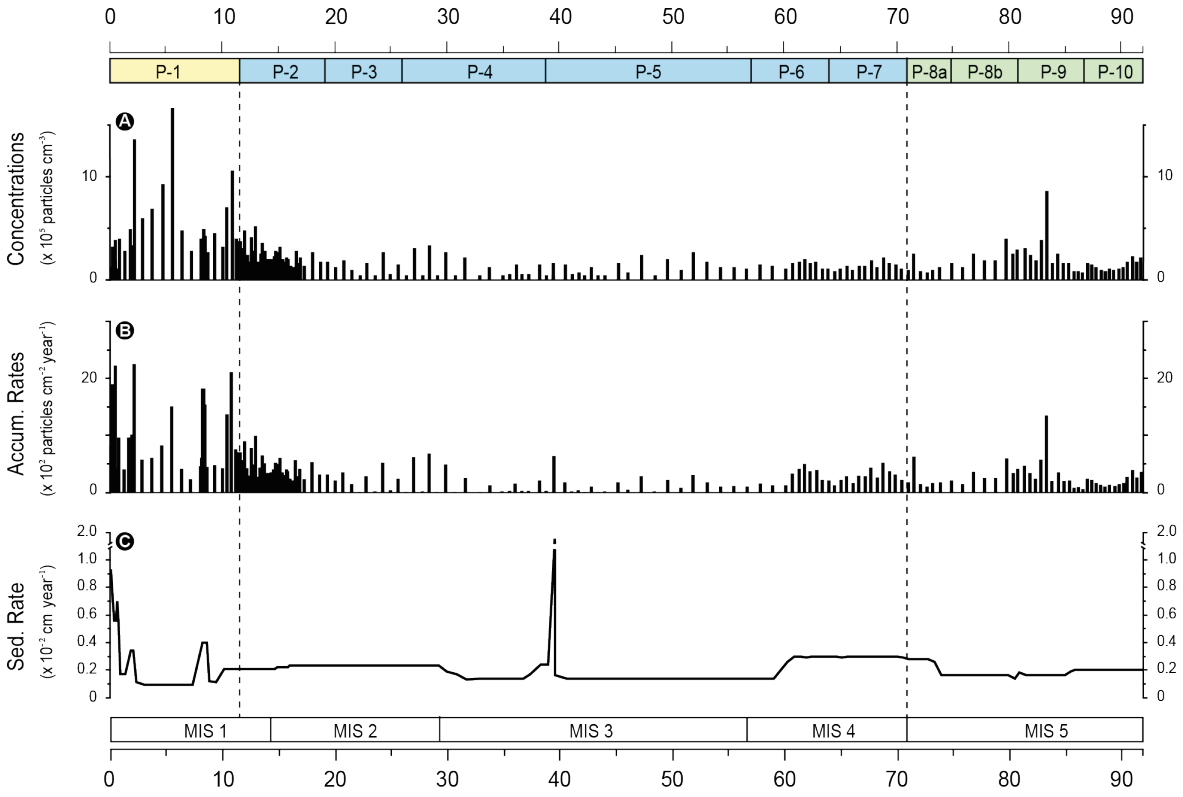

Figure 7.1: Microcharcoal fragment concentrations and accumulation rates in Co1215. Notice the accentuated peaks in the microcharcoal accumulation rate curve (b) within intervals of increased sedimentation rate (c). The Holocene (yellow) and MIS 5 (green) are separated by dashed lines from the interval including MIS 4, MIS 3, MIS 2 and the Lateglacial transition (blue).

7.2 Numerical analyses

7.2.1 Box plots

Exploratory data analysis was performed on selected variables (percentages and concentrations) or groups (groups are defined in Section **2.4.2**; the temperate group includes *Quercus* spp., the steppic group

comprises *Artemisia* and Chenopodiaceae) using PAST (Hammer et al., 2001), in order to visualize the dispersion and skewness of the data (**Figure 7.2**). Zonation of pollen percentage data was performed on selected species (i.e. taxa exceeding the 2% threshold) by agglomeration using stratigraphically constrained cluster analysis (Grimm, 1987; see also Section **5.4.2**). Subsequently, the zones identified with CONISS were grouped into three major intervals, namely the Holocene, the MIS 2-4, and the MIS 5.

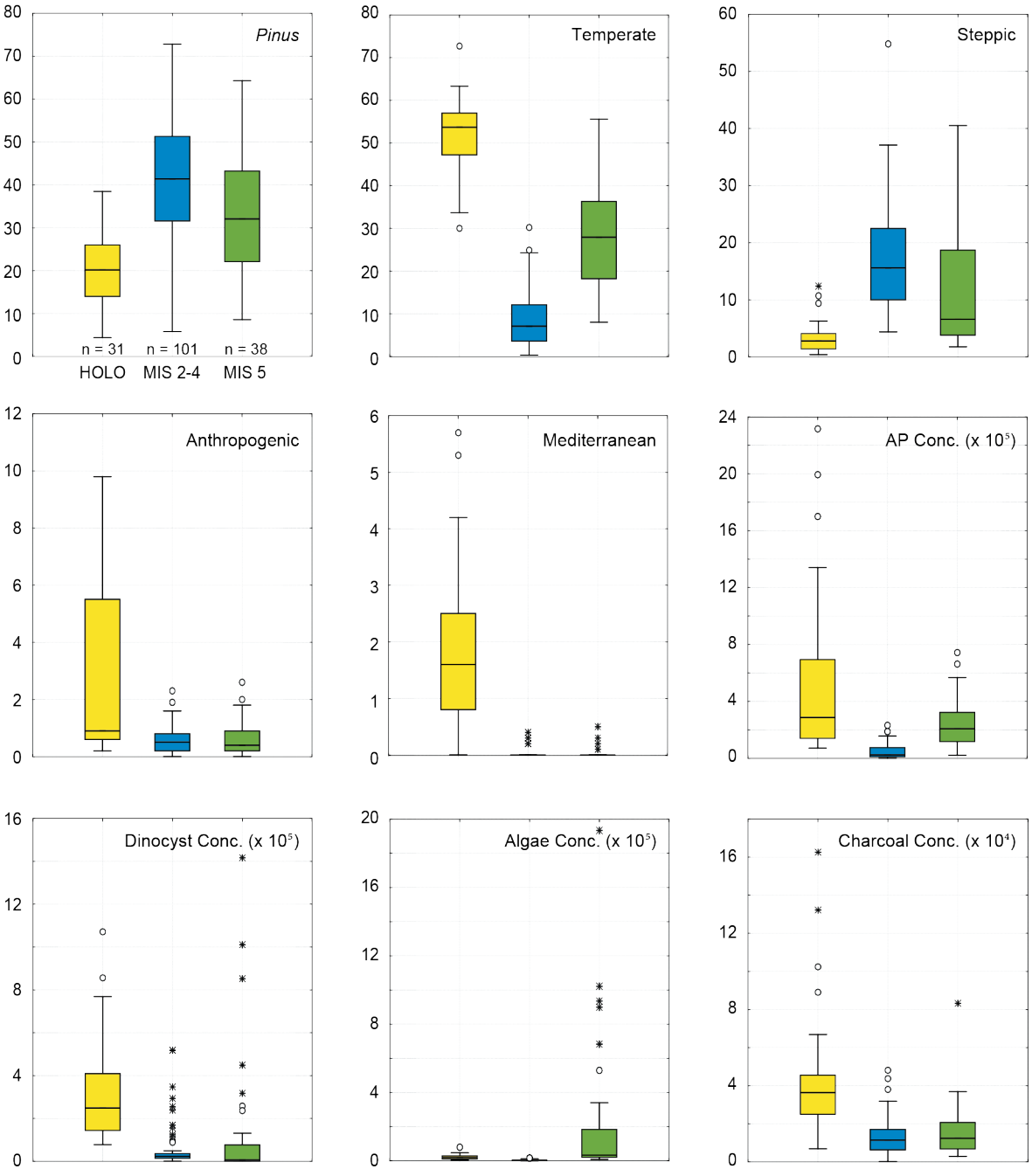

Figure 7.2: Box plots of selected palynological variables and groups in Co1215 during the Holocene, the MIS 2-4 and MIS 5. Note the different number of observations for each interval. The box contains the 25-75 percent quartiles, the median is indicated with a horizontal line within each box, while whiskers extend up to 1.5 times the inter-quartile range. Outliers are shown as circles (values outside the whiskers within 1.5 - 3 box length) and stars (more than 3 box length).

7.2.2 Ordination

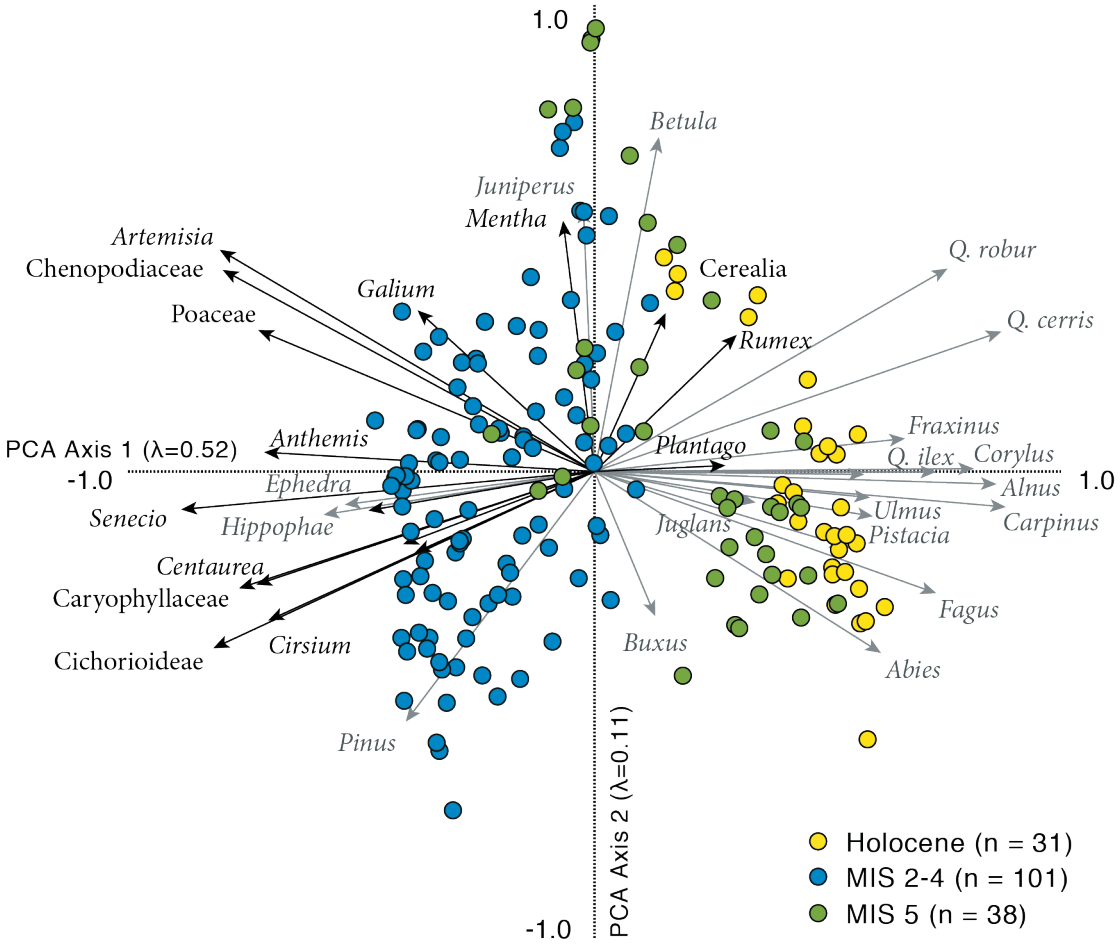

Figure 7.3: PCA biplot showing major species (n = 37) and samples (n = 170). NAP taxa are indicated in black, while AP taxa (trees and shrubs) in gray.

Principal Component Analysis (PCA) was performed on pollen relative percentages (for taxa crossing the 2% threshold) using CANOCO (ter Braak and Šmilauer, 2002). Pollen percentages of taxa included in the PCA were log transformed in order to reduce the asymmetry of the distributions (cf. Birks et al., 2012). The PCA results (**Figure 7.3**) summarize the major patterns of variation in the stratigraphical data in two axes PC 1 and PC 2, which explain 52% and 11% of the total variance respectively. The PC 1 separates the samples according to their proportion of drought- and cold-tollerant taxa (e.g. *Artemisia*, Chenopodiaceae, *Pinus*) versus temperate and thermophilous taxa (e.g. *Abies*, *Fagus*, *Quercus*, *Carpinus*). Notice how *Ephedra*, *Hippophae* and *Pinus* are placed together with NAP taxa, and Cerealia, *Rumex* and *Plantago* with AP taxa. Samples group into two distinct clusters (Holocene and MIS 2-4), while samples corresponding to MIS 5 span between the two clusters (**Figure 7.4**).

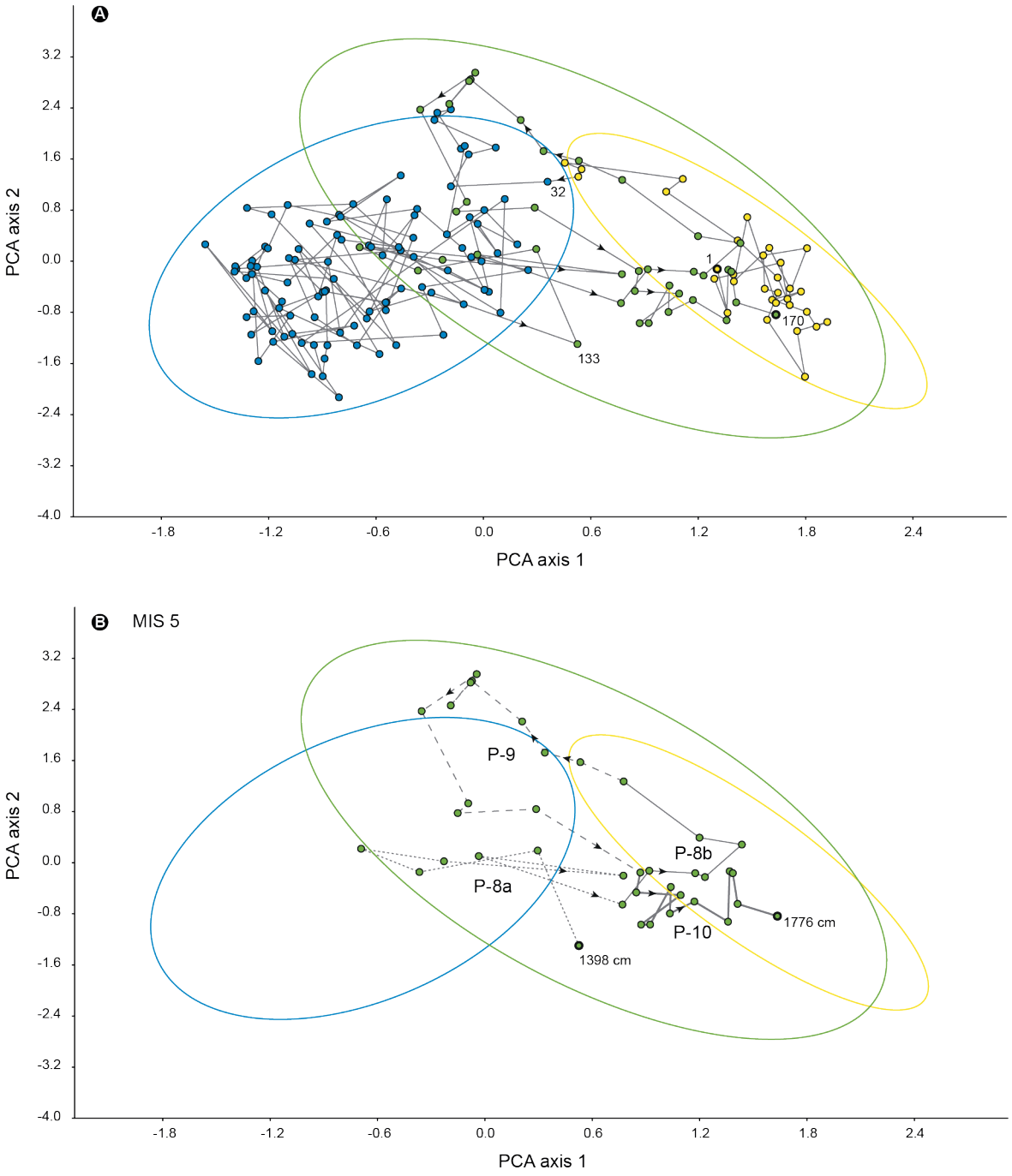

Figure 7.4: Plots of the Lake Prespa (Co1215) sample scores (n = 170) on the first and second principal component axes in stratigraphical order. The top and base of the sequence are indicated, as well as transitions between the three major intervals, which follow the color code of this chapter, the 95% sample concentration ellipses for each interval are also marked. (b) Local pollen assemblage zones are indicated for the MIS 5 interval (n = 38). Excursions of samples belonging to P-9 and P-8a in the direction of the MIS 2-4 ellipse are indicated by dashed lines.

7.2.3 Rarefaction

The total number of different pollen taxa present in a sample and the relative frequencies of different taxa are dependant, among other factors, on differences in pollen production and dispersal. Rarefaction analysis provides minimum variance unbiased estimates of the expected number of taxa (t) in a random sample of n individuals taken from a collection of N individuals containing T taxa (Birks and Line, 1992). Consequently, it enables comparison of richness between samples of different size by standardizing pollen counts to a single sum. The expected number of taxa ($E(T_n)$) for each sample is based on a common value of n, usually the smallest total count in the samples to be compared, and the rarefied sample will thus contain $t \leq T$ taxa and consist of $n \leq N$ (cf. Birks and Line, 1992). Palynological richness was determined in 165 samples (five samples with a main pollen sum less than 300 grains were left out of the analysis) with a standard pollen sum of 300 terrestrial grains ($E(T_{300})$) using PSIMPOLL (Bennett, 2011; **Figure 7.5**).

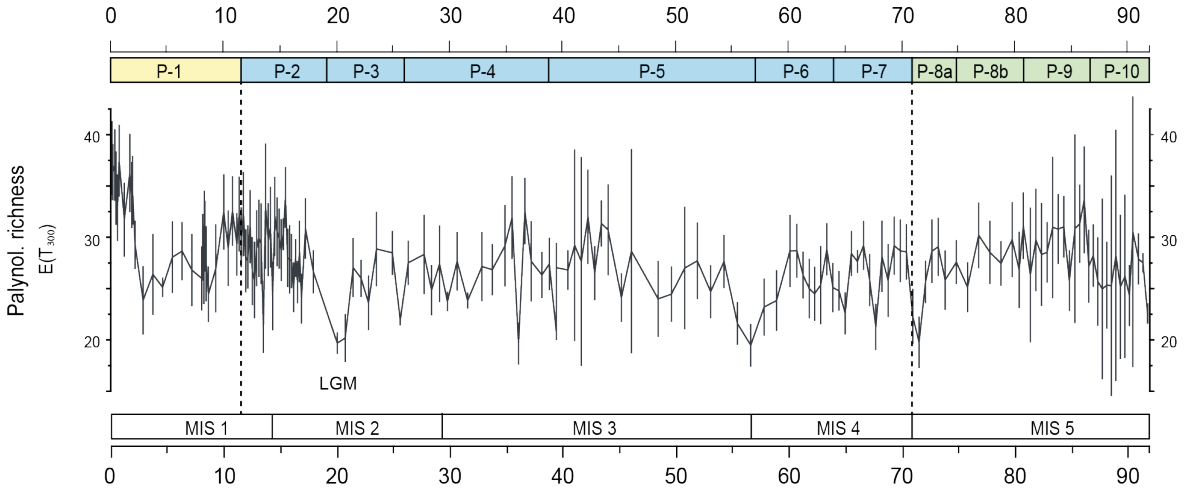

Figure 7.5: Plot of expected number of pollen taxa for 165 samples with 95% confidence intervals. The dashed lines delimit the Holocene, MIS 2-4 and MIS 5 intervals. The Last Glacial Maximum is also indicated

VIII Synthesis and Discussion

8.1 Watershed hydrology and sedimentation mechanisms

The large lake surface and the absence of a surface outlet lead to a negative net annual water balance at Lake Prespa at present and a rather short residence time (owing to the underground outflow to Lake Ohrid; Section **1.3.5**). The oxygen and hydrogen isotope composition of modern waters from Lake Prespa suggests that the lake is recharged mostly by spring water from high altitude and/or winter precipitation (snow and rain) that controls the strong seasonal and annual lake level fluctuations in turn (cf. Hollis and Stevenson, 1997; Leng et al., 2013; **Figure 1.7**; Section **4.5.1**). As a result, Lake Prespa is expected to react sensitively to winter precipitation, lake ice cover, and summer aridity at a decadal resolution (Section **4.6.1**).

There is evidence of glaciers forming on the mountains surrounding Lake Prespa (e.g. Galičica Mountain) during the Last Glacial, which were tentatively assigned a LGM age (Ribolini et al., 2011). In the absence of chronological data (Uranium series or cosmogenic radionuclides) these findings should be treated with caution, although ages obtained from neighboring sites (e.g. Hughes et al., 2006, 2010, 2011) as well as indirect evidence from core Co1215 substantiate the existence of local icecaps during this interval (see also Sections **2.5.1** and **5.5.1.3**). Belmecheri et al. (2009) postulated that glaciers reached the shores of Lake Prespa within the Last Glacial, however the intensely weathered glacial deposits in the lowlands suggest a much older age (most likely they formed within MIS 12; Ribolini et al., 2011).

A transect of multiple correlated cores is usually required for the reconstruction of lake level changes (e.g. at Lake Xinias by Digerfeldt et al., 2000 and at Lake Maliq by Fouache et al., 2010). In his methodology review, Dearing (1997) points out the difficulties in distinguishing between modifications of the sedimentation limit caused by lake-level change and by changes in the wind regime (in particular extreme storm events) or the sedimentation mechanisms (e.g. sediment focusing). At present, prevailing northern winds lead to the formation of traceable gyres on the lake surface and subsequent current activity accounts for a contourite drift visible in hydroacoustic profiles from Lake Prespa (Stefouli et al., 2011; Wagner et al., 2012; **Figure 1.8**). As the region is tectonically active, mass wasting deposits similar to the ones recorded in Lake Ohrid (e.g. Wagner, 2008) may occur; however, no such deposits are reported for Lake Prespa (cf. Wagner et al., 2012). The three cores from Lake Prespa (i.e. Co1215, Co1204 and Co1216) are described briefly in Section **1.4.1** (**Figure 1.9**). Considering the shortcomings listed above and the existence of underground outlets that were most likely active over longer periods, e.g. specialized endemic phytoplankton species occur at depths where karst springs discharge into Lake Ohrid (Matzinger et al., 2006), a robust reconstruction of past lake levels is not feasible with the material available to date. Nevertheless, some basic conclusions can be drawn from the correlation between the cores as well as from complimentary lines of evidence based on lithology, geochemical and palynological analyses (for details see also Sections **5.5.1.1** and **5.5.1.3**).

Sediment accumulation rates are relatively low (mean value of 0.23 mm $year^{-1}$) and besides some extreme events, e.g. Y–5 tephra deposition and the 8.2 cooling event, range between 0.18 mm

year^{-1} in MIS 5, 0.23 mm year^{-1} in MIS 2-4, and 0.3 mm year^{-1} in the Holocene (**Figure 8.1**). There is also a significant increase of sediment accumulation rates (0.65 mm year^{-1}) in the upper 34 cm of core Co1215 that correspond to the last 140 years. Over the last 92 ka, sediment focusing (greater sediment accumulation in the deeper part of a lake) does not appear to play an important role given the rather uniform sedimentation at core location (cf. Likens and Davis, 1975). During periods of elevated sediment accumulation (e.g. deposition of the c. 20 cm Y–5 tephra layer in Co1215), resuspension and redeposition to deeper parts of the basin by wave activity and water currents most likely occurred. The thickness of the Y–5 tephra layer in Co1204, retrieved from a lateral location, is 3 cm less in comparison to Co1215. In Co1216, the tephra encountered at the basal part of the sequence can not be correlated unequivocally (Sulpizio et al., 2010; Wagner et al., 2012) and together with the absence of other age control points impede comparison with the other cores.

Organic-rich sediments deposited during the Holocene are present in all three sequences, although discontinuities in Co1216 do not permit a direct comparison with the other cores (**Figure 8.1**). Lithology, geochemistry and radiocarbon dating suggest that recovery of the Holocene interval in Co1204 is complete, but the termination of the Last Glacial is partly missing. Focusing on this interval, Core Co1204 shows a higher sedimentation rate than the one observed in Co1215 (e.g. Holocene sediments of 300 cm in contrast to 200 cm in Co1215). This is a result of differential deposition most likely caused by some or several of the following factors: lake morphology, wind direction, wave and current action, mixing, and stream discharge. The latter

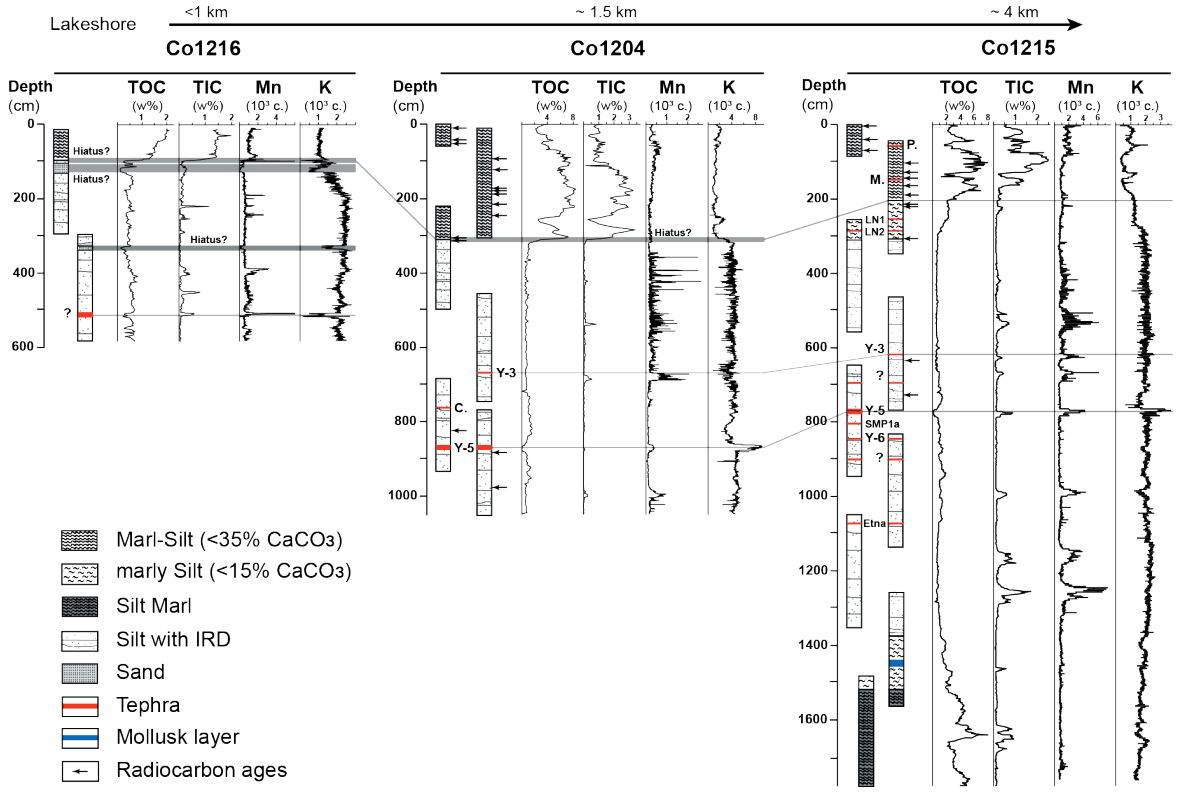

Figure 8.1: Lithology and geochemistry of existing composite cores from Lake Prespa to date. Correlation between cores is indicated by gray lines (modified from Böhm, 2012).

may have been a key mechanism during periods of extended snow (ice) cover, given the proximity to snow fields and glaciers, leading to events of extreme runoff with high erosional force in springtime. Further cores are required to assess the importance of local snow cover or icecaps and their potential impact on the sedimentation regime of Lake Prespa.

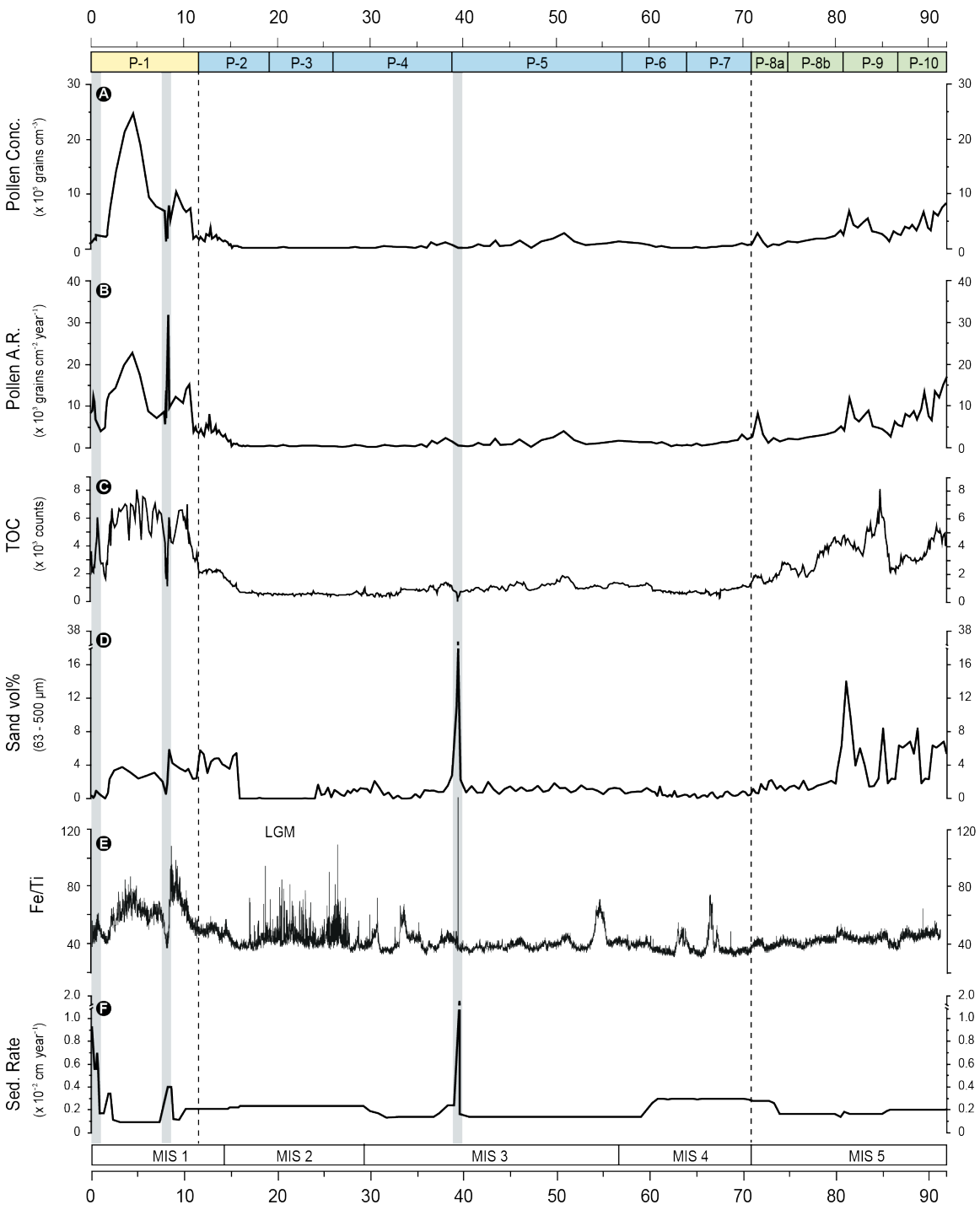

Figure 8.2: Pollen concentrations and accumulation rates, total organic carbon, sand percentages, iron/titanium ratio and sediment accumulation rates in Co1215. The gray bars delimit intervals with peaking sedimentation rate.

As a lake fills in, water depth and underwater slope angles decrease gradually. However, aeolian controlled processes such as waves and currents may lead to a more complex basin morphology particularly in larger basins such as Lake Prespa (**Figure 1.8**). Wagner et al. (2012) described the lateral depressions visible in hydroacoustic profiles from the northern part of the lake and argued that the formation of a contourite drift was initiated at c. 40 ka BP and intensified during the last c. 15 ka. Total sand percentages from Co1215 provide insights into sediment transport mechanisms and deposition conditions at the coring location. Sand percentages are relatively low (< 15%) in Co1215 with the exception of a pronounced peak corresponding to the deposition of the Y–5 tephra (**Figure 8.2** a). The low sand content suggests relatively calm sedimentation and is in agreement with the distal location of the core away from stream inflows. Therefore, higher sand percentages occurring at the base (MIS 5) and top (Lateglacial and Holocene) of the sequence imply changes in sedimentation processes (e.g. intensification of wind-stress and/or lower lake levels). A similar pattern of increased aeolian activity during these intervals emerges from Lake Ohrid (e.g. Vogel et al., 2010), suggesting changes in atmospheric circulation patterns at a regional scale. Increased aeolian activity during the MIS 5 may have led to the formation of a contourite drift between 92 ka and 80 ka (**Figure 8.2** d). Sedimentation of finer particles (< 60 μm) and the occurrence of Fe and Mn concretionary horizons (**Figure 8.2** e; Section **2.5.1**) imply deposition under calm and anoxic conditions during the MIS 2. A prolonged period of ice cover (extending in the springtime) and/or less wind-stress (or a change in prevalent wind direction) may be the mechanisms behind the weakening/cessation of the contourite drift during the Last Glacial Maximum.

There is a risk of reaching incorrect conclusions about regional paleovegetation from measurements made in basins were sedimentation mechanisms are not fully understood. In addition, inherent uncertainties in age-depth models, especially beyond the limit of radiocarbon dating, render the use of pollen accumulation rates problematic in sequences missing independent age control such as tephra horizons or varves (cf. Telford et al., 2004). Assuming robust age control and sound understanding of sedimentation processes at core location, pollen accumulation rates can be a

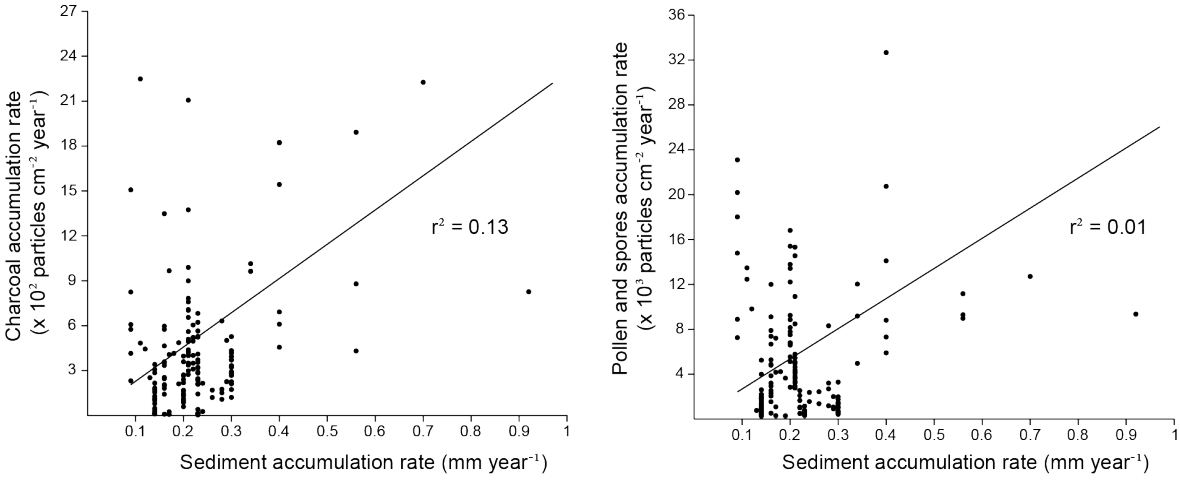

Figure 8.3: The relationship between pollen and charred particle accumulation rates and sedimentation rates in Co1215. Analysis based on 169 samples (a sample within the Y–5 tephra layer was removed).

valuable tool to infer terrestrial pollen production and together with pollen concentrations offer critical information about the openness of paleolandscapes (Section **3.5**; see Section **5.5.1.1** for a discussion over the susceptibility of relative percentages to effect of closure). Moreover, if age control is adequate, pollen influx can also help to elucidate the local presence of a pollen taxon or may indicate the time of its immigration within the pollen source area (e.g. *Fagus* refugia in the Balkans, Section **3.5.6**; **Figure 3.7**). Over the last 92 ka, charcoal and total pollen accumulation rates are not dependent on sedimentation rates in Co1215 (**Figure 8.3**). However, during short intervals of rapid sediment accumulation, e.g. 8.2 ka cooling event and over the last 140 years, pollen (and charcoal) accumulation rates are found to be dependent on core sediment accumulation (**Figure 8.2** b; **Figure 7.1** b). Overall, pollen accumulation rates are coupled to changes in pollen concentrations reflecting changes in pollen productivity and ecosystem development through time (**Figure 8.2**).

8.2 Reconstructing Prespa's ecosystems over the last 92 ka

PCA analysis performed on log-transformed assemblage composition data supports the partition of the Co1215 sequence into three major intervals, namely the MIS 5, the MIS 2-4 (including the Lateglacial transition) and the Holocene (Section **7.2.2**). There is a significant overlap between pollen samples grouped in the MIS 5 (green ellipse) and samples belonging to the other two groups (the MIS 2-4 and the Holocene; **Figure 7.4** b). Within the MIS 5, samples included in PAZs characterized by 'glacial' pollen spectra (**Figure 7.3**), i.e. P-9 and P-8a, are placed closer to samples of PAZs from the MIS 2-4.

Exploratory analysis of untransformed palynological data suggests that the Holocene stands out in most of the variables examined, while differences between the MIS 5 and the MIS 2-4 are not always clear (**Figure 7.2**). As box plot analysis is independent of the underlying distribution, it can prove useful in revealing outliers and asymmetries in the Prespa data set. For instance, the skewness in the distribution of dinocyst concentrations is much greater within the MIS 5 in comparison with the Holocene. Having a closer look at the dinocyst concentration curve (Fig 8.4 c) it becomes apparent that dinoflagellate concentrations were high only for short periods within the Last Glacial (notably in the MIS 5), but show sustained higher values during the Holocene. In ecological terms, the distribution of this phytoplankton species within MIS 5 can be ascribed to its immigration into Lake Prespa at c. 87 ka cal BP followed by an exponential growth of its population due to favorable environmental conditions around 84 ka cal BP (Section **5.5.1.3**).

Rarefaction analysis was used to estimate palynological richness ($E(T_n)$) for each pollen sample counted in Co1215 at a fixed sum of 300 terrestrial pollen grains (Section **7.2.3**). Diversity indices commonly used in ecology are not appropriate for pollen percentage data, as the latter are strongly dependent on differences in pollen productivity and dispersal mechanisms (e.g. wind or insects) among species. Birks and Line (1992) introduced this statistical technique into paleoecology, which is independent of data distribution, as an index for estimating floristic diversity (species richness) in the pollen source area. However, the relationship between species richness and palynological richness is not linear (Odgaard, 1999). Moreover, herbaceous pollen is usually underrepresented in forested stages due to limited wind dispersal below the canopy.

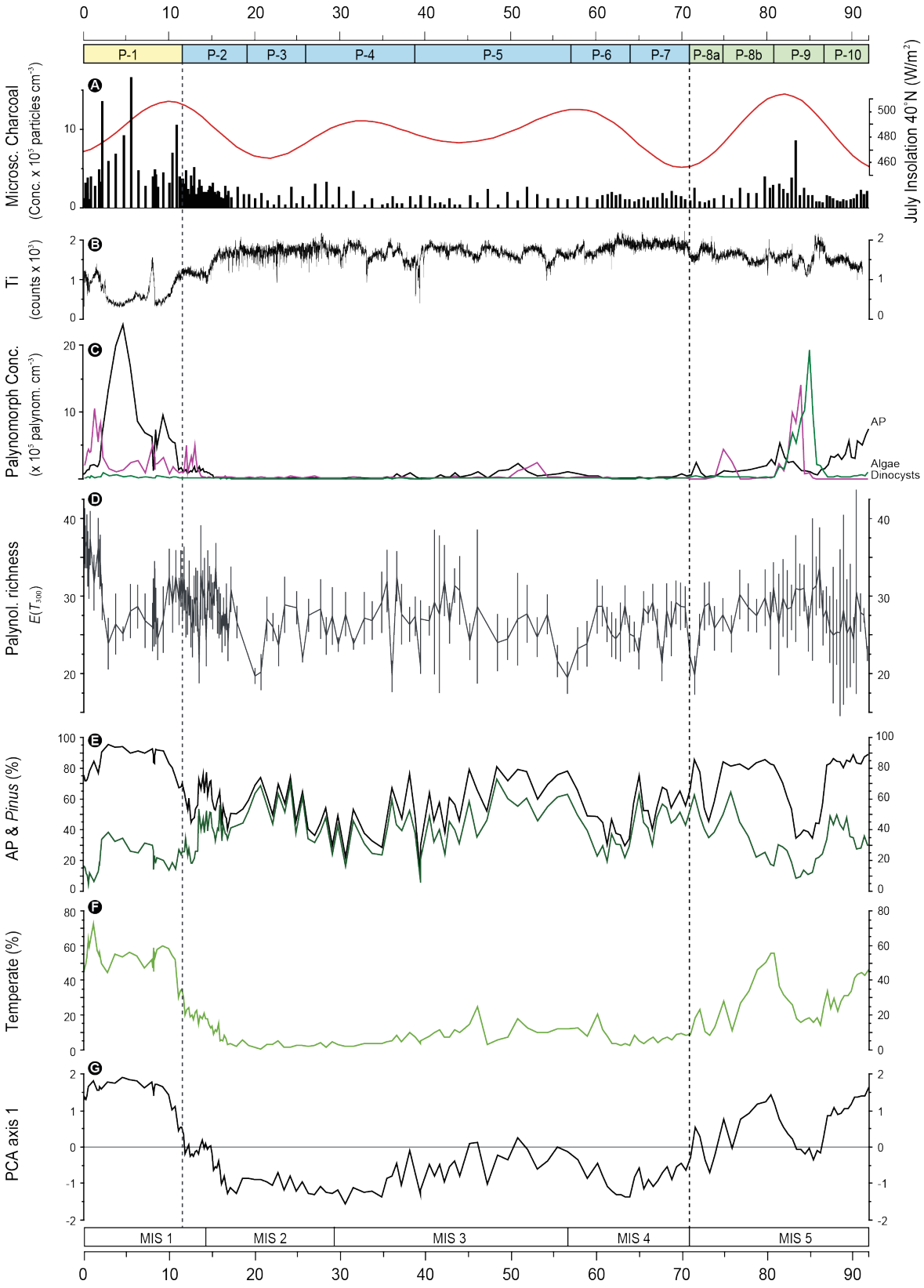

Figure 8.4: Synoptic diagram of selected proxies from Lake Prespa (Co1215).

It should also be stressed that rarefaction analysis does not address the question of species evenness (relative frequency of taxa) and is influenced by factors affecting pollen dispersal. Therefore, the outcome of the analysis should be treated with caution as there is a number of assumptions (e.g. samples compared should have similar flora) related to it and along with the taxonomic precision bias inherent in palynological analysis (i.e. numerous plant species corresponding to one morphological pollen type) may lead to erroneous interpretations (cf. Birks and Line, 1992; Odgaard, 1999). Considering the size of the basin, the curve of $E(T_{300})$) at Prespa is most likely capturing changes in taxonomic richness at a landscape scale (γ-diversity sensu Whittaker, 1972) and is influenced by climate, vegetational succession and disturbance (natural or anthropogenic). Thus, processes affecting floristic richness of the constituent vegetation types within the pollen source area, such as deforestation, may result in an increase of palynological richness by allowing for a greater representation of open ground taxa in pollen spectra (cf. Birks and Line, 1992). According to the 'intermediate disturbance hypothesis' (e.g. Petraitis et al., 1989), the maximum richness occurs at intermediate levels of disturbance. For example, van Odgaard (1994) demonstrated that highest floristic richness for three Danish sites spanning the Holocene occurred at intermediate fire intensities that were inferred from microscopic charcoal. At Prespa, a distinct increase of palynological richness is recorded after c. 2 ka cal BP and is most likely triggered by intensifying anthropogenic disturbance (e.g. agriculture and pastoralism; Panagiotopoulos et al., 2013) that produced a mosaic vegetational structure.

Pollen taxa scores of the first PCA axis, which explains half of the variance in the stratigraphic dataset (Section **7.2.2**), are remarkably similar to deciduous temperate tree percentages (**Figure 8.4** f and g). Both curves are considered to reflect changes along an environmental gradient of moisture availability and temperature at Prespa (with positive values and higher percentages respectively suggesting an increase of temperature and moisture availability). In addition, the highest values of AP concentration and percentages coupled with a parallel decrease in allochthonous clastic input, which is indicated by low Ti values, are documented during the MIS 5 and notably during the Holocene in Co1215 (**Figure 8.4** c). In terms of landscape evolution, these intervals enclose the only forested landscape phases inferred from the Lake Prespa pollen (for a detailed discussion see Section **5.5.1**). This conclusion appears to be in agreement with periods of relatively low palynological richness estimated for this time (**Figure 8.4** d). However, there are also some periods within these zones, such as P-9, and the Early and Late Holocene, when estimated floristic diversity rises. A coeval increase of microscopic charred particle concentrations -related to enhanced fuel availability- during these periods suggests the opening of the landscape, and is most likely one of the drivers behind the increase in $E(T_{300})$. Peaks in summer insolation in the MIS 5 and the Holocene can generally be correlated with increases in microscopic charcoal concentration (**Figure 8.4** a). However, after c. 5.5 ka cal BP this does not appear to be the case suggesting the synchronous operation of other perturbation mechanisms (most likely related to human activity).

The MIS 2-4 interval encompasses the highest *Pinus* and steppe herbaceous percentages of the Prespa pollen sequence (**Figure 7.2**). The open landscape inferred for most of this period (AP concentration and percentages, **Figure 8.4**; for details see also Section **5.5.1**) appears to be in line

with relatively low microscopic charcoal values and high palynological richness and Ti counts. Within this interval comprising almost 60 ka, there are times when tree values rose (e.g. AP concentrations and percentages in P-5 and P-2 corresponding to the MIS-3 and the Lateglacial) and this increase is also reflected in $E(T_{300})$, charcoal and Ti. However, a deviation from this pattern (similar to the one observed in the Holocene) is documented during two intervals lasting c. 3 ka each (at c. 55 ka and 20 ka cal BP). Contrary to the Holocene one, the minima registered in the palynological richness curve can be ascribed to climate forcing. Interestingly, AP and *Pinus* percentages are peaking, though extremely low AP concentrations within both intervals suggest an open landscape. The minimum in $E(T_{300})$ around 20 ka cal BP can be linked with the Last Glacial Maximum, a time when local glaciers reached their maximum extent (Ribolini et al., 2011; Section **8.1**) and most likely Prespa ecosystems crossed a critical threshold. The second minimum in palynological richness follows the H6 event (**Figure 5.6**; Section **5.5.2.2**) and probably indicates the reorganization of the vegetation at Prespa.

8.3 Vegetation dynamics at the Dessarate Lake region

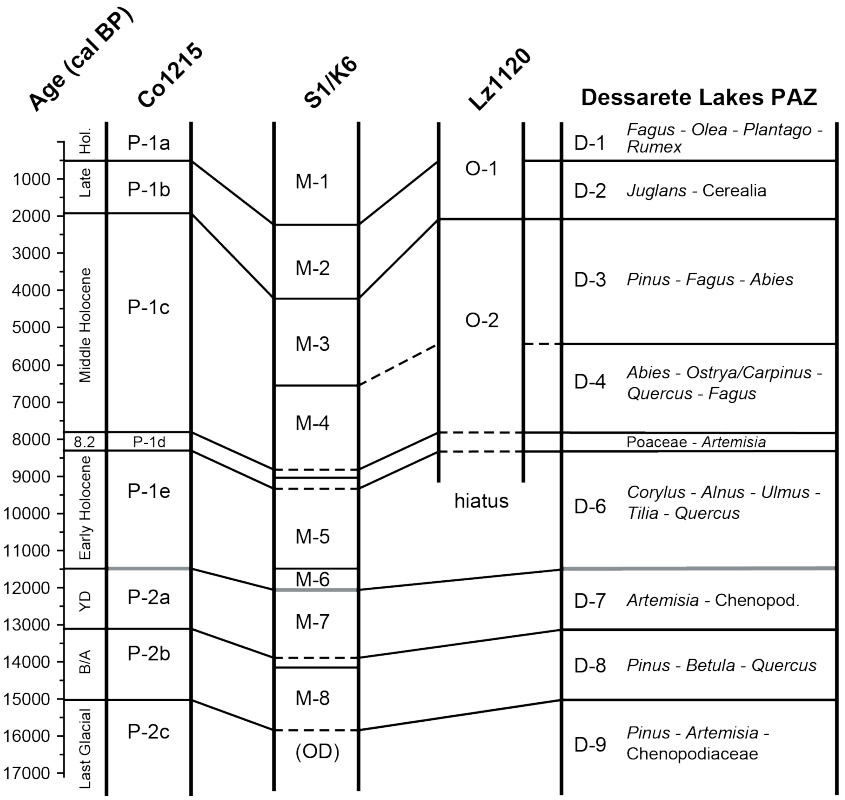

Figure 8.5: Regional pollen assemblage zones inferred from three representative Dessarete Lakes pollen records: Co1215 (Panagiotopoulos et al., 2013), S1/K6 (Denèfle et al., 2000; Bordon et al., 2009) and Lz1120 (Wagner et al., 2009). Zonation of the Prespa pollen record was performed using cluster analysis and the resulting local PAZs are described in detail in Chapters **III** and **V**. For S1/K6 solid lines represent the PAZ limits found in Denèfle et al.(2000), while dashed lines show modifications after Bordon et al. (2009). Zone names were assigned following the naming scheme of Co1215 in order to facilitate comparison. The onset of the Holocene is marked in gray. The 8.2 event can be distinguished in all pollen records from the region (it is indicated with dashed lines in Lz1120).

Considering the robust age-depth model of Co1215 and the undisturbed sedimentation at core location, the Prespa paleoarchive is employed in this section to reconstruct the vegetation history for the Dessarate Lakes region. Besides the records shown in **Figure 8.5** and **Figure 8.6**, there is an additional pollen sequence from Lake Ohrid spanning the Last Glacial cycle. However, it suffers from discontinuous sedimentation (between MIS 5 and MIS 4) and only a limited selection of herbaceous taxa is published (Lézine et al., 2010). Consequently, description of regional PAZs (D-9 to D-1) shown in **Figure 8.5** and reconstruction of the Dessarate Lake paleoenvironment are limited to the last c. 17 ka.

There is a striking resemblance between the pollen records originating from Lake Ohrid and Lake Prespa (**Figure 8.6**) that can be ascribed to geographical and geomorphological characteristics (e.g. similar basin size and partly common pollen source area). The pollen record from former Lake Maliq (S1/K6) is strongly influenced by local hydrology (transitions from lacustrine sedimentation to peat accumulation and vice versa; Denèfle et al., 2000) and shows a consistent time lag which is accentuated in the upper part of the core (**Figure 8.5**). Considering the significant hard-water/reservoir effect (up to c. 1 ka) evident in parallel dating of bulk and macrofossils in two horizons from Lake Prespa (Co1215; Section **2.4.4**), it is expected that bulk material dated at Maliq is also affected and as a result in the absence of other independent markers (e.g. tephra) the ages of S1/K6 are most likely biased.

On a regional scale, the Last Glacial interval (D-9; up to c. 15 ka cal BP) is characterized by the dominance of herbaceous communities, mostly composed of *Artemisia* and Chenopodiaceae, associated with *Pinus*. Poaceae percentages are high at both lakes and in the case of Maliq reach particularly high values (~ 60%) that perhaps can be a sign of aquatic provenance (e.g. *Phragmites australis*) and, consequently, can be tentatively related to changes in lake levels. The landscape inferred was rather open (low pollen accumulation rate and concentration at Prespa; Section **3.5.1**; **Figure 8.2**) and tree stands were most likely concentrated in sheltered locations at lower elevations within the catchment. Moreover, relatively high palynological richness documented at Prespa during this interval (**Figure 8.4 d**) suggests the dominance of open ground plants (herbs and shrubs). The refugial character of the greater area was deduced from occurrences of numerous deciduous tree pollen (such as *Quercus*, *Ulmus* and *Acer*; Denèfle et al., 2000; Panagiotopoulos et al., 2013). Local presence of these trees within the respective catchments can be indisputably indicated by recovery of the respective macrofossils (cf. Birks and Birks, 2000). This is especially the case when interpreting relative percentages of prolific pollen producers such as *Quercus* (cf. van der Knaap et al., 2005). Occurrences of *Acer* and *Ulmus* pollen, which are known for extremely low pollen production and poor long-distance transport ability of their grains, point to the survival of several deciduous tree species within the catchment limits. However, in the absence of macrofossil analyses from the area, the question whether these trees may have occurred within or in the vicinity of the respective lake catchment remains open.

A substantial increase in arboreal percentages at Prespa and Maliq (mainly *Pinus* and *Quercus*) associated with continuous curves of *Betula*, *Abies*, *Corylus* suggest the increase of moisture availability in the region during the Bølling/Allerød (D-8). However, accumulation rates of *Pinus* and *Quercus* increase gradually in Co1215 and imply a parkland landscape (**Figure 3.7**).

The notion of a landscape mosaic with scattered tree stands is backed by retreating *Artemisia* and Chenopodiaceae percentages and increasing palynological richness (**Figure 8.4**).

During the Younger Dryas (D-7), pronounced peaks of *Artemisia* and Chenopodiaceae percentages are documented at Prespa and Maliq and imply the opening of the landscape at the Dessarate Lake region. Panagiotopoulos et al. (2013) suggested a lowering of the treeline affecting mostly pines on higher terrain as a possible mechanism for the declining *Pinus* accumulation rate and percentages at Prespa between c. 13 and 11.7 ka cal BP. Relatively stable *Quercus* but decreasing *Pinus* percentages are also registered at Maliq. At Prespa, palynological diversity remains relatively high indicating the dominance of herbaceous vegetation in this interval.

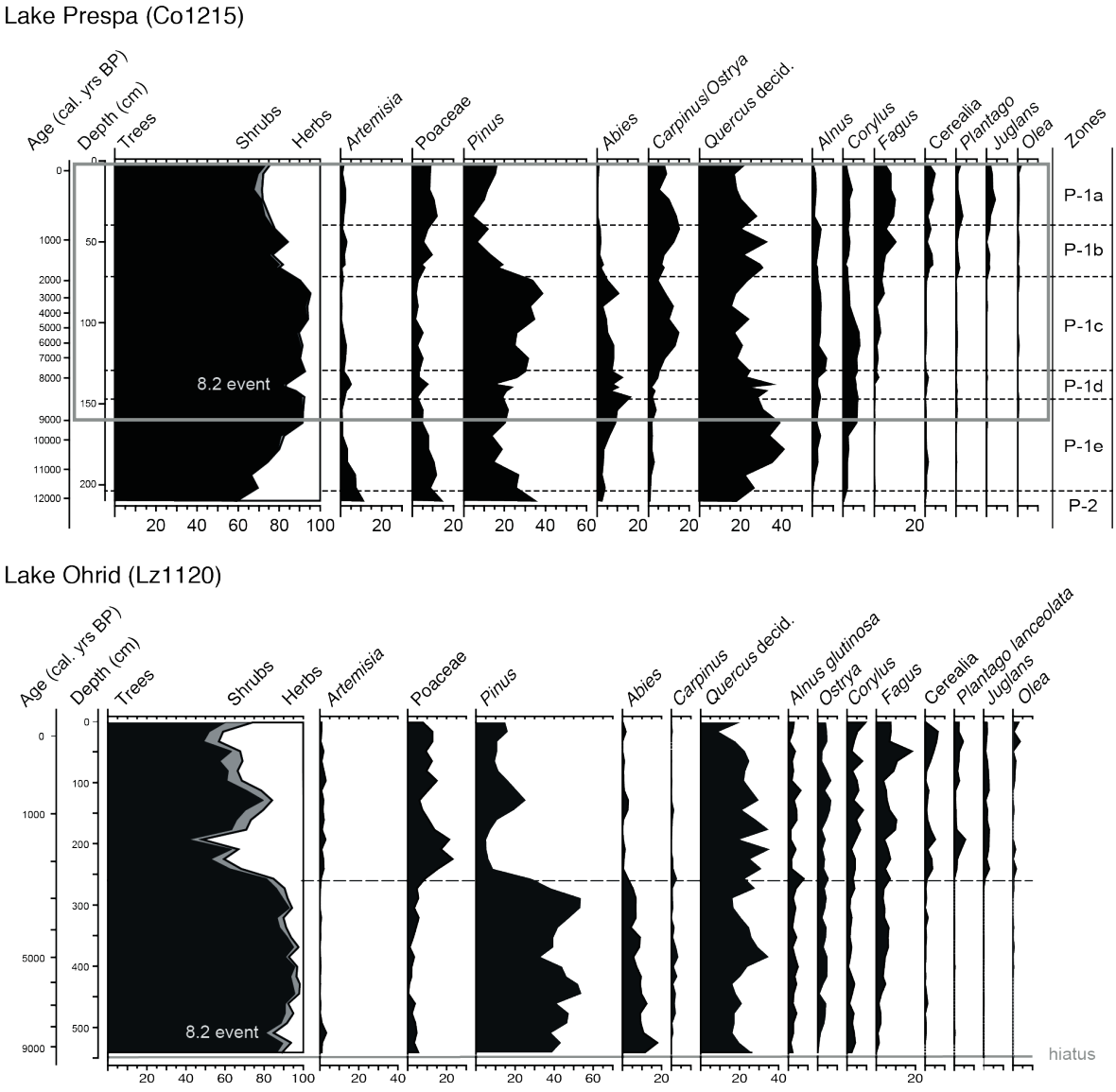

Figure 8.6: Simplified pollen diagrams from Lake Prespa (Co1215; Panagiotopoulos et al., 2013) and Lake Ohrid (Lz1120; Wagner et al., 2009) plotted against depth. The gray box includes the interval documented in both cores.

The onset of the Holocene (D-6) signals the expansion of numerous deciduous trees such as *Corylus*, *Ulmus*, *Tilia*, and *Alnus*, which occurred sporadically up to this point in the Maliq and Prespa archives. *Quercus* percentages and accumulation rates at Prespa suggest the closing of the landscape and a shift in vegetation zones. Contrary to rather stable *Pinus* percentages at Maliq, pine percentages are declining (down to 20%) at Prespa. The succession of pioneer trees (e.g. *Pinus*, *Betula*, *Quercus* and *Corylus*) followed by shade-tolerant species (e.g. *Abies*, *Ulmus*, *Tilia*) indicates optimal conditions for growth and the progressive formation of closed forests in the Dessarate Lake region. At Maliq, an expansion of fen trees (*Alnus* and *Salix*) associated with high Poaceae (reeds?) percentages during the Early Holocene indicate low lake levels. AP percentages at Prespa also suggest a distinct regression phase of tree communities that was tentatively related to the centennial PBO event (Section **3.5.4**). Water stress or frosts during late spring may have played a critical role in limiting the expansion of drought- and frost-sensitive species (e.g. *Fagus* and *Phillyrea*). Pollen taxa diversity in the Prespa record is high till c. 10 ka and decreases abruptly thereafter indicating the closing of the tree canopy (**Figure 8.4**). Interestingly, significant changes in microscopic charcoal concentration (and accumulation rates) and forest composition at Prespa overlap. Climatic (e.g. maximum in summer insolation) and non-climatic (e.g. type of vegetation and fuel availability) parameters most likely controlled forest development and fire regimes during this time. A prolonged dry summer period and an amplification of seasonal variability can be invoked to explain the reshaping of landscapes in the area (**Figure 8.4**). Despite the gradual afforestation (maxima in AP percentages around 10 ka) of the wider area, occurrences of most arboreal pollen types (excluding pines and oaks) can be traced back to the Last Glacial at both lake catchments. Hence, immigration (migration lag) was not behind the delayed expansion of some trees, and most likely climate and/or edaphic factors controlled regional vegetation response.

The regional PAZ encompassing the 8.2 event (D-5) is distinguishable in all pollen records originating from the Dessarete Lakes. This short climate oscillation is marked by a distinct peak of *Artemisia* and Poaceae coupled with a retreat of AP percentages and indicates cold and dry conditions persisting in the Dessarate Lake area (Denèfle et al., 2000; Wagner et al., 2009; Panagiotopoulos et al., 2013). The opening of the landscape is also implied by a peak in palynological diversity and decreasing terrestrial pollen influx in Co1215 (**Figure 8.2** b and **Figure 8.4**). A distinct spike of charcoal accumulation rates is not matched with a significant increase of charcoal concentrations, pointing to changes in sedimentation processes at Prespa (**Figure 8.4**; Sections **2.5.4**, **3.5.5**, and **8.1**).

In the Middle Holocene (D-4), AP percentages are consistently high (above 80%) in all archives suggesting extensive forests in the surroundings of the three lakes. Increasing *Pinus* percentages at Maliq and Prespa most likely indicate a shift of the treeline and the expansion of pines at higher and more challenging grounds. At c. 5.5 ka cal BP, a significant peak in microscopic charcoal accumulation rates and a pronounced peak in microscopic charcoal concentrations (**Figure 8.4 a**) can be linked with enhanced fire occurrence at Prespa and most likely with increasing summer aridity. However, evidence of increasing anthropogenic impact complicate the interpretation of the Prespa pollen in this interval (Section **3.5.6**). Periodical gaps in the tree canopy favored the

expansion of understory vegetation as it is shown in rising palynological richness for this interval. Increasing percentages of *Carpinus orientalis*/*Ostrya carpinifolia* and *Quercus cerris*-type at the expense of *Quercus robur*-type point to a reorganization of vegetation (expanding thermophilous belt) within the Prespa watershed (**Figure 3.5**). At Maliq, *Abies* percentages reach a maximum (>20%) at the beginning of D-4 while *Quercus* percentages at the end of the zone. Rising *Fagus* percentages (and influx in Co1215) and a continuous curve in the three records suggest the persistence of beech in the area, however due to climatic and/or ecological constraints *Fagus* expanded in the region only after c. 7 ka cal BP (Panagiotopoulos et al., 2013). In D-3, *Pinus* and *Quercus* accumulation rates as well as total arboreal concentration (**Figure 5.5**) peak at c. 4.5 ka and decline gradually thereafter. Interestingly, this maximum in AP concentration, which indicates a very productive interval for vegetation at Lake Prespa, is not as pronounced in AP percentages. Increasing *Pinus* and to a lesser degree *Abies* and *Fagus* percentages are recorded till c. 2.5 ka at Maliq, Ohrid and Prespa. After c. 2.5 ka, pollen abundance of most tree taxa starts to decline in the Dessarate Lake region with the exception of *Quercus* (*cerris*-type) at Prespa.

The Late Holocene (D-2 and D-1) is characterized by declining AP values and increasing occurrences of pollen taxa associated with anthropogenic activities (cf. Behre, 1981). A decreasing trend in AP percentages is documented at Ohrid (~ 40%) and Prespa (~ 15%), but not at Maliq. At the latter, sporadic occurrences of *Juglans* and *Olea* pollen, as well as an increase in *Artemisia* percentages suggest human presence. It is surprising that anthropogenic impact in the pollen record is rather limited at Maliq, although archaeological excavations suggest continuous human occupation dating back to c. 8 ka cal BP (Fouache et al., 2010). Given the lack of age control points in the upper 2.5 m of core S1/K6 as well as the artificial drying of the lake and the ensuing intensive agricultural activity at Maliq since the Fifties, most probably the last couple of hundred years are missing. At Prespa, on the contrary, there is a significant rise of pollen taxa diversity during this period (**Figure 8.4**) suggesting the opening of the landscape. Pollen of food crops such as *Juglans* and Cerealia show continuous curves at Ohrid and Prespa, as well as other herbaceous species considered as perennial weeds such as *Plantago* and *Rumex* (**Figure 3.5**, **Figure 3.6**; Section **3.5.6**). The highest *Olea* percentages are documented in the pollen record from Ohrid, which has the lowest elevation (693 m a.s.l.). *Fagus* percentages reach maximum values at the Dessarate Lake region within D-1. Pollen spectra from the upper centimeters of the Ohrid and Prespa cores indicate a reversal in the deforestation trend.

8.4 Conclusions and outlook

Sedimentological, geochemical and summary biological data (i.e. ostracods and pollen) for the last 17 ka provide evidence for a gradual increase of temperatures and precipitation at the study region (Chapter **II**). The data suggest a transition from oligotrophic and well-mixed lake conditions between 17 ka and 11.5 ka to a more productive, ice-free and seasonally stratified lake over the Holocene. The pollen data corroborate the gradual climate warming and rise in precipitation, but also illustrate a regression phase in the afforestation process corresponding to the Younger Dryas. Short periods of strong decomposition of organic matter, enhanced mixing and soil erosion tied to retreating forest cover are documented at c. 8.2 ka and after 2 ka.

Deglaciation left its imprint on aquatic and terrestrial ecosystems at Prespa. Palynological data provide evidence for the survival of numerous deciduous trees at Prespa or its vicinity during the Last Glacial (Chapter **III**). The wooded-steppe landscape inferred for the Lateglacial, which was dominated by *Artemisia* and Chenopodiaceae associated with pines, suggests low temperatures and precipitation. Oaks were probably restricted to lower elevations and expanded gradually in the Bølling interstadial. An opening of the landscape and a shift of the treeline documented during the Younger Dryas can be ascribed to cold and dry conditions favoring the spread of steppe vegetation. The onset of the Holocene signaled the increase of primary production in Lake Prespa and its surroundings pointing to rising temperatures and moisture. Increased seasonality was most likely responsible for changes in floristic composition and in fire regime through this period. Expansion and diversification of forests at Prespa was deduced for the Early and Middle Holocene. A distinct peak of *Artemisia* percentages at c. 8.2 was the only significant expansion of herbs preceding the intensification of human activity around 2 ka. Increasing weed and crop plant pollen indicate the onset of arable farming, while decreasing arboreal percentages point to the opening of the landscape.

Stable isotope data from modern waters show that hydrological balance in Lake Prespa is a function of summer aridity and winter precipitation. The sediments (1556 cm) fall into zones based on their sedimentology, geochemistry and palynology that correspond to Marine Isotope Stages 5 to 1 (Chapter **IV**). During the Last Glacial, the lake was oligotrophic and well-mixed indicated by peaks in OI and siderite. However, within sediment reducing conditions and methanogenesis most likely occurred. In contrast, MIS 5 and MIS 1 sediments suggest higher productivity (higher phytoplankton concentrations and calcite content) and a better preservation of organic matter due to anoxic conditions in the hypolimnion. Oxygen isotope data from glacial siderites suggest that the lake was less evaporative in the Glacial, probably as a consequence of longer ice cover and cooler summers. The oxygen isotope composition of calcites from the Holocene corroborate the notion of increased humidity inferred from pollen data.

Sedimentological, geochemical and palynological data from the longest Prespa sequence to date (1776 cm) offer insights into changes of aquatic and terrestrial vegetation in response to climate forcing (Chapter **V**). Pollen data suggest the survival of deciduous temperate trees in the Prespa region over the last 92 ka. A forested landscape and high lake productivity were inferred for intervals within the MIS 5 and the Holocene, a parkland landscape for MIS 3, and an open landscape with scattered tree stands and enhanced clastic input for MIS 4 and MIS 2 when temperatures and moisture declined. Orbital and suborbital climate variability can be discerned in biotic and abiotic proxies of the Prespa paleoarchive and appears to be in phase with other Mediterranean and global paleorecords given the age and sampling constraints. The Prespa and other regional records suggest the persistence of relatively favorable environmental conditions during MIS 3 that may have facilitated modern human dispersal into Europe.

The dynamic model of adaptive cycles presented in Chapter **VI** aims at bridging the gap between principles (e.g. geosciences, archaeology and sociocultural anthropology) as well as between the different temporal and spatial scales. This model, which is based on the theories of resilience and adaptive cycles, distinguishes among phases of growth (r-phase), conservation (K-phase), distor-

tion/decline (Ω-phase) and reorganization (α-phase). In the Lake Prespa case study, different phases in landscape evolution over the last 17 ka were distinguished and discussed. The revised adaptive cycle model allows the pooling of data from very diverse sources (i.e. ethnography, Paleolithic, Neolithic, paleodemography, paleoenvironment and geomorphology) and attempts to resolve questions of human-climate interaction, and of human mobility and dispersal.

A wide range of methodologies, proxies and principles was employed in this dissertation in an attempt to improve our understanding of ecosystem-human-climate interactions in southwestern Balkans. Under this scope, the research undertaken hitherto shed light to several mechanisms acting at centennial and millennial scales that control the response of biotic and abiotic components of the Prespa ecosystems. Owing to the robust chronology of the Prespa core, it was possible to trace the sensitive reaction of the vegetation within the lake and its catchment to climatic and environmental change over the last 92 ka. In addition, microscopic charcoal and rarefaction analysis provided insights into the impacts of disturbance (natural or anthropogenic) on landscape openness as well as on floristic composition and diversity. The vegetation history of the region was examined focusing on ecological processes such as species immigration, competition, succession, population growth and stability. However, over the last two millennia, anthropogenic activities overprinted the signature of climate variability and obscured the natural response of vegetation at Prespa.

This study underscores the sensitivity of the Lake Prespa region to climate forcing over the Last Glacial and the Holocene. Considering the potential and limitations of Prespa sediments, a decadal temporal resolution can be reached by decreasing sampling intervals. For instance, decreasing pollen sample intervals (to 2 cm) allowed for observation of vegetation dynamics in a sub-centennial scale during the 8.2 event. Refining the temporal resolution may yield a better correlation with short-term climate oscillations, in particular during the Last Glacial. Moreover, macrofossil analysis can provide indisputable evidence for local presence of trees and, thus, will complement pollen analysis in resolving questions about species immigration. Given the complex hydrology, additional and longer sequences originating from more lateral locations are required in order to decipher lake development and reconstruct lake-level fluctuations.

Ongoing investigations on material from Co1215 focusing on proxies such as diatoms (Z. Levkov, Ss Cyril and Methodius University), ostracods (F. Viehberg, University of Cologne), stable isotopes (M. Leng, BGS, NIGL), and paleomagnetics (N. Nowaczyk, GFZ Potsdam) will eventually improve age control (especially in the basal part) and provide further insights into the hydrology, limnology (e.g. lake water pH) and climate of the study area. In addition, surface samples collected at Prespa will be used in calibrating the transfer functions developed in collaboration with the B3 Project within the CRC 806 (T. Litt, A. Hense, B. Thoma, Bonn University). The first results of pollen-based reconstructions of temperatures and precipitation during the last 17 ka using Bayesian statistics are promising and in line with the qualitative reconstruction approach presented here (B. Thoma, personal communication). Finally, successful completion of the ongoing ICDP drilling at Lake Ohrid is expected to extend our current understanding about the paleoenvironment and paleoclimate of the Dessarete Lake region over several glacial-interglacial cycles.

References*

Aliaj, S., Baldassarre, G., Shkupi, D., 2001. Quaternary subsidence zones in Albania: some case studies. Bull Eng Geol Env 59, 313-318.

Amataj, S., Anovski, T., Benischke, R., Eftimi, R., Gourcy, L., Kola, L., Leontiadis, I., Micevski, E., Stamos, A., Zoto, J., 2007. Tracer methods used to verify the hypothesis of Cvijić about the underground connection between Prespa and Ohrid Lake. Environmental Geology 51(5), 749-753.

Aufgebauer, A., Panagiotopoulos, K., Wagner, B., Schaebitz, F., Viehberg, F.A., Vogel, H., Zanchetta, G., Sulpizio, R., Leng, M.J., Damaschke, M., 2012. Climate and environmental change in the Balkans over the last 17 ka recorded in sediments from Lake Prespa (Albania/F.Y.R. of Macedonia/Greece). Quaternary International 274, 122-135.

Behre, K.E., 1981. The interpretation of anthropogenic indicators in pollen diagrams. Pollen et spores 23(2), 225-245.

Belmecheri, S., Namiotko, T., Robert, C., Von Grafenstein, U., Danielopol, D.L., 2009. Climate controlled ostracod preservation in Lake Ohrid (Albania, Macedonia). Palaeogeography, Palaeoclimatology, Palaeoecology 277(3-4), 236-245.

Bennett, K D, PSIMPOLL and PSCOMB (version 4.26) programs for plotting and analysis, retrieved 05.10.2011, from http://chrono.qub.ac.uk/psimpoll/psimpoll.html.

Birks, H.J.B., Line, J.M., 1992. The use of rarefaction analysis for estimating palynological richness from Quaternary pollen-analytical data. The Holocene 2(1), 1-10.

Tracking Environmental Change Using Lake Sediments., in: Developments in Paleoenvironmental Research, Vol.5: Data Handling and Numerical Techniques. Birks, H.J.B., Lotter, A.F., Juggins, S., Smol, J.P. (Eds.), Springer, Dordrecht, 2012.

Birks, H.H., Birks, H., 2000. Future uses of pollen analysis must include plant macrofossils. Journal of Biogeography 27(1), 31-35.

Böhm, A., 2012. Die Klima- und Umweltgeschichte des Balkans während des letzten Glazials und des Holozäns, rekonstruiert anhand von Seesedimenten des Prespasees (Mazedonien/Albanien/Griechenland). Universität zu Köln, Cologne,pp. 113, (in German).

Bordon, A., Peyron, O., Lézine, A.M., Brewer, S., Fouache, E., 2009. Pollen-inferred Late-Glacial and Holocene climate in southern Balkans (Lake Maliq). Quaternary International 200, 19-30.

Damaschke, M., Sulpizio, R., Zanchetta, G., Wagner, B., Böhm, A., Nowaczyk, N., Rethemeyer, J., Hilgers, A., 2013. Tephrostratigraphic studies on a sediment core from Lake Prespa in the Balkans. Climate of the Past 9(1), 267-287.

De Vivo, B., Rolandi, G., Gans, P.B., Calvert, A., Bohrson, W.A., Spera, F.J., Belkin, H.E., 2001. New constraints on the pyroclastic eruptive history of the Campanian volcanic Plain (Italy). Mineralogy and Petrology 73(1), 47-65.

Dearing, J.A., 1997. Sedimentary indicators of lake-level changes in the humid temperate zone: a critical review. Journal of Paleolimnology 18(1), 1-14.

Denèfle, M., Lézine, A., Fouache, E., Dufaure, J., 2000. A 12,000-year pollen record from Lake Maliq, Albania. Quaternary Research 54(3), 423-432.

Di Vito, M.A., Sulpizio, R., Zanchetta, G., D'Orazio, M., 2008. The late Pleistocene pyroclastic deposits of the Campanian Plain: New insights into the explosive activity of Neapolitan volcanoes. Journal of Volcanology and Geothermal Research 177(1), 19-48.

Digerfeldt, G., Olsson, S., Sandgren, P., 2000. Reconstruction of lake-level changes in lake Xinias, central Greece, during the last 40 000 years. Palaeogeography, Palaeoclimatology, Palaeoecology 158(1-2), 65-82.

Dumurdzanov, N., Serafimovski, T., Burchfiel, B.C., 2005. Cenozoic tectonics of Macedonia and its relation to the South Balkan extensional regime. Geosphere 1(1), 1-22.

Fouache, E., Desruelles, S., Magny, M., Bordon, A., Oberweiler, C., Coussot, C., Touchais, G., Lera, P., Lézine, A.M., Fadin, L., Roger, R., 2010. Palaeogeographical reconstructions of Lake Maliq (Korça Basin, Albania) between 14,000 BP and 2000 BP. Journal of Archeological Science 37, 525-535.

* for Chapters I, VII and VIII.

Geological Map of Albania, 1983, Scale 1:200 000, Geological Institute, Tirana.

Geological Maps of Yugoslavia, 1977, Scale 1:100 000, sheets K34-114 Podgradec, K34-102 Ohrid, K34-103 Bitola, K34-115 Lerin, Geological Institute, Belgrade.

Balkan Biodiversity: Pattern and Process in the European Hotspot., Griffiths, H.I., Kryštufek, B., Reed, J.M. (Eds.), Kluwer Academic Publishers, Dodrecht, The Netherlands, 2004.

Grimm, E.C., 1987. CONISS: a FORTRAN 77 program for stratigraphically constrained cluster analysis by the method of incremental sum of squares. Computers & Geosciences 13(1), 13-35.

Hammer, Ø., Harper, D.A.T., Ryan, P.D., 2001. PAST: paleontological statistics software package for education and data analysis. Palaeontologia electronica 4(1), 9.

Hijmans, R.J., Cameron, S.E., Parra, J.L., Jones, P.G., Jarvis, A., 2005. Very high resolution interpolated climate surfaces for global land areas. International Journal of Climatology 25(15), 1965-1978.

Hollis, G.E., Stevenson, A.C., 1997. The physical basis of the Lake Mikri Prespa systems: geology, climate, hydrology and water quality. Hydrobiologia 351, 1-19.

Hughes, P.D., 2010. Little Ice Age glaciers in the Balkans: low altitude glaciation enabled by cooler temperatures and local topoclimatic controls. Earth Surface Processes and Landforms 35, 229-241.

Hughes, P.D., Woodward, J.C., Gibbard, P.L., 2006. Late Pleistocene glaciers and climate in the Mediterranean. Global and Planetary Change 50(1-2), 83-98.

Hughes, P.D., Woodward, J.C., Van Calsteren, P.C., Thomas, L.E., 2011. The glacial history of the Dinaric Alps, Montenegro. Quaternary Science Reviews 30(23-24), 3393-3412.

Hydrogeological map of western Macedonia water district (09), 2010, Definition and assessment of hydrogeologic characteristics of aquifer systems of Greece, Institute of Geology and Mineral Expoloration (IGME), Athens.

IPCC., 2007. Climate Change 2007: Synthesis Report. Contribution of Working Groups I, II and III to the Fourth Assessment Report of the Intergovernmental Panel on Climate Change. (IPCC Fourth Assessment Report). IPCC, Geneva, Switzerland.

Keller, J., Ryan, W.B.F., Ninkovich, D., Altherr, R., 1978. Explosive volcanic activity in the Mediterranean over the past 200,000 yr as recorded in deep-sea sediments. Geological Society of America Bulletin 89(4), 591-604.

Leadley, P., Pereira, H.M., Alkemade, R., Fernandez-Manjarrés, J.F., Proenca, V., Scharlemann, J.P.W., Walpole, M.J., 2010. Biodiversity Scenarios: Projects Of 21st Century Change In Biodiversity And Associated Ecosystem Services (Cbd Technical Series). (50). Secretariat of the Convention on Biological Diversity, Montreal.

Leng, M.J., Baneschi, I., Zanchetta, G., Jex, C.N., Wagner, B., Vogel, H., 2010. Late Quaternary palaeoenvironmental reconstruction from Lakes Ohrid and Prespa (Macedonia/Albania border) using stable isotopes. Biogeosciences 7(10), 3109-3122.

Leng, M.J., Wagner, B., Boehm, A., Panagiotopoulos, K., Vane, C.H., Snelling, A., Haidon, C., Woodley, E., Vogel, H., Zanchetta, G., Baneschi, I., 2013. Understanding past climatic and hydrological variability in the Mediterranean from Lake Prespa sediment isotope and geochemical record over the Last Glacial cycle. Quaternary Science Reviews 66, 123-136.

Levin, I., Kromer, B., 2004. The tropospheric 14CO2 level in mid-latitudes of the Northern Hemisphere (1959-2003). Radiocarbon 46(3), 1261-1272.

Lézine, A.M., Von Grafenstein, U., Andersen, N., Belmecheri, S., Bordon, A., Caron, B., Cazet, J.P., Erlenkeuser, H., Fouache, E., Grenier, C., 2010. Lake Ohrid, Albania, provides an exceptional multi-proxy record of environmental changes during the last glacial–interglacial cycle. Palaeogeography, Palaeoclimatology, Palaeoecology 287(1-4), 116-127.

Likens, G.E., Davis, M.B., 1975. Post-glacial history of Mirror Lake and its watershed in New Hampshire: an initial report. Verh. Int. Verein. Limnol. 19, 982-993.

Malakou, M., Parisopoulos, G.A., Kazoglou, Y., Koutseri, I., Rigas, A., Belidis, T.,Guidelines for management and remediation of wet meadows in Micro Prespa, 2007, LIFE2002NAT/GR/8494, pp. 203, Agios Germanos, Greece, (in Greek).

Matevski, V., Čarni, A., Avramovski, O., Juvan, N., Kostadinovski, M., Košir, P., Marinšek, A., Paušič, A., Šilc, U., 2011. Forest vegetation of the Galičica mountain range in Macedonia. Založba ZRC, Ljubljana.

Matzinger, A., Jordanoski, M., Veljanoska-Sarafiloska, E., Sturm, M., Müller, B., Wüest, A., 2006. Is Lake Prespa jeopardizing the ecosystem of ancient Lake Ohrid? Hydrobiologia 553(1), 89-109.

Médail, F., Diadema, K., 2009. Glacial refugia influence plant diversity patterns in the Mediterranean Basin. Journal of Biogeography 36(7), 1333-1345.

Myers, N., Mittermeier, R.A., Mittermeier, C.G., Da Fonseca, G.A.B., Kent, J., 2000. Biodiversity hotspots for conservation priorities. Nature 403(6772), 853-858.

Odgaard, B.V., 1999. Fossil pollen as a record of past biodiversity. Journal of Biogeography 26(1), 7-17.

Odgaard, B.V., 1994. The Holocene vegetation history of northern West Jutland. Opera Botanica 123, 1-171.

Panagiotopoulos, K., Aufgebauer, A., Schäbitz, F., Wagner, B., 2013. Vegetation and climate history of the Lake Prespa region since the Lateglacial. Quaternary International 293, 157-169.

Parisopoulos, G.A., Malakou, M., Giamouri, M., 2009. Evaluation of lake level control using objective indicators: The case of Micro Prespa. Journal of Hydrology 367(1-2), 86-92.

Pavlides, G., 1997. The flora of Prespa National Park with emphasis on species of conservation interest. Hydrobiologia 351(1), 35-40.

Pereira, H.M., Leadley, P.W., Proenca, V., Alkemade, R., Scharlemann, J.P., Fernandez-Manjarres, J.F., Araujo, M.B., Balvanera, P., Biggs, R., Cheung, W.W., Chini, L., Cooper, H.D., Gilman, E.L., Guenette, S., Hurtt, G.C., Huntington, H.P., Mace, G.M., Oberdorff, T., Revenga, C., Rodrigues, P., Scholes, R.J., Sumaila, U.R., Walpole, M., 2010. Scenarios for global biodiversity in the 21st century. Science 330(6010), 1496-1501.

Petraitis, P.S., Latham, R.E., Niesenbaum, R.A., 1989. The maintenance of species diversity by disturbance. Quarterly Review of Biology 64(4), 393-418.

Polunin, O., 1980. Flowers of Greece and the Balkans - A Field Guide. Oxford University Press, Oxford.

Popovska, C., Bonacci, O., 2007. Basic data on the hydrology of Lakes Ohrid and Prespa. Hydrological Processes 21(5), 658-664.

Reimer, P.J., Baillie, M.G.L., Bard, E., Bayliss, A., Beck, J.W., Blackwell, P.G., Bronk Ramsey, C., Buck, C.E., Burr, G.S., Edwards, R.L., Friedrich, M., Grootes, P.M., Guilderson, T.P., Hajdas, I., Heaton, T.J., Hogg, A.G., Hughen, K.A., Kaiser, K.F., Kromer, B., Mccormac, F.G., Manning, S.W., Reimer, R.W., Richards, D.A., Southon, J.R., Talamo, S., Turney, C.S.M., Van Der Plicht, J., Weyhenmeyer, C.E., 2009. IntCal09 and Marine09 Radiocarbon Age Calibration Curves, 0 - 50,000 years cal BP. Radiocarbon 51, 1111-1150.

Ribolini, A., Isola, I., Zanchetta, G., Bini, M., Sulpizio, R., 2011. Glacial features on the Galicica Mountains, Macedonia: preliminary report. Geogr. Fis. Dinam. Quat. 34, 247-255.

Richter, J., Melles, M., Schäbitz, F., 2012. Temporal and spatial corridors of Homo sapiens sapiens population dynamics during the Late Pleistocene and early Holocene. Quaternary International 274, 1-4.

Sala, O.E., Chapin, F.S., Armesto, J.J., Berlow, E., Bloomfield, J., Dirzo, R., Huber-Sanwald, E., Huenneke, L.F., Jackson, R.B., Kinzig, A., 2000. Global biodiversity scenarios for the year 2100. Science 287(5459), 1770-1774.

Santacroce, R., Cioni, R., Marianelli, P., Sbrana, A., Sulpizio, R., Zanchetta, G., Donahue, D.J., Joron, J.L., 2008. Age and whole rock-glass compositions of proximal pyroclastics from the major explosive eruptions of Somma-Vesuvius: a review as a tool for distal tephrostratigraphy. Journal of Volcanology and Geothermal Research 177, 1-18.

Siani, G., Sulpizio, R., Paterne, M., Sbrana, A., 2004. Tephrostratigraphy study for the last 18,000 14C years in a deep-sea sediment sequence for the South Adriatic. Quaternary Science Reviews 23, 2485-2500.

Society for the Protection of Prespa, SPP, 2011. Number of species, retrieved 27.11.2011, from http://www.spp.gr/spp/species%20chart_en.pdf.

Stanković, S.: The Balkan Lake Ohrid and its living world., in: Monographiae Biologicae, Vol.IX. Bodenheimer, F.S., Weisbach, W.W. (Eds.), Dr. W. Junk, Den Haag, 1960.

Stefouli, M., Charou, E., Katsimpra, E.: Monitoring Lake Ecosystems Using Integrated Remote Sensing / Gis Techniques: An Assessment in the Region of West Macedonia, Greece., in: Environmental Monitoring, Ekundayo, E.O. (Ed.), InTech, 2011.

Stockmarr, J., 1971. Tablets with spores used in absolute pollen analysis. Pollen et spores 13, 615-621.

Strubenhoff, H.W., Hoyos, C.G., 2005. KfW Feasibility Study, Project Preparation & Development of the Transboundary Prespa Park Project, Part V: Hydrology Report. Hamburg,pp. 94.

Stuiver, M, Reimer, P J, Reimer, R, 2012. CALIB Radiocarbon Calibration (Version 6.1.0), retrieved 02.11.2012, from http://calib.qub.ac.uk/calib/.

Sulpizio, R., Zanchetta, G., D'Orazio, M., Vogel, H., Wagner, B., 2010. Tephrostratigraphy and tephrochronology of lakes Ohrid and Prespa, Balkans. Biogeosciences 7(10), 3273-3288.

Taberlet, P., Cheddadi, R., 2002. Ecology. Quaternary refugia and persistence of biodiversity. Science 297(5589), 2009-2010.

Telford, R., Heegaard, E., Birks, H.J.B., 2004. All age-depth models are wrong: but how badly? Quaternary Science Reviews 23(1-2), 1-5.

Ter Braak, C.J.F., Šmilauer, P., 2002. CANOCO reference manual and CanoDraw for Windows user's guide: software for canonical community ordination (version 4.5). Micro-computer Power Ithaca, NY, pp. 500.

Thomas, C.D., Cameron, A., Green, R.E., Bakkenes, M., Beaumont, L.J., Collingham, Y.C., Erasmus, B.F.N., De Siqueira, M.F., Grainger, A., Hannah, L., Hughes, L., Huntley, B., Van Jaarsveld, A.S., Midgley, G.F., Miles, L., Ortega-Huerta, M.A., Townsend Peterson, A., Phillips, O.L., Williams, J.W., 2004. Extinction risk from climate change. Nature 427(6970), 145-148.

Thuiller, W., Lavorel, S., Araújo, M.B., Sykes, M.T., Prentice, I.C., 2005. Climate change threats to plant diversity in Europe. Proceedings of the National Academy of Sciences of the United States of America 102(23), 8245-8250.

Van Der Knaap, W.O., Van Leeuwen, J.F.N., Finsinger, W., Gobet, E., Pini, R., Schweizer, A., Valsecchi, V., Ammann, B., 2005. Migration and population expansion of Abies, Fagus, Picea, and Quercus since 15000 years in and across the Alps, based on pollen-percentage threshold values. Quaternary Science Reviews 24(5-6), 645-680.

Vogel, H., Wagner, B., Zanchetta, G., Sulpizio, R., Rosén, P., 2010. A paleoclimate record with tephrochronological age control for the last glacial-interglacial cycle from Lake Ohrid, Albania and Macedonia. Journal of Paleolimnology 44(1), 295-310.

Wagner, B., Lotter, A., Nowaczyk, N., Reed, J., Schwalb, A., Sulpizio, R., Valsecchi, V., Wessels, M., Zanchetta, G., 2009. A 40,000-year record of environmental change from ancient Lake Ohrid (Albania and Macedonia). Journal of Paleolimnology 41(3), 407-430.

Wagner, B., Reicherter, K., Daut, G., Wessels, M., Matzinger, A., Schwalb, A., Spirkovski, Z., Sanxhaku, M., 2008. The potential of Lake Ohrid for long-term palaeoenvironmental reconstructions. Palaeogeography, Palaeoclimatology, Palaeoecology 259(2-3), 341-356.

Wagner, B., Vogel, H., Zanchetta, G., Sulpizio, R., 2010. Environmental change within the Balkan region during the past ca. 50 ka recorded in the sediments from lakes Prespa and Ohrid. Biogeosciences 7, 3187-3198.

Wagner, B., Aufgebauer, A., Vogel, H., Zanchetta, G., Sulpizio, R., Damaschke, M., 2012. Late Pleistocene and Holocene contourite drift in Lake Prespa (Albania/F.Y.R. of Macedonia/Greece). Quaternary International 274, 112-121.

Whittaker, R.H., 1972. Evolution and measurement of species diversity. Taxon 21(2), 213-251.

Willis, K.J., Bailey, R.M., Bhagwat, S.A., Birks, H.J., 2010. Biodiversity baselines, thresholds and resilience: testing predictions and assumptions using palaeoecological data. Trends in Ecology & Evolution 25(10), 583-591.

Zacharias, I., Bertachas, I., Skoulikidis, N., Koussouris, T., 2002. Greek lakes: Limnological overview. Lakes & Reservoirs: Research & Management 7(1), 55-62.

Zanchetta, G., Sulpizio, R., Giaccio, B., Siani, G., Paterne, M., Wulf, S., D'Orazio, M., 2008. The Y-3 tephra: A Last Glacial stratigraphic marker for the central Mediterranean basin. Journal of Volcanology and Geothermal Research 177(1), 145-154.

Zanchetta, G., Sulpizio, R., Roberts, N., Cioni, R., Eastwood, W., Siani, G., Paterne, M., Santacroce, R., 2011. Tephrostratigraphy, chronology and climatic events of the Mediterranean basin during the Holocene: an overview. The Holocene 21, 33-52.

Summary

The transboundary Lake Prespa and its watershed enclose a remarkable biodiversity that is protected by several national and international treaties. Situated at 849 m a.s.l., the area is characterized by a transitional climate and the closed nature of the basin controls Lake Prespa's modern hydrology. An 18 m-long sediment sequence was retrieved from a distal location, away from stream inflow, where preliminary hydroacoustic investigations suggested undisturbed sedimentation. Consequently, the sediments were dated and analyzed using palynological, sedimentological and geochemical techniques. The age model is based on AMS and ESR dating, tephrochronology and cross correlation with the Greenland ice record (NGRIP) and suggests an age of c. 92 ka cal BP for the base of the sequence.

The pollen spectra allow for the zoning of the record in three major phases of vegetation development corresponding to Marine Isotope Stages 5 to 1. The forested phases of MIS 5 and MIS 1 are dominated by thermophilous and drought-sensitive trees (e.g. *Quercus*, *Carpinus*, *Fagus*) suggesting higher temperatures and moisture availability during their growing season. Increased lake productivity, hypolimnion anoxia and calcite precipitation are recorded in these intervals. Continuous presence of Mediterranean frost-sensitive species (e.g. *Pistacia*, *Phillyrea*) during the Holocene implies rising temperatures in late winter and spring. Sporadic occurrence of maquis pollen in MIS 5 suggest that temperature was probably limiting their expansion. Increasing fuel availability and summer aridity most likely account for a higher microscopic charred particle concentration during the Holocene (in particular after c. 5.5 ka). However, intensifying anthropogenic activity has probably overridden climate forcing over the last c. 2 ka. Within MIS 5 and MIS 1, brief periods (centennial to millennial) of open landscape are also documented and are ascribed to colder and drier climate conditions persisting at Prespa. During MIS 3, the relatively open landscape is characterized by several deciduous trees besides *Pinus*. An open steppe landscape with scattered tree stands comprising mostly *Pinus* prevailed in MIS 4 and MIS 2. High *Artemisia* and Chenopodiaceae abundances point to rather cold and arid conditions at Prespa. This appears to be in agreement with low lake productivity, enhanced mixing and increased ice-cover documented for this time. However, occurrences of deciduous tree pollen throughout the Last Glacial provide evidence for the survival of several tree species in sheltered locations at Prespa or its vicinity.

This study underscores the sensitivity of the Lake Prespa region to climate forcing over the Last Glacial and the Holocene. The vegetation history of the region was examined focusing on ecological processes such as immigration, competition, succession, population growth and stability. Ongoing investigations may offer further insights into the paleoenvironment and paleoclimate at Prespa. The Prespa pollen underline the potential of the region to serve as refugium over longer time scales. In spite of systematic conservation efforts over the last decades, the question of whether Prespa's ecosystems will withstand increasing anthropogenic pressures remains open.

Zusammenfassung

Der trinationale Prespasee und sein Einzugsgebiet beherbergen eine bemerkenswerte Artenvielfalt, die derzeit durch mehrere nationale und internationale Verträge geschützt wird. Der in einer Höhe von 849 m üNN gelegene See wird von einem eumediterranen Klima geprägt. Die moderne Hydrologie des Sees ist durch die geschlossene Lage des Seebeckens charakterisiert. Eine 18m-lange Sedimentsequenz wurde vom nördlichen zentralen Seegrund abseits des Mündungsbereichs der Gebirgsbäche erbohrt, nachdem dort hydroakustische Untersuchungen auf ungestörte Sedimentation hingewiesen hatten. Die Sedimente wurden datiert und unter Verwendung palynologischer, sedimentologischer und geochemischer Analysemethoden untersucht. Das Altersmodell basiert auf AMS-und ESR-Datierungen, Tephrochronologie und Kreuzkorrelation mit dem grönländischen Eisbohrkern (NGRIP). Für die Basis der Sedimentsequenz ergibt sich ein Alter von c. 92 ka cal BP.

Die Pollenspektren ermöglichen die Einordnung dreier großer Vegetationsentwicklungsphasen entsprechend der marinen Isotopenstadien (MIS) 5 bis 1. Die bewaldeten Phasen des MIS 5 und MIS 1 sind von wärmeliebender und Dürre empfindlicher Waldvegetation (z.B. *Quercus*, *Carpinus*, *Fagus*) geprägt, was auf höhere Temperaturen und Niederschläge während der Vegetationsperiode hindeutet. Der Prespasee zeigt während dieser Intervalle eine erhöhte Produktivität, hypolimnische Anoxie und verstärkte Calcitfällung. Das kontinuierliche Auftreten der Pollen mediterraner, frostempfindlicher Arten (z.B. *Pistacia* und *Phillyrea*) während des Holozäns impliziert steigende Temperaturen im späten Winter und Frühjahr. Ein sporadisches Auftreten von Pollen Macchia-typischer Arten in MIS 5 zeigt, dass niedrigere Temperaturen wahrscheinlich ihre weitere Expansion limitierte. Eine steigende Verfügbarkeit brennbarer Biomasse und erhöhte Trockenheit im Sommer sind höchstwahrscheinlich der Grund für die höhere Konzentration mikroskopischer Holzkohle- Partikel im Holozän (insbesondere nach c. 5.5 ka). Allerdings hat der zunehmende anthropogene Einfluss das Klimasignal der letzten c. 2 ka vermutlich verändert. Innerhalb von MIS 5 und MIS 1 zeigen sich kurzzeitige Perioden (100-1000 Jahre), die durch eine offenere Landschaft gekennzeichnet sind und auf kältere und trockenere Klimabedingungen im Gebiet des Prespasees hindeuten. Während MIS 3 ist die relativ offene Landschaft neben *Pinus* durch mehrere laubwerfende Baumarten gekennzeichnet. Eine offene Steppenlandschaft mit vereinzelten Bäumen (meist *Pinus*) herrschte in MIS 4 und MIS 2 vor. Hohe Häufigkeiten an *Artemisia* und Chenopodiaceae deuten hier auf eher kalte und trockene Bedingungen am Prespasee hin. Dies scheint mit der niedrigeren Produktivität des Sees, dem erhöhten klastischen Eintrag und der verstärkten Eisbedeckung während dieser Zeit zu korrelieren. Der Nachweis von Laubbaum-Pollen während dem letzten Glazial liefert Beweise für das Überleben von mehreren Baumarten an geschützten Stellen in der Region des Prespasees.

Diese Studie unterstreicht die Klimasensitivität des Prespasees und dessen Eignung für paläoökologische Untersuchungen zur regionalen Klimarekonstruktion der letzten Eiszeit und des Holozäns. Sie erlaubt ferner die Untersuchung der regionalen Vegetationsgeschichte, wobei der Schwerpunkt auf ökologische Prozesse wie Einwanderung, Konkurrenz, Sukzession, Populationswachstum und Stabilität gelegt wird. Laufende Untersuchungen können weitere Einblicke in Paläoumwelt- und Paläoklimabedingungen liefern. Die Prespasee-Pollen unterstreichen die Bedeutung der Region als wichtiges Refugium über längere Zeitskalen. Trotz der intensiven Naturschutzmassnahmen der letzten Jahrzehnte, bleibt die Frage, wie lange der Prespasee als Ökosystem noch den zunehmenden anthropogenen Belastungen standhalten kann.

Περίληψη

Η διασυνοριακή λίμνη Πρέσπα και η λεκάνη απορροής της προστατεύονται από εθνικές και διεθνείς συνθήκες και διακρίνονται για την βιοποικιλότητα τους. Η περιοχή, που βρίσκεται σε υψόμετρο 849 μ., χαρακτηρίζεται από ένα μεταβατικό κλίμα, ενώ η κλειστή λεκάνη απορροής της ρυθμίζει σε σημαντικό βαθμό την υδρολογία της λίμνης. Μια μακρά ακολουθία ιζημάτων (18 μ) ανακτήθηκε από γεώτρηση σε κεντρική τοποθεσία της λίμνης, η οποία επιλέχθηκε ύστερα από προκαταρκτικές υδροακουστικές έρευνες που υπέδειξαν συνεχή απόθεση. Εν συνεχεία, τα ιζήματα χρονολογήθηκαν και αναλύθηκαν χρησιμοποιώντας παλυνολογικές, ιζηματολογικές και γεωχημικές τεχνικές. Η ηλικία των ιζημάτων προσδιορίσθηκε με ράδιο- και φασματοσκοπική (ESR)- χρονολόγηση, με τεφροχρονολόγηση καθώς και με τη συσχέτιση τους με τα αρχεία πάγου της Γροιλανδίας (NGRIP) και παραπέμπει σε ηλικία 92.000 χρόνων για τη βάση της ακολουθίας.

Η παλυνολογική ανάλυση επιτρέπει την οριοθέτηση τριών κύριων φάσεων της βλάστησης που αντιστοιχούν στα Ισοτοπικά Στάδια (MIS) 5 έως 1. Κατά τη διάρκεια των MIS 5 και MIS 1 απαντώνται θερμόφιλα και υγρόφιλα δασικά είδη (π.χ. *Quercus*, *Carpinus*, *Fagus*), γεγονός που υποδηλώνει υψηλότερες θερμοκρασίες και μειωμένη εξατμισοδιαπνοή κατά τη διάρκεια της βλαστιτικής περιόδου. Αυξημένη πρωτογενής παραγωγή, παρατεταμένη ανοξία του υπολιμνίου και κατακρήμνιση ασβεστίτη καταγράφονται σε αυτές τις περιόδους. Η αδιάκοπη παρουσία κατά τη διάρκεια του Ολόκαινου μεσογειακών ειδών (π.χ. *Pistacia*, *Phillyrea*) ευαίσθητων στον παγετό συνεπάγεται την αύξηση της θερμοκρασίας στα τέλη του χειμώνα και την άνοιξη. Η σποραδική εμφάνιση γύρης μεσογειακών ειδών στο MIS 5 μαρτυρά ότι οι χαμηλές θερμοκρασίες πιθανώς περιόριζαν την εξάπλωσή τους. Η αυξημένη φυτική βιομάζα σε συνδυασμό με τη θερινή ξηρασία συντέλεσαν στην αυξημένη συγκέντρωση απανθρακωμένων μικροσκοπικών σωματιδίων κατά τη διάρκεια του Ολόκαινου (ιδιαίτερα πριν από 5.500 χρόνια). Ωστόσο, η εντατικοποίηση των ανθρωπογενών δραστηριοτήτων τα τελευταία 2.000 χρόνια πιθανώς επισκιάζει τον αντίκτυπο της φυσικής κλιματικής ακολουθίας στα τοπικά οικοσυστήματα. Σχετικά σύντομες περίοδοι (διάρκειας μερικών αιώνων), στις οποίες η δασοκάλυψη της λεκάνης απορροής υποχωρεί αισθητά, καταγράφονται κατά τη διάρκεια των MIS 5 και MIS 1 και μπορούν να αποδοθούν σε ψυχρότερες και ξηρότερες κλιματολογικές συνθήκες. Κατά τη διάρκεια του MIS 3, το σχετικά ανοιχτό τοπίο, πέρα από το είδος *Pinus,* χαρακτηρίζεται από αρκετά άλλα είδη φυλλοβόλων δένδρων. Ένα ανοιχτό τοπίο στέπας με διάσπαρτες συστάδες δένδρων, κυρίως *Pinus,* επικρατούσε στην περιοχή των Πρεσπών στις περιόδους MIS 4 και 2. Είδη *Artemisia* και Chenopodiaceae κυριαρχούσαν στη λεκάνη απορροής και υποδηλώνουν την επικράτηση χαμηλών θερμοκρασιών και άνυδρων συνθηκών σε αυτά τα χρονικά διαστήματα. Οι ολιγοτροφικές συνθήκες, η ενισχυμένη μίξη και η αυξημένη παγοκάλυψη της λίμνης υποστηρίζουν αυτή την ερμηνεία. Ωστόσο, η καταγραφή γύρης φυλλοβόλων δένδρων καθ' όλη τη διάρκεια της τελευταίας παγετώδης περιόδου παρέχει ισχυρές ενδείξεις για την επιβίωση πολλών ξυλωδών ειδών σε προστατευμένες τοποθεσίες εντός ή πλησίον της λεκάνης απορροής.

Αυτή η μελέτη υπογραμμίζει την ευαισθησία της περιοχής των Πρεσπών στην κλιματική αλλαγή κατά την τελευταία παγετώδη περίοδο και το Ολόκαινο. Η εξέλιξη της βλάστησης της περιοχής εξετάστηκε επικεντρώνοντας σε οικολογικές διαδικασίες όπως η μετανάστευση, ο ανταγωνισμός, η διαδοχή, η πληθυσμιακή αύξηση και σταθερότητα ενός είδους. Έρευνες που βρίσκονται ακόμα σε εξέλιξη θα συνεισφέρουν στην περαιτέρω κατανόηση των παρελθόντων περιβαλλοντολογικών και κλιματολογικών συνθηκών στην Πρέσπα. Η παρούσα παλυνολογική ανάλυση αναδεικνύει το δυναμικό της περιοχής να λειτουργεί ως καταφύγιο φυτικών ειδών σε μεγάλες χρονικές κλίμακες. Όμως, παρά τις συστηματικές προσπάθειες περιβαλλοντικής προστασίας των τελευταίων δεκαετιών, το ερώτημα πώς τα οικοσυστήματα των Πρεσπών θα αντεπεξέλθουν στις αυξανόμενες ανθρωπογενείς πιέσεις παραμένει ανοιχτό.

A SEM Images

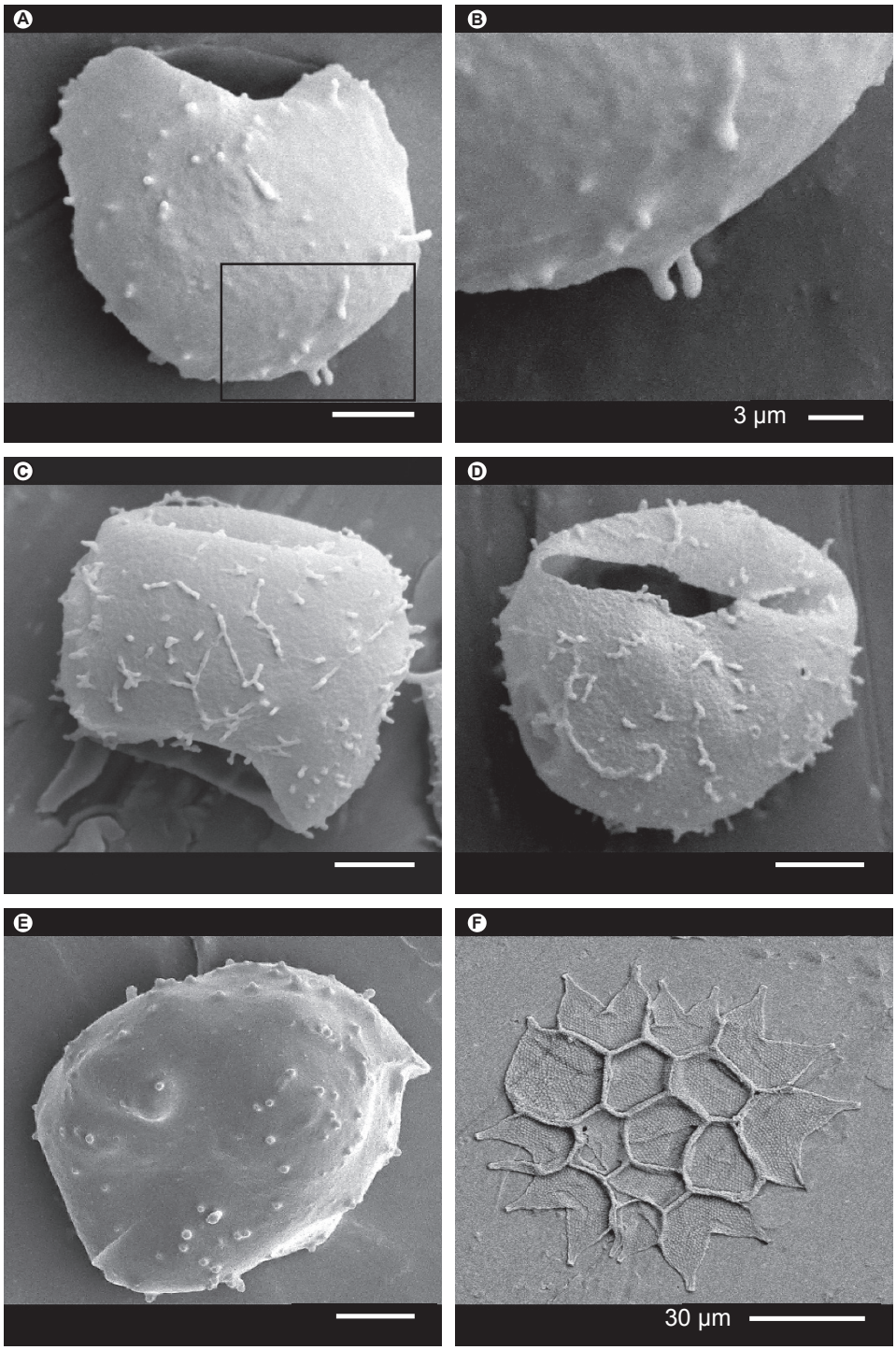

Figure A.1: Scanning electron microscope images of palynomorphs encountered in the upper 2 cm of Co1215. Samples from refrigerated material were processed using standard palynological techniques and stored in ethanol before mounting on a specimen pin stub. A scale of 10 µm is shown unless indicated otherwise. *Gonyaulax apiculata* (cf. Evitt et al., 1985; Kouli et al. 2001; a – e) and *Pediastrum boryanum* (f). Notice the morphological variations in parasutural development and the occasional formation of ridges (c, d).

B Pollen and spore taxa

Table B.1: Pollen of trees, shrubs, vines and tree parasites counted in Co1215.

Aceraceae	*Acer*
Adoxaceae	*Sambucus*
Anacardiaceae	*Pistacia*
Araliaceae	*Hedera*
Betulaceae	*Alnus*
	Betula
	Carpinus betulus
	Carpinus orientalis/ *Ostrya carpinifolia*
	Corylus
Buxaceae	*Buxus*
Cornaceae	*Cornus mas*-type
Cupressaceae	*Juniperus*
Elaeagnaceae	*Hippophae*
Ephedraceae	*Ephedra distachya*-type
	Ephedra fragilis-type
Ericaceae	*spp.*
	Vaccinium-type
Fagaceae	*Fagus*
	Quercus cerris-type
	Quercus ilex-type
	Quercus robur-type
Juglandaceae	*Juglans*
Loranthaceae	*Loranthus*
Malvaceae	*Tilia*
Oleaceae	*Fraxinus excelsior*-type
	Fraxinus ornus
	Olea
	Phillyrea
Pinaceae	*Abies*
	Picea
	Pinus
Rosaceae	*Sorbus*
Salicaceae	*Salix*
Sapindaceae	*Aesculus hippocastanum*
Thymelaeaceae	*Daphne*
Ulmaceae	*Ulmus/Zelkova*
Vitaceae	*Vitis*

Table B.2: Pollen of herbs counted in Co1215.

Amaranthaceae	*Polycnemum*
Apiaceae	spp.
Asteraceae	*Anthemis*-type
	Artemisia
	Centaurea jacea-type
	Cichorioideae
	Cirsium-type
	Senecio-type
Brassicaceae	spp.
	Capsella-type
	Sinapis-type
Campanulaceae	spp.
Cannabaceae	*Humulus*
Caryophyllaceae	spp.
Chenopodiaceae	spp.
Cistaceae	*Helianthemum*
	Fumana
Euphorbiaceae	spp.
Ericaceae	spp.
	Vaccinium-type
Hypericaceae	*Hypericum perforatum*-type
Lamiaceae	*Mentha*-type
Plantaginaceae	spp.
	Plantago lanceolata-type
	Plantago media/major-type
Plumbaginaceae	*Armeria*
Poaceae	spp.
	Cerealia
Polemoniaceae	spp.
Polygonaceae	spp.
	Persicaria
	Rumex
Ranunculaceae	spp.
	Helleborus
	Ranunculus acris-type
	Thalictrum
Rosaceae	spp.
	Sanguisorba minor
Rubiaceae	spp.
	Galium
Saxifragaceae	spp.
Urticaceae	*Urtica*
Valerianaceae	*Valeriana*
Zygophyllaceae	*Tribulus*

Table B.3: Pollen of aquatic plants, spores of ferns and fungi, coenobia of green algae and dinocysts counted in Co1215.

Aquatics

Alismataceae	*Alisma plantago-aquatica*
Cyperaceae	spp.
Haloragaceae	*Myriophyllum spicatum*
	Myriophyllum verticillatum
Nymphaeaceae	*Nymphaea*
Potamogetonaceae	*Potamogeton*
Typhaceae	*Sparganium*-type
	Typha latifolia-type

Ferns

Aspleniaceae	*Asplenium*
Dennstaedtiaceae	*Pteridium*
Polypodiaceae	*Polypodium*

Fungi

Sporomiaceae	*Sporormiella*

Green Algae

Botryococcaceae	*Botryococcus braunii*
	Botryococcus pila
Hydrodictyaceae	*Pediastrum boryanum*
	Pediastrum simplex

Dinoflagellata

Gonyaulacaceae	*Gonyaulax apiculata*

C Palynological data of Co1215

Palynological data will be made available to access online at the following link of the CRC 806 Database: http://crc806db.uni-koeln.de/

Sedimentological and geochemical data can be found in the PANGAEA repository accessible at: http://www.pangaea.de/

Chapter Contributions

Chapter II: Climate and environmental change in the Balkans over the last 17 ka recorded in sediments from Lake Prespa (Albania/F.Y.R. of Macedonia/Greece)

Aufgebauer provided lithological, sedimentological, geochemical and geophysical data and interpretation. Panagiotopoulos provided palynological data and interpretation. Viehberg provided ostracod data and interpretation. Damaschke, Sulpizio and Zanchetta contributed to tephra identification and correlation. Aufgebauer wrote the text with contributions from Panagiotopoulos, Wagner, Leng, Vogel, Schäbitz. Panagiotopoulos' overall contribution accounts for 35%.

Chapter III: Vegetation and climate history of the Lake Prespa region since the Lateglacial

Panagiotopoulos conducted palynological and microscopic charcoal analyses and provided the relevant data sets and interpretation. Aufgebauer provided chronological, lithological, geochemistry and geophysical data (through Chapter II). Panagiotopoulos undertook the main interpretation of all data and wrote the text with contributions from Aufgebauer, Schäbitz and Wagner. Overall contribution of Panagiotopoulos to Chapter III exceeds 90%.

Chapter IV: Understanding past climatic and hydrological variability in the Mediterranean from Lake Prespa sediment isotope and geochemical record over the Last Glacial cycle

Leng and Wagner undertook the main interpretation of all data. Panagiotopoulos provided pollen, green algae and dinoflagellate data and interpretation. Vane provided Rock Eval data and interpretation. Böhm provided geochemical data. Snelling, Haidon, Woodley and Baneschi provided isotope and mineralogy data. Vogel and Zanchetta contributed intellectually to the discussions of the data. Panagiotopoulos' contribution to Chapter IV accounts for 30%.

Chapter V: Climate variability since MIS 5 in SW Balkans inferred from multiproxy analysis of Lake Prespa sediments

Panagiotopoulos provided pollen, green algae and dinoflagellate data and interpretation. Böhm provided lithological, sedimentological and geochemical data and interpretation. Panagiotopoulos undertook the main interpretation of all data and wrote the text with contributions from Leng, Wagner, Böhm and Schäbitz. Panagiotopoulos' contribution to Chapter V exceeds 90%.

Chapter VI: Towards a theoretical framework for analyzing integrated socio-environmental systems

Widlok undertook the main interpretation of all data and wrote the text with contributions from Solich, Peters, Zimmermann, Kretschmer, Bradtmöller, Pastors, Schäbitz, Hoffmann, Dikau. For section 6.3.5 (The Prespa case study): Aufgebauer and Panagiotopoulos provided geophysical and palynological data and interpretation respectively; Schäbitz wrote the text with contributions from Panagiotopoulos, Aufgebauer and Wagner. Panagiotopoulos' contribution to section 6.3.5 is 30% and overall to Chapter VI is 5%.

Erklärung

Ich versichere, dass ich die von mir vorgelegte Dissertation selbständig angefertigt, die benutzten Quellen und Hilfsmittel vollständig angegeben und die Stellen der Arbeit –einschließlich Tabellen, Karten und Abbildungen–, die anderen Werken im Wortlaut oder dem Sinn nach entnommen sind, in jedem Einzelfall als Entlehnung kenntlich gemacht habe; dass diese Dissertation noch keiner anderen Fakultät oder Universität zur Prüfung vorgelegen hat; dass sie –abgesehen von unten angegebenen Teilpublikationen– noch nicht veröffentlicht worden ist, sowie, dass ich eine solche Veröffentlichung vor Abschluss des Promotionsverfahrens nicht vornehmen werde.

Die Bestimmungen der Promotionsordnung sind mir bekannt. Die von mir vorgelegte Dissertation ist von Prof. Dr. Frank Schäbitz betreut worden.

Nachfolgend genannte Teilpublikationen liegen vor:

1. Aufgebauer A., Panagiotopoulos K., Wagner B., Schäbitz F., Viehberg F. A., Vogel H., Zanchetta G., Sulpizio R., Leng M. J., Damaschke M., 2012, Climate and environmental change in the Balkans over the last 17 ka recorded in sediments from Lake Prespa (Albania/F.Y.R. of Macedonia/Greece), Quaternary International 274, 122-135.
2. Panagiotopoulos K., Aufgebauer A., Schäbitz F., Wagner B., 2013a, Vegetation and climate history of Lake Prespa since the Lateglacial, Quaternary International 293, 157-169.
3. Leng, M.J., Wagner, B., Boehm, A., Panagiotopoulos, K., Vane, C.H., Snelling, A., Haidon, C., Woodley, E., Vogel, H., Zanchetta, G., and Baneschi, I., 2013, Understanding past climatic and hydrological variability in the Mediterranean from Lake Prespa sediment isotope and geochemical record over the Last Glacial cycle, Quaternary Science Reviews 66, 123-136.
4. Panagiotopoulos, K., Böhm, A., Leng, M. J., Wagner, B., Schäbitz, F., 2013b, Climate variability since MIS 5 in SW Balkans inferred from multiproxy analysis of Lake Prespa sediments, Climate of the Past Discussions.
5. Widlok, T., Aufgebauer, A., Bradtmöller, M., Dikau, R., Hoffmann, T., Kretschmer, I., Panagiotopoulos, K., Pastoors, A., Peters, R., Schäbitz, F., Schlummer, M., Solich, M., Wagner, B., Weniger, G.-C., Zimmermann, A., 2012: Towards a theoretical framework for analyzing integrated socio-environmental systems. Quaternary International 274, 259-272.

Köln, den 22.04.2013

Konstantinos Panagiotopoulos